PCT WORLD INTELLECTUAL PROPERTY ORGANIZATION
International Bureau

INTERNATIONAL APPLICATION PUBLISHED UNDER THE PATENT COOPERATION TREATY (PCT)

(51) International Patent Classification 6 : G06F 17/50 | A2

(11) International Publication Number: **WO 98/06048**

(43) International Publication Date: 12 February 1998 (12.02.98)

(21) International Application Number: PCT/CA97/00539

(22) International Filing Date: 31 July 1997 (31.07.97)

(30) Priority Data:
9616105.4 31 July 1996 (31.07.96) GB

(71) Applicant *(for all designated States except US)*: QUEEN'S UNIVERSITY AT KINGSTON [CA/CA]; Kingston, Ontario K7L 3N6 (CA).

(72) Inventors; and
(75) Inventors/Applicants *(for US only)*: SHAMOVSKY, Igor, L. [RU/CA]; 6-202, 17 Van Order Drive, Kingston, Ontario K7M 1B5 (CA). ROSS, Gregory, M. [CA/CA]; 1090 Caitlin Crescent, Kingston, Ontario K7P 2S4 (CA). RIOPELLE, Richard, J. [CA/CA]; 32 Lakeshore Boulevard, Kingston, Ontario K7M 4J6 (CA). WEAVER, Donald, F. [CA/CA]; 27 Collegeview Crescent, Kingston, Ontario K7M 7J8 (CA).

(74) Agents: SCHUMACHER, Lynn, C. et al.; Hill & Schumacher, Suite 802, 335 Bay Street, Toronto, Ontario M5H 2R3 (CA).

(81) Designated States: AL, AM, AT, AU, AZ, BA, BB, BG, BR, BY, CA, CH, CN, CU, CZ, DE, DK, EE, ES, FI, GB, GE, GH, HU, IL, IS, JP, KE, KG, KP, KR, KZ, LC, LK, LR, LS, LT, LU, LV, MD, MG, MK, MN, MW, MX, NO, NZ, PL, PT, RO, RU, SD, SE, SG, SI, SK, SL, TJ, TM, TR, TT, UA, UG, US, UZ, VN, YU, ZW, ARIPO patent (GH, KE, LS, MW, SD, SZ, UG, ZW), Eurasian patent (AM, AZ, BY, KG, KZ, MD, RU, TJ, TM), European patent (AT, BE, CH, DE, DK, ES, FI, FR, GB, GR, IE, IT, LU, MC, NL, PT, SE), OAPI patent (BF, BJ, CF, CG, CI, CM, GA, GN, ML, MR, NE, SN, TD, TG).

Published
Without international search report and to be republished upon receipt of that report.

(54) Title: MOLECULAR MODELLING OF NEUROTROPHIN-RECEPTOR BINDING

(57) Abstract

The present invention relates to a computational method for identifying the bioactive conformations of peptide domains, in particular, the geometries of complexes of neurotrophins and their receptors. The bioactive conformation of the Nerve Growth Factor (NGF) amino and carboxyl termini (Trk binding domain) was determined. The complex of the NGF termini splits into two distinct regions: a rigid region (residues 9-11 and 112'-118') and a flexible loop (residues 1-8), the geometry of the rigid region, which is maintained by electrostatic interaction between Glu^{11} and $Arg^{118'}$, is conserved in active molecules only. The separation of the flexible loop from the rigid region is necessary in order to eliminate an influence of the loop on the biologically active conformation of the rigid region. The present invention also relates to a method for identifying and theoretically modelling specific receptor binding sites for Nerve Growth Factor (NGF) and Brain-Derived Neurotrophic Factor (BDNF) on their receptors, TrkA and TrkB, respectively. The present invention also relates to a method for identifying and theoretically modelling a receptor binding site for neurotrophins, such as NGF, BDNF, NT-3, and NT-4/5, of the common neurotrophin receptor $p75^{NTR}$.

FOR THE PURPOSES OF INFORMATION ONLY

Codes used to identify States party to the PCT on the front pages of pamphlets publishing international applications under the PCT.

AL	Albania	ES	Spain	LS	Lesotho	SI	Slovenia
AM	Armenia	FI	Finland	LT	Lithuania	SK	Slovakia
AT	Austria	FR	France	LU	Luxembourg	SN	Senegal
AU	Australia	GA	Gabon	LV	Latvia	SZ	Swaziland
AZ	Azerbaijan	GB	United Kingdom	MC	Monaco	TD	Chad
BA	Bosnia and Herzegovina	GE	Georgia	MD	Republic of Moldova	TG	Togo
BB	Barbados	GH	Ghana	MG	Madagascar	TJ	Tajikistan
BE	Belgium	GN	Guinea	MK	The former Yugoslav Republic of Macedonia	TM	Turkmenistan
BF	Burkina Faso	GR	Greece			TR	Turkey
BG	Bulgaria	HU	Hungary	ML	Mali	TT	Trinidad and Tobago
BJ	Benin	IE	Ireland	MN	Mongolia	UA	Ukraine
BR	Brazil	IL	Israel	MR	Mauritania	UG	Uganda
BY	Belarus	IS	Iceland	MW	Malawi	US	United States of America
CA	Canada	IT	Italy	MX	Mexico	UZ	Uzbekistan
CF	Central African Republic	JP	Japan	NE	Niger	VN	Viet Nam
CG	Congo	KE	Kenya	NL	Netherlands	YU	Yugoslavia
CH	Switzerland	KG	Kyrgyzstan	NO	Norway	ZW	Zimbabwe
CI	Côte d'Ivoire	KP	Democratic People's Republic of Korea	NZ	New Zealand		
CM	Cameroon			PL	Poland		
CN	China	KR	Republic of Korea	PT	Portugal		
CU	Cuba	KZ	Kazakstan	RO	Romania		
CZ	Czech Republic	LC	Saint Lucia	RU	Russian Federation		
DE	Germany	LI	Liechtenstein	SD	Sudan		
DK	Denmark	LK	Sri Lanka	SE	Sweden		
EE	Estonia	LR	Liberia	SG	Singapore		

MOLECULAR MODELLING OF NEUROTROPHIN-RECEPTOR BINDING

FIELD OF THE INVENTION

The present invention relates to a computational method for identifying minimum-energy structures in molecular systems, and more particularly for determining the bioactive conformations of peptide domains. The invention relates to determination of the bioactive conformations of the amino and carboxyl termini of Nerve Growth Factor (NGF) and analogues thereof, and the 3-dimensional structures of their complexes with the 24-amino acid second leucine-rich motif (LRM) of TrkA which represents the binding site for NGF. The invention further relates to the theoretically identified geometries of the TrkB and the $p75^{NTR}$ receptor binding sites and to the mechanisms of neurotrophin binding.

BACKGROUND OF THE INVENTION

The neurotrophins are a family of structurally and functionally related proteins, including Nerve Growth Factor (NGF), Brain-Derived Neurotrophic Factor (BDNF), Neurotrophin-3 (NT-3), Neurotrophin-4/5 (NT-4/5) and Neurotrophin-6 (NT-6). These proteins promote the survival and differentiation of diverse neuronal populations in both the peripheral and central nervous systems (Hefti, 1986; Hefti and Weiner, 1986; Levi-Montalcini, 1987; Barde, 1989; Leibrock *et al.*, 1989; Maisonpierre *et al.*, 1990; Rosenthal *et al.*, 1990; Hohn *et al.*, 1990; Gotz *et al.*, 1994; Maness *et al.*, 1994) and are involved in the pathogenesis of diverse neurological disorders. Neurotrophins exert certain of their biological effects through specific interactions with a class of transmembrane receptor tyrosine kinases (TrkA, TrkB and TrkC) (Kaplan *et al.*, 1991; Klein *et al.*, 1991, 1992; Soppet *et al.*, 1991; Squinto *et al.*, 1991; Berkemeier *et al.*, 1991; Escandon *et al.*, 1993; Lamballe *et al.*, 1991). Specificity of neurotrophin action results from their selective interactions with Trk. That is, TrkA only binds NGF (Kaplan *et al.*, 1991; Klein *et al.*, 1991); TrkB binds BDNF, NT-3 and NT-4/5 (Soppet *et al.*, 1991; Squinto *et al.*, 1991; Berkemeier *et al.*, 1991; Escandon *et al.*, 1993; Lamballe *et al.*, 1991; Klein *et al.*, 1992; Vale and Shooter, 1985; Barbacid, 1993); and TrkC exclusively binds NT-3 (Lamballe *et al.*, 1991; Vale and Shooter, 1985). This is particularly evident when the Trk receptors are coexpressed with the common neurotrophin receptor $p75^{NTR}$ (For review see Meakin and Shooter, 1992; Barbacid, 1993; Chao, 1994; Bradshaw *et al.*, 1994; Ibáñez, 1995).

The common neurotrophin receptor $p75^{NTR}$ is a transmembrane glycoprotein structurally related to the tumor necrosis factor and CD-40 receptors (Meakin and Shooter,

1992; Rydén and Ibáñez, 1996). As all neurotrophins bind to $p75^{NTR}$ with similar affinity (Rodriguez-Tébar *et al.*, 1990; Hallböök *et al.*, 1991; Rodriguez-Tébar *et al.*, 1992; Ibáñez, 1995), neurotrophin specificity is conventionally thought to be caused by the binding selectivity for Trk receptors which are differentially expressed in different neuronal populations (Ibáñez, 1995). However, accumulated experimental data on neurotrophin activity reveal important functional aspects of $p75^{NTR}$ (Heldin *et al.*, 1989; Jing *et al.*, 1992; Herrmann, 1993; Barker and Shooter, 1994; Dobrowsky *et al.*, 1994, Matsumoto *et al.*, 1995; Marchetti *et al.*, 1996; Washiyama *et al.*, 1996). The common neurotrophin receptor enhances functions and increases binding specificity of Trk receptors (Barker and Shooter, 1994; Mahadeo *et al.*, 1994; Chao and Hempstead, 1995; Rydén and Ibáñez, 1996). In addition, $p75^{NTR}$ possesses unique, Trk-independent signalling properties which involve ceramide production through activation of the sphingomyelin cycle (Dobrowsky *et al.*, 1994), apoptosis (cell death) (Van der Zee *et al.*, 1996; Cassacia-Bonnefil *et al.*, 1996; Frade *et al.*, 1996), and activation of the transcription factor NFκB (Carter *et al.*, 1996). Recently, $p75^{NTR}$ has been demonstrated to participate in human melanoma progression (Herrmann *et al.*, 1993; Marchetti *et al.*, 1996). Furthermore, NGF and NT-3 increase the production of heparin by 70W melanoma cells, which is associated with their metastatic potential (Marchetti *et al.*, 1996). Although this effect has been shown to be mediated by the common neurotrophin receptor, neither BDNF nor NT-4/5 appeared to be active. Explicit modelling of the various neurotrophin receptors will be critical to the rational design of neurotrophin-based drugs.

NGF displays high and low affinity binding sites in sensory and sympathetic neurons and in pheochromocytoma PC12 cells (Sutter *et al.*, 1979; Landreth and Shooter, 1980; Schechter and Bothwell, 1981). The coexpression of the common neurotrophin $p75^{NTR}$ receptor with TrkA is required to form the high affinity binding site (Hempstead *et al.*, 1991; Barker and Shooter, 1994; Mahadeo *et al.*, 1994; Chao and Hempstead, 1995). Several models of the TrkA-$p75^{NTR}$ interaction have been proposed to explain high affinity NGF binding (Bothwell, 1991; Chao, 1992b; Chao and Hempstead, 1995; Wolf *et al.*, 1995; Ross *et al.*, 1996; Ross *et al.*, 1997). These models differ with respect to direct (conformational model) or indirect (ligand-presentation model) interaction of $p75^{NTR}$ with TrkA. Direct TrkA-$p75^{NTR}$ interaction is consistent with much of the existing experimental data.

NGF, a 118 amino acid protein, is an extremely important neurotrophin, being implicated in the pathogenesis of Alzheimer's disease, epilepsy and pain (Ben and Represa, 1990; McKee *et al.*, 1991; Leven and Mendel, 1993; Woolf and Doubell, 1994; Rashid *et al.*, 1995; McMahon *et al.*, 1995). The binding of NGF to its receptors is determined by distinct sequences within its primary amino acid structure. While several regions of NGF participate in the NGF/TrkA interaction, mutation studies suggest that relatively few key residues, namely

those located in th NGF amino and carboxyl t rmini, are required for high affinity binding.

Th hairpin loop at residues 29-35 is responsible for recognition by $p75^{NTR}$ (Ibáñez *et al.*, 1992; Radziejewski *et al.*, 1992), while the amino and carboxyl t rmini are important binding d terminants for recognition by the TrkA receptor (Shih *et al.*, 1994; Moore and Shooter, 1975; Suter *et al.*, 1992; Burton *et al.*, 1992, 1995; Kahle *et al.*, 1992; Luo and Neet, 1992; Drinkwater *et al.*, 1993; Treanor *et al.*, 1995; Taylor *et al.*, 1991). Truncation of either the amino or carboxyl terminus of NGF produces less active NGF analogues; similarly most deletion or point mutations of the amino terminus also lead to NGF analogues with diminished activity (Shih *et al.*, 1994; Burton *et al.*, 1992, 1995; Kahle *et al.*, 1992; Drinkwater *et al.*, 1993; Treanor *et al.*, 1995; Taylor *et al.*, 1991). On the other hand, the NGFΔ2-8 (NGF with residues 2-8 removed) and NGFΔ3-9 deletion mutants are almost as active as wild type NGF (Drinkwater *et al.*, 1993). These NGF structure-activity relationships in combination with the considerable species variability (mouse, human, guinea pig and snake) of the amino acid sequence of the NGF termini (McDonald *et al.*, 1991) are of potential value in understanding the NGF/TrkA interaction.

NGF exerts its biological activity as a non-covalent dimer (Treanor *et al.*, 1995; Burton *et al.*, 1995; McDonald *et al.*, 1991; Ibáñez *et al.*, 1993; Bothwell and Shooter, 1977). Two 118 residue NGF monomers are dimerized by hydrophobic and van der Waals interactions between their three anti-parallel pairs of β-strands; consequently, the amino terminus of one NGF monomer and the carboxyl terminus of the other are spatially juxtaposed (McDonald *et al.*, 1991). Furthermore, although a dimer has 2 pairs of termini, only one pair of termini is required for TrkA receptor recognition (Treanor *et al.*, 1995; Burton *et al.*, 1995). Accordingly, solving the conformation of the complex formed by the amino terminus of one monomer and the carboxyl terminus of the other in dimeric NGF is of fundamental relevance to understanding the interaction of NGF with TrkA.

The X-ray crystallographic 3-dimensional structure of a dimeric mouse NGF (mNGF) has been reported recently (McDonald *et al.*, 1991). However, within this structure, the amino terminus (residues 1-11) and the carboxyl terminus (residues 112-118) remain unresolved for both pairs of termini. High flexibility of the NGF termini makes it difficult to *experimentally* determine their bioactive conformations, particularly since transition metal ions commonly used in X-ray crystallography (McDonald *et al.*, 1991) have high affinity for His residues (Gregory *et al.*, 1993) which are present in the NGF amino terminus (Bradshaw *et al.*, 1994). Indeed, conformational alterations in the receptor binding domains of NGF caused by Zn^{2+} cations leading to its inactivation have been described recently (Ross *et al.*, 1997). Since the amino and carboxyl termini are crucial for NGF bioactivity as mediated via TrkA and because of the significance of NGF in multipl neurologic diseas processes, th determination of the

biologically active conformation of these terminini is an important and challenging problem for computational chemistry.

In contrast with NGF, little is known about the BDNF binding determinant for TrkB activation. Although there were several attempts to identify structural elements of BDNF that determine its receptor specificity (Ibáñez *et al.*, 1991, 1993, 1995; Suter *et al.*, 1992; Ilag *et al.*, 1994; Kullander and Ebendal, 1994; Urfer *et al.*, 1994; Lai *et al.*, 1996), the results of mutational experiments are still controversial. Thus, the reported importance of residues 40-49 (variable loop region II) for TrkB related activity of BDNF (Ibáñez *et al.*, 1991; Ilag *et al.*, 1994) has not been confirmed by recent studies (Lai *et al.*, 1996), in which it has also been shown that the key residues of the TrkB receptor binding domain of BDNF are situated between residues 80 and 109. The latter result is consistent with earlier observations that the BDNF termini are not involved in TrkB binding and that the key residues of the BDNF binding epitope are Arg^{81} and Gln^{84} (Ibáñez *et al.*, 1993). In addition, it has been found that receptor binding domains of BDNF and NT-3 are located in the same regions of the molecules, i.e. in their "waist" parts (Ibáñez *et al.*, 1993; Urfer *et al.*, 1994). As far as the NT-3 receptor binding domain is concerned, detailed mutational studies carried out by Urfer *et al.* (1994) revealed that it comprises a surface that includes major parts of the central β-strand stem, with the most important residues being Arg^{103}, Thr^{22}, Glu^{54}, Arg^{56}, Lys^{80} and Gln^{83}. These residues correspond to Arg^{104}, Thr^{21}, Glu^{55}, Lys^{57}, Arg^{81} and Gln^{84} of BDNF, respectively (McDonald *et al.*, 1991).

The location of the neurotrophin binding sites within the Trk receptors is the subject of debate (MacDonald and Meakin, 1996). Published data indicate the existence of two putative neurotrophin binding sites of Trk proteins: the "second immunoglobulin-like domain" (residues Trp^{299}-Asn^{365}, denoted IgC2) and the "second leucine-rich motif" (LRM-2A and LRM-2B, residues Thr^{97}-Leu^{120} of TrkA and TrkB, respectively) (Schneider and Schweiger, 1991; Kullander and Ebendal, 1994; Pérez *et al.*, 1995; Urfer *et al.*, 1995; Windisch *et al.*, 1995a, 1995b, 1995c; MacDonald and Meakin, 1996; Rydén and Ibáñez, 1996).

$p75^{NTR}$ belongs to a family of cell surface proteins that share a common pattern of four repeated cysteine-rich domains (CRDs) in the extracellular portion (Yan and Chao, 1991; Baldwin and Shooter, 1994). X-ray crystallographic studies on the extracellular portion of the related protein $p55^{TNFR}$ revealed that CRDs fold independently of each other, and three conserved disulfide bonds maintain a specific geometry of each CRD which consists of two loops (Banner *et al.*, 1993) (loops A and B, Fig. 1a). Very little is known about the $p75^{NTR}$ receptor functional epitope and, particularly, about residues directly participating in molecular recognition processes. All four CRD repeats of $p75^{NTR}$ are found to be required for binding, with the second CRD being most important (Baldwin and Shooter, 1995). Residues Tyr^{50} of

$p75^{NTR}$ seems to b ess ntial for NGF binding (Baldwin and Shooter, 1995).

The results of site-directed mutagenesis sugg st that the $p75^{NTR}$ receptor binding domains within n urotrophins are juxtaposed positively charged residues located in two adjacent hairpin loops which represent variable region I (residues 23-35) and V (residues 93-98) (Ibáñez *et al.*, 1992; Rydén *et al.*, 1995; Ibáñez, 1994; Ibáñez, 1995; Rydén and Ibáñez, 1996) (Fig. 1c). In NGF, residues Lys^{32}, Lys^{34}, and Lys^{95} have been found to be involved in $p75^{NTR}$ receptor binding, with Lys^{32} making the strongest contact, followed by Lys^{34} and Lys^{95}. In addition, some role of Asp^{30}, Glu^{35}, Arg^{103}, Arg^{100}, Lys^{88}, and Ile^{31} in $p75^{NTR}$ binding and biological activity has been demonstrated (Ibáñez *et al.*, 1992; Ibáñez, 1994). Two residues of variable region I, namely Arg^{31} and His^{33}, have been demonstrated to be essential for binding of NT-3 to $p75^{NTR}$, whereas similarly located Arg^{34} and Arg^{36} mediate binding of NT-4/5 (Rydén *et al.*, 1995). In contrast to NGF, a positively charged residue in variable region V is not critical for binding of NT-3 or NT-4/5 to $p75^{NTR}$ (Rydén *et al.*, 1995). In BDNF, however, only residues of variable region V, Lys^{95}, Lys^{96} and Arg^{97}, bind to $p75^{NTR}$ and compensate for the lack of positively charged residues in variable loop region I (Rydén *et al.*, 1995).

Therefore, it is an object of the invention to establish explicit atom-level models of the Trk and $p75^{NTR}$ recognition sites for neurotrophins.

It is a further object of the invention to provide atom-level models of the mechanism of interaction of neurotrophins and their receptors.

SUMMARY OF THE INVENTION

The inventors describe a method of characterizing the interaction between non-contiguous domains of a ligand and its receptor. The specific examples of the method described in detail below concern the interaction of nerve growth factor (NGF) with its TrkA receptor binding site, brain-derived neurotrophic factor (BDNF) with its TrkB receptor binding site, and the interaction of the neurotrophins (e.g., NGF, BDNF, NT-3, and NT-4/5) with the neurotrophin binding site of the common neurotrophin receptor $p75^{NTR}$.

In one aspect of the invention there is provided a variable basis Monte-Carlo (VBMC) simulated annealing method for identifying an optimal structure in a molecular system. The method comprises:

(a) providing a Markov chain with an initial basis set of N configurational variables which define a structure for said molecular system;

(b) translating the N configurational variables simultaneously along a basis vector to produce a new structure for the molecular system, wherein magnitude of translation is chosen randomly within a preselected range;

(c) calculating potential nergy of the new stat of the molecular syst m;

(d) deciding whether to accept or rej ct the new structure using an effective temperature dependent transition function, and if the new structure is accept d, replacing the current structure with the accepted structure;

(e) repeating steps (b) to (d), each repetition having a new basis vector, for a preselected first number of repetitions at a preselected upper temperature; then

(f) decreasing temperature according to a preselected cooling schedule;

(g) repeating steps (b) to (d) and (f), each repetition having a new basis vector, for a preselected second number of repetitions; then

(h) storing current structure of the molecular system;

(I) repeating steps (g) and (h) until a preselected number of stored structures have been accumulated; then

(j) rotating the basis set of configurational variables according to an effective distribution of the accumulated structures so that basis vectors are directed along low-energy valleys of a potential energy hypersurface thereby accelerating conformational motions and structural transitions of the molecular system, and erasing accumulated structures from steps (h) and (I);

(k) repeating steps (I) and (j) until, after an effective third number of repetitions, a preselected lower temperature limit is reached, thereby producing an unrefined global minimum structure; and

(l) refining the global energy minimum structure so that at least one local minimum on the potential energy hypersurface is identified.

The present invention also provides a method of identifying structures of a peptide domain of a neurotrophin to bind with a binding site of a receptor. The method comprises providing a plurality of neurotrophin analogues wherein at least one of neurotrophin analogue binds the receptor, identifying an optimal or near-optimal structure for respective peptide domains of the neurotrophin analogues that bind the receptor by applying a preselected number of the variable basis Monte-Carlo (VBMC) annealing simulations described above to each of the respective peptide domains to identify minimum or near-minimum energy structures for the peptide domains, and comparing said minimum or near-minimum energy structures to identify common structural features shared by neurotrophin analogues exhibiting receptor mediated activity.

The step of providing neurotrophin analogues may include providing wild-type neurotrophin analogues or mutants thereof.

The present invention also provides a method of identifying structures of a domain of a ligand to bind with a binding site of a receptor, comprising providing a plurality of ligand

analogues wherein at least on ligand analogu binds th receptor, identifying an optimal or near-optimal structure for respectiv domains of the ligand analogues that bind th receptor by applying a preselected numb r of the variable basis Monte-Carlo (VBMC) annealing simulations described above to each of the respective domains to identify minimum or near-minimum energy structures for the domains; and comparing said minimum or near-minimum energy structures to identify common structural features shared by ligands exhibiting receptor mediated activity.

As would be apparent to a person skilled in the art, methods of the present invention are not limited to neurotrophin-receptor interactions, but are applicable to the characterization of other ligand-receptor interactions. That is, an array of ligands that are either known to interact with a specific receptor or are candidate ligands that may potentially interact with this receptor may be computationally analyzed to identify optimal or near-optimal structures that provide the desired interaction. In some embodiments of the invention, the ligand may have a peptide domain, e.g., the ligand may be a peptide hormone, such as insulin, prolactin, or growth hormone. In some embodiments, the ligands or candidate ligands under study may be native ligands, mutants of native ligands, or isosteres of native ligands. They may be structurally different but have similar binding activity or functional effect(s). The optimal or near-optimal structure identified may act as an agonist or antagonist. "Isosteric" is an art-recognized term and, for purposes of this disclosure, a first moiety is "isosteric" to a second when they have similar molecular topography and functionality. This term should not, therefore, be restricted to mere similarity in chemical bond configuration. Two compounds may have different chemical bond configurations but nonetheless be isosteric due their 3-dimensional similarity of form and chemical nature, e.g. relevant centers such as heteroatoms are located in the same position, charges and/or dipoles are comparable, and the like.

The present invention provides a ligand for binding with TrkA, wherein TrkA comprises a leucine rich motif (LRM) comprising amino acid residues 93 to 117, the coordinates of the residues of said LRM given in Appendix 1, said LRM motif having five binding areas, area A comprising amino acid residue Phe^{105tA} capable of hydrophobic bonding, area B comprising residues Phe^{111tA}, Phe^{113tA}, and Thr^{114tA} capable of hydrophobic bonding, area C comprising residues Asp^{109tA} and His^{112tA} capable of ionic interaction, area D comprising residue Lys^{100tA} capable of ionic interaction, and area E comprising residues Asn^{95tA} to Ile^{98tA} capable of multiple parallel β-strand type hydrogen bonding. The ligand includes at least three moieties each comprising effective atomic elements having spatial occupancy, relative atomic position, bond type and charge to define a three dimensional conformation of said ligand so that a first moiety can bind with a first binding area, a second moiety can bind with a second binding

area, and a third moi ty can bind with a third binding area.

Put another way, the ligand comprises at least three moieties ffectively spaced relative to each other so that a first moiety can bind with a first binding area, a second moiety can bind with a second binding area, and a third moiety can bind with a third binding area.More specifically, the ligand comprises at least one moiety being capable of hydrophobic bonding and being present in an effective position in the ligand to hydrophobically bind to area A, at least one positively charged moiety being present in an effective position in said ligand to ionically bind to area C, and at least one negatively charged moiety being present in an effective position in said ligand to ionically bind to area D.

The present invention also provides a method of designing a ligand to bind with an LRM of TrkA. The method comprises providing a template of said LRM of TrkA, said LRM comprising amino acid residue sequence 93 to 117 inclusive, said amino acid residues having spatial Cartesian coordinates given in Appendix 1 wherein binding area A in the sequence comprises residue Phe^{105tA} capable of hydrophobic bonding, binding area B comprises residues Phe^{111tA}, Phe^{113tA}, Thr^{114tA} capable of hydrophobic bonding, binding area C comprises residues Asp^{109tA} and His^{112tA} capable of ionic interaction, binding area D comprises Lys^{100tA} capable of ionic interactions, and binding area E comprises residues Asn^{95tA} to Ile^{98tA} capable of multiple parallel β-strand type hydrogen bonding and computationally evolving a chemical ligand using any effective algorithm with preselected spatial constraints so that said evolved ligand comprises at least three effective moieties of suitable identity and spatially located relative to each other in the ligand so that a first of the moieties hydrophobically interacts with binding area A, a second of the moieties ionically interacts with binding area C, and a third of the moieties ionically interacts with binding area D of the LRM of TrkA. The algorithm may be a genetic algorithm and the LRM may be the second LRM of a plurality of LRMs.

The invention further provides a method of designing a ligand to bind with an LRM of TrkA, comprising providing a template of said LRM of TrkA, said LRM comprising amino acid residue sequence 93 to 117 inclusive, the amino acid residues having spatial Cartesian coordinates given in Appendix 1 wherein binding area A comprises Phe^{105tA} capable of hydrophobic bonding, binding area B comprises Phe^{111tA}, Phe^{113tA}, Thr^{114tA} capable of hydrophobic bonding, binding area C comprises Asp^{109tA} and His^{112tA} capable of ionic interaction, binding area D comprises Lys^{100tA} capable of ionic interaction, and binding area E comprises Asn^{95tA} to Ile^{98tA} capable of hydrogen bonding. The method comprises computationally evolving a ligand using an effective algorithm so that said evolved ligand comprises at least three effective moieties located relative to each other in the ligand so that a first moiety can bind with a first of the five binding areas, a second moiety can bind with a second of the five binding areas, and a third moiety can bind with a third of the binding areas.

In another aspect the invention provides a ligand for binding with TrkB, wherein TrkB comprises a leucine-rich motif (LRM) comprising amino acid residues 93 to 117, the coordinates of the residues of said LRM given in Appendix 2, said LRM having five binding areas, binding area F comprising amino acid residue Asp^{100B} capable of ionic interaction, binding area G comprising amino acid residue Lys^{109B} capable of ionic interaction, binding area H comprising amino acid residues Lys^{113B} capable of ionic interaction, binding area I comprising amino acid residue Arg^{94B} capable of ionic interaction, and binding area K comprising amino acid residue Lys^{104B} capable of hydrogen bonding or ionic interaction. The ligand comprises at least three moieties effectively spaced relative to each other so that a first moiety can bind with a first binding area, a second moiety can bind with a second binding area, and a third moiety can bind with a third binding area.

The present invention provides a method of designing a ligand to bind with TrkB, wherein TrkB comprises a leucine-rich motif (LRM) comprising amino acid residues 93 to 117, the coordinates of the residues of said LRM given in Appendix 2, said LRM having five binding areas, binding area F comprising amino acid residue Asp^{100B} capable of ionic interaction, binding area G comprising amino acid residue Lys^{109B} capable of ionic interaction, binding area H comprising amino acid residue Lys^{113B} capable of ionic interaction, binding area I comprising amino acid residue Arg^{94B} capable of ionic interaction, and binding area K comprising amino acid residue Lys^{104B} capable of hydrogen bonding or ionic interaction. The method comprises computationally evolving a ligand using an effective algorithm so that the evolved ligand comprises at least three effective moieties located relative to each other in the ligand so that a first moiety can bind with a first of said five binding areas, a second moiety can bind with a second of said five binding areas, and a third moiety can bind with a third of the binding areas. The algorithm may be a genetic algorithm.

The invention also provides a ligand for binding with the common neurotrophin receptor $p75^{NTR}$, wherein $p75^{NTR}$ comprises a binding site including amino acid residues Cys^{39p} to Cys^{94p} inclusive, said residues of said binding site having spatial coordinates given in Appendix 3, said binding site having three binding areas including binding loop 2A comprising region Cys^{39p} to Cys^{58p} capable of attractive electrostatic interactions, binding loop 2B comprising region Cys^{58p} to Cys^{79p} capable of attractive electrostatic interactions, and binding loop 3A comprising region Cys^{79p} to Cys^{94p} capable of attractive electrostatic interactions. The ligand comprises at least two moieties effectively spaced relative to each other so that a first moiety can bind to a first loop and a second moiety can bind to a second loop.

The present invention also provides a method of designing a ligand for binding with the common neurotrophin receptor $p75^{NTR}$, wherein $p75^{NTR}$ comprises a binding site including amino acid residues Cys^{39p} to Cys^{94p} inclusive. The residues of the binding site have spatial

coordinates giv n in Appendix 3. The binding site has three binding areas including binding loop 2A comprising region Cys^{39p} to Cys^{58p} capabl of attractive lectrostatic interaction, binding loop 2B comprising region Cys^{58p} to Cys^{79p} capable of attractive lectrostatic interaction, and binding loop 3A comprising region Cys^{79p} to Cys^{94p} capable of attractive electrostatic interaction. The method comprises computationally evolving a ligand using an effective algorithm so that the evolved ligand comprises at least two effective moieties located relative to each other in the ligand so that a first moiety can bind to a first of the three loops and a second moiety can bind to a second loop of the three loops.

The invention provides a method of identifying a ligand to bind with a leucine rich motif (LRM) of TrkA. The method comprises providing a three dimensional conformation for the LRM. The LRM comprises amino acid residue sequence 93 to 117 inclusive, the amino acid residues having spatial Cartesian coordinates given in Appendix 1. The LRM has five binding areas, area A comprising amino acid residue Phe^{105tA} capable of hydrophobic interaction, area B comprising amino acid residues Phe^{111tA}, Phe^{113tA}, and Thr^{114tA} capable of hydrophobic interaction, area C comprising amino acid residues Asp^{109tA} and His^{112tA} capable of ionic interaction, area D comprising amino acid residue Lys^{100tA} capable of ionic interaction, and area E comprising Asn^{85tA} to Ile^{98tA} capable of multiple parallel β-strand type hydrogen bonding. The method includes providing a data base containing molecules coded for spatial occupancy, relative atomic position, bond type and/or charge; and screening the data base to select those molecules comprising moieties having a three dimensional conformation and effective charge that can bind with at least three of the five binding areas.

The invention provides a method of identifying a ligand to bind with a leucine rich motif (LRM) of TrkB. The method comprises providing a three dimensional conformation for the LRM. The LRM comprises amino acid residues 93 to 117, the coordinates of the residues of the LRM are given in Appendix 2, the LRM having five binding areas, binding area F comprising amino acid residue Asp^{100tB} capable of ionic interaction, binding area G comprising amino acid residue Lys^{109tB} capable of ionic interaction, binding area H comprising amino acid residue Lys^{113tB} capable of ionic interaction, binding area I comprising amino acid residue Arg^{94tB} capable of ionic interaction, and binding area K comprising amino acid residue Lys^{104tB} capable of hydrogen bonding or ionic interaction. The method includes providing a data base containing molecules coded for spatial occupancy, relative atomic position, bond type and/or charge; and screening the data base to select those molecules comprising moieties having a three dimensional conformation and effective charge that can bind with at least three of the five binding areas.

The present invention also provides a method of identifying a ligand to bind with common neurotrophin receptor $p75^{NTR}$. The method comprises providing a three dimensional

conformation for the common n urotrophin receptor $p75^{NTR}$, wh rein $p75^{NTR}$ compris s a binding site including amino acid residues Cys^{39p} to Cys^{94p} inclusive. The residues of th binding site have spatial coordinates giv n in Appendix 3, the binding sit having three binding areas including binding loop 2A comprising region Cys^{39p} to Cys^{58p} capable of attractive electrostatic interaction, binding loop 2B comprising region Cys^{58p} to Cys^{79p} capable of attractive electrostatic interaction, and binding loop 3A comprising region Cys^{79p} to Cys^{94p} capable of attractive electrostatic interaction. The method includes providing a data base containing molecules coded for spatial occupancy, relative atomic position, bond type and/or charge; and screening the data base to select those molecules comprising moieties that can bind with at least two of the three binding loops.

In one aspect of the invention, a ligand (e.g., small molecule) designed to interact with a receptor such as Trk or p75NTR may be bifunctional, such that a first portion of the ligand binds to one receptor monomer and a second portion of the ligand binds to a second receptor monomer. Thus, a receptor dimer is effectively cross-linked by the interaction of ligand with both receptor monomers.

According to the invention, detailed information is provided regarding those amino acid residues of neurotrophins and of neutrophin receptors which are involved in neurotrophin-receptor binding. Such information includes the bioactive conformations of the respective peptide domains of the neurotrophins and receptors. This in turn permits the design of small molecules which interact with said amino acid residues or domains. Where such interaction block the residues or changes the conformation of the domain, the small molecule can inhibit neurotrophin-receptor binding, in certain cases abolishing it completely. As would be appreciated by a person skilled in the art, small molecule design according to this aspect of the invention is applicable to other ligand-receptor interactions in addition to neurotrophins, according to the methods disclosed herein.

As a person skilled in the art would appreciate, the invention not only provides molecules (ligands) that interact with receptors, but also molecules which, in their mimicry of a receptor's bioactive conformation, can bind to the receptor binding site of a ligand such as, for example, a neurotrophin. Such molecules, whether they interact with ligand or with receptor, can block native ligand-receptor interaction. In some embodiments of the invention, a small molecule which binds to a receptor may even trigger signal transduction similar to that of the native ligand, i.e., act as an agonist.

BRIEF DESCRIPTION OF THE DRAWINGS

The invention will be described, by example only, reference being had to the accompanying drawings, in which:

Figure 1 shows the amino acid sequences of the conformationally variable termini of the dimeric NGF analogues under study. The residues are numbered from 1 to 118 for the first monomer, and from 1' to 118' for the second monomer. The fixed parts of the proteins simulated by the X-ray geometry of mouse NGF (McDonald *et al.*, 1991) are underlined.

Figure 2 shows the structure of the complex of the amino and carboxyl termini of (1-118)hNGF homodimer. The carboxyl terminus is shown in grey, the amino terminus in white, and the interacting conservative region $His^{75'}$ -$Asn^{77'}$ of the "south" part of the NGF dimer, in black.

Figure 3 shows the structure of the complex of the amino and carboxyl termini of (1-118)mNGF homodimer.

Figure 4 shows the structure of the complex of the amino and carboxyl termini of dimeric mNGFΔ3-9 molecule.

Figure 5 shows the structure of the complex of the amino and carboxyl termini of dimeric hNGF-H4D molecule.

Figure 6 shows the structure of the complex of the amino and carboxyl termini of dimeric mNGFΔ1-8 molecule.

Figure 7 shows the structure of the complex of the amino and carboxyl termini of BDNF homodimer.

Figure 8 illustrates the TrkA leucine-rich motifs. Locations of parallel β-strands are illustrated by the shaded areas designated by symbol β. Fragments B1-B4 demonstrate NGF binding affinity, while N1-N4 do not (Windisch *et al.*, 1995a, 1995b).

Figure 9 shows sequences of the amino and carboxyl termini of fully active NGF analogues. Regions with rigid structures are underlined.

Figure 10 shows the predicted bioactive conformation of the NGF binding domain (a) and the structures of the NGF/LRM-2A complexes of hNGF (b), mNGF (c), mNGFΔ3-9 (d), and hNGF:NT-4/5 (e). Only residues essential for discussion are designated. A, B, C, D and E represent specific NGF/LRM-2A binding areas. The LRM-2A is illustrated in grey, NGF in white.

Figure 11 shows the TrkB receptor binding site of BDNF (a), predicted features of the BDNF/LRM-2B complex (b), and geometry of the "improper" NGF/LRM-2B complex (c). Only residues essential for discussion are designated. F, G, H, I and K represent specific BDNF/LRM-2B binding areas. The LRM-2B is illustrated in grey, BDNF and NGF in white.

Figure 12 is a d tail of th LRM-2A conformation when bound to hNGF. The three groups of the β-strand involv d in H-bonding with th parallel β-strand motif of the NGF analogues are designat d by NH or CO. Hydrophobic residues are illustrated as light, polar uncharged as dark, charged as black.

Figure 13 presents principal residues of the NGF binding domain essential for TrkA receptor recognition. Conserved residues of NGF molecules among all characterized species (McDonald *et al.*, 1991) are designated by X, whereas those which are substituted in NGF molecules derived from different species by similar amino acids and NGF residues maintaining the bioactive conformation or interacting with specific binding areas A-E of the LRM-2A are indicated by X.

Figure 14 presents principal residues of the LRM-2A. The residues which are specific for TrkA (Windisch *et al.*, 1995a, 1995b) and critical for the present model are designated by X and X, respectively.

Figure 15 is a schematic representation of the second leucine-rich motif of TrkA (residues 93tA to 116tA) (a) and TrkB (residues 93tB to 116tB) (b) as specific binding sites for NGF and BDNF, respectively. General consensus residues are shaded. Arrows designate distinct positions essential for molecular recognition processes.

Figure 16 represents the X-ray crystallography-derived geometry of the α-carbon trace of the two loops (2A and 2B) of the second cysteine-rich domain (white bonds) and the first loop (3A) of the third cysteine-rich domain (grey bonds) of $p55^{TNFR}$ (Banner *et al.*, 1993) (a), the preferred geometry of the α-carbon trace of the corresponding fragment of $p75^{NTR}$ (b), and the predicted bioactive conformation of mouse NGF (McDonald *et al.*, 1991); (c). White and grey bonds in panel (c) illustrate different protomers. The $p75^{NTR}$ binding determinant of NGF (loops I and V) is denoted. Disulfide bonds are shown in black.

Figure 17 shows the sequence of a putative binding site for neurotrophins within $p75^{NTR}$ aligned with the corresponding sequence of homologous $p55^{TNFR}$. Conserved pattern of disulfide bonds is illustrated. Abbreviation (h) stands for human (Johnson *et al.*, 1986), (r) for rat (Radeke *et al.*, 1987), and (c) for chicken (Large *et al.*, 1989) $p75^{NTR}$.

Figure 18 illustrates the most stable geometries of the complexes of the neurotrophins with the common neurotrophin receptor $p75^{NTR}$: with NGF (a); with BDNF (b); with NT-3 (c); with NT-4/5 (d). The α-carbon traces of the neurotrophins are shown in white, while that of the $p75^{NTR}$ binding site is shown in grey. Disulfide bonds are illustrated in black. Only residues mentioned in the text are denoted.

Figure 19 demonstrates geometric compatibility of the van der Waals surfaces of BDNF (light) and the $p75^{NTR}$ binding site (dark).

Figure 20 illustrates conformational changes of the $p75^{NTR}$ binding site upon BDNF

binding. Conformation of the $p75^{NTR}$ receptor binding site before binding is illustrated in white, after binding in grey. The two conformations have been superimposed using the equilibrium positions of the reference α-carbon atoms located in loops 2A and 3A. Straight lines denote linear approximations of the conformations of the α-carbon traces of loop 2B in both structures.

DETAILED DESCRIPTION OF THE INVENTION

PART A

THEORETICAL STUDIES OF THE BIOACTIVE CONFORMATION OF NERVE GROWTH FACTOR USING VBMC - A NOVEL VARIABLE BASIS MONTE-CARLO SIMULATED ANNEALING ALGORITHM FOR PEPTIDES

BACKGROUND TO THE VBMC ALGORITHM

The structural optimization of the peptide domains under study required a rigorous search of conformational space. As with other theoretical peptide studies, such calculations are plagued by a multiple-minima problem (Gibson and Scheraga, 1988) which traditionally is addressed using either molecular dynamics, Monte Carlo approaches or other algorithms. The Monte Carlo method, although exceedingly powerful, is limited by the excessive CPU time requirements on existing computers. To remedy this problem, we have devised a novel Variable Basis Monte Carlo simulated annealing algorithm for peptides (VBMC).

The potential energy hypersurface of a peptide has an enormous number of local minima (Gibson and Scheraga, 1988; Piela *et al.*, 1989, 1994), but usually only the global energy minimum structure is required. Despite efforts to elaborate an efficient method of global energy minimization (Gibson and Scheraga, 1988; Judson *et al.*, 1994), the multiple-minima problem is far from being solved. Although simulated annealing (Kirkpatrick *et al.*, 1983; Vanderbilt *et al.*, 1984) is mathematically correct and guarantees convergence to the global minimum in principle, the suggested "cooling" schedule appears to be far too slow for practical purposes, and faster "cooling" has to be used (Gidas, 1985; Kushner, 1987). Within the simulated annealing approach, thermal molecular motion can be simulated either by Monte Carlo (Kirkpatrick *et al.*, 1983; Nayeem *et al.*, 1991; Wilson *et al.*, 1988; Snow, 1992; Shamovsky *et al.*, 1992) or molecular dynamics (Lelj *et al.*, 1991; Villani and Tamburro, 1994) methods.

The major problem of the Monte Carlo technique is that motion of a molecular system along a Markov chain is very slow (Piela *et al.*, 1994; Scheraga, 1989; Nayeem *et al.*, 1991). On the other hand, the Monte Carlo technique has several considerable advantages over

molecular dynamics. First, it does not require calculating forces. Second, potential energy functions do not have to be continuous. Third, much larger steps in conformational space can be utilized (Li and Scheraga, 1988; Kincaid and Scheraga, 1982). Fourth, the additional iterative self-consistent SHAKE routine (Ryckaert *et al.*, 1977), which is used in molecular dynamics simulations to deal with holonomic constraints (Brooks III and Case, 1993), is not required in the Monte Carlo method. This has led to efforts to accelerate configurational motion within the Monte Carlo approach (Raj *et al.*, 1994; Snow, 1992; Kincaid and Scheraga, 1982; Rao *et al.*, 1979; Rossky *et al.*, 1978). The main reason for inefficiency with the conventional Monte Carlo method (Metropolis *et al.*, 1953) is a slow and cumbersome sequential change of configurational variables.

To overcome these problems, lessons can be learned from molecular dynamics. In molecular dynamics (Allen and Tildesley, 1987) configurational variables move simultaneously, and the soft modes of the system explicitly direct these motions. Soft modes are defined as low-energy valleys on the potential energy hypersurface. Although there have been attempts to direct Monte Carlo configurational motion along the soft modes (Raj *et al.*, 1994; Rao *et al.*, 1979; Rossky *et al.*, 1978), these improvements require calculating forces and, consequently, result in losing the main advantages of the Monte Carlo approach. An algorithm which would retain the advantages of the Monte Carlo method and direct configurational changes along the soft modes is thus required. One possible solution has recently been suggested (Szentpaly *et al.*, 1994).

The classical Monte Carlo-Metropolis method (Metropolis *et al.*, 1953) consists of modelling a Markov chain containing subsequent conformations of the molecule under study: x_0, x_1, x_2,..., x_i,..., where x ($x_i = \{x_i^1 \ldots x_i^m \ldots x_i^N\}$) is the vector of independent structural parameters. Each vector x_{i+1} is derived from the preceding one, x_i, by means of a random change of one randomly chosen variable:

$$x_{i+1}^m = x_i^m + \lambda_m \cdot \xi \qquad (1)$$

where ξ is a random quantity from the interval (-1,1) and λ_m is a maximal allowed increment of the given variable. N moves of the Markov chain (where N is the number of independent parameters) represent a Monte Carlo step. Whether the new state x_{i+1} is accepted or rejected is decided according to a transition probability function. The following functional form of transition probability is used in the present expression (2) (Gunningham and Meijer, 1976):

$$W(x_i \Rightarrow x_{i+1}) = 1/[1 + \exp(\Delta E_i / kT)] \qquad (2)$$

where ΔE_i is the difference between conformational energies of the states x_{i+1} and x_i, k is the Boltzmann constant and T is absolute temperature.

Those skilled in the art will appreciate that other functional forms of transition functions may be used to screen state a new state x_{i+1}. For example, another effective temperature dependent transition function for screening a new state x_{i+1} derived from a previous state x_i is given by:

$$W(x_i \Rightarrow x_{i+1}) = 1, \qquad \text{if } E(x_{i+1}) \leq E(W(x_i))$$

$$= \exp(-\Delta E_i / kT), \qquad \text{if } E(x_{i+1}) \geq E(W(x_i))$$

where ΔE_i is the difference between conformational energies of the states x_{i+1} and x_i, k is the Boltzmann constant and T is absolute temperature.

The direct application of this conventional Monte Carlo technique to the conformational space study of protein structure is not efficient because the conformational variables of peptide chains appear to be mutually dependent, i.e., low-energy conformational motions involve several conformational variables. When applied to molecular systems such as protein secondary, tertiary or quaternary structure, equation (1), in which structural parameters are sequentially changed one after another, results in very small values of ξ and, consequently, in a very slow conformational motion (Piela *et al.*, 1994; Scheraga, 1989; Nayeem *et al.*, 1991). In order to model a *simultaneous* change of the structural parameters, we have used Eq.(3) (instead of the conventional (1)),

$$x_{i+1} = x_i + \lambda_m \cdot \xi \cdot g^m \qquad (3)$$

where g^m is a randomly or sequentially chosen *basis vector* from a basis $G=\{g^m\}$, ξ is a random quantity from an interval (-1,1) and λ_m is a maximal acceptable move in direction g^m. In this study λ_m was constant and equal to 10°.

A basis G is formed from linear combinations of independent conformational parameters x for their change to be realized *along the soft modes* of the molecule. These modes are revealed by dispersion analysis of the distribution of the sequential configurational points of the Markov chain. The soft modes of the molecular system are to be directed along the axes of the dispersion ellipsoid because they should correspond to the directions of maximal deviations made by the independent variables during a certain period of simulation. Initially, basis G coincides with a unit matrix, i.e., G = I, and Eq.(3) is equivalent to (1). The rotation of basis G is carried out after every 150 Monte Carlo steps based on the particular scattering of the previous 150 configurations x. Basis vectors g^m are made equal to the eigenvectors of the covariant matrix D which has the following elements:

$$d_{ij} = (1/M) \cdot \sum_{n=1}^{M} (x_n^i - (1/M) \cdot \sum_{n=1}^{M} x_n^i) \cdot (x_n^j - (1/M) \cdot \sum_{n=1}^{M} x_n^j) \quad (4)$$

where M is the number of points in the distribution (M=150), and x_n^i is the i-th structural parameter at the n-th Monte Carlo step. Vectors $\mathbf{g}^m$ form the orthonormalized basis and are used in the Markov chain instead of independent conformational parameters. Periodic rotations of basis G in Monte Carlo simulations result in a simultaneous change of all the conformational variables along the valleys of a potential energy surface, which considerably accelerates conformational motions and transitions (Szentpaly *et al.*, 1994).

The method disclosed herein is highly advantageous over known processes for several reasons. In the present process the preselected range from which the magnitude of translation is chosen is constant and does not depend on the basis set. Thus the present method is much more efficient than previous methods in part because the magnitude of translation along the basis vector is limited by a preselected range. The present method is also more efficient because rotation of the basis set of configurational variables is avoided at the upper temperatures and is implemented only at the lower temperatures.

IMPLEMENTATION OF THE VBMC ALGORITHM

VBMC was written in Fortran-77. The algorithm was then interfaced with the CHARMM force field (Brooks *et al.*, 1983; The force field parameters are extracted from CHARMM release 23.1, Molecular Simulations, Inc., Waltham, MA). Torsional distortion, van der Waals and electrostatic interactions, and hydrogen bonding were thus explicitly considered. The united atom approach was used for all carbons with non-polar hydrogens. Point atomic charges of Weiner *et al.* (Weiner *et al.*, 1984) were used. A dielectric constant equal to the interatomic separation in angstroms was utilized to implicitly simulate solvation effects (Weiner *et al.*, 1984). All calculations were performed on an 8-node IBM Scalable POWERparallel 2 [SP2] high performance computer at Queen's University, Kingston, Canada. Each Monte Carlo simulated annealing computation required up to 120 hours of CPU time.

Appendix 4 is attached. Appendix 4 is a computer program written in Fortran-77 and is a non-limiting example of a program used to perform the VBMC simulated annealing method in accordance with the present invention.

Each run of the VBMC algorithm provides a unique final structure which would represent the global energy minimum structure, regardless of the initial geometry, if the "cooling" was performed infinitely slowly. However, since this is impossible, several Monte Carlo simulated annealing computations must be performed from different starting points x_0, using different initial temperatures T_0, "cooling" schedules and random sequences. An initial temperature of 1000° K is sufficient. The Markov chain is kept at a constant temperature T_0

for 10^4 Monte Carlo steps before the initiation of "cooling". The temperature T is then decreased at v ry Monte Carlo move (3) by a small increment such that aft r $2 \cdot 10^4$ Monte Carlo steps it reach s 120° K producing an unrefined global energy minimum structure.

The global energy minimum structure is then refined to identify the nearest local minimum or stationary point on the potential energy hypersurface. Refinement may be accomplished using any one of several non-linear minimization routines to identify the local minimum on the potential energy hypersurface. For example, gradient descent minimization and conjugate gradient minimization may be used. Quasi-Newton minimization methods such as the Newton-Raphson method may also be used. Other non-linear methods include the Marquardt method, the Powell method and a variable metric method. Those skilled in the art will be aware of the various non-linear routines which may be used for refinement and those mentioned herein are more fully described in *Nonlinear Programming: Theory, Algorithms, and Applications.* 1983. New York: John Wiley & Sons.

APPLYING VBMC TO NGF

The aim of this computational study was to ascertain the biologically active conformation of the TrkA receptor binding determinant of NGF. A comprehensive review of the literature identified an initial study set of 17 proteins which have been assessed for TrkA mediated activity using comparable experimental methods. From these 17 analogues, a subset of six (three active and three inactive) which reflects the range of structural diversity was selected for preliminary study. Accordingly, in the present invention the low-energy conformations of the amino and carboxyl termini of six NGF analogues were obtained by means of Monte Carlo simulated annealing calculations. Three of these analogues retain full TrkA mediated activity: human NGF (hNGF; Shih *et al.*, 1994; Burton *et al.*, 1992), mouse NGF (mNGF; Burton *et al.*, 1992; Drinkwater *et al.*, 1993), and mNGFΔ3-9 (deletion 3-9 of mNGF; Drinkwater *et al.*, 1993). The other three analogues are biologically inactive: hNGF-H4D (a point mutation of hNGF in which His [H] in position 4 is replaced by Asp [D]; Shih *et al.*, 1994), mNGFΔ1-8 (Burton *et al.*, 1992; Drinkwater *et al.*, 1993; Taylor *et al.*, 1991) and BDNF (Suter *et al.*, 1992). The results and conclusions obtained from these six analogues were then validated by being applied to the remaining 11 analogues of the initial study set.

The amino acid sequences of the termini of the neurotrophin molecules under study are presented in Figure 1. Residues are numbered from 1 to 118 for the first monomer, and from 1' to 118' for the second monomer. The mutual orientation of the termini of the different monomers is determined by the disulfide bonds Cys^{15} - Cys^{80} and $Cys^{68'}$ - $Cys^{110'}$ and hydrophobic interactions Val^{14} :$Val^{14'}$ and Val^{109} :$Val^{109'}$, which are absolutely conserved in all neurotrophins (McDonald *t al.*, 1991). The conformational space of the peptide molecules

consists of flexible torsional angles determining geometry of the amino terminus of one monomer and the carboxyl terminus of the other, while keeping the rest of the dimer fixed in the known geometry of mNGF (McDonald *et al.*, 1991). Covalent bond lengths and bond angles of the termini are kept fixed. The geometry of each residue is determined only by flexible torsional angles of the peptide backbone (ϕ and ψ) and the side chain (χ_1, χ_2,...). All torsional angles of amino acid Pro except for ψ are fixed. Torsional angles describing structural motifs with the essentially planar geometry (such as peptide bonds or conjugated regions in side chains) are kept fixed. Likewise, the configurations of the sp^3-carbons are fixed. With these constraints, the total conformational space of the flexible termini of hNGF, mNGF and BDNF consists of 74, 73 and 67 variables, respectively.

RESULTS AND DISCUSSION

By diagonalizing the covariant matrix in the framework of the VBMC algorithm, rigid modes of a molecular system, which should slow down conformational changes, are supposed to be revealed simultaneously with soft modes of the system. To test the efficiency of the VBMC algorithm, its performance was compared with the conventional Monte-Carlo method at the equilibrium parts of the Markov chains generated at different constant temperatures. These comparisons showed that at high temperatures (700^0-1000^0K) the basis variability results in decreasing acceptance rates. On the other hand, the temperature decrease reinforces the advantage of the VBMC approach, and at temperatures below 600^0 acceptance rates of the VBMC Markov chains were significantly higher. Thus, at T=300^0 K the acceptance rate of the conventional Markov chain was found to be 0.22, which is very close to that recommended by Kincaid and Scheraga (1982) as optimal (0.20). The acceptance rate of the VBMC algorithm obtained at the same conditions was 0.26, i.e. 18% higher. These evaluations are in agreement with what one would expect. Indeed, at low temperatures only soft modes of molecules are involved in thermal motions, hence, they are especially populated in corresponding Monte-Carlo generated conformational ensembles and can be revealed from them. Higher acceptance rates of the low temperature VBMC Markov chains over conventional Markov chains mean that the average increase of the sizes of the Monte-Carlo moves along soft modes of the system are higher than their decrease along the rigid modes. Thus, the VBMC disclosed herein for evaluating peptide conformations not only changes directions of the Monte-Carlo moves, but also accelerates conformational changes by directing them along the soft modes of the molecule. Consequently, the present VBMC algorithm is more efficient than conventional Monte-Carlo method only at moderate and low temperatures, when thermal motions tend to take place along the valleys of the potential energy surface. This particular temperature region causes serious problems in known simulated annealing algorithms, and the VBMC method disclosed herein provides a solution

to these probl ms.

S v n independent VBMC simulations for each of the six molecular syst ms und r study were p rform d. Simultaneously, local nergy refinem nts were periodically carried out from a number of points generat d during th "slow cooling" stage. All local minimizations resulted in higher energy stationary points on the potential energy surface than those produced by VBMC computations. This means that the VBMC technique as an approach to global minimization cannot be replaced by relatively inexpensive periodic energy refinements from the high-temperature conformational space; at high temperatures only high-energy conformers are sufficiently populated. Although VBMC runs did not converge to the same conformation, the final structures differed insignificantly; i.e., the peptide backbone conformation remained unchanged but there were limited differences in the side chain torsional angles. Multiple VBMC simulations identified rigid and flexible parts of the molecules. Minimum energy structures of all molecules are displayed in Figures 2-7 while Table 1 presents optimized conformational parameters of the amino and carboxyl termini of the considered NGF analogues.

GEOMETRIC SIMILARITY OF BIOACTIVE NGF CONFORMERS

Rigid regions of hNGF and mNGF which maintain the same conformation in all independent VBMC simulations are formed by residues 9-11 and 112'-118', creating a richly hydrogen bonded (H-bonded) 3-dimensional complex. Conformational variability within this rigid zone is primarily restricted to side chains and does not affect the geometry of the backbone. An interesting example of such side chain mobility occurs with $Arg^{114'}$, which is H-bonded to the carbonyl oxygen of the ninth amino acid of the amino terminus and which is therefore expected to have a fixed conformation. Nevertheless, $Arg^{114'}$ has two distinct conformers in which the H-bonding is realized by the hydrogen atoms attached to the different NH_2 groups, with the energy difference being about 1 kcal/mol. In addition to local conformational variability, hNGF and mNGF have a region of "cooperative" flexibility which is made up of residues 1-8. Several distinct conformations exist within this region, with its conformational variability being caused by a number of possibilities for the H-bond network formed by residues 1-3.

Comparison of the most stable conformers of hNGF (Figure 2) and mNGF (Figure 3) reveals striking conformational similarity between their rigid regions in spite of several differences in the primary structure of the amino and carboxyl termini (Figure 1). As shown in Table 1, both termini have the same conformation, except for the variable region consisting of residues 1-3. The most stable H-bond networks in this area differ considerably because of the mT3hS substitution.

The essential difference between the amino acid sequences of the termini of hNGF

and mNGF is the mM9hR substitution, which does not change the geometry of the rigid region. Residues Met and Arg have different side chain types, i.e., the former is non-polar while the latter is polar and positively charged under physiological conditions. It is surprising that this substitution does not affect geometry since it introduces the positive charge of Arg^9 which is located in an electrostatic field created by at least five neighbouring charged functional groups. Conformational stability of the rigid region of hNGF is maintained by the exact fit of the Arg^9 side chain into a "hollow" in the rigid region, which is occupied by the Met^9 side chain in mNGF. Furthermore, the Arg^9 side chain, being in this "hollow", forms two additional interchain H-bonds with carbonyl oxygens of residues Val^{117} and Arg^{118}. This further stabilizes the rigid region of hNGF.

The physical reason for the geometric similarity of the rigid regions of hNGF and mNGF is that the structural features of these two complexes are determined by similar H-bonding and electrostatic interactions. The major stabilizing factor is the H-bonding and electrostatic interaction of charged side chains of residues Glu^{11} and Arg^{118}. In addition, these side chains are involved in other H-bonding: the carboxyl oxygens of Glu^{11} are bonded to the δ-NH group of His^8, the hydroxyl group of Ser^{113} and the backbone NH group of Lys^{115}; the side chain NH and NH_2 groups of Arg^{118} are bonded to the backbone Phe^7 and Lys^{115} carbonyl groups. There are some other common interchain H-bonds in hNGF and mNGF. The ε-amino group of the Lys^{115} side chain forms a H-bond with the δ-carbonyl oxygen of the Asn^{77} residue, situated at the "south" part of NGF structure (McDonald *et al.*, 1991).

In addition to H-bonding, the particular geometry of the rigid region in both molecules is also maintained by electrostatic interactions of positively charged residues, specifically His^4, His^8, Arg^{114}, Arg^{118} and His^{75}. An electrostatic repulsion between His^4 and boundary residues His^8 and Arg^{118} of the rigid region forces His^4 to be located as far as possible from the rigid region, separating the 1-8 loop from the rest of the structure. This tendency is further reinforced in hNGF by the presence of a third positively charged boundary residue Arg^9. The His^{75} amino acid located in the "south" part of NGF also participates in maintaining the structure of the rigid region. An electrostatic repulsion between His^{75} and Arg^{114} prevents H-bonding of the amino group of Arg^{114} with the Asn^{77} side chain and the Ser^{113} backbone: indeed, removing the ε-proton from His^{75} results in two H-bond contacts which change the global energy minimum structure of the complex.

The separation of flexible loop 1-8 from the rigid region is also determined by residue Pro^5. This amino acid imposes restrictions on conformational motion of the loop, making it "bent" at this particular point, and thereby defining the location of the adjacent His^4 residue at the most distant point from the rigid region. Thus, residues His^4 and Pro^5 are primarily responsible for the separation of the flexible loop from the rigid region.

Although mNGFΔ3-9 does not have the flexible loop, the energy optimized g ometric f atures of its t rmini are very similar to those of the hNGF and mNGF rigid regions (Table 1, Figures 2-4). There are only two structural lem nts which are specific for the rigid region of mNGFΔ3-9. First, although Arg^{118} has a different conformation, the result is functionally the same, namely both NH_2 groups of the Arg^{118} side chain are H-bonded to the Glu^{11} side chain. In addition, the ε-NH group of Arg^{118}, which is H-bonded to the Phe^{7} carbonyl group of the flexible loop in both hNGF and mNGF, faces the carbonyl terminus in mNGFΔ3-9. Second, the "hollow", which is occupied by the ninth amino acid side chain in hNGF and mNGF, is now filled with the protein backbone of the remainder of the loop, i.e., residues 1-2. Functionally, the structure of the rigid region of mNGFΔ3-9 resembles that of hNGF because of the stabilizing interchain H-bond contacts of the moieties located in the "hollow".

GEOMETRIC DISTINCTION OF NGF ANALOGUES INACTIVE FOR TrkA BINDING

The energy minimum structures of the complexes formed by the amino and carboxyl termini of molecules, hNGF-H4D, mNGFΔ1-8 and BDNF, which are inactive with respect to TrkA binding, do not possess the common structural features found in active molecules. Point mutation H4D in hNGF incorporates negative instead of positive charge into the 1-8 loop. As a result of this mutation, the loop is no longer separated from the rigid region, forming a united complex instead (Figure 5). In this complex the negatively charged carboxyl group of Asp^{4} is surrounded by four positively charged NH_2 groups of Arg^{9} and Arg^{114}, and residue His^{8} is not H-bonded to the Glu^{11} carboxyl group. Thus, because of the H4D point mutation, the common structural features inherent in hNGF and mNGF are lost from hNGF-H4D.

Deletion 1-8 also changes dramatically the most stable structure of the rigid region of mNGF (Figure 6). The newly created positively charged amino terminus is located between negatively charged carboxyl groups of Glu^{11} and Arg^{118}, with charged side chains of Arg^{114}, Lys^{115} and Arg^{116} being substantially shifted from their preferred positions in active molecules. Thus, the electrostatic field caused by the positive charge of the new amino terminus in mNGFΔ1-8, located in the vicinity of the carboxyl group of Glu^{11}, is responsible for the destruction of the geometry of the rigid region inherent in the active molecules.

The complex formed by the amino and carboxyl termini of BDNF is also significantly different from those formed by the molecules active for TrkA binding (Figure 7, Table 1). There are several reasons for the considerable conformational changes in BDNF. First, negatively charged residue Asp^{5} eliminates the separation of the flexible loop from the rigid region, and interacts with the positively charged His^{3}, Arg^{9} and amino terminus. Second, because of its long tail, Arg^{8} is unable to form the H-bond contact with the Glu^{11} side chain and forms bifurcated H-bonds with the carbonyl group of Gly^{10}. Third, Arg^{116} is H-bonded to

Glu^{65} located in the "south" part of the molecule, which imposes a specific restriction on conformational possibilities of the carboxyl terminus of BDNF.

EXPLANATION FOR THE OBSERVED STRUCTURE-ACTIVITY RELATIONSHIPS

The principal result of the molecular simulations presented is that the NGF molecules with full TrkA mediated activity considered in this study have regions with similar 3-dimensional structure, whereas in all inactive analogues, the geometry of this region is altered, mainly by novel electrostatic interactions. It is therefore reasonable to attribute the TrkA mediated activity to a specific conformation of this particular region. The amino and carboxyl terminal regions therefore represent a "functional epitope" which contains relatively few contact residues mediating high affinity binding. The ability of a small number of residues to cause high affinity binding has previously been demonstrated in other systems and may represent a general property of protein-protein interfaces. Some experimental data consistent with this concept are presented below.

The VBMC computations show that the following amino acids are critical in determining the structure of the complex in wild type NGF dimers: His^4, Pro^5, His^8, Arg^9, Glu^{11}, His^{75}, Asn^{77}, Lys^{115} and Arg^{118}. This is significant since residues His^4, Pro^5, Glu^{11}, His^{75}, Asn^{77} and Lys^{115} are conserved in NGF molecules across all species (McDonald *et al.*, 1991). The overlap between these two sets reflects a tendency to maintain the particular geometry of the complex in natural NGF molecules. In addition, as demonstrated, the substitution of the important residue Arg^9 by the essentially different Met^9 does not result in geometric changes of the complex, which is consistent with equivalent bioactivity of hNGF and mNGF (Burton *et al.*, 1992). Thus, because of multiple physical factors maintaining the geometry of the complex, some species variability observed in NGF termini (McDonald *et al.*, 1991) is acceptable and does not cause geometric changes in the rigid region.

It is shown that each NGF terminus has several important residues, which determine the particular structure of the complex. This is consistent with high sensitivity of biological activity of NGF to the primary structure of both the amino and carboxyl termini (Klein *et al.*, 1991; Shih *et al.*, 1994; Burton *et al.*, 1992, 1995; Kahle *et al.*, 1992; Drinkwater *et al.*, 1993; Treanor *et al.*, 1995; Taylor *et al.*, 1991). The lack of the TrkA mediated activity of the mNGFΔ3-11, mNGFΔ3-12, mNGFΔ3-13, mNGFΔ3-14, mNGFΔ9-14 and mNGFΔ112-118 deletion mutants (Drinkwater *et al.*, 1993) is thus explained by the absence of the key residues Glu^{11} and Arg^{118}.

The separation of the flexible loop from the rest of the complex is crucial in permitting the rigid region to exist with definite geometric features. Residues His^4 and Pro^5 which cause this separation are absolutely conserved elements of the wild type NGF molecules derived from different species (McDonald *et al.*, 1991), and their compulsory location in the middle of

th flexible loop is well suited for facilitating th maximal separation. Point mutation P5A or H4D w akens or destroys the tend ncy of the lo p to separate from th rigid region; accordingly, th se mutati ns result in dramatic loss of TrkA related activity (Shih *et al.*, 1994).

The flexible loop is not an ess ntial structural element for TrkA activation since the mNGFΔ3-9 deletion mutant, which does not contain the loop (Figure 4), is as active as wild type mNGF (Drinkwater *et al.*, 1993). However, complete elimination of all loop residues results in almost inactive mutants mNGFΔ1-8 (Burton *et al.*, 1992; Drinkwater *et al.*, 1993; Taylor *et al.*, 1991) and hNGFΔ1-9 (Shih *et al.*, 1994; Burton *et al.*, 1992, 1995; Kahle *et al.*, 1992; Luo and Neet, 1992). Our molecular simulation studies enable the explanation for this apparent contradiction. It is demonstrated that the backbone of residues Ser^{8}-Ser^{9} in the mNGFΔ3-9 mutant is naturally incorporated into the structure of the rigid region because it matches the geometry of the "hollow" occupied by either Met^{9} or Arg^{9} side chain in wild type NGF dimers. On the contrary, total truncation of the flexible loop in the mNGFΔ1-8 deletion mutant results in placing the positively charged amino end in the vicinity of the key H-bonded Glu^{11} and $Arg^{118'}$ charged side chains (Figure 3), which abolishes the desired geometry of the rigid region (Figure 6). The same applies to the hNGFΔ1-9 deletion mutant which has neither the 1-8 loop nor the stabilizing Arg^{9} residue (Figure 2). This being the case, biological activity of amino terminus deletions of NGF should be determined by the length of the remainder of the terminus rather than its particular sequence. Indeed, available experimental data confirm this point. Deletion mutant mNGFΔ2-8 which has exactly the same number of residues in the amino terminus as the highly active mNGFΔ3-9 mutant is also very active (Drinkwater *et al.*, 1993). Some decrease in biological activity of mNGFΔ2-8 is likely to be caused by unfavorable directing of the Met^{9} hydrophobic side chain away from the complex whereas in the mNGFΔ3-9 deletion mutant this side chain is replaced by the hydrophilic hydroxyl group (Figure 4). Deletion mutants mNGFΔ3-8 (Drinkwater *et al.*, 1993) and hNGFΔ1-5 (Shih *et al.*, 1994), which contain a greater number of amino terminus residues, are remarkably less active than wild type NGF because the remainder of the loop is too long to occupy the "hollow" but too short to separate from the rigid region. The present explanations for the observed structure-activity relationships enable the prediction that, for example, a S2G mutation in the mNGFΔ3-9 deletion mutant would retain high biological activity.

Although the bioactive conformation of the NGF binding determinant has been disclosed above, the question of which NGF residues are involved in NGF/TrkA recognition was not yet addressed. One would reason, most probably, those residues which are primarily responsible for maintaining the particular structure of the NGF termini do not directly interact with the receptor. Thus, side chains of His^{4}, Pro^{5}, His^{6}, Met^{9}, Arg^{9}, Glu^{11} and $Arg^{118'}$ are not expected to play a crucial role in molecular recognition. On the oth r hand, charged residu s

$Arg^{114'}$ and $Lys^{115'}$ which are conserved in NGF molecules across all species (McDonald *et al.*, 1991) but not involved in principal intramolecular electrostatic interactions are candidates for the centres of intramolecular electrostatic recognition. Although both $Arg^{114'}$ and $Lys^{115'}$ participate in stabilizing intramolecular H-bonding within the bioactive conformations of the NGF termini, their electrostatic properties as charged residues are not utilized for this purpose.

The other structural element of the termini with potential for stereochemical fit to the TrkA receptor is a short exposed β-sheet motif located between the α-carbons of residues 7 and 9 (Figures 2,3). On the one hand, H-bonding between β-pleated sheets is rather common for protein-protein interactions (Kobe and Deisenhofer, 1993, 1994, 1995; Yoder *et al.*, 1993; Baumann *et al.*, 1993). On the other hand, a short exposed β-sheet motif is generally inherent in the structure of a leucine-rich repeat (Kobe and Deisenhofer, 1993, 1994, 1995) which has been recently identified as the TrkA recognition site for NGF (Windisch *et al.*, 1995a, 1995b). Other regions of NGF might also be involved in the NGF/TrkA recognition (Shih *et al.*, 1994; Ibáñez *et al.*, 1993). This will be discussed in depth below.

CONCLUSIONS

The Variable Basis Monte Carlo simulated annealing technique disclosed herein enables analysis of the low-energy conformational space of peptide molecules. Although multiple VBMC calculations do not consistently converge to the global energy minimum structure, they do permit the biologically active conformation to be evaluated. Definite physical factors maintain and distinguish the bioactive conformation of a molecule, and these factors can be understood by analyzing the low-energy conformational space. The precisely defined global energy minimum structure is unnecessary, especially considering that any empirical force field functions are not ideal. In biologically relevant molecular modelling, exploring the bioactive conformation is more important than determining the global energy minimum. VBMC is a useful tool for facilitating this exploration.

The present VBMC simulations predict that the amino (1-11) and carboxyl (112'-118') termini of dimeric (1-118)NGF form a complex comprised of a rigid region and a conformationally variable loop. The rigid region is formed by residues 9-11 and 112'-118' while the variable loop is formed by residues 1-8. The major stabilizing factor of the rigid region is the ionic contact of the Glu^{11} and $Arg^{118'}$ side chains. The separation of the loop from the rigid region arises from the electrostatic repulsion between His^4 and boundary residues of the rigid region His^8, Arg^9 (in hNGF) and $Arg^{118'}$. The geometry of the complex explains observed structure-activity relationships. Accordingly, it is the conformation of the rigid region which is recognized by the TrkA receptor, defining the biologically active

conformation of NGF for TrkA activation.

The split of the complex of the NGF t rmini into two distinct moi ties could hav important bi logical implications. Although only the structure of the rigid region is recognized by the TrkA receptor, the flexible loop is able to control conformational stability of the biologically active conformation of the rigid region and, consequently, NGF-induced TrkA phosphorylation.

PART B

THEORETICAL MODELLING OF Trk-RECEPTOR RECOGNITION SITES FOR NGF AND BDNF

INTRODUCTION

As mentioned above, the location of the neurotrophin binding sites within the Trk receptors is the subject of debate (MacDonald and Meakin, 1996). Based upon published data, there is reason to believe that Trk proteins have two putative neurotrophin binding sites: the "second immunoglobulin-like domain" (IgC2, residues Trp^{299}-Asn^{365}) and the "second leucine-rich motif" (LRM-2A and LRM-2B, residues Thr^{97}-Leu^{120} of TrkA and TrkB, respectively) (Schneider and Schweiger, 1991; Kullander and Ebendal, 1994; Pérez *et al.*, 1995; Urfer *et al.*, 1995; Windisch *et al.*, 1995a, 1995b, 1995c; MacDonald and Meakin, 1996; Rydén and Ibáñez, 1996). LRM containing proteins are a diverse group with different functions and cellular locations, and are known to mediate strong and selective protein-protein interactions (Kobe and Deisenhofer, 1993, 1994, 1995). The amino acid sequence of an LRM is characterized by conserved hydrophobic consensus residues (Schneider *et al.*, 1988; Schneider and Schweiger, 1991; Kobe and Deisenhofer, 1993, 1994, 1995). Typically, LRMs exist as repetitive cassettes, with an individual LRM representing a right-handed β-α hairpin unit (Kobe and Deisenhofer, 1993, 1994, 1995). Recent crystallographic studies on porcine ribonuclease inhibitor indicate that the side chains of the consensus residues form the hydrophobic core of the LRM modules, thereby determining their geometric features (Kobe and Deisenhofer, 1993).

According to the invention, the inventors report explicit atom-level models of the receptor sites for NGF and BDNF based on the structures of the second LRMs of TrkA (LRM-2A) and of TrkB (LRM-2B), respectively. To deduce these models, we have investigated the interaction of the bioactive conformation of the NGF amino and carboxyl termini region with the LRM-2A and of the "waist" region of BDNF with the LRM-2B. A series of four active NGF analogues, namely human NGF (hNGF) (Burton *et al.*, 1992; Shih *et al.*, 1994), mouse NGF (mNGF) (Burton *et al.*, 1992; Drinkwater *et al.*, 1993), the 3-9 deletion of mNGF (mNGFΔ3-9) (Drinkwater *et al.*, 1993) and the hNGF:NT-4/5 heterodimer (Treanor *et al.*, 1995), have been

docked to th LRM-2A of rat TrkA. For all four NGF molecul s studied, a st reochemical fit of the LRM-2A to the amino and carboxyl region was achieved. Th s results indicate that the bioactiv conformation of the NGF t rmini is a functional epitope which mediates high affinity binding via an interaction with the LRM-2A. This approach has also been applied to BDNF/LRM-2B docking, and their stereochemical fit, based mainly on electrostatic complementarity, has been identified and is described below.

METHODS

A sequence of three logical steps has been used to deduce the models of the interactions of NGF and BDNF with their respective Trk receptor binding sites: *Step 1:* The bioactive conformations of the amino and carboxyl termini of NGF analogues were determined. *Step 2:* The residues of the Trk proteins which form potential binding sites for NGF and BDNF were identified. *Step 3:* The interaction of the bioactive conformation of the NGF amino and carboxyl termini with the TrkA binding site and the BDNF β-strand stem region with the TrkB binding site were modeled computationally. Finally, the predicted features of the NGF/TrkA and BDNF/TrkB interaction models were validated against available experimental data. Residues of the first monomer of a neurotrophin are designated 1 to 118, those of the second monomer are designated 1' to 118'. Residues of the TrkA LRM-2A and the TrkB LRM-2B binding sites are designated by abbreviations tA and tB, respectively. Residues of the BDNF monomer are designated 1 to 119.

Step 1: **REVEALING THE BIOACTIVE CONFORMATION OF THE NGF TERMINI**

The most energetically favored conformations of the amino and carboxyl termini of NGF analogues have been obtained by VBMC computations and are described above. Since the 3-dimensional structures of the termini of fully active NGF molecules were found to be different from those of TrkA-inactive analogues, the former conformations were predicted to be "bioactive" for TrkA-mediated activity of NGF. That is, those geometric features that are exclusively inherent to active NGF molecules are expected to be compatible with the structure of the TrkA binding site for NGF. Since the geometry of the central β-strand stem of BDNF is rigid and has been established by X-ray crystallography (Radziejewski and Robinson, 1993), this logical step is bypassed for BDNF. Instead, it is assumed that the X-ray crystallography deduced conformation of the amino acid backbone of the TrkB binding determinant of BDNF represents its "bioactive" conformation.

Step 2: **SELECTION OF THE LRM-2 BOUNDARIES WITHIN THE TRK RECEPTORS**

Since there is controversy in the literature regarding the actual boundaries of LRMs (Schneider *et al.*, 1988; Schneider and Schweiger, 1991; Kobe and Deisenhofer, 1993, 1994, 1995; Windisch *et al.*, 1995a, 1995b), the following experimental background (Figure 8) was used to define boundaries for this computational study. According to Schneider and

colleagues (1988, 1991), the LRM domains of TrkA begin with Leu^{68IA}, Leu^{93IA} and Leu^{117IA}, whereas those boundaries are slightly shifted in the crystallographic studies of Kobe and Deisenhofer (1993). Furthermore, the boundaries of the "minimal" LRM module of TrkA (designated B4 in Figure 8), which demonstrates the same NGF binding affinity as wild type TrkA, are substantially shifted towards the carboxyl terminus (Windisch *et al.*, 1995a, 1995b) with respect to those suggested by Schneider and colleagues (1988, 1991). The same boundary shift has been suggested for the LRM-2B module (Windisch *et al.*, 1995a, 1995b, 1995c). However, a comparison of active (B1 and B4) and inactive (N4) LRM domains indicates that the presence of the "minimal" amino acid sequence (B4) does not ensure NGF binding. Understanding those factors which maintain the essential features of the LRM geometry in segments B1 and B4, and those factors which destroy them in N4, is of fundamental relevance to the correct assignment of the LRM boundaries.

β-Strand motifs exist in proteins only if hydrogen bonded (H-bonded) to other β-strands; otherwise their structure is unstable (Kobe and Deisenhofer, 1994). Tandem repeats of LRMs represent a prominent example of H-bonded parallel β-strand motifs. The general location of the β-strand motifs in the LRM, according to X-ray data, is illustrated in Figure 8; however, in a single LRM their particular geometry is destroyed (Kobe and Deisenhofer, 1993, 1994, 1995). Consequently, the only possibe way to exclude dramatic conformational changes in a protein domain upon disruption of the inter-strand H-bonding between β-strand motifs is to avoid those motifs. Accordingly, both boundaries of segment B4 are located in the middle of the β-strand regions of the adjacent LRMs such that this segment appears to be free of any β-strand. Nevertheless, the β-strand motif is a characteristic structural unit of LRMs, and thus it is likely that this unit is involved in the NGF/TrkA recognition process. Additionally, a short exposed β-strand motif has been detected in the bioactive conformation of the NGF termini, as described above. The incorporation of the β-strand regions at both sides of the B4 segment (as in N4) results in cooperative H-bonding between these β-strands and a complete loss of NGF binding, which indicates that accessibility of the β-strand motif for intermolecular contacts is essential. On the other hand, the separation of the entire LRM segment from the adjacent LRMs within the B1 molecule as a result of conformational kinking is likely to be energetically more favorable, since the entire LRM module has the internal stabilizing factors. Moreover, kinking between adjacent LRMs does not disrupt the structure of their β-strand motifs (since they remain H-bonded with their opposite sides), but makes them accessible for molecular recognition processes.

Accordingly, in the modelling of the present invention we used the conventional boundaries of the LRMs of TrkA and TrkB (Schneider *et al.*, 1988; Schneider and Schwiger,

1991), which keep the β-strand motif in the LRM, and we explicitly arranged H-bonding of this unit with the parallel β-strand motif of the NGF amino terminus to preserve it from conformational reorganizations. Thus, the segments between residues Leu^{93A} and Leu^{117A} in TrkA, and Leu^{93B} and Leu^{117B} in TrkB, were respectively designated the LRM-2A and the LRM-2B.

Step 3: **COMPUTATIONAL SIMULATION OF THE NEUROTROPHIN/RECEPTOR INTERACTIONS**

Docking interactions NGF/LRM-2A and BDNF/LRM-2B were simulated using a combined VBMC/CHARMM approach. As described above, the VBMC algorithm permits conformational space search; CHARMM (Brooks *et al.*, 1983) is a force field which defines conformational energy. The same approach was also used to study improper docking interactions of the central β-strand stem region of NGF with the LRM-2B, as a negative control.

The VBMC algorithm performs conformational and orientational space searches of a complicated molecular system with the aim of finding the structure which corresponds to the global minimum on the potential energy E_{tot} surface.

$$E_{tot} = E_t + E_w + E_e + E_{hb} + E_{qq} + E_{hy} + E_c \qquad (4)$$

The following potential energy terms have been considered in the framework of the united atom CHARMM force field (Brooks *et al.*, 1983; The force field parameters are extracted from CHARMM version 23.1, Molecular Simulations, Inc., Waltham, MA): torsional distortion E_t, van der Waals interactions E_w, electrostatic interactions E_e, and hydrogen bonding E_{hb}. Since the united atom approach is not appropriate to treat rigorously the quadrupole-quadrupole interactions of benzene rings (which are important for determining their mutual orientations in proteins (Hunter and Sanders, 1990; Hunter *et al.*, 1991), single quadrupoles have been placed at the centers of the benzene rings of phenylalanine, tryptophan and tyrosine, and the energy of the quadrupole-quadrupole interactions, E_{qq}, has been calculated as suggested by Schauer and Bernstein (1985). (The potential energy function of two interacting benzene molecules, comprising E_{qq} and E_w terms, has stationary points corresponding to both known electrostatically favorable "edge-to-face" and "offset stacked" orientations, with the dimerization energy of 1.94 kcal/mol agreeing well with *ab initio* quantum mechanical calculations (Hobza *et al.*, 1994).) In addition, the conformationally dependent free energy of hydration, E_{hy}, has been calculated according to the hydration shell model including both nonspecific and specific hydration terms (Hopfinger, 1973; Hodes *et al.*, 1979). Point atomic charges of Weiner and colleagues (1984) have been used. A dielectric constant equal to the interatomic separation in angstroms has been used to implicitly simulate solvation effects (Weiner *et al.*, 1984).

The E_c term is used only for the NGF/LRM-2A complex and represents the distance constraints which restrain the H-bonding of residues Glu^{11} and $Arg^{118'}$ within the bioactive conformation of the NGF terminii, as described above. In addition, two intermolecular H-bonds, arising from the alignment of complementary parallel β-strand motifs of NGF and LRM-2A, are also constrained and contribute to E_c. In the Monte Carlo conformational space search, E_c is defined as follows:

$$E_c = 10 \times \sum (d_{AB} - 1.8)^2 , \qquad (5)$$

where d_{AB} is the distance in angstroms between atoms A and B which are to be H-bonded. The E_c term is neglected when performing final energy minimization following the VBMC simulated annealing. In addition, this term has not been utilized when studying the mNGFΔ3-9/LRM-2A complex. Since, as described above, the mNGFΔ3-9 deletion mutant does not have a β-strand region, the geometry of its LRM-2A counterpart, namely Leu^{93tA}-Ile^{98tA}, has been kept fixed in the crystallographic conformation (Kobe and Deisenhofer, 1993) during Monte Carlo simulations. The E_c term, being "soft", does not preclude conformational and orientational changes to occur during Monte Carlo simulations. This term increases rigidity of the bioactive conformation of the ligand, which allows us to utilize the knowledge obtained at *Step 1*, instead of explicit considerations of inactive NGF analogues, in *Step 3*. In addition, this term keeps conformations of the β-strands of both ligand and binding site from destruction, and thereby allows us to avoid an explicit consideration of the adjacent first LRM of TrkA. Furthermore, this term maintains the known orientation of the parallel β-strand motifs in the NGF/LRM-2A complex.

The amino acid sequences of the binding determinants of the NGF molecules studied are presented in Figure 9. The conformational space of the NGF analogues consists of torsional angles determining geometry of the amino terminus of one monomer (residues 1-11) and the carboxyl terminus of the other (residues 112'-118'), while keeping the rest of the dimer in the experimental geometry of mNGF (McDonald *et al.*, 1991). The conformational spaces of the LRM domains of TrkA and TrkB consist of torsional angles representing fragments Arg^{94tA}-Leu^{117tA} and Arg^{94tB}-Leu^{117tB}, respectively. Covalent bond lengths and bond angles have been kept fixed. The geometry of each i-th residue is determined only by flexible torsional angles of the backbone (ϕ_i and ψ_i) and the side chain (χ_i1, χ_i2,...). All torsional angles for prolines, except ψ_i have been fixed. Torsional angles describing structural motifs with planar geometries (such as peptide bonds or conjugated regions in side chains) were fixed. Likewise, the configurations of the sp^3-carbons were fixed. The conformational space of BDNF consists only of torsional angles determining side-chain geometries of those residues which are located in the vicinity of its central β-strand stem and define a molecular surface (Table 2). In addition to the conformational variables of each complex, the six

orientational variables (three Euler angles and three translations along the coordinate axes) were used to describe the ligand-receptor orientations.

In accordance generally with the simulated annealing approach (Kirkpatrick *et al.*, 1983; Vanderbilt and Louie, 1984; Brünger, 1998; Nilges *et al.*, 1988; Wilson *et al.*, 1988; Wilson and Doniach, 1989), the molecular systems were kept at a constant temperature of 800°K for 2×10^6 Monte Carlo moves before the initiation of "cooling". The temperature was then decreased at every Monte Carlo move by a small increment such that after 2×10^6 Monte Carlo moves it reached 120°K. At this time, a local energy refinement was performed to identify the nearest stationary point on the potential energy surface. According to the VBMC algorithm described above, the basis of independent structural parameters was recalculated after every 7×10^4 Monte Carlo moves to direct them along the valleys of the potential energy surface, thereby accelerating conformational and orientational changes.

All calculations were performed on an Indigo-2 Silicon Graphics Workstation and an 8-node IBM Scalable POWER parallel 2 [SP2] high performance computer.

RESULTS AND DISCUSSION

CONFORMATIONAL FLEXIBILITY WITHIN RECEPTOR ENVIRONMENTS

Five independent VBMC simulations from different initial configurations were performed for each of the six molecular complexes under study. The elimination of the distance constraints E_c in the complexes with the LRM-2A did not result in any noticeable conformational changes within the complexes. Although independent VBMC simulations did not always converge to the same geometry for the same molecule, the final structures differed insignificantly; i.e., the conformations of the peptide backbones remained unchanged with the exception of residues 1-3 of the NGF amino terminus and the terminal residue Leu^{117A} of the LRM-2A. The differences between the VBMC generated structures were located in side-chain conformations of a limited number of residues, specifically Ser^{1}, $Val^{117'}$ ($Thr^{117'}$ in mNGF), Thr^{97tA} and Ser^{101tA}. These residues are not involved in intermolecular or intramolecular interactions, and do not affect the overall structures of the complexes. No considerable differences were identified in the independent VBMC-generated conformations of the BDNF/LRM-2B and the NGF/LRM-2B complexes.

A grid search of the internal space of the complexes using the water molecule radius 1.4 Å as a probe (Ponnuswamy and Manavalan, 1976) (as incorporated into the QUANTA program, Version 4.1, Molecular Simulations, Inc., Waltham, MA) showed that there is no internal cavity available for a solvent molecule in the hNGF/LRM-2A complex. This explains the rigidity of the complex and demonstrates the "perfect" stereochemical fit of the hNGF amino-carboxyl termini complex to the LRM-2A. Other complexes have some internal cavities, especially with the LRM-2B binding site.

SPECIFIC BINDING AREAS WITHIN RECEPTOR ENVIRONMENTS

The TrkA Receptor Binding Site

Comparison of the most stabl structures of th different complex s with the LRM-2A binding site (Figure 10) shows their striking conformational similarity. In all molecules, ligand-receptor binding is caused by similar hydrophobic, ionic, H-bonding and van der Waals interactions. There are five distinct areas (A-E) within the NGF/LRM-2A fit: areas A and B have hydrophobic interactions, areas C and D have ionic H-bonding, and area E has cooperative H-bonding between parallel β-strand motifs.

Area A represents the hydrophobic region at which residue Phe^{105tA} interacts with $Trp^{76'}$, which in turn forms hydrophobic contacts with Phe^{12} and $Leu^{112'}$. The aromatic rings of Phe^{12}, $Trp^{76'}$ and Phe^{105tA} are approximately perpendicular to each other, which is energetically favorable (Hunter and Sanders, 1990; Hunter *et al.*, 1991; Hobza *et al.*, 1994). This particular geometry would create a hole within the complex, if it was not filled by hydrophobic residue $Leu^{112'}$.

In area B, Phe^{7} of NGF is placed within the hydrophobic core of the LRM-2A created by the consensus residues (Schneider *et al.*, 1988; Schneider and Schweiger, 1991; Kobe and Deisenhofer, 1993, 1994, 1995). Similar to the favorable orientation of the aromatic residues in area A, the aromatic rings of Phe^{111tA} and Phe^{113tA} are perpendicular to that of Phe^{7}. On the other hand, residues Phe^{111tA} and Phe^{113tA} are not perpendicular to each other; their orientation instead resembles the favorable "offset stacked" geometry described by Hunter and others (Hunter and Sanders, 1990; Hunter *et al.*, 1991; Hobza *et al.*, 1994). As in area A, a hole created by the three neighboring favorably oriented aromatic rings is filled by a fourth residue, Thr^{114tA}. Interactions between aromatic rings in proteins is very common and represent an important conformational driving force (Warme and Morgan, 1978; Hunter *et al.*, 1991). Consequently, the fact that all three phenylalanine residues of the LRM-2A find their counterparts within the NGF binding domain supports the calculated structure of the NGF/LRM-2A complex.

In ionic binding area C, the negatively charged residue Asp^{109tA} exerts a central role. It is surrounded by the three positively charged amino acids His^{112tA}, $Arg^{114'}$ and $Lys^{115'}$ in hNGF, mNGF and mNGFΔ3-9, and by His^{112tA}, $Arg^{115'}$ and Arg^{9} in hNGF:NT-4/5. Residue His^{112tA} plays a secondary role: it creates the electrostatic dipole Asp^{109tA}→His^{112tA} in the LRM-2A, which imposes constraints on the spatial positions of the recognized positively charged residues of NGF, thereby reinforcing geometric selectivity in this area. Although the hNGF:NT-4/5 heterodimer has two substitutions in the C-area segment of the NT-4/5 carboxyl terminus, namely R114S and K115R, the geometry of the C area remains qualitatively the same, since residues Arg^{9} and $Arg^{115'}$ of hNGF:NT-4/5 functionally replace the absent $Lys^{115'}$

and Arg$^{114'}$ amino acids, respectiv ly. Alth ugh Arg^{9} also exists in the hNGF homodim r, it is not involv d in the ionic binding in this molecule, since it is separated from area C due to lectrostatic repulsions. Similarly, th charged amino end of mNGFΔ3-9, which functionally replaces Arg^{9}, is also separated from area C. There is no plac for the fourth positively charged residue in area C. Thus, in all molecules studied, the two positively charged amino acids of the ligand saturate the coordination possibilities of the receptor residue Asp^{109tA}.

Area C is partially isolated from its surrounding environment by flanking hydrophobic residues Val^{106tA} and Pro^{115tA}. Similarly, the principal charged residues of NGF, namely His^{8}, Glu^{11} and Arg$^{118'}$, are located between hydrophobic residues Ile^{8} (Val^{8} in mNGF), Val$^{111'}$ (Leu$^{113'}$ in hNGF:NT-4/5) and Val^{99tA} within the complexes. Thus, residues Val^{99tA}, Val^{106tA} and Pro^{115tA} of the LRM-2A participate in "compartmentalization" of the principal ionic interactions of the complexes, thereby shielding them from the conformation destructive influence of solvation..

The organization of ionic binding area D is similar to that of area C. Positively charged residues Arg^{59} and Arg^{69} are located in the vicinity of negatively charged Asp^{16} within the NGF structure (McDonald *et al.*, 1991; Bradshaw *et al.*, 1994), such that the coordination of the latter is not full. The third positively charged residue, Lys^{100tA}, comes from the LRM-2A to complete the Asp^{16} coordination. In addition to the ionic binding, residue Lys^{100tA} forms an H-bond with the Ser^{13} side chain.

Area E consists of the H-bonded parallel β-strand motifs of the LRM-2A and NGF (Figure 10b, 10c and 10e), each of the β-strands having three peptide bonds. The LRM-2A β-strand motif is located between the α-carbon atoms of Asn^{95tA} and Ile^{98tA}, whereas the NGF β-strand is located between the α-carbons of the sixth and ninth residues. The locations of the β-strand regions in the uncomplexed LRM (Kobe and Deisenhofer, 1993) and NGF (see above) resemble those in the complexes considered. In the complexed LRM-2A, the β-strand motif is shortened by one peptide bond at its amino end to accommodate the His^{4} side chain of NGF. On the other hand, the two peptide bond β-strand of the uncomplexed NGF is lengthened by one peptide bond at its amino end in the complexes.

The TrkB Receptor Binding Site

Figure 11a illustrates the central β-strand stem region of BDNF, and Figure 11b presents the VBMC-generated structure of the BDNF/LRM-2B complex. In this complex, ligand-receptor binding is based mainly on intermolecular electrostatic interactions of either ionic or hydrogen bonding origin. There are five distinct binding areas (F-K) within the TrkB receptor environment: four salt bridges (areas F, G, H and I) and one H-bonding area K. In contrast with the NGF/LRM-2A binding pattern, there is no participation of the LRM-2B β-strand motif in cooperative H-bonding with the BDNF binding epitope.

In area F, the primary positively charged residue (Ibáñez *et al.*, 1993) of the BDNF

binding domain, Arg^{81}, is bound to Asp^{100B}, th only negativ ly charged residue of the LRM-2B. It should b noted that Arg^{81} is xclusiv ly inh rent in BDNF molecules while being substituted by lectrostatically n utral Thr in NGF or by Lys in NT-3 or NT-4/5 molecul s (Bradshaw *et al.*, 1994), which indicates the importance of this area in neurotrophin recognition processes (see also Urfer *et al.*, 1994). On the contrary, residue Gln^{84}, identified by Ibáñez and co-workers (1993) as important, is not directly involved in specific intermolecular interactions within the LRM-2B domain.

In binding area G, the negatively charged residue Glu^{55}, which is absolutely conserved in all neurotrophins (Bradshaw *et al.*, 1994), exerts a central role. It is surrounded by the three positively charged amino acids, Lys^{25}, Lys^{57} and Lys^{109B}. Two of them, belonging to the neurotrophin, are also highly conserved (Bradshaw *et al.*, 1994). The third one, Lys^{109B}, is specific for the TrkB receptor site (Windisch *et al.*, 1995a, 1995b, 1995c). All BDNF residues of the G binding area, namely Lys^{25}, Lys^{57} and Glu^{55}, have been shown to be essential in NT-3 structure for TrkC receptor activation (Urfer *et al.*, 1994), which is in agreement with observations that the TrkB and TrkC binding domains are located in the same region of these neurotrophins. This particular arrangement of the three positively charged residues around one with a negative charge seems to be very common in neurotrophin-receptor recognition processes, since the NGF/LRM-2A interaction also includes two binding areas of this type (C and D). Existence of the absolutely conserved negatively charged residue Asp^{106} in direct proximity to area G increases binding affinity of Lys^{109B}, thereby highlighting some importance of this area in the BDNF/TrkB recognition processes. Although detailed mutational experiments did not demonstrate importance of the equivalent residue Asp^{105} in NT-3 for TrkC related activities (Urfer *et al.*, 1994), its direct involvement in the Zn^{2+} mediated regulation of neurotrophin bioactivities has been recently proven by multidisciplinary studies (Ross *et al.*, 1997), and, therefore, its location within the binding determinants of BDNF and NT-3 is consistent with these observations.

In area H, conserved residue Asp^{24} of BDNF forms a salt bridge with specific TrkB residue Lys^{113B}. Although Asp^{24} has not been demonstrated to be involved in direct neurotrophin-receptor interactions, either for TrkB or TrkC related activities, it is highly conserved in neurotrophins (Bradshaw *et al.*, 1994) and located in direct proximity to Thr^{22} in NT-3, which has been shown to be included in the TrkC receptor binding domain (Urfer *et al.*, 1994). These observations are consistent with the present model of BDNF/TrkB binding, since substitution of the equivalent residue of BDNF, Thr^{21}, by bulky Gln (Urfer *et al.*, 1994) would sterically hinder proper location of the LRM-2B domain (Figure 11b), whereas mutation D24A, although lacking one specific ligand-receptor interaction, would not significantly alter the BDNF/LRM-2B orientation resulting from multiple-point electrostatic complementarity. In

addition, the absence of negatively charged residue Asp^{24} is shown to induce salt bridge interaction of Lys^{113B} with neighboring Glu^{18}, with only minor conformational alterations of the LRM-2B.

In area I, Glu^{18}, a specific residue of BDNF (Bradshaw *et al.*, 1994), forms a salt bridge with the LRM-2B amino acid Arg^{94B}. Residue Glu^{18} is also involved in intramolecular electrostatic interactions with Lys^{57}.

Area K is the only region of the distinct BDNF/LRM-2B interactions which is not of ionic nature. The positively charged residue Lys^{104B} forms multiple H-bond contacts with the BDNF loop I backbone carbonyl groups and the neutral Thr^{35} side chain. The energy of such H-bonding is much lower than that of salt bridge contact, and, therefore, a substitution of the uncharged amino acid Thr^{35} by a negatively charged residue would stabilize the particular structure of the BDNF/LRM-2B complex. In accordance with the present model, the experimental substitution of BDNF residues 34-41 by the corresponding segment of NGF, which includes the substitution of negatively charged residue Glu^{35} for Thr^{35}, resulted in a significant increase in bioactivity of the resulting chimeric molecule relative to wild type BDNF in TrkB mediated survival (Lai *et al.*, 1996).

In addition to these five distinct binding areas of the BDNF/LRM-2B complex, there is one more area which reinforce binding specificity. The side chain of Pro^{60}, a specific residue of BDNF (Bradshaw *et al.*, 1994), demonstrates a perfect geometric fit into the hollow in the "zigzag"-shaped β-strand region of the LRM-2B (Figure 11b). This geometric complementarity indicates that Pro^{60} "recognizes" the β-strand motif of the receptor binding site. This interaction, obviously, does not significantly contribute to the total energy of the complex in the case of a perfect fit, but does represent a steric hindrance when this fit cannot be readily achieved. Accordingly, BDNF is very selective and does not bind non-cognate Trk receptors.

Figure 11c illustrates the VBMC-generated geometry of the "improper" NGF/LRM-2B complex. In this complex, specific binding areas F and I are absent due to lack of properly charged residues at positions 20 and 81, which would correspond to BDNF residues Glu^{18} and Arg^{81}, respectively. In addition, residue Pro^{60}, determining the proper BDNF/LRM-2B orientation, is substituted in NGF molecules (Bradshaw *et al.*, 1994). These substitutions cause dramatic conformational and orientational alterations in the complexed LRM-2B domain (compare Figure 11b and 11c). Predicted Cartesian 3-dimensional coordinates of atoms of the TrkB LRM-2B binding site in the complex with BDNF are presented in Appendix 2.

LIGAND-RECEPTOR INTERACTION ENERGY

NGF/TrkA Interactions

Table 3 presents the components of the intermolecular energies of the NGF/TrkA

complex s. Stability of the NGF/LRM-2A complexes results primarily from attractiv lectrostatic and van der Waals interactions, with intermolecular H-bonding playing a secondary role. It should be not d, however, that in the framework of the molecular m chanical approach, th H-bonding energy is partially incorporated into the lectrostatic interaction energy term, so the tabulated E_{hb} values reflect only part of the H-bonding energy. Accordingly, intermolecular H-bonding is more important for the NGF/LRM-2A interaction than it appears in Table 3. On the other hand, the intermolecular component of the E_{qq} term seems to be insignificant. The reason for the latter is that the aromatic moieties of Phe^{7}, Trp^{76}, Phe^{105tA}, Phe^{111tA} and Phe^{113tA} are "preorganized" for intermolecular contacts with their counterparts in the complexes in electrostatically attractive geometry in which the quadrupole-quadrupole interaction energy term is not significant. In addition, hydrophobic ligand-receptor interaction energy is presumably extremely important for NGF/LRM-2A complex formation, but rigorous quantitative evaluation is currently not possible.

Since neither electrostatic interactions nor hydrogen bonding can significantly stabilize a ligand-receptor complex in a water environment, the stability of the complex generally results from van der Waals and hydrophobic interactions (Clackson and Wells, 1995). Considerable contribution of intermolecular van der Waals interaction energy E_w (Table 3) arises from the geometric complementarity of the NGF binding domain and the TrkA recognition site, such that the high value of the E_w term is due to a large number of intermolecular van der Waals contacts. This complementarity is a consequence of the right-handed twists of both the NGF amino-carboxyl termini complex and the LRM-2A, this geometric feature being characteristic of each of these domains in both uncomplexed (Kobe and Deisenhofer, 1993; Shamovsky *et al.*, 1996) and complexed conformations. Thus, purely geometric ligand-receptor compatibility together with distinct hydrophobic contacts play a crucial role in NGF/TrkA recognition, while attractive electrostatic interactions and H-bonding further reinforce specificity of binding, which is in agreement with generalizations made by Clackson and Wells (1995).

BDNF/TrkB and NGF/TrkB Interactions

Table 4 presents the components of the potential energies of the complexes of BDNF and NGF with the LRM-2B in their minimum-energy conformations. Data presented in section A of Table 4 indicate that the difference in total energies (92.0 kcal/mol) is almost exclusively a consequence of more favorable electrostatic interactions in the BDNF/LRM-2B complex than in the NGF/LRM-2B complex (negative control). Section B of Table 4 illustrates that the BDNF complex is also more favorable in terms of intermolecular electrostatic energy by 77.2 kcal/mol (85% of the difference in total electrostatic energies). On the contrary, intermolecular van der Waals interactions are more favorable in the "improper" NGF/LRM-2B complex.

Furthermore, the value of intermolecular van der Waals energy is significantly lower for NGF/LRM-2B than for the NGF/LRM-2A complex, whereas electrostatic contribution is more than twice as high. Consequently, in contrast to the NGF/TrkA binding pattern, molecular recognition of BDNF by the TrkB receptor binding site is almost exclusively based on electrostatic complementarity, whereas the roles of van der Waals and hydrophobic interactions are insignificant. At the same time, such a perfect electrostatic fit could not be achieved without a purely geometric compatibility of the BDNF and the LRM-2B binding domains in size and shape (Figure 11b).

INDUCED CONFORMATIONAL CHANGES

The NGF Amino and Carboxyl Termini

Conformations of the NGF amino and carboxyl termini remain almost the same after complexation with the LRM-2A (Table 5; compare Figure 10a with 10b, 10c, 10d and 10e). A few local conformational changes occur in the $Arg^{114'}$ and the $Lys^{115'}$ side chains, and in the backbones of residues Ser^{2} and Phe^{7}. As predicted above, conserved charged residues $Arg^{114'}$ and $Lys^{115'}$ do not participate in principal intermolecular interactions within the NGF termini but are expected to form ionic intermolecular contacts with the TrkA binding site. Indeed, these are the intermolecular ionic NGF/LRM-2A interactions in area C, which change considerably the side-chain conformations of $Arg^{114'}$ and $Lys^{115'}$ while keeping their backbone geometry intact. The LRM-2A-induced conformational changes in residue Phe^{7} are caused by the intermolecular H-bonding in area E while the geometry of Ser^{2} is slightly changed to accommodate the LRM-2A residue Thr^{114tA}. The rest of the structure of the LRM-2A-complexed NGF termini retains the energy minimum conformation of the uncomplexed molecules because it is controlled by multiple intramolecular H-bonds. Consequently, the geometry of the NGF termini is "preorganized" for complexation with the LRM-2A, and only local conformational changes, primarily in residues $Arg^{114'}$ and $Lys^{115'}$, occur upon complexation. Geometric "preorganization" of the NGF termini as a ligand for binding to a leucine-rich motif is consistent with X-ray studies of Kobe and Deisenhofer (1995), who have demonstrated that ribonuclease A maintains a fixed geometry upon binding to the LRMs of ribonuclease inhibitor.

The LRM-2A Domain

Figure 12 illustrates the isolated structure of the LRM-2A from the hNGF/LRM-2A complex. Table 6 presents the equilibrium torsional angles of the hNGF-bound LRM-2A. As seen, the side chains of the general consensus residues, Leu^{93tA}, Leu^{96tA}, Ile^{98tA}, Leu^{103tA} and Phe^{111tA} (Schneider *et al.*, 1988; Schneider and Schweiger, 1991), form the hydrophobic core, similarly to their conformations in intact leucine-rich repeats (Kobe and Deisenhofer, 1993). Terminal consensus residue Leu^{117tA} is solvent-exposed due to a boundary effect. Amino

acids Ala^{107tA}, Pro^{108tA}, Ala^{110tA} and Phe^{113tA} are also incorporated into the LRM-2A hydrophobic core. On th other hand, residu s Val^{99tA}, Ph ^{105tA}, Val^{106tA} and Pro^{115tA} are not involved in hydrophobic int raction within th core, and apparently have specific rol s in the recognition sit of TrkA. Th most hydrophilic residues of the LRM-2A, nam ly Arg^{94tA}, Lys^{100tA}, Arg^{104tA}, Asp^{109tA}, His^{112tA} and Arg^{116tA} are exposed from the hydrophobic core in the complexes. Amino acids Lys^{100tA}, Asp^{109tA} and His^{112tA} participate in specific intermolecular interactions, while the other three are solvent-exposed. The reasonable locations of the hydrophobic and hydrophilic residues of the LRM-2A within the NGF/LRM-2A complexes with respect to water environment supports the calculated structures.

NGF/LRM-2A binding spans almost the whole LRM-2A domain, i.e., an interval between residues Leu^{93tA} and Pro^{115tA} comprising three distinct regions: β-strand, α-helix, and loop connecting the carboxyl terminus of the β-strand and the amino terminus of the α-helix. This is in agreement with recent crystallographic studies on the ribonuclease A - porcine ribonuclease inhibitor complex (Kobe and Deisenhofer, 1995), in which these particular regions of leucine-rich repeats of ribonuclease inhibitor are also involved in the molecular recognition process. While the β-strand structure exists in the complexed LRM-2A, the α-helix motif is destroyed by intermolecular interactions with NGF. Accordingly, the LRM-2A β-strand determines the proper orientation of the ligand with respect to the recognition site of TrkA, but does not undergo noticeable conformational changes. Consequently, the cooperative ligand-receptor H-bonding in area E cannot directly mediate those changes in receptor conformation which trigger receptor phosphorylation processes. Available experimental data confirm this point. First, the mNGFΔ3-9 deletion mutant, which does not have the β-strand motif and, consequently, cannot specifically bind area E, is as active as wild type mNGF (Drinkwater *et al.*, 1993). Second, the 24-residue LRM fragment Thr^{97tA}-Leu^{120tA} lacking the β-strand region (Kobe and Deisenhofer, 1993), demonstrates the same kinetics of binding to NGF as wild type TrkA (Windisch *et al.*, 1995a, 1995b).

The LRM-2B Domain

Table 7 presents the equilibrium torsional angles of the LRM-2B in the complex with BDNF. Side chains of all general consensus residues of the LRM-2B, except for Phe^{111tB} and terminal amino acid Leu^{117tB}, form the hydrophobic core and thereby stabilize the characteristic hairpin shape of the LRM (Figure 11b). In contrast with the LRM-2A, aromatic residues of the LRM-2B, namely Phe^{105tB}, Tyr^{108tB} and Phe^{111tB}, do not seem to have any specific roles in BDNF/LRM-2B molecular recognition. They form a cluster in which their aromatic rings interact with each other and are about mutually perpendicular (Figure 11b). On the contrary, all charged residues of the LRM-2B, namely Arg^{94tB}, Asp^{100tB}, Lys^{104tB}, Lys^{109tB} and Lys^{113tB}, are involved in specific electrostatic interactions with BDNF.

Similar to th NGF/LRM-2A complex, almost th whol LRM-2B domain, from Leu^{93tB} to Lys^{113tB}, fits to th BDNF binding d terminant (Figure 11b). On the other hand, there are significant diff rences of the n urotrophin-induced conformational alterations in th two LRM domains. First, since the BDNF binding domain does not have a β-strand motif which would fit to the β-strand of the LRM-2B, the characteristic geometric features of the latter are lost. Second, region Tyr^{108tB} to Asn^{116tB} retains its α-helical structure in the BDNF-bound LRM-2B domain. The reason of this conformational stability is that the spacer between the two BDNF-bound residues, Lys^{109tB} and Lys^{113tB} (3 residues), is consistent with the period of an α-helix (3.5 residues).

PRINCIPAL AMINO ACIDS INVOLVED IN MOLECULAR RECOGNITION

Principal NGF Residues

The amino acids of NGF which are primarily responsible for maintaining bioactive conformations (McDonald *et al.*, 1991; Shamovsky *et al.*, 1996) or which directly participate in NGF/TrkA recognition are specified in Figure 13. Almost all residues of the amino and carboxyl termini of NGF as well as the His$^{75'}$-Asn$^{77'}$ region are involved in specific intra- or intermolecular interactions. Only five amino acids of the 30-residue binding domain of NGF do not seem to be essential for either maintaining its bioactive conformation or binding to the recognition site of TrkA. These include Ser^{1}, Ser^{2}, Ser^{3}, Ala$^{116'}$ and Val$^{117'}$.

The observation that the important amino acids of the NGF binding domain are conserved across all species while the apparently unimportant five residues are variable (Figure 13) (McDonald *et al.*, 1991) supports the particular structural features of the NGF/LRM-2A complexes calculated herein. There are, however, exceptions which require explanation. In most cases, principal amino acids of NGF molecules derived from different species appear to be substituted by similar residues, e.g. I6V, F7L, L112I, S113T or R114K. In some special cases, the substituted amino acid is quite different but the particular substitution is still consistent with the present model, e.g. R9M, R9L or R118Q (McDonald *et al.*, 1991; Shamovsky *et al.*, 1996); in the case of the H8N substitution (McDonald *et al.*, 1991), histidine and asparagine have the same topology with respect to H-bonding to the Glu^{11} carboxyl oxygen. The structure of snake NGF (sNGF) requires special consideration. Principal hydrophobic residues Phe^{7} and Phe^{12} are replaced by histidine residues in sNGF. Although these mutations could be accompanied by structural differences in snake TrkA, they are consistent with the present model. According to the survey of Warme and Morgan (1978), side-chain interactions of histidine with tryptophan or threonine are very common in natural proteins, which implies the existence of specific inter-residue affinities. This being the case, attractive interactions His^{7}...Thr^{114A} and His^{12}...Trp$^{76'}$ in areas B and A, respectively, may replace corresponding hydrophobic interactions with Phe^{7} and Ph ^{12}.

Principal LRM-2A Residues

Th principal residues of th LRM-2A are shown in Figure 14. The g n ral consensus residues (Schneider *et al.*, 1988; Schn ider and Schweiger, 1991) maintain the specific geometry of th LRM (Kob and Deis nhof r, 1993, 1994, 1995). Th amino acids which form the distinct binding areas are involved in specific intermolecular interactions with the NGF binding domain. Since NGF does not activate the TrkB receptor, those residues which are specific for the TrkA receptor have been postulated to be directly involved in NGF/LRM-2A recognition (Windisch *et al.*, 1995a, 1995b). As shown, the LRM-2A segment has nine specific residues, seven of them directly participating in NGF/LRM-2A recognition in the framework of the present model. Thus, Lys^{100tA} binds Asp^{16} in area D, Pro^{106tA} is completely buried inside the NGF/LRM-2A complex, residues Asp^{109tA}, His^{112tA} and Pro^{115tA} form binding area C, and residues Phe^{113tA} and Thr^{114tA} are involved in forming area B. The other specific residues, Arg^{104tA} and Arg^{116tA}, do not seem to be required for specific NGF/LRM-2A interactions. It is seen, furthermore, that binding areas A and E are not specific for the recognition site of TrkA, indicating that binding specificity of the LRM-2A is determined by Lys^{100tA}, Asp^{109tA} and Phe^{113tA}. The fact that these particular amino acids are replaced in the recognition site of TrkB by residues of a different chemical nature, namely Asp^{100tA}, Lys^{109tA} and Lys^{113tA}, respectively (Windisch *et al.*, 1995a, 1995b), making NGF/TrkB binding impossible, supports the herein predicted details of NGF/LRM-2A recognition. Principal residue Phe^{105tA}, although common to both the TrkA and TrkB recognition sites (Windisch *et al.*, 1995a, 1995b), is also important for the NGF/TrkA recognition process, since oxidation of its counterpart, Trp^{76}, results in a complete loss of receptor binding (Merrell *et al.*, 1975).

Principal BDNF residues

Since BDNF/TrkB molecular recognition is predicted to be primarily based on electrostatic complementarity, principal BDNF and LRM-2B residues are identified by analysing their contribution to the intermolecular electrostatic energy. Table 8 presents a comparison of individual contributions of residues of BDNF, NGF and the LRM-2B to the intermolecular electrostatic energy for the BDNF/LRM-2B and the NGF/LRM-2B complexes, with cutoff being ±10 kcal/mol. BDNF/TrkB molecular recognition is achieved by those residues that make significantly more favourable contacts with their counterparts than do corresponding residues in the "improper" NGF/LRM-2B interaction. Accordingly, in section A of Table 8, residues of BDNF that make more favourable contacts with the LRM-2B than do those of NGF by at least 10 kcal/mol, are highlighted. They are: Glu^{18}, Asp^{24}, Glu^{55}, Arg^{81} and Gln^{84}. These residues make up the BDNF binding epitope for TrkB activation. Only two of them, Arg^{81} and Gln^{84}, have been previously identified (Ibáñez *et al.*, 1993). The most unusual case is residu Gln^{84}, which does not markedly participate in electrostatic interactions

with th LRM-2B; howev r, its substitution by His^{84} results in consid rable repulsive interactions with positively charged residu s of the receptor site. Therefore, Gln^{84} cannot be referred to as a principal residu by itself in terms of the TrkB receptor binding, and its apparent importance (Ibáñ z *t al.*, 1993) comes from unfavorable substitution by a positiv ly charged His^{84}. The only residue of NGF which binds to the TrkB receptor site significantly more strongly than does the corresponding residue of BDNF is Glu^{35}, in agreement with observations (Lai *et al.*, 1996).

Principal LRM-2B residues

Section B of Table 8 identifies the LRM-2B residues which significantly contribute to specificity of binding. Amino acids Arg^{94tB}, Asp^{100tB}, Ser^{101tB}, Lys^{109tB} and Lys^{113tB} make significantly more favorable contacts with their counterparts in BDNF than with those in NGF. Additionally, these residues are responsible for specific binding in areas F-K. The only residue of the LRM-2B that favours the NGF counterpart is Lys^{104tB}, which is caused by the abovementioned effect of Glu^{35}.

Figure 15 illustrates schematically the geometry of the LRM-2A and the LRM-2B receptor sites. Those residues which are predicted to form specific bonds with their preferred ligand are shown by arrows. The similarity of the binding patterns of the two LRMs is striking, especially bearing in mind the differences pointed out in the nature of the intermolecular interactions, and that the binding patterns were identified in independent computations. Thus, binding specificity of TrkA and TrkB is determined by the residues located in distinct positions of their second LRMs, with their respective binding patterns being incompatible with each other.

It is shown that van der Waals and hydrophobic interactions play a more important role in TrkA than in TrkB recognition. As a part of this phenomenon, we have demonstrated that NGF/LRM-2A binding is characterized by greater geometric complementarity, such that the ligand-receptor complex does not contain marked internal cavities. A plausible explanation for these particular features of Trk receptor recognition is that the NGF binding determinant is flexible and, because of that, more is required to stabilize its bioactive conformation in solution. Accordingly, TrkA receptor binding involves physical factors that are more effective in an aqueous environment, namely van der Waals and hydrophobic interactions.

EXPLANATION FOR STRUCTURE-ACTIVITY RELATIONSHIPS

TrkA mediated activity has been evaluated for 27 point and deletion mutants of the TrkA binding domain of NGF: hNGF (Burton *et al.*, 1992; Shih *et al.*, 1994), mNGF (Burton *et al.*, 1992; Drinkwater *et al.*, 1993), mNGFΔ3-9 (Drinkwater *et al.*, 1993), (1-120)hNGF (Schmelzer *t al.*, 1992), (1-120)mNGF (Luo and Neet, 1992), (1-117)hNGF (Schmelzer *et al.*,

1992) and hNGF:NT-4/5 (Treanor *et al.*, 1995) retain full activity; mNGFΔ2-8, mNGFΔ61-66 (Drinkwater *et al.*, 1993), hNGF-R9A, hNGFΔ1-5 and hNGF-P5A (Shih *et al.*, 1994) demonstrat intermediate potency; hNGFΔ1-9 (Burton *et al.*, 1992; Kahl *et al.*, 1992; Luo and Neet, 1992; Drinkwater *t al.*, 1993; Shih *t al.*, 1994; Burton *et al.*, 1995), mNGFΔ1-8 (Taylor *et al.*, 1991; Burton *et al.*, 1992), mNGFΔ1-9, mNGFΔ9-13 (Woo *et al.*, 1995), mNGFΔ3-8, mNGFΔ3-11, mNGFΔ3-12, mNGFΔ3-13, mNGFΔ3-14, mNGFΔ9-14, mNGFΔ112-118 (Drinkwater *et al.*, 1993), hNGF-H4A, hNGF-H4D (Shih *et al.*, 1994), BDNF (Suter *et al.*, 1992), and NT-4/5 (Treanor *et al.*, 1995) are almost or completely inactive. The present model of NGF/LRM-2A recognition enables a comprehensive explanation for the structure-activity relationships.

As demonstrated, fully active hNGF, mNGF and hNGF:NT-4/5 fit to the five binding areas A-E of the recognition site of TrkA, while the mNGFΔ3-9 deletion mutant fits only to A, C and D, without any specific binding taking place in areas B or E. Therefore, there are three common geometric features of the four fully active molecules which distinguish them from the less active analogues. First, conformations of the amino and carboxyl termini of these NGF analogues are "preorganized" for binding to the principal LRM-2A binding areas A, C and D. Second, there is no stereochemical incompatibility in the binding areas B and E. Third, there is no hole inside the NGF/LRM-2A complexes.

The structures of the other three fully active NGF analogues, (1-120)hNGF, (1-120)mNGF and (1-117)hNGF, are consistent with the above criteria. Indeed, since the NGF carboxyl end is located on the surface of the NGF/LRM-2A complexes (Figure 10) and does not directly participate in principal intermolecular interactions, the lengthening of the NGF carboxyl terminus by two amino acids does not explicitly affect NGF/LRM-2A compatibility. As far as the (1-117)hNGF molecule is concerned, terminal residue Arg^{118} of NGF has been shown to form inter-chain ionic H-bonds with Glu^{11} (see above) and, hence, seems to be important in maintaining the structure of the NGF bioactive conformation. On the other hand, there is a second factor stabilizing the bioactive conformation of the hNGF termini, namely inter-chain H-bonding of residue Arg^{9}. Because of the latter binding, the above criteria are still fulfilled for (1-117)hNGF.

The deletion of principal residue Phe^{12}, which participates in hydrophobic interactions in area A, results in a substantial loss of TrkA mediated activity of the mNGFΔ3-12, mNGFΔ3-13, mNGFΔ3-14 and mNGFΔ9-14 deletion mutants (Drinkwater *et al.*, 1993). Likewise, the absence of principal residues Arg^{114} and Lys^{115}, essential for the ionic binding in area C, results in dramatic loss of bioactivity of mNGFΔ112-118 (Drinkwater *et al.*, 1993). Similarly, geometric perturbations of the essential residues Arg^{59} and Arg^{69} in the mNGFΔ61-66 del tion mutant result in incomplete NGF/LRM-2A compatibility in area D and,

accordingly, a considerable loss of activity.

The specific location of the NGF ninth amino acid side chain in the "hollow" xisting on the surface of the NGF rigid region has been predicted herein to be critical for high TrkA mediated activity. The present inv ntion provides a d tailed explanation for this prediction. That is, the "hollow" is buried inside the NGF/LRM-2A complex, and a moiety located in this "hollow" fills the cavity which otherwise would exist inside the complex and destroy NGF/LRM-2A compatibility. Since this moiety is located in the internal cavity of the complex (Figure 10), severe limitations are imposed on its size. A short side chain does not fill this cavity; therefore, the hNGF-R9A mutant demonstrates noticeably diminished activity (Shih *et al.*, 1994). The cavity preferably is filled either by a bulky amino acid side chain, such as arginine (e.g. hNGF), methionine (e.g. mNGF) or leucine (sNGF), or by the two residue peptide backbone (mNGFΔ3-9 or mNGFΔ2-8). A longer amino terminus tail (e.g. in mNGFΔ3-8, mNGFΔ9-13 or mNGFΔ1-5) cannot be accommodated in the internal cavity of the NGF/LRM-2A complex and, hence, interferes with binding areas B and E.

Most deletion or point mutations of the NGF amino terminus destroy the exposed β-strand motif Phe^{7}-Arg^{9} and change the proper orientation of the Phe^{7} side chain, thereby affecting NGF/LRM-2A compatibility in areas B and E. Thus, incorporation of a negatively charged residue into the relatively long NGF amino terminus, as in hNGF-H4D, BDNF, NT-3 and NT-4/5, or substitution H8R, which is characteristic for BDNF and NT-4/5, has each been demonstrated to cause dramatic conformational changes in the complex of the neurotrophin amino-carboxyl termini, making it incompatible with the LRM-2A. This stereochemical incompatibility of the geometry of the NGF amino terminus with binding areas B and E of the LRM-2A is the reason for the partial or complete loss of TrkA-related activity of mNGFΔ3-8, mNGFΔ1-5, hNGF-P5A, hNGF-H4A, hNGF-H4D, mNGFΔ1-8, hNGFΔ1-9, mNGFΔ1-9, mNGFΔ9-13, mNGFΔ3-11, BDNF and NT-4/5.

As demonstrated, both NGF monomers are directly involved in specific ligand-receptor interactions, i.e., the first monomer binds areas B, D and E, whereas the second one binds areas A and C. Consequently, the dimeric structure of NGF is necessary to retain high biological activity, which is also consistent with experimental data (Maness *et al.*, 1994). On the contrary, only one BDNF protomer is essential for TrkB binding (Figure 11a, 11b).

In addition, recent reports of experiments have demonstrated the importance of residues Phe^{7} (Kullander and Ebendal, 1996), Leu^{112}, Arg^{114} and Lys^{115} (Krüttgen *et al.*, 1996) for TrkA mediated activity of NGF. This is consistent with their participation in the specific NGF/LRM-2A binding in the framework of the present model.

CONCLUSIONS

The complexes of the amino and carboxyl termini of the four fully active NGF

analogues with the second leucine-rich motif of TrkA were obtained using Variabl Basis Monte Carlo simulated annealing calculations. Th same methodology was utilized to define the structure of th complex f the second l ucine-rich motif of TrkB with th BDNF receptor binding determinant. Th structural features of the resulting NGF/TrkA and BDNF/TrkB binding predictions are supported by the following: (i) geometric and electrostatic complementarity of the binding domains of NGF and BDNF to binding sites of TrkA and TrkB, respectively, without considerable conformational changes of the ligands; (ii) appropriate environments for hydrophobic and hydrophilic residues within the complexes; (iii) analysis of structural variability of both binding domains; and (iv) comprehensive explanation of currently published structure-activity relationships. Within these complexes, NGF/TrkA molecular recognition is based upon multiple-point intermolecular interactions of hydrophobic, van der Waals, ionic and hydrogen bonding type. Extensive intermolecular van der Waals contacts arise from complementarity of the NGF binding domain and the TrkA recognition site in size and shape. In addition, there are five specific binding areas within the receptor model: hydrophobic A and B, ionic C and D and cooperative hydrogen bonding E. The NGF/TrkA stereochemical compatibility in areas A, C and D is required for TrkA receptor activation, whereas areas B and E reinforce binding specificity, making the NGF molecule a very sophisticated key triggering the chain of biological events following receptor phosphorylation. The 3-dimensional structures of the binding domains of the fully active NGF analogues are "preorganized" for stereochemical fit to the second leucine-rich motif of TrkA. Five distinct binding areas F-K were also identified in the BDNF/TrkB complex, although, in contrast with NGF/TrkA binding, BDNF/TrkB recognition is based primarily on ionic and hydrogen bonding interactions. In spite of significant differences in the nature of ligand-receptor interactions involved in TrkA and TrkB recognition processes, binding patterns of their receptor binding sites for NGF and BDNF are almost identical. The predicted mechanism of high affinity NGF/TrkA and BDNF/TrkB binding is consistent with the conformational model of TrkA-$p75^{NTR}$ interactions (Chao and Hempstead, 1995).

PART C

THEORETICAL MODELLING OF THE $P75^{NTR}$ RECEPTOR RECOGNITION SITE FOR NEUROTROPHINS

INTRODUCTION

As summarized above, the neurotrophins represent a family of structurally and functionally related proteins which play a crucial role in the development, survival and maintenance of th sympathetic and s nsory neurons (Purves, 1988; Snider and Johnson,

1989; Barde, 1989; Thoenen, 1991; Korsching, 1993; Persson and Ibáñez, 1993; Davies, 1994; Ibáñez, 1995). The neurotrophin family consists of nerve growth factor (NGF), brain-derived neurotrophic factor (BDNF), neurotrophin-3 (NT-3), neurotrophin-4/5 (NT-4/5), and more recently discovered neurotrophin-6 (NT-6) (Berkmeier *et al.*, 1991; Barde, 1991; Barbacid, 1993; Bradshaw *et al.*, 1994; Chao, 1994; Gotz *et al.*, 1994). Each neurotrophin is capable of binding independently with the common neurotrophin receptor $p75^{NTR}$, as opposed to specific Trk receptor interactions.

METHODS

The geometric features of complexes of monomeric neurotrophins with the $p75^{NTR}$ receptor binding site have been obtained by multiple molecular dynamics runs of 200-300 ps at constant temperatures between 300 and 400°K, followed by local energy refinements. The QUANTA V4.1 molecular modelling program (Molecular Simulations Inc., Waltham, MA) with the united atom CHARMM potential energy terms (Brooks *et al.*, 1983) has been used. Residues of $p75^{NTR}$ are designated by abbreviation p.

According to the invention, we superimposed the binding domains of NGF, BDNF, NT-3 and NT-4/5 with a putative binding site of $p75^{NTR}$ and carried out multiple molecular dynamics computations of the ligand-receptor complexes. These calculations revealed the 3-dimensional structures of the binding domains of the neurotrophins and $p75^{NTR}$, demonstrated their geometric and electrostatic complementarity, and identified principal residues involved in receptor recognition. All neurotrophins are believed to induce similar conformational changes in the $p75^{NTR}$ binding site, generally located in the orientation of the sequential loops within the cysteine-rich repeats.

Initial geometries of individual components of the complexes were based upon the X-ray crystallographic coordinates of neurotrophins NGF (McDonald *et al.*, 1991), BDNF and NT-3 (Robinson *et al.*, 1995) and the $p55^{TNFR}$ receptor extracellular domain (Banner *et al.*, 1993) which is homologous to $p75^{NTR}$. Geometry of the NT-4/5 monomer was constructed from the X-ray derived structure of NT-3 (Robinson *et al.*, 1995). Since NGF and other neurotrophins fold in similar rigid conformations, their molecular motions were restricted by imposing the following atom constraints. First, peptide backbones of the neurotrophins were fixed at their crystallographic coordinates. Further, conformations of the amino acid side chains of the neurotrophins were also fixed except for those located within and in the vicinity of the variable loop regions I and V (the $p75^{NTR}$ binding determinant). Thus, amino acid side-chain motions were allowed for residues 23-35 and 93-98 (NGF numbering) as well as for eight additional neighboring residues, namely His^{84} (Gln in other neurotrophins), Phe^{86} (Tyr in other neurotrophins), Lys^{88} (Arg in other neurotrophins), Trp^{99}, Arg^{100}, Phe^{101} (Trp in NT-3 and NT-4/5), Arg^{103}, and Asp^{105}. The flexible amino and carboxyl termini of the neurotrophins were

exclud d to avoid artefactual spacial hindrances for the receptor binding.

Fig. 16a represents a fragment of the crystallographically resolved structure of the $p55^{TNFR}$ extracellular domain (Bann r *et al.*, 1993), corresponding to the second CRD (loops 2A and 2B) and the first loop of th third CRD (loop 3A). Fig. 17 illustrates th sequence of this fragment and its alignment with the three known $p75^{NTR}$ peptides (Johnson *et al.*, 1986; Radeke *et al.*, 1987; Large *et al.*, 1989). Fig. 16b presents the minimum energy conformation of the corresponding fragment of human $p75^{NTR}$. As is apparent, its size and shape are complementary to the exposed $p75^{NTR}$ binding determinant of NGF (Fig. 16c). Accordingly, this 58-amino acid fragment of $p75^{NTR}$, including the second and the beginning of the third CRDs (Fig. 17), has been considered as a putative binding site for neurotrophins. The artefactual charges on the terminal amino and carboxyl groups of the peptide representing the $p75^{NTR}$ binding site were neglected.

Once the most stable equilibrium 3-dimensional structures of the complexes being studied were obtained, the residues contributing the most to the energy of intermolecular interactions were identified. Point atomic charges of Weiner *et al.* (1984) and a dielectric constant equal to the interatomic separation in angstroms (to implicitly simulate solvation effects) (Weiner *et al.*, 1984) were utilized to calculate the electrostatic intermolecular terms. The van der Waals intermolecular terms were evaluated by the united atom CHARMM force field (Brooks *et al.*, 1983). The calculations were performed on a 200 MHz Indigo-2 SiliconGraphics Workstation.

RESULTS AND DISCUSSION

The most stable structures of the complexes of the neurotrophins with the putative $p75^{NTR}$ receptor binding site obtained by the molecular dynamics computations described herein are illustrated in Fig. 18. Table 9 presents net values of the electrostatic and van der Waals terms of the ligand-receptor interaction energy. Tables 9 and 10 list individual residues of the neurotrophins and the $p75^{NTR}$ receptor which significantly contribute to the intermolecular electrostatic interaction energy. The highlighted residues represent the functional epitopes of the ligands (Table 9) and the receptor (Table 10), whereas the other listed residues, although being located within the binding interfaces, apparently do not participate in major ligand-receptor electrostatic interactions in the particular complex. Predicted Cartesian 3-dimensional coordinates of atoms of the $p75^{NTR}$ binding sites in the complexes with NGF and BDNF are presented in Appendix 3.

Significant contributions of electrostatic interactions to the ligand-receptor interaction energy (Table 9) result from opposite net charges of the binding domains of neurotrophins (positively charged) and the common neurotrophin receptor (negatively charged), which effect is consistent with published predictions (Ryd´n *et al.*, 1995). Data pres nted in Tables 9 and

10 demonstrate that, on th average, th int raction between the functional epitopes is responsible for 94% of intermolecular electrostatic energy, but only 43% of van der Waals interaction energy. Consequ ntly, residues participating in strong and specific ligand-receptor interactions represent only a part of a bigg r binding int rface in which significant van d r Waals contribution is accumulated from a large number of weak contacts, which is possible only as a consequence of geometric complementarity of the binding domains. Fig. 19 presents the structure of the BDNF/p75^{NTR} complex as atomic van der Waals spheres and demonstrates the geometric fit of the binding domains. The van der Waals energy and, therefore, geometric complementarity of the binding interfaces in the NGF/p75^{NTR} complex is significantly lower than in the other neurotrophin/p75^{NTR} complexes (Table 9), which is consistent with its fastest rate of dissociation (Ibáñez, 1995). However, the pure geometric factor cannot explain the slowest rate of dissociation observed for the BDNF/p75^{NTR} complex (Ibáñez, 1995). Thus, stability of the complex arises from a combination of geometric and electrostatic complementarities of the binding interfaces, consistent with the generalizations of Clackson and Wells (1995). A specific feature of the neurotrophin/p75^{NTR} binding interfaces is that they do not include substantially hydrophobic residues, so they do not have a hydrophobic core, which has been found in many other protein-protein complexes (Clackson and Wells, 1995; Livnah *et al.*, 1996). The predominant interactions within the binding domains of the complexes under study are of the salt-bridge type.

Specificity of binding of the neurotrophins to the p75^{NTR} receptor is determined by charged residues within the binding domains (Rydén *et al.*, 1995). As seen in Fig. 18, they create 3-dimensional networks in which most of them are in contact with more than one residue of the opposite charge. Therefore, any missing charge would destroy more than just one bond, but a significant portion of, if not the whole, network. That is, the electrostatic complementarity of the binding interfaces would be altered, which is consistent with the experimentally observed sensitivity of binding to mutations of charged residues (Ibáñez *et al.*, 1992; Rydén *et al.*, 1995; Rydén and Ibáñez, 1996). Both ligand and receptor provide the network with positive and negative charges (Table 9 and 10, Fig. 18), even though negative charges dominate in the receptor, and positive in the ligands. This particular spatial arrangement of the charges increases specificity of binding and prevents electrostatic repulsions within the same binding domains. For example, in all the complexes, positively charged residue Lys^{56p} of the receptor forms salt-bridges with negatively charged residues Asp^{75p} and Asp^{76p} of the receptor, thereby occupying one site of their coordination, such that only the opposite sides of the latter residues remain available for intermolecular ionic interactions (Fig. 18). Negatively charged residue Asp^{93} of BDNF holds together positively charged residues Arg^{97} and Arg^{101} of BDNF, such that they are both able to interact with

juxtaposed amino acids Asp^{75p} and Asp^{76p} of th receptor (Fig. 18b). Similarly, n gativ ly charged residue Asp^{30} of th neurotrophins forms a salt-bridg int raction with Arg^{100}, which directly int racts with $p75^{NTR}$.

In spit f the differences in the binding interfaces of the respectiv complexes, binding patterns of the $p75^{NTR}$ receptor are similar. All three loops of the receptor binding site (2A, 2B and 3A) are involved in binding (Fig. 18). The principal residues of loop 2A are Asp^{47p} and Lys^{58p}; those of loop 2B are Asp^{75p} and Asp^{76p}; and those of loop 3A are Asp^{88p} and Glu^{89p}. As is seen in Table 10, loop 2B forms the strongest contacts. In addition to the principal binding pattern, the $p75^{NTR}$ binding domain comprises specific residues for ionic interactions with particular neurotrophins (Table 10, Fig. 18). Thus, Arg^{80p} interacts only with Glu^{35} of NGF; residue Glu^{53p} interacts only with Lys^{86} of BDNF, and Glu^{60p} and Glu^{73p} interact only with residues of NT-3 and NT-4/5.

Site-directed mutagenesis studies of the $p75^{NTR}$ binding site have suggested that mutation of any one of the residues Asp^{75p}, Asp^{76p} or Glu^{89p} to Ala does not affect NGF binding, whereas mutation of Ser^{50p}, which does not participate in major ionic interactions, results in the complete abolishment of binding (Baldwin and Shooter, 1995). The apparent discrepancy with the present theoretical studies can be explained, since the cited experimental observations are still controversial. Indeed, although both Asp^{75p} and Asp^{76p} are involved in ionic interactions in the loop 2B region with positively charged residues of neurotrophins, one of them might be enough to maintain binding to NGF. Likewise, the functional role of the missing residue Glu^{89p} in loop 3A might be fulfilled by adjacent Asp^{88p}. Residue Ser^{50p} of $p75^{NTR}$ is predicted to be hydrogen bonded to Gln^{96} of NGF (Fig. 18a), and its mutation to Asn, Ala or Thr, which abolishes receptor binding (Baldwin and Shooter, 1995), may create steric hindrances in the NGF/$p75^{NTR}$ interface. The present molecular modelling studies suggest that Ser^{50p} is not important for binding of any other neurotrophin (Fig. 18, b-d).

In contrast to the $p75^{NTR}$ receptor binding pattern, there are only two common residues of the binding interfaces of neurotrophins which directly interact with the receptor site, Arg^{100} and Arg^{103}. Contribution of Arg^{103} is significant in all the complexes, while Arg^{100} seems to be less important for the NGF/$p75^{NTR}$ binding.

As is seen in Table 9, most important residues of the NGF binding domain are (in order of decreasing significance) Lys^{32}, Lys^{34}, Arg^{103}, Lys^{95}, and His^{84}, all of them forming specific ionic contacts with negatively charged residues of $p75^{NTR}$ (Fig. 18a). Involvement of Lys^{32}, Lys^{34}, and Lys^{95} in $p75^{NTR}$ binding has been very well established experimentally, with the same order of significance being observed (Ibáñez, 1994). The most important residues of NGF, Lys^{32} and Lys^{34}, bind to the loop 2B residues of $p75^{NTR}$ (Fig. 18a). Here we

d monstrate that residu Lys^{88} is not critical for p75^{NTR} binding, whereas residu s Arg^{103} and His^{84} make direct ionic contacts with the receptor binding site. Importance of th latter residue has not been previously reported in the cont xt of p75^{NTR} binding. Th roles of Asp^{30}, Glu^{35} and Arg^{100} seem to be secondary, since their contributions are relatively small. Hydrophobic residue Ile^{31} is not directly involved in ligand-receptor interactions.

In BDNF, all three positively charged residues of variable region V, Lys^{95}, Lys^{96} and Arg^{97} (Rydén *et al.*, 1995), bind to negatively charged residues of the p75^{NTR} binding site, namely Asp^{47p}, Glu^{53p} and Asp^{75p}, respectively (Fig. 18b). In addition, the residues Arg^{88} and Arg^{101} play a more important role than in the NGF case (Table 9); they bind to the loop 2B residues Asp^{75p} and Asp^{76p} of p75^{NTR}, thereby fulfilling the function of missing positively charged residues of loop I. The increased importance of residue Arg^{88} in BDNF and other neurotrophins relative to that of Lys^{88} in NGF (Table 9) is permitted by a longer side chain of Arg, which results in a decrease of the separation between opposite charges (Fig. 18). Because of missing residue His^{84}, only the positively charged residue Arg^{104} binds to the loop 3A residues Asp^{88p} and Glu^{89p} of p75^{NTR}.

In NT-3, the loop 2B residues of the receptor Glu^{73p}, Asp^{75p}, and Asp^{76p} bind to Arg^{31}, His^{33}, Arg^{100}, and Arg^{87}. Residue Asp^{47p} of loop 2A of the receptor also binds to Arg^{100}. Residue Lys^{95} of variable region V does not form any salt-bridge contact with the receptor, consistent with its reported insignificance for NT-3 binding (Rydén *et al.*, 1995). Thus, the present results agree well with the established roles of Arg^{31} and His^{33} of NT-3 (Rydén *et al.*, 1995; Rydén and Ibáñez, 1996) and predict the increased importance of residue Arg^{100} in NT-3 for p75^{NTR} binding (Table 9). The binding pattern of NT-4/5 is similar to that of NT-3 (Fig. 18, c,d). The increased electrostatic contribution of Arg^{36} with respect to corresponding NT-3 residue His^{33} (Table 9) is caused by the longer side chain of the former, which results in formation of a salt-bridge contact with residue Glu^{60p} of the receptor (Fig. 18d).

Binding of a neurotrophin induces conformational changes in the p75^{NTR} binding site. The conformational space of the three loops (2A, 2B and 3A) is limited by eight disulfide bonds; therefore, the most significant changes occur in the junction areas of those loops. Fig. 20 illustrates the superimposed equilibrium geometries of the free and the BDNF-complexed p75^{NTR} binding site. The superimposition is performed by a least-square minimization technique using the α-carbon reference atoms of loops 2A and 3A. As is apparent, the orientation of loop 2B with respect to the two flanking loops is considerably changed upon binding. Because of striking similarities between the binding patterns of the p75^{NTR} receptor with the different neurotrophins, a similar conformational change takes place in all four complexes under investigation. The driving force behind this particular conformational transition is ionic interactions of the principal residues of loop 2B, Asp^{75p} and

Asp^{76p}, with positively charged residues of the n urotrophins, taking into account that spacial positions of th flanking loops 2A and 3A are fixed by ionic int ractions of residu s Asp^{47p}, Lys^{56p}, Asp^{88p}, and Glu^{89p} with corresponding residu s of the neurotrophins (Fig. 18). Thus, structural variability between the neurotrophins does not preclude them from inducing similar conformational change in the common neurotrophin receptor.

The binding pattern of neurotrophins to the $p75^{NTR}$ receptor predicted by the present molecular modelling studies can be additionally verified by checking conservation of the identified principal residues. The sequences of the binding site of the $p75^{NTR}$ receptor from different species (Fig. 17) demonstrate that principal residues forming its common binding pattern, namely Asp^{47p}, Lys^{56p}, Asp^{75p}, Asp^{76p}, Asp^{88p}, and Glu^{89p}, are conserved in $p75^{NTR}$. The known variability of regions I and V among neurotrophins (Rydén *et al.*, 1995) implies that conservation of the principal residues of the $p75^{NTR}$ binding determinants may be checked only within the same neurotrophin derived from different species. Study of a recent sequence alignment of neurotrophins (Bradshaw *et al.*, 1994) allowed us to conclude that the functional epitope of the neurotrophins (Table 9) is generally conserved within the same neurotrophin even though there are some exceptions, often represented by the substitution by a similar amino acid. Arg^{100} and Arg^{103} are the only two residues of the binding epitopes which are conserved throughout all neurotrophins (Bradshaw *et al.*, 1994). Other residues within the functional epitopes maintain specificity of binding of different neurotrophins.

The present model also represents a key to understanding the conservation of residues which do not directly participate in receptor binding. For example, Gly^{33} is absolutely conserved in all neurotrophins, yet is not involved in any specific interactions with the receptor binding site. However, within the present model, its conservation can be understood, since it is located very close to loop 3A of the receptor and forms van der Waals contacts with it (Fig. 18), such that any other residue would impose steric hindrance which would alter or destroy the ligand-receptor geometric complementarity.

The principal NGF/TrkA binding areas necessary to trigger TrkA phosphorylation and subsequent biological events have been discovered by the inventors. Specifically, the inventors have discovered that essentially the full binding site of the second leucine rich motif (LRM) of TrkA, amino acid residues 93 to 117, forms the binding site for NGF, and comprises five distinct binding areas, A, B, C, D and E. Appendix 1 provides the Cartesian coordinates of the LRM-2A residues defining the areas A to E in PDB format. Binding areas A and B bind hydrophobically to ligands, areas C and D form ionic bonds with charged portions on ligands and area E forms hydrogen bonds with ligands.

The stereochemical fit to at least three of these binding sites, A, C and D by a ligand is necessary to activate TrkA receptor. Binding areas B and E reinforce stereoselectivity of

th TrkA binding site by selecting an NGF analogue with a stereoch mically compatible amino t rminus.

Binding area A of the second LRM comprises hydrophobic int raction of residue Phe^{105tA}. Binding area B compris s hydrophobic int raction of residues Phe^{111tA}, Phe^{113tA} and Thr^{114tA}. Binding area C comprises attractive ionic interaction between a suitable portion on the ligand and Asp^{109tA}. Binding area D comprises attractive ionic interaction between a suitable portion on the ligand and residue Lys^{100tA}. Binding area E comprises multiple parallel β-strand type hydrogen bonding with region Asn^{95tA}-Ile^{98tA}.

Main structural features of the bioactive conformation of NGF include: 1) ionic hydrogen bonding between Glu^{11} in the amino terminus and $Arg^{118'}$ in the carboxyl terminus; 2) separation of the flexible loop 1-8 from the rigid region (9-11 and 112' to 118') because of electrostatic repulsions caused by His^4 and conformational restrictions imposed by Pro^5; 3) packing the side chain of Arg^9 or Met^9 in the "hollow" of the rigid region, this "hollow" being an indentation in the protein structure by residues $Lys^{115'}$-$Arg^{118'}$; and 4) an embryonic β-sheet structure present between the α-carbons of the 7th and 9th residues.

Within NGF, residues $Trp^{76'}$, $Arg^{114'}$, $Lys^{115'}$ and Asp^{16} comprise the pharmacophore which binds TrkA. Any synthetic molecule, whether peptide or non-peptide, which fits into binding areas A, C and D is contemplated to elicit a biological response (agonist) or block biological response (antagonist).

The present invention provides a ligand for binding with TrkA, wherein TrkA comprises a second leucine rich motif (LRM) region comprising amino acid residues 93 to 117, the coordinates of the residues of said LRM given in Appendix 1, said LRM motif having five binding areas, area A comprising hydrophobic interaction of amino acid residue Phe^{105tA}, area B comprising hydrophobic interaction of amino acid residues Phe^{111tA}, Phe^{113tA}, and Thr^{114tA}, area C comprising ionic interaction of amino acid residues Asp^{109tA} and His^{112tA}, area D comprising ionic interaction of amino acid residue Lys^{100tA}, and area E comprising multiple parallel β-strand type hydrogen bonding of region Asn^{95tA} to Ile^{98tA}. The ligand comprises at least one functional group being capable of hydrophobic bonding and being present in an effective position in the ligand to hydrophobically bind to area A, at least one positively charged functional group being present in an effective position in the ligand to ionically bind to area C, and at least one negatively charged functional group being present in an effective position in the ligand to ionically bind to area D.

Secondary features of the ligand include at least one effective functional group present in a position in the ligand to hydrophobically bind to area B of TrkA, and a functional group present in an effective position in the ligand to hydrogen bind to area E of TrkA.

The invention further provides the ligand comprising amino acid residues, at least one

of th residues being capable of hydrophobic bonding and being present in an effective position in th ligand to hydrophobically bind to Phe^{105A} in area A on the TrkA receptor, at least one of the residues being a positiv ly charged residu present in an ffective position in the ligand to ionically interact with Asp^{109A} and His^{112A} forming area C on th TrkA receptor, and one of the residues being a negatively charged residue present in an effective position in the ligand to ionically bind to Lys^{100A} in area D on the TrkA receptor.

The present invention also provides a method of designing a ligand to bind with an LRM binding site on TrkA. The method includes computationally evolving a chemical ligand using an effective genetic algorithm with preselected spatial constraints so that the evolved ligand comprises at least three effective functional groups of suitable identity and spatially located relative to each other in the ligand so that a first of the functional groups hydrophobically interacts with binding area A, a second of the functional groups ionically interacts with binding area C, and a third one of the functional groups ionically interacts with binding area D of the second LRM of TrkA. Those skilled in the art will be aware of the various techniques which may be used for *de novo* ligand design. For example, packages such as Quanta, Discover and Insight provide computational methodologies for generating ligands.

Some ligands according to the present invention may be peptides or peptidomimetics. Morgan and co-workers (Morgan *et al.*, 1989) define peptide mimetics as "structures which serve as appropriate substitutes for peptides in interactions with receptors and enzymes". The mimetic must possess not only affinity but also efficacy and substrate function. For purposes of this disclosure, the terms "peptide mimetic" and "peptidomimetic" are used interchangeably according to the above excerpted definition. That is, a peptidomimetic exhibits function(s) of a particular peptide, without restriction of structure. Peptidomimetics of the invention, e.g., analogues of the neurotrophin and receptor binding sites described herein, may include amino acid residues or other chemical moieties which provide functional characteristics described herein.

Known compounds may also be screened to determine if they satisfy the spatial and functional requirements for binding with the second LRM of TrkA. The molecules in the data bases are screened to determine if they contain effective moieties spaced relative to each other so that a first moiety hydrophobically interacts with binding area A, a second of moiety ionically interacts with binding area C, and a third moiety ionically interacts with binding area D of the second LRM of TrkA.

The contents of all references and appendices (see Appendices 1, 2, 3, and 4) cited throughout this application are hereby expressly incorporated by reference.

EQUIVALENTS

Those skilled in the art will recognize, or b abl to ascertain using no more than routine xperimentation, many equival nts to the specific mbodiments of the inv ntion described herein. Such equival nts are intended to be encompassed by th following claims.

Tabl 1. Equilibrium variable torsional angles (in degrees) of th amino and carboxyl termini of the most stabl conformations of th NGF dim rs and analogues.*

No.		Active structures						Inactive structures					
		hNGF		mNGF		mNGFD3-9		hNGF-H4D		mNGFD1-8		BDNF	
Amino terminus													
11	ψ	E	82.9	E	85.9	E	89.2	E	80.9	E	63.7	E	68.2
	ϕ		55.7		56.3		57.8		57.2		47.9		56.3
	χ1		-69.8		-72.0		-72.1		-75.0		-66.2		-76.9
	χ2		72.7		71.7		66.0		72.6		71.2		70.1
	χ3		-120.4		-111.7		-107.0		-104.8		-102.8		-97.7
10	ψ	G	-89.1	G	-95.1	G	-88.0	G	-129.5	G	-81.6	G	-134.1
	ϕ		-172.5		-178.6		-177.5		104.7		-80.8		155.0
9	ψ	R	-36.1	M	-21.1	S	146.5	R	-46.5	M	-66.6	R	71.4
	ϕ		-92.8		-91.4		-103.6		-80.9		157.5		-128.5
	χ1		-77.2		-75.2		-66.7		-115.0		-142.4		-73.5
	χ2		-173.9		-179.7		64.0		69.5		-69.7		-179.8
	χ3		-175.5		179.9		-		-141.9		178.3		-71.4
	χ4		134.3		-		-		98.1		-		-109.8
8	ψ	H	118.6	H	110.4	S	106.1	H	151.6		-	R	105.2
	ϕ		-116.5		-110.4		52.8		-53.7		-		-100.1
	χ1		-89.7		-90.9		-45.9		-62.0		-		179.6
	χ2		-73.8		-71.5		-172.3		-72.5		-		-105.5
	χ3		-		-		-		-		-		162.1
	χ4		-		-		-		-		-		133.7
7	ψ	F	135.7	F	129.4		-	F	142.3		-	A	161.6
	ϕ		-68.8		-89.0		-		-114.8		-		-166.6
	χ1		-171.6		-163.9		-		-170.7		-		-
	χ2		-96.3		-91.5		-		-100.2		-		-
6	ψ	I	40.3	V	61.7		-	I	40.0		-	P	114.4
	ϕ		40.4		47.7		-		39.9		-		-
	χ1		-159.7		-177.3		-		-159.7		-		-
	χ2		87.1		-		-		88.6		-		-

	5	ψ	P	156.0	P	149.8	-	P	105.5	-	D	82.8
		ϕ		-		-	-		-	-		56.5
		χ1		-		-	-		-	-		-176.9
		χ2		-		-	-		-	-		-112.8
	4	ψ	H	121.4	H	122.1	-	D	117.9	-	S	136.2
		ϕ		-129.2		-129.8	-		-102.8	-		-53.4
		χ1		-162.5		-163.3	-		-66.4	-		-172.9
		χ2		-69.1		-69.2	-		-97.5	-		-178.3
	3	ψ	S	2.1	T	-1.9	-	S	-25.0	-	H	153.8
		ϕ		-91.9		-84.5	-		-68.2	-		48.2
		χ1		-171.8		-174.9	-		39.3	-		82.1
		χ2		-53.2		-51.2	-		-120.5	-		69.8
	2	ψ	S	138.5	S	139.4	-	S	38.5	-		-
		ϕ		-128.9		-114.1	-		50.8	-		-
		χ1		173.3		169.7	-		-173.2	-		-
		χ2		-141.9		-139.8	-		-120.6	-		-
	1	ψ	S	133.0	S	127.9	-	S	131.9	-		-
		ϕ		48.6		49.4	-		-133.8	-		-
		χ1		-43.2		-44.1	-		-43.5	-		-
		χ2		-171.5		-172.4	-		-173.6	-		-

Carboxyl terminus

	112'	ϕ	L	-113.3	L	-113.0	L	-112.4	L	-112.0	L	-111.5	L	-110.6
		ψ		98.8		98.7		99.2		97.7		89.9		100.1
		χ1		-72.3		-71.6		-71.6		-71.7		-71.8		-72.1
		χ2		163.7		163.0		162.6		162.2		161.9		161.1
	113'	ϕ	S	-83.4	S	-77.2	S	-77.4	S	-76.8	S	-91.9	T	-89.5
		ψ		136.1		146.0		143.5		141.7		149.4		134.0
		χ1		177.0		179.4		176.3		175.6		169.6		57.4
		χ2		65.2		60.6		59.0		57.5		73.2		-179.7
	114'	ϕ	R	-66.7	R	-71.5	R	-78.0	R	-75.1	R	-117.0	I	-57.9
		ψ		-47.0		-53.7		-59.3		-57.1		-31.9		-32.2
		χ1		-99.1		-145.6		-93.4		177.5		-168.1		-162.1
		χ2		-173.1		-179.8		-171.5		-159.7		86.5		87.9
		χ3		170.4		-173.6		-172.9		58.1		-73.8		-

		χ4		138.4		140.3		141.5		124.7		173.4	-
	115'	ϕ	K	-163.2	K	-162.1	K	-167.1	K	-163.0	K	-133.4	K -167.7
		ψ		110.6		132.0		153.3		157.6		141.7	126.1
		χ1		-139.8		-143.3		-140.1		-137.8		-164.0	-142.2
		χ2		78.7		81.7		85.0		79.3		172.4	83.5
		χ3		-96.4		-97.9		-95.8		-97.4		133.9	-100.4
		χ4		129.5		120.9		131.0		133.6		-73.6	109.2
		χ5		-39.1		-35.6		-47.7		-44.1		9.6	-9.5
	116'	ϕ	A	-60.5	A	-69.6	A	-58.2	A	-63.9	A	-51.6	R -61.4
		ψ		-47.5		-40.7		-47.5		-42.4		-45.3	-39.3
		χ1		-		-		-		-		-	-80.9
		χ2		-		-		-		-		-	-173.4
		χ3		-		-		-		-		-	174.3
		χ4		-		-		-		-		-	129.6
	117'	ϕ	V	-71.8	T	-85.5	T	-64.6	V	-41.0	T	-114.6	G -73.3
		ψ		112.0		116.4		108.2		130.2		168.4	77.3
		χ1		-74.3		53.4		50.9		-66.2		57.2	-
		χ2		-		60.5		58.0		-		-170.5	-
	118'	ϕ	R	-93.8	R	-118.2	R	-58.5	R	-125.2	R	-51.5	R -49.0
		ψ		-57.9		-48.4		-37.6		141.3		-56.3	-40.3
		χ1		-104.3		-80.9		-109.5		-126.2		-153.8	-125.9
		χ2		79.1		109.1		73.3		106.7		88.0	98.0
		χ3		147.7		116.1		-76.3		-78.8		-74.9	-76.6
		χ4		147.0		116.1		-87.2		-98.5		-125.9	-111.5

*Torsional angles are designated according to the IUPAC-IUB rules (1970).

Table 2. Residues of BDNF and NGF defining the surfaces of their central β-strand stems, the side-chain thermal motion of which is taken into account when optimizing the structures of the complexes with the LRM-2B.

BDNF		NGF	
Ile^{16}	Lys^{57}	-	Lys^{57}
Glu^{18}	Asn^{59}	Val^{18}	Arg^{59}
Val^{20}	Met^{61}	Val^{20}	Ser^{61}
Thr^{21}	Lys^{65}	Val^{22}	-
Asp^{24}	Gln^{79}	Asp^{24}	Tyr^{79}
Lys^{25}	Arg^{81}	Lys^{25}	Thr^{81}
Lys^{26}	Thr^{82}	Thr^{26}	Thr^{82}
Thr^{27}	Gln^{84}	Thr^{27}	His^{84}
Val^{29}	Tyr^{86}	Thr^{29}	Phe^{86}
Thr^{35}	Arg^{104}	Glu^{35}	Arg^{103}
Glu^{55}	Asp^{106}	Glu^{55}	Asp^{105}

Table 3. Components of the molecular mechanical potential energy of the intermolecular NGF/LRM-2A interactions (in kcal/mol)

Term	hNGF	mNGF	mNGFΔ3-9	hNGF:NT-4/5
E_w	-61.2	-57.9	-39.3	-65.1
E_e	-96.2	-87.9	-99.0	-65.2
E_{hb}	-7.4	-5.9 -3.1	-4.6	
E_{qq}	-0.3	-0.3 -0.1	-0.1	
Total	-165.1	-152.0	-141.5	-135.1

Table 4. Components of th mol cular mechanical pot ntial nergy of the BDNF/LRM-2B and the NGF/LRM-2B complexes (in kcal/mol)

A. Components of the potential energy

	BDNF/LRM-2B	NGF/LRM-2B	Difference*
E_w	89.3	82.3	-7.0
E_{el}	-183.8	-93.1	**90.7**
E_{hb}	-31.0	-21.5	9.5
Et	114.9	114.0	-0.9
E_{qq}	0.4	0.0	-0.4
Total	-10.2	81.8	**92.0**

B. Components of the intermolecular interactions energy

	BDNF/LRM-2B	NGF/LRM-2B	Difference*
E_w	-48.0	-64.9	-16.9
E_{el}	-221.4	-144.2	**77.2**
E_{hb}	-5.6	-4.3	1.3
Total	-275.0	-213.5	61.5

*Difference of the energy terms within the minimum-energy structures of the NGF/LRM-2B and the BDNF/LRM-2B complexes. Underlined values demonstrate that the difference in intermolecular electrostatic interactions dominates in the differences in potential energies of the complexes.

Table 5. Equilibrium variable torsional angles (in degrees) of the amino and carboxyl terminii of the most stable conformations of the uncomplexed (UC) and complexed (C) NGF analogues.*

No.			hNGF			mNGF			mNGFΔ3-9	
			UC	C		UC	C		UC	C
					Amino terminus					
11	ψ	E	82.9	78.2	E	85.9	85.4	E	89.2	96.6
	φ		55.7	60.3		56.3	56.3		57.8	60.3
	χ1		-69.8	-69.3		-72.0	-69.4		-72.1	-73.7
	χ2		72.7	70.2		71.7	71.3		66.0	67.0
	χ3		-120.4	-117.6		-111.7	-117.1		-107.0	-109.2
10	ψ	G	-89.1	-122.1	G	-95.1	-103.2	G	-88.0	-94.8
	φ		-172.5	-166.5		-178.6	174.1		-177.5	168.7
9	ψ	R	-36.1	-25.7	M	-21.1	-14.3	S	146.5	166.1
	φ		-92.8	-84.2		-91.4	-77.3		-103.6	-132.1
	χ1		-77.2	-92.9		-75.2	-84.9		**-66.7**	**-179.1**
	χ2		-173.9	-174.1		-179.7	179.0		**64.0**	**122.2**
	χ3		-175.5	158.1		179.9	171.5		-	-
	χ4		134.3	136.4		-	-		-	-
8	ψ	H	118.6	98.3	H	110.4	96.1	S	**106.1**	**156.1**
	φ		-116.5	-127.3		-110.4	-121.8		52.8	46.0
	χ1		-89.7	-108.0		-90.9	-104.1		-45.9	-35.5
	χ2		-73.8	-87.9		-71.5	-65.8		-172.3	-174.1
7	ψ	F	135.7	113.6	F	129.4	106.7		-	-
	φ		**-68.8**	**-122.4**		**-89.0**	**-130.8**		-	-
	χ1		-171.6	-147.2		-163.9	-143.9		-	-
	χ2		-96.3	-85.8		-91.5	-87.5		-	-
6	ψ	I	40.3	57.9	V	61.7	67.9		-	-
	φ		40.4	38.5		47.7	48.3		-	-
	χ1		-159.7	-165.7		-177.3	-177.3		-	-
	χ2		87.1	88.3		-	-		-	-
5	ψ	P	156.0	164.8	P	149.8	153.3		-	-

	4	ψ	H	121.4	125.4	H	122.1	122.9	-	-
		ϕ		-129.2	-133.8		-129.8	-125.9	-	-
		χ1		-162.5	-163.2		-163.3	-161.8	-	-
		χ2		-69.1	-71.9		-69.2	-69.9	-	-
	3	ψ	S	2.1	-4.9	T	-1.9	-5.1	-	-
		ϕ		-91.9	-78.9		-84.5	-82.3	-	-
		χ1		-171.8	-172.3		-174.9	-171.4	-	-
		χ2		-53.2	-51.2		-51.2	-52.3	-	-
	2	ψ	S	138.5	135.7	S	139.4	139.4	-	-
		ϕ		**-128.9**	**-157.5**		**-114.1**	**-160.3**	-	-
		χ1		173.3	173.4		169.7	170.3	-	-
		χ2		-141.9	-133.0		-139.8	-134.5	-	-
	1	ψ	S	133.0	129.5	S	127.9	128.6	-	-
		ϕ		48.6	46.6		49.4	53.8	-	-
		χ1		-43.2	-41.9		-44.1	-44.0	-	-
		χ2		-171.5	-171.0		-172.4	-170.9	-	-
					Carboxyl terminus					
	112'	ϕ	L	-113.3	-113.1	L	-113.0	-114.1	L -112.4	-113.7
		ψ		98.8	95.5		98.7	99.3	99.2	103.9
		χ1		-72.3	-72.1		-71.6	-72.1	-71.6	-72.1
		χ2		163.7	163.2		163.0	164.1	162.6	163.8
	113'	ϕ	S	-83.4	-72.5	S	-77.2	-70.5	S -77.4	-63.0
		ψ		136.1	147.9		146.0	148.6	143.5	145.8
		χ1		177.0	179.1		179.4	-177.9	176.3	-177.0
		χ2		65.2	56.0		60.6	56.3	59.0	52.4
	114'	ϕ	R	-66.7	-101.6	R	-71.5	-92.5	R -78.0	-92.3
		ψ		-47.0	-41.9		-53.7	-43.8	-59.3	-50.4
		χ1		**-99.1**	**-175.3**		**-145.6**	**-173.2**	**-93.4**	**-167.4**
		χ2		**-173.1**	**-130.0**		**-179.8**	**-114.8**	**-171.5**	**-101.4**
		χ3		170.4	159.9		-173.6	151.4	-172.9	172.3
		χ4		**138.4**	**-117.4**		**140.3**	**-139.0**	**141.5**	**-130.9**
	115'	ϕ	K	-163.2	-155.3	K	-162.1	-152.2	K -167.1	-161.4
		ψ		110.6	111.2		132.0	111.0	153.3	132.6

	$\chi 1$		-139.8	-150.7		-143.3	-156.2	-140.1	-144.6
	$\chi 2$		**78.7**	**-170.9**		**81.7**	**-170.0**	**85.0**	**-177.7**
	$\chi 3$		**-96.4**	**177.2**		**-97.9**	**-174.3**	**-95.8**	**-169.3**
	$\chi 4$		**129.5**	**-165.4**		**120.9**	**-173.7**	**131.0**	**175.4**
	$\chi 5$		-39.1	-63.2		-35.6	-61.4	-47.7	-53.3
116'	ϕ	A	-60.5	-62.3	A	-69.6	-61.7	A -58.2	-67.9
	ψ		-47.5	-43.9		-40.7	-47.8	-47.5	-40.4
117'	ϕ	V	-71.8	-106.1	T	-85.5	-106.0	T -64.6	-74.3
	ψ		112.0	107.0		116.4	98.5	108.2	107.7
	$\chi 1$		-74.3	-75.0		53.4	55.1	50.9	56.6
	$\chi 2$		-	-		60.5	63.2	58.0	54.0
118'	ϕ	R	-93.8	-58.0	R	**-118.2**	**-58.4**	R -58.5	-79.4
	ψ		-57.9	-53.7		-48.4	-59.7	-37.6	-49.6
	$\chi 1$		-104.3	-88.5		-80.9	-84.7	-109.5	-135.3
	$\chi 2$		79.1	74.4		109.1	79.7	73.3	108.0
	$\chi 3$		147.7	161.4		116.1	147.5	-76.3	-70.1
	$\chi 4$		147.0	119.7		116.1	118.7	-87.2	-135.3

*Torsional angles are designated according to the IUPAC-IUB rules (1970). Torsional angles undergoing considerable changes upon LRM-2A binding are shown in bold.

Table 6. Optimized conformational variables (in degre s) of hNGF-complexed LRM-2A.*

No.	Type	ϕ	ψ	$\chi 1$	$\chi 2$	$\chi 3$	$\chi 4$	$\chi 5$
94tA	Arg	-161.6	-62.5	-169.2	-164.9	66.8	172.2	
95tA	Asn	-114.1	132.0	33.0	-111.6			
96tA	Leu	-131.9	114.2	-161.2	141.1			
97tA	Thr	-145.0	125.0	-179.9	-176.6			
98tA	Ile	-123.1	21.6	61.3	105.7			
99tA	Val	-61.2	107.3	175.7				
100tA	Lys	54.4	40.8	-75.6	161.7	-174.8	166.2	-41.3
101tA	Ser	-97.4	-40.0	-176.4	167.7			
102tA	Gly	144.4	46.5					
103tA	Leu	-135.6	155.5	-85.0	90.0			
104tA	Arg	-81.7	179.3	-33.6	165.0	-52.8	-144.7	
105tA	Phe	-68.6	-40.8	-159.4	93.3			
106tA	Val	-106.1	94.3	176.1				
107tA	Ala	-173.5	-54.8					
108tA	Pro		-26.2					
109tA	Asp	-85.5	64.7	-116.1	102.8			
110tA	Ala	-117.5	-57.2					
111tA	Phe	-79.4	135.3	38.4	89.8			
112tA	His	-132.1	78.5	-67.1	89.9			
113tA	Phe	-120.8	-29.0	54.6	95.4			
114tA	Thr	-59.9	-56.0	-23.4	-176.5			
115tA	Pro		-47.9					
116tA	Arg	-150.8	142.7	46.8	98.5	-100.4	155.7	
117tA	Leu	-76.3	-39.4	57.0	117.9			

*Torsional angles are designated according to the IUPAC-IUB rules (1970).

Table 7. Optimized conformational variabl s (in degrees) of BDNF-complexed LRM-2B.*

No.	Type	ϕ	ψ	$\chi 1$	$\chi 2$	$\chi 3$	$\chi 4$	$\chi 5$
94tB	Arg	-109.3	-54.2	-69.7	169.4	-171.6	119.4	
95tB	Asn	-163.6	141.0	-129.4	-109.4			
96tB	Leu	-81.9	86.5	-92.9	-58.2			
97tB	Thr	-138.3	143.5	-177.9	169.6			
98tB	Ile	-136.4	136.6	-164.6	86.9			
99tB	Val	-107.6	151.8	-70.1				
100tB	Asp	-68.8	-72.8	23.6	95.2			
101tB	Ser	36.4	36.0	-156.1	157.6			
102tB	Gly	42.0	44.4					
103tB	Leu	-118.2	149.0	49.9	87.1			
104tB	Lys	-92.9	68.5	-147.2	173.5	91.3	-169.5	45.1
105tB	Phe	73.7	-78.5	-160.5	-111.0			
106tB	Val	52.6	19.9	-174.2				
107tB	Ala	-113.9	26.4					
108tB	Tyr	-58.7	-20.3	-46.5	102.7	-74.2		
109tB	Lys	-71.4	-27.6	62.1	-113.2	176.6	176.6	-55.9
110tB	Ala	-91.7	-32.6					
111tB	Phe	-63.5	-37.4	-168.3	83.6			
112tB	Leu	-60.3	-43.2	-169.7	91.0			
113tB	Lys	-61.5	-48.0	-78.9	152.7	-167.9	63.2	22.9
114tB	Asn	-59.4	-36.6	-70.9	-107.4			
115tB	Ser	-68.6	-32.9	-60.0	68.6			
116tB	Asn	-80.7	-45.4	-83.4	-96.8			
117tB	Leu	-127.8	-58.8	-75.6	105.5			

*Torsional angles are designated according to the IUPAC-IUB rules (1970).

Table 8. Contributions of individual residues to intermolecular electrostatic interaction energies of the complexes BDNF/LRM-2B and NGF/LRM-2B (in kcal/mol)*.

A. Binding epitopes of neurotrophins

BDNF/LRM-2B		NGF/LRM-2B		Difference‡
Glu^{18}	-61.6	Val^{18}	0.3	61.9
Asp^{24}	-65.1	Asp^{24}	-44.9	20.2
Lys^{25}	25.3	Lys25	15.5	-9.8
Gly^{33}	-11.9	Gly^{33}	-13.4	-1.5
Thr^{35}	-11.4	Glu^{35}	-50.5	-39.1
Glu^{55}	-50.2	Glu^{56}	-18.9	31.3
Lys^{57}	27.1	Lys^{57}	22.5	-4.6
Arg^{81}	-32.2	Thr^{81}	0.1	32.3
Gln^{84}	1.2	His^{84}	11.5	10.3
Arg^{104}	-14.3	Arg^{103}	-9.5	4.8
Asp^{106}	-39.7	Asp^{105}	-46.4	-6.7
Total	-232.8		-133.7	99.1

B. Binding epitopes of the LRM-2B

BDNF/LRM-2B		NGF/LRM-2B	Difference‡
Arg^{94B}	-40.9	4.2	45.1
Asn^{95B}	0.2	-12.8	-13.0
Asp^{100B}	-42.1	-9.3	32.8
Ser^{101B}	-17.9	-0.1	17.8
Gly^{102B}	-1.3	-12.0	-10.7
Lys^{104B}	-18.5	-48.1	-29.6
Lys^{109B}	-46.4	-21.5	24.9
Lys^{113B}	-54.6	-37.2	17.4
Total	-221.5	-136.8	84.7

*The ±10 kcal/mol cutoff of intermolecular electrostatic interaction energy has been used to identify binding epitopes within the complexes. ‡Difference of the intermolecular electrostatic interaction energies of the given residue within the minimum-energy structures of the NGF/LRM-2B and the BDNF/LRM-2B complexes. Residues within the binding epitopes of BDNF and the LRM-2B which cause their binding specificity are bolded.

Table 9. Contributions of individual residues of th neurotrophins to th intermolecular interaction n rgy of their complex s with the common neurotrophin receptor $p75^{NTR}$ (kcal/mol)*

NGF			BDNF			NT-3			NT-4/5		
Res.	EL	VDW	Res.	EL	VDW	Res.	EL	VDW	Res.	EL	VDW
D-30	17.9	-0.9	**D-30**	25.0	-1.8	**D-29**	24.6	-2.6	**D-32**	19.8	-1.8
K-32	-94.9	-6.0	S-32	0.5	-4.5	**R-31**	-48.2	-8.0	**R-34**	-42.6	-9.3
K-34	-88.8	-3.3	G-34	-1.8	-3.1	**H-33**	-35.0	-7.1	**R-36**	-57.2	-7.7
E-35	-10.0	-2.2	T-35	1.7	-1.4	Q-34	0.5	-2.3	D-37	-0.8	-1.7
H-84	-30.9	-1.0	Q-84	1.19	-2.4	Q-83	0.8	-0.7	Q-83	0.6	-1.0
F-86	-0.2	-0.3	Y-86	-0.5	-0.5	**Y-85**	-13.4	0.3	Y-96	-9.2	-0.3
K-88	-8.5	-0.1	**R-88**	-12.7	-0.2	**R-87**	-20.0	-0.3	**R-98**	-16.2	-0.2
D-93	-9.0	-1.3	**D-93**	13.7	-2.2	**E-92**	24.1	-2.8	D-103	9.0	-2.1
K-95	-63.7	-5.6	**K-95**	-82.9	-7.6	N-94	-0.1	-0.2	Q-105	-0.3	-0.2
Q-96	-0.3	-3.7	**K-96**	-58.2	2.0	**K-95**	-49.6	-2.6	G-106	-0.6	-0.6
A-97	0.2	-0.2	**R-97**	-79.3	-5.7	L-96	-0.5	-6.7	**R-107**	-28.0	-11.2
R-100	-11.8	-0.7	**R-101**	-59.2	-1.1	**R-100**	-79.3	1.7	**R-111**	-57.8	-1.9
R-103	-64.5	0.0	**R-104**	-64.2	-1.6	**R-103**	-51.5	0.6	**R-114**	-55.3	-2.9
D-105	10.6	-0.2	D-106	8.3	-0.2	D-105	5.5	-0.1	D-116	4.8	-0.1
Total	-336.1	-15.6		-317.8	-18.2		-248.3	-15.6		-237.3	-35.0
	100%	55%		99%	39%		97%	32%		102%	61%
Net	-337.3	-32.3		-321.4	-46.7		-254.8	-48.9		-233.0	-57.5

*EL and VDW denote electrostatic and van der Waals terms of the ligand-receptor interaction energy, respectively. The ±10 kcal/mol cutoff of the intermolecular electrostatic interaction energy has been used to identify the functional epitopes (bolded). "Total" electrostatic and van der Waals contributions of the functional epitopes to the "net" values of the intermolecular interaction energy calculated over the whole binding interface are presented. Residue numbering corresponds to the general alignment of neurotrophins (Bradshaw *et al.*, 1994).

Table 10. Contributions of individual residues of $p75^{NTR}$ to the intermolecular interaction energy of their complexes with neurotrophins (kcal/mol)*.

NGF			BDNF			NT-3			NT-4/5		
Res.	EL	VDW	Res.	EL	VDW	Res.	EL	VDW	Res.	EL	VDW
D-47	-46.0	0.2	**D-47**	-67.1	0.1	**D-47**	-50.5	-0.3	**D-47**	-26.7	-4.1
E-53	-2.6	-0.2	**E-53**	-55.4	1.6	E-53	-6.6	-0.2	E-53	-3.6	-0.1
P-54	-12.4	-2.8	**P-54**	-13.5	-2.5	**P-54**	-15.1	0.2	P-54	-5.3	-0.8
C-55	-1.4	-0.9	C-55	-8.4	-1.3	**C-55**	-14.9	-1.0	C-55	-3.0	-1.2
K-56	21.8	-4.5	**K-56**	13.2	-4.8	**K-56**	32.9	-5.0	**K-56**	14.8	-5.8
E-60	-6.2	-0.3	E-60	-3.0	-0.1	**E-60**	-10.0	-0.2	**E-60**	-10.4	-0.4
E-73	-4.2	0.0	E-73	-9.7	-0.2	**E-73**	-12.5	-0.3	**E-73**	-11.2	-0.3
D-75	-56.5	0.6	**D-75**	-77.1	0.4	**D-75**	-65.5	-1.1	**D-75**	-59.4	-2.7
D-76	-91.6	-2.0	**D-76**	-22.3	-8.4	**D-76**	-39.9	-3.7	**D-76**	-39.3	-5.1
R-80	-18.5	-3.9	R-80	2.9	-2.1	R-80	5.3	-4.0	R-80	3.1	-4.3
D-88	-49.1	0.4	**D-88**	-39.8	-0.4	**D-88**	-34.4	0.4	**D-88**	-33.1	-1.2
E-89	-32.5	-1.6	**E-89**	-25.2	-6.2	**E-89**	-33.8	-3.8	**E-89**	-33.0	-5.9
Total	-285.4	-13.6		-287.2	-20.2		-243.7	-14.8		-198.3	-25.5
	84%	42%		89%	43%		96%	30%		85%	44%

*See footnote to Table 9.

Appendix 1. Geometry of the LRM-2A in PDB format.*

```
REMARK  1 The bioactive conformation of the second LRM of TrkA.
REMARK  2    HSC stands for charged HIS
REMARK  3
ATOM      1  N   LEU S  93      19.399 -23.034 -15.306  1.00 -0.45
ATOM      2  CA  LEU S  93      18.757 -22.140 -14.332  1.00 -0.07
ATOM      3  C   LEU S  93      19.555 -20.869 -14.130  1.00  0.53
ATOM      4  O   LEU S  93      20.777 -20.864 -14.044  1.00 -0.50
ATOM      5  CB  LEU S  93      18.635 -22.886 -13.002  1.00  0.02
ATOM      6  CG  LEU S  93      17.661 -22.206 -12.037  1.00  0.05
ATOM      7  CD1 LEU S  93      16.251 -22.083 -12.617  1.00 -0.01
ATOM      8  CD2 LEU S  93      17.517 -22.968 -10.718  1.00 -0.01
ATOM      9 1H   LEU S  93      19.651 -23.930 -14.841  1.00  0.15
ATOM     10 2H   LEU S  93      18.742 -23.223 -16.089  1.00  0.15
ATOM     11 3H   LEU S  93      20.260 -22.582 -15.677  1.00  0.15
ATOM     12  N   ARG S  94      18.551 -20.159 -13.624  1.00 -0.52
ATOM     13  CA  ARG S  94      18.777 -19.044 -12.708  1.00  0.24
ATOM     14  C   ARG S  94      17.460 -18.800 -12.010  1.00  0.53
ATOM     15  O   ARG S  94      17.364 -18.941 -10.781  1.00 -0.50
ATOM     16  CB  ARG S  94      19.316 -17.812 -13.451  1.00  0.05
ATOM     17  CG  ARG S  94      19.818 -16.700 -12.515  1.00  0.06
ATOM     18  CD  ARG S  94      20.009 -15.345 -13.215  1.00  0.11
ATOM     19  NE  ARG S  94      18.720 -14.803 -13.642  1.00 -0.49
ATOM     20  CZ  ARG S  94      18.631 -13.550 -14.138  1.00  0.81
ATOM     21  NH1 ARG S  94      19.703 -12.767 -14.256  1.00 -0.63
ATOM     22  NH2 ARG S  94      17.444 -13.087 -14.518  1.00 -0.63
ATOM     23  H   ARG S  94      17.611 -20.389 -13.873  1.00  0.25
ATOM     24  HE  ARG S  94      17.892 -15.358 -13.571  1.00  0.29
ATOM     25 1HH1 ARG S  94      19.604 -11.843 -14.627  1.00  0.36
ATOM     26 2HH1 ARG S  94      20.606 -13.094 -13.977  1.00  0.36
ATOM     27 1HH2 ARG S  94      17.363 -12.161 -14.887  1.00  0.36
ATOM     28 2HH2 ARG S  94      16.633 -13.666 -14.434  1.00  0.36
ATOM     29  N   ASN S  95      16.446 -18.435 -12.789  1.00 -0.52
ATOM     30  CA  ASN S  95      15.116 -18.165 -12.251  1.00  0.22
ATOM     31  C   ASN S  95      14.111 -19.178 -12.745  1.00  0.53
```

```
ATOM   32  O   ASN S  95      14.047 -19.466 -13.950  1.00 -0.50
ATOM   33  CB  ASN S  95      14.629 -16.742 -12.566  1.00  0.00
ATOM   34  CG  ASN S  95      15.171 -16.300 -13.911  1.00  0.68
ATOM   35  OD1 ASN S  95      16.007 -15.410 -13.997  1.00 -0.47
ATOM   36  ND2 ASN S  95      14.657 -16.965 -14.959  1.00 -0.87
ATOM   37  H   ASN S  95      16.591 -18.340 -13.774  1.00  0.25
ATOM   38 1HD2 ASN S  95      14.948 -16.750 -15.892  1.00  0.34
ATOM   39 2HD2 ASN S  95      13.976 -17.684 -14.820  1.00  0.34
ATOM   40  N   LEU S  96      13.325 -19.720 -11.819  1.00 -0.52
ATOM   41  CA  LEU S  96      12.308 -20.713 -12.151  1.00  0.20
ATOM   42  C   LEU S  96      11.023 -20.296 -11.479  1.00  0.53
ATOM   43  O   LEU S  96      10.934 -20.287 -10.242  1.00 -0.50
ATOM   44  CB  LEU S  96      12.767 -22.109 -11.701  1.00  0.02
ATOM   45  CG  LEU S  96      12.022 -23.268 -12.383  1.00  0.05
ATOM   46  CD1 LEU S  96      12.921 -24.464 -12.732  1.00 -0.01
ATOM   47  CD2 LEU S  96      10.797 -23.704 -11.562  1.00 -0.01
ATOM   48  H   LEU S  96      13.428 -19.444 -10.863  1.00  0.25
ATOM   49  N   THR S  97      10.026 -19.951 -12.289  1.00 -0.52
ATOM   50  CA  THR S  97       8.726 -19.526 -11.778  1.00  0.27
ATOM   51  C   THR S  97       7.604 -19.988 -12.678  1.00  0.53
ATOM   52  O   THR S  97       7.607 -19.702 -13.884  1.00 -0.50
ATOM   53  CB  THR S  97       8.692 -18.000 -11.598  1.00  0.21
ATOM   54  OG1 THR S  97       7.420 -17.594 -11.097  1.00 -0.55
ATOM   55  CG2 THR S  97       9.014 -17.248 -12.899  1.00  0.01
ATOM   56  H   THR S  97      10.163 -19.980 -13.279  1.00  0.25
ATOM   57  HG1 THR S  97       7.431 -16.635 -11.053  1.00  0.31
ATOM   58  N   ILE S  98       6.645 -20.701 -12.095  1.00 -0.52
ATOM   59  CA  ILE S  98       5.499 -21.213 -12.841  1.00  0.20
ATOM   60  C   ILE S  98       4.166 -20.765 -12.292  1.00  0.53
ATOM   61  O   ILE S  98       3.134 -21.406 -12.544  1.00 -0.50
ATOM   62  CB  ILE S  98       5.633 -22.735 -13.006  1.00  0.03
ATOM   63  CG1 ILE S  98       5.655 -23.480 -11.662  1.00  0.02
ATOM   64  CG2 ILE S  98       6.841 -23.109 -13.880  1.00  0.00
ATOM   65  CD1 ILE S  98       4.338 -24.216 -11.369  1.00  0.00
ATOM   66  H   ILE S  98       6.703 -20.897 -11.116  1.00  0.25
ATOM   67  N   VAL S  99       4.183 -19.667 -11.541  1.00 -0.52
```

ATOM 68 CA VAL S 99 2.969 -19.119 -10.945 1.00 0.20
ATOM 69 C VAL S 99 1.976 -18.727 -12.013 1.00 0.53
ATOM 70 O VAL S 99 2.172 -17.725 -12.717 1.00 -0.50
ATOM 71 CB VAL S 99 3.389 -17.945 -10.045 1.00 0.03
ATOM 72 CG1 VAL S 99 2.188 -17.207 -9.432 1.00 0.01
ATOM 73 CG2 VAL S 99 4.444 -18.324 -8.993 1.00 0.01
ATOM 74 H VAL S 99 5.050 -19.197 -11.376 1.00 0.25
ATOM 75 N LYS S 100 0.911 -19.514 -12.136 1.00 -0.52
ATOM 76 CA LYS S 100 -0.131 -19.257 -13.126 1.00 0.23
ATOM 77 C LYS S 100 0.517 -19.154 -14.486 1.00 0.53
ATOM 78 O LYS S 100 0.146 -18.291 -15.296 1.00 -0.50
ATOM 79 CB LYS S 100 -0.916 -17.989 -12.753 1.00 0.04
ATOM 80 CG LYS S 100 -1.911 -18.178 -11.597 1.00 0.05
ATOM 81 CD LYS S 100 -2.337 -16.845 -10.961 1.00 0.05
ATOM 82 CE LYS S 100 -3.230 -17.043 -9.726 1.00 0.22
ATOM 83 NZ LYS S 100 -3.328 -15.780 -8.983 1.00 -0.27
ATOM 84 H LYS S 100 0.814 -20.308 -11.536 1.00 0.25
ATOM 85 1HZ LYS S 100 -2.395 -15.321 -8.953 1.00 0.31
ATOM 86 2HZ LYS S 100 -3.649 -15.972 -8.012 1.00 0.31
ATOM 87 3HZ LYS S 100 -4.008 -15.150 -9.454 1.00 0.31
ATOM 88 N SER S 101 1.485 -20.030 -14.739 1.00 -0.52
ATOM 89 CA SER S 101 2.199 -20.048 -16.012 1.00 0.36
ATOM 90 C SER S 101 1.652 -21.075 -16.974 1.00 0.53
ATOM 91 O SER S 101 1.546 -20.813 -18.182 1.00 -0.50
ATOM 92 CB SER S 101 3.695 -20.297 -15.758 1.00 0.19
ATOM 93 OG SER S 101 4.426 -20.237 -16.981 1.00 -0.55
ATOM 94 H SER S 101 1.736 -20.701 -14.041 1.00 0.25
ATOM 95 HG SER S 101 5.354 -20.203 -16.738 1.00 0.31
ATOM 96 N GLY S 102 1.302 -22.243 -16.444 1.00 -0.52
ATOM 97 CA GLY S 102 0.758 -23.329 -17.254 1.00 0.25
ATOM 98 C GLY S 102 1.148 -24.732 -16.854 1.00 0.53
ATOM 99 O GLY S 102 1.526 -25.548 -17.708 1.00 -0.50
ATOM 100 H GLY S 102 1.413 -22.390 -15.461 1.00 0.25
ATOM 101 N LEU S 103 1.058 -25.015 -15.558 1.00 -0.52
ATOM 102 CA LEU S 103 1.402 -26.331 -15.027 1.00 0.20
ATOM 103 C LEU S 103 0.326 -26.726 -14.045 1.00 0.53

ATOM 104 O LEU S 103 -0.356 -25.860 -13.476 1.00 -0.50
ATOM 105 CB LEU S 103 2.792 -26.289 -14.372 1.00 0.02
ATOM 106 CG LEU S 103 3.957 -26.492 -15.354 1.00 0.05
ATOM 107 CD1 LEU S 103 4.502 -25.183 -15.949 1.00 -0.01
ATOM 108 CD2 LEU S 103 5.078 -27.333 -14.723 1.00 -0.01
ATOM 109 H LEU S 103 0.745 -24.311 -14.920 1.00 0.25
ATOM 110 N ARG S 104 0.170 -28.031 -13.843 1.00 -0.52
ATOM 111 CA ARG S 104 -0.832 -28.558 -12.921 1.00 0.24
ATOM 112 C ARG S 104 -0.225 -28.464 -11.541 1.00 0.53
ATOM 113 O ARG S 104 0.920 -28.016 -11.387 1.00 -0.50
ATOM 114 CB ARG S 104 -1.253 -29.984 -13.311 1.00 0.05
ATOM 115 CG ARG S 104 -1.250 -30.233 -14.827 1.00 0.06
ATOM 116 CD ARG S 104 -1.308 -31.721 -15.207 1.00 0.11
ATOM 117 NE ARG S 104 -0.254 -32.467 -14.521 1.00 -0.49
ATOM 118 CZ ARG S 104 0.365 -33.502 -15.129 1.00 0.81
ATOM 119 NH1 ARG S 104 0.042 -33.880 -16.366 1.00 -0.63
ATOM 120 NH2 ARG S 104 1.319 -34.159 -14.478 1.00 -0.63
ATOM 121 H ARG S 104 0.754 -28.678 -14.334 1.00 0.25
ATOM 122 HE ARG S 104 0.018 -32.215 -13.592 1.00 0.29
ATOM 123 1HH1 ARG S 104 0.519 -34.651 -16.789 1.00 0.36
ATOM 124 2HH1 ARG S 104 -0.672 -33.401 -16.875 1.00 0.36
ATOM 125 1HH2 ARG S 104 1.786 -34.927 -14.915 1.00 0.36
ATOM 126 2HH2 ARG S 104 1.569 -33.884 -13.549 1.00 0.36
ATOM 127 N PHE S 105 -0.990 -28.886 -10.538 1.00 -0.52
ATOM 128 CA PHE S 105 -0.535 -28.854 -9.152 1.00 0.21
ATOM 129 C PHE S 105 0.558 -29.894 -9.090 1.00 0.53
ATOM 130 O PHE S 105 1.596 -29.679 -8.447 1.00 -0.50
ATOM 131 CB PHE S 105 -1.656 -29.230 -8.170 1.00 0.04
ATOM 132 CG PHE S 105 -1.354 -28.726 -6.778 1.00 0.01
ATOM 133 CD1 PHE S 105 -1.851 -27.471 -6.366 1.00 -0.01
ATOM 134 CD2 PHE S 105 -0.575 -29.526 -5.913 1.00 -0.01
ATOM 135 CE1 PHE S 105 -1.566 -27.007 -5.067 1.00 0.00
ATOM 136 CE2 PHE S 105 -0.290 -29.063 -4.616 1.00 0.00
ATOM 137 CZ PHE S 105 -0.788 -27.809 -4.206 1.00 0.00
ATOM 138 H PHE S 105 -1.906 -29.236 -10.732 1.00 0.25
ATOM 139 N VAL S 106 0.329 -31.021 -9.758 1.00 -0.52

```
ATOM  140 CA  VAL S 106     1.297 -32.114  -9.787  1.00  0.20
ATOM  141 C   VAL S 106     1.984 -32.186 -11.130  1.00  0.53
ATOM  142 O   VAL S 106     1.469 -32.815 -12.067  1.00 -0.50
ATOM  143 CB  VAL S 106     0.545 -33.403  -9.418  1.00  0.03
ATOM  144 CG1 VAL S 106     1.433 -34.654  -9.506  1.00  0.01
ATOM  145 CG2 VAL S 106    -0.212 -33.313  -8.084  1.00  0.01
ATOM  146 H   VAL S 106    -0.530 -31.131 -10.258  1.00  0.25
ATOM  147 N   ALA S 107     3.145 -31.545 -11.226  1.00 -0.52
ATOM  148 CA  ALA S 107     3.920 -31.529 -12.463  1.00  0.22
ATOM  149 C   ALA S 107     5.237 -30.854 -12.163  1.00  0.53
ATOM  150 O   ALA S 107     6.308 -31.425 -12.415  1.00 -0.50
ATOM  151 CB  ALA S 107     3.199 -30.751 -13.576  1.00  0.03
ATOM  152 H   ALA S 107     3.504 -31.056 -10.432  1.00  0.25
ATOM  153 N   PRO S 108     5.161 -29.640 -11.625  1.00 -0.26
ATOM  154 CA  PRO S 108     6.351 -28.871 -11.283  1.00  0.11
ATOM  155 C   PRO S 108     7.264 -29.638 -10.357  1.00  0.53
ATOM  156 O   PRO S 108     8.481 -29.403 -10.336  1.00 -0.50
ATOM  157 CB  PRO S 108     5.782 -27.574 -10.686  1.00  0.00
ATOM  158 CG  PRO S 108     4.356 -27.900 -10.256  1.00  0.04
ATOM  159 CD  PRO S 108     3.932 -28.917 -11.305  1.00  0.08
ATOM  160 N   ASP S 109     6.680 -30.556  -9.591  1.00 -0.52
ATOM  161 CA  ASP S 109     7.439 -31.374  -8.649  1.00  0.25
ATOM  162 C   ASP S 109     7.956 -32.544  -9.451  1.00  0.53
ATOM  163 O   ASP S 109     7.574 -33.697  -9.200  1.00 -0.50
ATOM  164 CB  ASP S 109     6.510 -31.884  -7.536  1.00 -0.21
ATOM  165 CG  ASP S 109     6.933 -31.318  -6.195  1.00  0.62
ATOM  166 OD1 ASP S 109     6.290 -30.391  -5.711  1.00 -0.71
ATOM  167 OD2 ASP S 109     7.907 -31.800  -5.626  1.00 -0.71
ATOM  168 H   ASP S 109     5.692 -30.697  -9.657  1.00  0.25
ATOM  169 N   ALA S 110     8.824 -32.252 -10.416  1.00 -0.52
ATOM  170 CA  ALA S 110     9.406 -33.282 -11.270  1.00  0.22
ATOM  171 C   ALA S 110    10.898 -33.275 -11.034  1.00  0.53
ATOM  172 O   ALA S 110    11.481 -34.304 -10.662  1.00 -0.50
ATOM  173 CB  ALA S 110     9.132 -33.009 -12.758  1.00  0.03
ATOM  174 H   ALA S 110     9.090 -31.300 -10.566  1.00  0.25
ATOM  175 N   PHE S 111    11.517 -32.118 -11.249  1.00 -0.52
```

ATOM 176 CA PHE S 111 12.956 -31.964 -11.061 1.00 0.21
ATOM 177 C PHE S 111 13.127 -31.810 -9.568 1.00 0.53
ATOM 178 O PHE S 111 12.376 -31.064 -8.923 1.00 -0.50
ATOM 179 CB PHE S 111 13.497 -30.712 -11.770 1.00 0.04
ATOM 180 CG PHE S 111 12.526 -29.559 -11.656 1.00 0.01
ATOM 181 CD1 PHE S 111 12.618 -28.673 -10.561 1.00 -0.01
ATOM 182 CD2 PHE S 111 11.542 -29.391 -12.654 1.00 -0.01
ATOM 183 CE1 PHE S 111 11.710 -27.601 -10.462 1.00 0.00
ATOM 184 CE2 PHE S 111 10.634 -28.321 -12.556 1.00 0.00
ATOM 185 CZ PHE S 111 10.727 -27.436 -11.461 1.00 0.00
ATOM 186 H PHE S 111 10.987 -31.324 -11.549 1.00 0.25
ATOM 187 N HSC S 112 14.112 -32.515 -9.019 1.00 -0.52
ATOM 188 H HSC S 112 14.681 -33.099 -9.597 1.00 0.25
ATOM 189 CA HSC S 112 14.393 -32.465 -7.587 1.00 0.19
ATOM 190 CB HSC S 112 13.775 -33.685 -6.885 1.00 0.21
ATOM 191 CG HSC S 112 12.263 -33.637 -6.920 1.00 0.10
ATOM 192 CD2 HSC S 112 11.396 -33.062 -5.986 1.00 0.35
ATOM 193 ND1 HSC S 112 11.533 -34.176 -7.915 1.00 -0.61
ATOM 194 HD1 HSC S 112 11.881 -34.643 -8.703 1.00 0.48
ATOM 195 CE1 HSC S 112 10.215 -33.947 -7.619 1.00 0.72
ATOM 196 NE2 HSC S 112 10.132 -33.262 -6.434 1.00 -0.69
ATOM 197 HE2 HSC S 112 9.308 -32.971 -5.991 1.00 0.49
ATOM 198 C HSC S 112 15.841 -32.262 -7.208 1.00 0.53
ATOM 199 O HSC S 112 16.534 -33.221 -6.836 1.00 -0.50
ATOM 200 N PHE S 113 16.299 -31.017 -7.301 1.00 -0.52
ATOM 201 CA PHE S 113 17.678 -30.673 -6.967 1.00 0.21
ATOM 202 C PHE S 113 17.554 -29.654 -5.860 1.00 0.53
ATOM 203 O PHE S 113 18.444 -29.545 -5.003 1.00 -0.50
ATOM 204 CB PHE S 113 18.418 -30.047 -8.160 1.00 0.04
ATOM 205 CG PHE S 113 17.666 -28.854 -8.702 1.00 0.01
ATOM 206 CD1 PHE S 113 18.011 -27.554 -8.270 1.00 -0.01
ATOM 207 CD2 PHE S 113 16.627 -29.064 -9.635 1.00 -0.01
ATOM 208 CE1 PHE S 113 17.306 -26.447 -8.780 1.00 0.00
ATOM 209 CE2 PHE S 113 15.922 -27.959 -10.145 1.00 0.00
ATOM 210 CZ PHE S 113 16.268 -26.661 -9.712 1.00 0.00

```
ATOM   211  H   PHE S 113     15.686 -30.289  -7.608  1.00  0.25
ATOM   212  N   THR S 114     16.454 -28.908  -5.874  1.00 -0.52
ATOM   213  CA  THR S 114     16.200 -27.883  -4.866  1.00  0.27
ATOM   214  C   THR S 114     16.150 -28.477  -3.478  1.00  0.53
ATOM   215  O   THR S 114     16.898 -28.053  -2.585  1.00 -0.50
ATOM   216  CB  THR S 114     14.903 -27.124  -5.185  1.00  0.21
ATOM   217  OG1 THR S 114     14.606 -27.224  -6.576  1.00 -0.55
ATOM   218  CG2 THR S 114     14.967 -25.648  -4.762  1.00  0.01
ATOM   219  H   THR S 114     15.774 -29.046  -6.595  1.00  0.25
ATOM   220  HG1 THR S 114     13.824 -26.691  -6.734  1.00  0.31
ATOM   221  N   PRO S 115     15.270 -29.457  -3.296  1.00 -0.26
ATOM   222  CA  PRO S 115     15.113 -30.124  -2.008  1.00  0.11
ATOM   223  C   PRO S 115     16.420 -30.691  -1.510  1.00  0.53
ATOM   224  O   PRO S 115     16.789 -30.490  -0.343  1.00 -0.50
ATOM   225  CB  PRO S 115     14.024 -31.174  -2.277  1.00  0.00
ATOM   226  CG  PRO S 115     14.008 -31.384  -3.788  1.00  0.04
ATOM   227  CD  PRO S 115     14.364 -29.999  -4.305  1.00  0.08
ATOM   228  N   ARG S 116     17.122 -31.399  -2.390  1.00 -0.52
ATOM   229  CA  ARG S 116     18.405 -32.006  -2.048  1.00  0.24
ATOM   230  C   ARG S 116     19.201 -32.059  -3.330  1.00  0.53
ATOM   231  O   ARG S 116     18.642 -32.307  -4.408  1.00 -0.50
ATOM   232  CB  ARG S 116     18.212 -33.381  -1.388  1.00  0.05
ATOM   233  CG  ARG S 116     17.213 -34.284  -2.128  1.00  0.06
ATOM   234  CD  ARG S 116     17.881 -35.312  -3.055  1.00  0.11
ATOM   235  NE  ARG S 116     17.832 -34.856  -4.444  1.00 -0.49
ATOM   236  CZ  ARG S 116     18.735 -35.300  -5.346  1.00  0.81
ATOM   237  NH1 ARG S 116     19.694 -36.161  -5.009  1.00 -0.63
ATOM   238  NH2 ARG S 116     18.663 -34.866  -6.600  1.00 -0.63
ATOM   239  H   ARG S 116     16.767 -31.523  -3.317  1.00  0.25
ATOM   240  HE  ARG S 116     17.128 -34.209  -4.737  1.00  0.29
ATOM   241 1HH1 ARG S 116     20.347 -36.471  -5.701  1.00  0.36
ATOM   242 2HH1 ARG S 116     19.767 -36.501  -4.072  1.00  0.36
ATOM   243 1HH2 ARG S 116     19.324 -35.186  -7.279  1.00  0.36
ATOM   244 2HH2 ARG S 116     17.947 -34.219  -6.864  1.00  0.36
ATOM   245  N   LEU S 117     20.506 -31.828  -3.216  1.00 -0.52
ATOM   246  CA  LEU S 117     21.399 -31.846  -4.370  1.00  0.23
```

```
ATOM   247  C   LEU S 117     21.643 -33.299  -4.741  1.00  0.50
ATOM   248  O   LEU S 117     21.687 -33.594  -5.933  1.00 -0.25
ATOM   249  CB  LEU S 117     22.706 -31.110  -4.038  1.00  0.02
ATOM   250  CG  LEU S 117     23.454 -31.672  -2.818  1.00  0.05
ATOM   251  CD1 LEU S 117     24.851 -32.222  -3.147  1.00 -0.01
ATOM   252  CD2 LEU S 117     23.506 -30.647  -1.674  1.00 -0.01
ATOM   253  OXT LEU S 117     21.785 -34.114  -3.834  1.00 -0.25
ATOM   254  H   LEU S 117     20.894 -31.634  -2.315  1.00  0.25
END
```

*Principal residues are bolded.

Appendix 2. Geometry of the LRM-2B in PDB format.*

REMARK 1 The bioactive conformation of the second LRM of TrkB.

REMARK 2

ATOM 1 N LEU S 93 -32.287 14.723 17.944 1.00 -0.45
ATOM 2 CA LEU S 93 -33.186 15.831 17.679 1.00 -0.07
ATOM 3 C LEU S 93 -32.411 17.027 17.215 1.00 0.53
ATOM 4 O LEU S 93 -31.203 17.150 17.385 1.00 -0.50
ATOM 5 CB LEU S 93 -33.996 16.167 18.941 1.00 0.02
ATOM 6 CG LEU S 93 -35.339 15.426 19.042 1.00 0.05
ATOM 7 CD1 LEU S 93 -36.286 15.694 17.861 1.00 -0.01
ATOM 8 CD2 LEU S 93 -35.131 13.920 19.266 1.00 -0.01
ATOM 9 1H LEU S 93 -31.777 14.490 17.116 1.00 0.15
ATOM 10 2H LEU S 93 -32.810 13.922 18.239 1.00 0.15
ATOM 11 3H LEU S 93 -31.641 14.971 18.665 1.00 0.15
ATOM 12 N ARG S 94 -33.510 17.650 16.801 1.00 -0.52
ATOM 13 CA ARG S 94 -33.484 19.028 16.320 1.00 0.24
ATOM 14 C ARG S 94 -34.175 19.857 17.377 1.00 0.53
ATOM 15 O ARG S 94 -33.609 20.841 17.874 1.00 -0.50
ATOM 16 CB ARG S 94 -34.128 19.146 14.929 1.00 0.05
ATOM 17 CG ARG S 94 -33.300 18.494 13.811 1.00 0.06
ATOM 18 CD ARG S 94 -34.051 18.379 12.475 1.00 0.11
ATOM 19 NE ARG S 94 -33.282 17.579 11.523 1.00 -0.49
ATOM 20 CZ ARG S 94 -33.792 16.435 11.016 1.00 0.81
ATOM 21 NH1 ARG S 94 -35.003 15.996 11.360 1.00 -0.63
ATOM 22 NH2 ARG S 94 -33.068 15.730 10.153 1.00 -0.63
ATOM 23 H ARG S 94 -34.386 17.167 16.817 1.00 0.25
ATOM 24 HE ARG S 94 -32.370 17.873 11.238 1.00 0.29
ATOM 25 1HH1 ARG S 94 -35.352 15.145 10.968 1.00 0.36
ATOM 26 2HH1 ARG S 94 -35.565 16.510 12.008 1.00 0.36
ATOM 27 1HH2 ARG S 94 -33.433 14.882 9.769 1.00 0.36
ATOM 28 2HH2 ARG S 94 -32.159 16.050 9.887 1.00 0.36
ATOM 29 N ASN S 95 -35.397 19.461 17.721 1.00 -0.52
ATOM 30 CA ASN S 95 -36.183 20.166 18.729 1.00 0.22
ATOM 31 C ASN S 95 -37.332 19.318 19.219 1.00 0.53
ATOM 32 O ASN S 95 -37.969 18.605 18.430 1.00 -0.50
ATOM 33 CB ASN S 95 -36.706 21.522 18.229 1.00 0.00

```
ATOM   34 CG  ASN S  95   -36.363  22.606  19.233  1.00  0.68
ATOM   35 OD1 ASN S  95   -37.231  23.137  19.913  1.00 -0.47
ATOM   36 ND2 ASN S  95   -35.056  22.909  19.294  1.00 -0.87
ATOM   37 H   ASN S  95   -35.797  18.657  17.281  1.00  0.25
ATOM   38 1HD2 ASN S  95   -34.725  23.610  19.925  1.00  0.34
ATOM   39 2HD2 ASN S  95   -34.397  22.435  18.709  1.00  0.34
ATOM   40 N   LEU S  96   -37.598  19.391  20.520  1.00 -0.52
ATOM   41 CA  LEU S  96   -38.679  18.626  21.134  1.00  0.20
ATOM   42 C   LEU S  96   -39.965  19.383  20.901  1.00  0.53
ATOM   43 O   LEU S  96   -40.388  20.181  21.751  1.00 -0.50
ATOM   44 CB  LEU S  96   -38.396  18.419  22.630  1.00  0.02
ATOM   45 CG  LEU S  96   -37.665  17.107  22.956  1.00  0.05
ATOM   46 CD1 LEU S  96   -38.413  15.848  22.489  1.00 -0.01
ATOM   47 CD2 LEU S  96   -36.219  17.129  22.436  1.00 -0.01
ATOM   48 H   LEU S  96   -37.044  19.987  21.103  1.00  0.25
ATOM   49 N   THR S  97   -40.588  19.136  19.753  1.00 -0.52
ATOM   50 CA  THR S  97   -41.840  19.794  19.394  1.00  0.27
ATOM   51 C   THR S  97   -42.809  18.826  18.759  1.00  0.53
ATOM   52 O   THR S  97   -42.400  17.929  18.007  1.00 -0.50
ATOM   53 CB  THR S  97   -41.572  20.990  18.466  1.00  0.21
ATOM   54 OG1 THR S  97   -42.795  21.657  18.160  1.00 -0.55
ATOM   55 CG2 THR S  97   -40.854  20.578  17.171  1.00  0.01
ATOM   56 H   THR S  97   -40.193  18.480  19.110  1.00  0.25
ATOM   57 HG1 THR S  97   -42.562  22.479  17.722  1.00  0.31
ATOM   58 N   ILE S  98   -44.093  19.003  19.059  1.00 -0.52
ATOM   59 CA  ILE S  98   -45.140  18.142  18.518  1.00  0.20
ATOM   60 C   ILE S  98   -46.361  18.894  18.043  1.00  0.53
ATOM   61 O   ILE S  98   -46.834  19.818  18.721  1.00 -0.50
ATOM   62 CB  ILE S  98   -45.444  17.014  19.516  1.00  0.03
ATOM   63 CG1 ILE S  98   -46.244  15.862  18.888  1.00  0.02
ATOM   64 CG2 ILE S  98   -46.123  17.547  20.788  1.00  0.00
ATOM   65 CD1 ILE S  98   -45.346  14.810  18.219  1.00  0.00
ATOM   66 H   ILE S  98   -44.356  19.747  19.673  1.00  0.25
ATOM   67 N   VAL S  99   -46.872  18.500  16.880  1.00 -0.52
ATOM   68 CA  VAL S  99   -48.051  19.135  16.298  1.00  0.20
ATOM   69 C   VAL S  99   -49.253  18.226  16.395  1.00  0.53
```

ATOM 70 O VAL S 99 -49.110 16.994 16.408 1.00 -0.50
ATOM 71 CB VAL S 99 -47.698 19.525 14.854 1.00 0.03
ATOM 72 CG1 VAL S 99 -46.688 20.681 14.780 1.00 0.01
ATOM 73 CG2 VAL S 99 -47.287 18.331 13.978 1.00 0.01
ATOM 74 H VAL S 99 -46.441 17.747 16.383 1.00 0.25
ATOM 75 N ASP S 100 -50.436 18.829 16.461 1.00 -0.52
ATOM 76 CA ASP S 100 -51.684 18.077 16.557 1.00 0.25
ATOM 77 C ASP S 100 -51.849 17.392 15.222 1.00 0.53
ATOM 78 O ASP S 100 -51.673 16.169 15.115 1.00 -0.50
ATOM 79 CB ASP S 100 -52.858 19.041 16.789 1.00 -0.21
ATOM 80 CG ASP S 100 -52.508 20.428 16.287 1.00 0.62
ATOM 81 OD1 ASP S 100 -52.854 20.755 15.156 1.00 -0.71
ATOM 82 OD2 ASP S 100 -51.889 21.189 17.023 1.00 -0.71
ATOM 83 H ASP S 100 -50.481 19.828 16.445 1.00 0.25
ATOM 84 N SER S 101 -52.187 18.177 14.202 1.00 -0.52
ATOM 85 CA SER S 101 -52.382 17.652 12.854 1.00 0.29
ATOM 86 C SER S 101 -53.017 16.282 12.846 1.00 0.53
ATOM 87 O SER S 101 -52.684 15.439 12.000 1.00 -0.50
ATOM 88 CB SER S 101 -51.034 17.621 12.116 1.00 0.19
ATOM 89 OG SER S 101 -51.236 17.656 10.705 1.00 -0.55
ATOM 90 H SER S 101 -52.314 19.157 14.356 1.00 0.25
ATOM 91 HG SER S 101 -50.419 17.987 10.324 1.00 0.31
ATOM 92 N GLY S 102 -53.930 16.058 13.786 1.00 -0.52
ATOM 93 CA GLY S 102 -54.626 14.779 13.900 1.00 0.25
ATOM 94 C GLY S 102 -53.788 13.536 13.720 1.00 0.53
ATOM 95 O GLY S 102 -54.199 12.596 13.024 1.00 -0.50
ATOM 96 H GLY S 102 -54.153 16.782 14.439 1.00 0.25
ATOM 97 N LEU S 103 -52.615 13.527 14.347 1.00 -0.52
ATOM 98 CA LEU S 103 -51.701 12.392 14.263 1.00 0.20
ATOM 99 C LEU S 103 -51.521 11.844 15.658 1.00 0.53
ATOM 100 O LEU S 103 -51.586 12.596 16.643 1.00 -0.50
ATOM 101 CB LEU S 103 -50.367 12.833 13.641 1.00 0.02
ATOM 102 CG LEU S 103 -49.757 14.089 14.284 1.00 0.05
ATOM 103 CD1 LEU S 103 -48.873 13.793 15.505 1.00 -0.01
ATOM 104 CD2 LEU S 103 -49.015 14.944 13.244 1.00 -0.01
ATOM 105 H LEU S 103 -52.343 14.319 14.894 1.00 0.25

```
ATOM  106  N   LYS S 104   -51.296  10.536  15.747  1.00 -0.52
ATOM  107  CA  LYS S 104   -51.102   9.870  17.032  1.00  0.23
ATOM  108  C   LYS S 104   -49.623   9.824  17.329  1.00  0.53
ATOM  109  O   LYS S 104   -49.013   8.744  17.326  1.00 -0.50
ATOM  110  CB  LYS S 104   -51.738   8.471  17.005  1.00  0.04
ATOM  111  CG  LYS S 104   -52.308   8.008  18.355  1.00  0.05
ATOM  112  CD  LYS S 104   -53.074   6.679  18.249  1.00  0.05
ATOM  113  CE  LYS S 104   -52.171   5.461  18.503  1.00  0.22
ATOM  114  NZ  LYS S 104   -52.891   4.233  18.143  1.00 -0.27
ATOM  115  H   LYS S 104   -51.256   9.986  14.913  1.00  0.25
ATOM  116 1HZ  LYS S 104   -53.368   4.364  17.227  1.00  0.31
ATOM  117 2HZ  LYS S 104   -53.600   4.018  18.873  1.00  0.31
ATOM  118 3HZ  LYS S 104   -52.219   3.443  18.071  1.00  0.31
ATOM  119  N   PHE S 105   -49.043  10.993  17.585  1.00 -0.52
ATOM  120  CA  PHE S 105   -47.619  11.101  17.889  1.00  0.21
ATOM  121  C   PHE S 105   -46.933  10.882  16.562  1.00  0.53
ATOM  122  O   PHE S 105   -46.495  11.844  15.914  1.00 -0.50
ATOM  123  CB  PHE S 105   -47.162  10.024  18.886  1.00  0.04
ATOM  124  CG  PHE S 105   -45.861  10.412  19.549  1.00  0.01
ATOM  125  CD1 PHE S 105   -44.683   9.692  19.251  1.00 -0.01
ATOM  126  CD2 PHE S 105   -45.849  11.493  20.457  1.00 -0.01
ATOM  127  CE1 PHE S 105   -43.474  10.058  19.873  1.00  0.00
ATOM  128  CE2 PHE S 105   -44.641  11.860  21.078  1.00  0.00
ATOM  129  CZ  PHE S 105   -43.466  11.139  20.780  1.00  0.00
ATOM  130  H   PHE S 105   -49.592  11.829  17.571  1.00  0.25
ATOM  131  N   VAL S 106   -46.838   9.619  16.156  1.00 -0.52
ATOM  132  CA  VAL S 106   -46.200   9.259  14.893  1.00  0.20
ATOM  133  C   VAL S 106   -44.818   9.859  14.800  1.00  0.53
ATOM  134  O   VAL S 106   -44.261   9.989  13.699  1.00 -0.50
ATOM  135  CB  VAL S 106   -47.136   9.709  13.760  1.00  0.03
ATOM  136  CG1 VAL S 106   -46.649   9.261  12.372  1.00  0.01
ATOM  137  CG2 VAL S 106   -48.612   9.356  14.005  1.00  0.01
ATOM  138  H   VAL S 106   -47.213   8.889  16.726  1.00  0.25
ATOM  139  N   ALA S 107   -44.263  10.225  15.951  1.00 -0.52
ATOM  140  CA  ALA S 107   -42.930  10.820  16.013  1.00  0.22
ATOM  141  C   ALA S 107   -42.034   9.846  16.740  1.00  0.53
```

ATOM 142 O ALA S 107 -41.035 10.247 17.354 1.00 -0.50
ATOM 143 CB ALA S 107 -42.939 12.156 16.772 1.00 0.03
ATOM 144 H ALA S 107 -44.766 10.093 16.805 1.00 0.25
ATOM 145 N TYR S 108 -42.388 8.565 16.671 1.00 -0.52
ATOM 146 CA TYR S 108 -41.616 7.513 17.325 1.00 0.25
ATOM 147 C TYR S 108 -40.181 7.445 16.861 1.00 0.53
ATOM 148 O TYR S 108 -39.320 6.888 17.557 1.00 -0.50
ATOM 149 CB TYR S 108 -42.269 6.142 17.090 1.00 0.02
ATOM 150 CG TYR S 108 -43.761 6.173 17.332 1.00 0.00
ATOM 151 CD1 TYR S 108 -44.625 6.208 16.220 1.00 -0.04
ATOM 152 CD2 TYR S 108 -44.248 6.166 18.656 1.00 -0.04
ATOM 153 CE1 TYR S 108 -46.012 6.237 16.436 1.00 0.10
ATOM 154 CE2 TYR S 108 -45.636 6.196 18.871 1.00 0.10
ATOM 155 CZ TYR S 108 -46.500 6.231 17.759 1.00 -0.12
ATOM 156 OH TYR S 108 -47.863 6.259 17.970 1.00 -0.37
ATOM 157 H TYR S 108 -43.207 8.308 16.159 1.00 0.25
ATOM 158 HH TYR S 108 -48.199 7.127 17.791 1.00 0.34
ATOM 159 N LYS S 109 -39.921 8.011 15.685 1.00 -0.52
ATOM 160 CA LYS S 109 -38.579 8.021 15.112 1.00 0.23
ATOM 161 C LYS S 109 -37.724 8.976 15.910 1.00 0.53
ATOM 162 O LYS S 109 -36.497 8.811 15.985 1.00 -0.50
ATOM 163 CB LYS S 109 -38.641 8.396 13.622 1.00 0.04
ATOM 164 CG LYS S 109 -39.200 9.801 13.345 1.00 0.05
ATOM 165 CD LYS S 109 -40.553 9.764 12.617 1.00 0.05
ATOM 166 CE LYS S 109 -41.148 11.167 12.416 1.00 0.22
ATOM 167 NZ LYS S 109 -42.394 11.066 11.645 1.00 -0.27
ATOM 168 H LYS S 109 -40.662 8.444 15.173 1.00 0.25
ATOM 169 1HZ LYS S 109 -42.761 12.020 11.449 1.00 0.31
ATOM 170 2HZ LYS S 109 -43.099 10.531 12.191 1.00 0.31
ATOM 171 3HZ LYS S 109 -42.209 10.576 10.746 1.00 0.31
ATOM 172 N ALA S 110 -38.368 9.974 16.509 1.00 -0.52
ATOM 173 CA ALA S 110 -37.671 10.972 17.314 1.00 0.22
ATOM 174 C ALA S 110 -37.673 10.482 18.742 1.00 0.53
ATOM 175 O ALA S 110 -36.724 10.741 19.497 1.00 -0.50
ATOM 176 CB ALA S 110 -38.368 12.341 17.251 1.00 0.03
ATOM 177 H ALA S 110 -39.360 10.050 16.409 1.00 0.25

```
ATOM  178  N   PHE S 111   -38.736   9.775  19.114  1.00 -0.52
ATOM  179  CA  PHE S 111   -38.873   9.238  20.465  1.00  0.21
ATOM  180  C   PHE S 111   -37.731   8.259  20.599  1.00  0.53
ATOM  181  O   PHE S 111   -37.123   8.144  21.673  1.00 -0.50
ATOM  182  CB  PHE S 111   -40.207   8.499  20.656  1.00  0.04
ATOM  183  CG  PHE S 111   -40.461   8.200  22.115  1.00  0.01
ATOM  184  CD1 PHE S 111   -41.035   9.191  22.942  1.00 -0.01
ATOM  185  CD2 PHE S 111   -40.116   6.930  22.626  1.00 -0.01
ATOM  186  CE1 PHE S 111   -41.269   8.906  24.301  1.00  0.00
ATOM  187  CE2 PHE S 111   -40.349   6.645  23.983  1.00  0.00
ATOM  188  CZ  PHE S 111   -40.924   7.636  24.807  1.00  0.00
ATOM  189  H   PHE S 111   -39.467   9.602  18.455  1.00  0.25
ATOM  190  N   LEU S 112   -37.439   7.552  19.511  1.00 -0.52
ATOM  191  CA  LEU S 112   -36.360   6.568  19.494  1.00  0.20
ATOM  192  C   LEU S 112   -35.074   7.293  19.811  1.00  0.53
ATOM  193  O   LEU S 112   -34.249   6.798  20.594  1.00 -0.50
ATOM  194  CB  LEU S 112   -36.305   5.868  18.127  1.00  0.02
ATOM  195  CG  LEU S 112   -35.374   4.646  18.082  1.00  0.05
ATOM  196  CD1 LEU S 112   -36.074   3.321  18.421  1.00 -0.01
ATOM  197  CD2 LEU S 112   -34.628   4.563  16.740  1.00 -0.01
ATOM  198  H   LEU S 112   -37.970   7.692  18.675  1.00  0.25
ATOM  199  N   LYS S 113   -34.900   8.464  19.205  1.00 -0.52
ATOM  200  CA  LYS S 113   -33.705   9.275  19.417  1.00  0.23
ATOM  201  C   LYS S 113   -33.633   9.650  20.878  1.00  0.53
ATOM  202  O   LYS S 113   -32.578   9.508  21.513  1.00 -0.50
ATOM  203  CB  LYS S 113   -33.728  10.505  18.496  1.00  0.04
ATOM  204  CG  LYS S 113   -33.318  10.217  17.043  1.00  0.05
ATOM  205  CD  LYS S 113   -33.954  11.198  16.045  1.00  0.05
ATOM  206  CE  LYS S 113   -33.790  10.739  14.587  1.00  0.22
ATOM  207  NZ  LYS S 113   -34.498   9.467  14.390  1.00 -0.27
ATOM  208  H   LYS S 113   -35.605   8.807  18.585  1.00  0.25
ATOM  209 1HZ  LYS S 113   -35.239   9.365  15.113  1.00  0.31
ATOM  210 2HZ  LYS S 113   -33.826   8.678  14.472  1.00  0.31
ATOM  211 3HZ  LYS S 113   -34.933   9.453  13.446  1.00  0.31
ATOM  212  N   ASN S 114   -34.754  10.128  21.412  1.00 -0.52
ATOM  213  CA  ASN S 114   -34.832  10.531  22.813  1.00  0.22
```

```
ATOM  214  C   ASN S 114    -34.508   9.379  23.733  1.00  0.53
ATOM  215  O   ASN S 114    -33.878   9.570  24.784  1.00 -0.50
ATOM  216  CB  ASN S 114    -36.198  11.131  23.180  1.00  0.00
ATOM  217  CG  ASN S 114    -36.349  12.495  22.535  1.00  0.68
ATOM  218  OD1 ASN S 114    -37.101  12.669  21.585  1.00 -0.47
ATOM  219  ND2 ASN S 114    -35.597  13.457  23.097  1.00 -0.87
ATOM  220  H   ASN S 114    -35.572  10.217  20.844  1.00  0.25
ATOM  221 1HD2 ASN S 114    -35.623  14.393  22.746  1.00  0.34
ATOM  222 2HD2 ASN S 114    -35.002  13.248  23.873  1.00  0.34
ATOM  223  N   SER S 115    -34.937   8.182  23.342  1.00 -0.52
ATOM  224  CA  SER S 115    -34.696   6.977  24.131  1.00  0.29
ATOM  225  C   SER S 115    -33.240   6.580  24.160  1.00  0.53
ATOM  226  O   SER S 115    -32.755   6.037  25.165  1.00 -0.50
ATOM  227  CB  SER S 115    -35.553   5.825  23.584  1.00  0.19
ATOM  228  OG  SER S 115    -36.939   6.156  23.655  1.00 -0.55
ATOM  229  H   SER S 115    -35.440   8.096  22.482  1.00  0.25
ATOM  230  HG  SER S 115    -37.081   6.859  23.017  1.00  0.31
ATOM  231  N   ASN S 116    -32.540   6.850  23.062  1.00 -0.52
ATOM  232  CA  ASN S 116    -31.121   6.522  22.949  1.00  0.22
ATOM  233  C   ASN S 116    -30.264   7.559  23.632  1.00  0.53
ATOM  234  O   ASN S 116    -29.329   7.216  24.372  1.00 -0.50
ATOM  235  CB  ASN S 116    -30.671   6.343  21.490  1.00  0.00
ATOM  236  CG  ASN S 116    -30.988   4.935  21.025  1.00  0.68
ATOM  237  OD1 ASN S 116    -30.139   4.053  21.046  1.00 -0.47
ATOM  238  ND2 ASN S 116    -32.252   4.764  20.603  1.00 -0.87
ATOM  239  H   ASN S 116    -32.991   7.290  22.286  1.00  0.25
ATOM  240 1HD2 ASN S 116    -32.564   3.872  20.275  1.00  0.34
ATOM  241 2HD2 ASN S 116    -32.898   5.528  20.611  1.00  0.34
ATOM  242  N   LEU S 117    -30.578   8.828  23.387  1.00 -0.52
ATOM  243  CA  LEU S 117    -29.835   9.937  23.980  1.00  0.23
ATOM  244  C   LEU S 117    -30.840  10.862  24.645  1.00  0.50
ATOM  245  O   LEU S 117    -31.725  11.354  23.951  1.00 -0.25
ATOM  246  CB  LEU S 117    -29.015  10.660  22.900  1.00  0.02
ATOM  247  CG  LEU S 117    -27.751   9.905  22.458  1.00  0.05
ATOM  248  CD1 LEU S 117    -27.875   9.246  21.075  1.00 -0.01
ATOM  249  CD2 LEU S 117    -26.506  10.802  22.546  1.00 -0.01
```

ATOM 250 OXT LEU S 117 -30.723 11.077 25.849 1.00 -0.25

ATOM 251 H LEU S 117 -31.344 9.038 22.780 1.00 0.25

END

*Principal residues are bolded.

Appendix 3. Geometry of the $p75^{NTR}$ binding site for neurotrophins in PDB format.*

```
REMARK   1 Second CRD of p75NTR, bound to NGF.
REMARK   2
ATOM      1  N   CYS R  39     -32.488 -11.161   6.915  1.00  0.00
ATOM      2  CA  CYS R  39     -33.024  -9.817   7.111  1.00  0.00
ATOM      3  C   CYS R  39     -33.595  -9.148   5.878  1.00  0.00
ATOM      4  O   CYS R  39     -34.221  -8.095   5.967  1.00  0.00
ATOM      5  CB  CYS R  39     -31.991  -8.907   7.780  1.00  0.00
ATOM      6  SG  CYS R  39     -30.272  -9.354   7.401  1.00  0.00
ATOM      7 1H   CYS R  39     -31.698 -11.178   6.287  1.00  0.00
ATOM      8 2H   CYS R  39     -32.170 -11.586   7.775  1.00  0.00
ATOM      9 3H   CYS R  39     -33.166 -11.799   6.523  1.00  0.00
ATOM     10  N   LEU R  40     -33.398  -9.779   4.707  1.00  0.00
ATOM     11  CA  LEU R  40     -34.095  -9.260   3.530  1.00  0.00
ATOM     12  C   LEU R  40     -35.322 -10.097   3.220  1.00  0.00
ATOM     13  O   LEU R  40     -36.442  -9.632   3.041  1.00  0.00
ATOM     14  CB  LEU R  40     -33.148  -9.230   2.327  1.00  0.00
ATOM     15  CG  LEU R  40     -31.880  -8.404   2.561  1.00  0.00
ATOM     16  CD1 LEU R  40     -30.862  -8.604   1.438  1.00  0.00
ATOM     17  CD2 LEU R  40     -32.184  -6.924   2.806  1.00  0.00
ATOM     18  H   LEU R  40     -32.867 -10.625   4.675  1.00  0.00
ATOM     19  N   ASP R  41     -35.034 -11.407   3.188  1.00  0.00
ATOM     20  CA  ASP R  41     -36.070 -12.408   2.947  1.00  0.00
ATOM     21  C   ASP R  41     -35.822 -13.609   3.848  1.00  0.00
ATOM     22  O   ASP R  41     -34.792 -13.673   4.525  1.00  0.00
ATOM     23  CB  ASP R  41     -36.054 -12.772   1.449  1.00  0.00
ATOM     24  CG  ASP R  41     -37.195 -13.703   1.074  1.00  0.00
ATOM     25  OD1 ASP R  41     -38.299 -13.520   1.568  1.00  0.00
ATOM     26  OD2 ASP R  41     -36.979 -14.633   0.314  1.00  0.00
ATOM     27  H   ASP R  41     -34.111 -11.739   3.385  1.00  0.00
ATOM     28  N   SER R  42     -36.757 -14.563   3.825  1.00  0.00
ATOM     29  CA  SER R  42     -36.565 -15.812   4.545  1.00  0.00
ATOM     30  C   SER R  42     -35.305 -16.572   4.150  1.00  0.00
ATOM     31  O   SER R  42     -34.755 -17.350   4.918  1.00  0.00
```

```
ATOM   32  CB  SER R 42    -37.816 -16.678   4.398  1.00  0.00
ATOM   33  OG  SER R 42    -38.988 -15.930   4.780  1.00  0.00
ATOM   34  H   SER R 42    -37.497 -14.449   3.168  1.00  0.00
ATOM   35  HG  SER R 42    -39.404 -15.604   3.984  1.00  0.00
ATOM   36  N   VAL R 43    -34.794 -16.284   2.940  1.00  0.00
ATOM   37  CA  VAL R 43    -33.503 -16.883   2.574  1.00  0.00
ATOM   38  C   VAL R 43    -32.270 -16.339   3.305  1.00  0.00
ATOM   39  O   VAL R 43    -31.128 -16.743   3.081  1.00  0.00
ATOM   40  CB  VAL R 43    -33.300 -16.823   1.054  1.00  0.00
ATOM   41  CG1 VAL R 43    -34.389 -17.623   0.337  1.00  0.00
ATOM   42  CG2 VAL R 43    -33.208 -15.383   0.537  1.00  0.00
ATOM   43  H   VAL R 43    -35.321 -15.679   2.336  1.00  0.00
ATOM   44  N   THR R 44    -32.539 -15.360   4.166  1.00  0.00
ATOM   45  CA  THR R 44    -31.443 -14.732   4.879  1.00  0.00
ATOM   46  C   THR R 44    -31.701 -14.680   6.367  1.00  0.00
ATOM   47  O   THR R 44    -32.659 -14.063   6.830  1.00  0.00
ATOM   48  CB  THR R 44    -31.171 -13.339   4.300  1.00  0.00
ATOM   49  OG1 THR R 44    -32.382 -12.578   4.130  1.00  0.00
ATOM   50  CG2 THR R 44    -30.430 -13.431   2.962  1.00  0.00
ATOM   51  H   THR R 44    -33.481 -15.090   4.359  1.00  0.00
ATOM   52  HG1 THR R 44    -33.031 -12.981   4.718  1.00  0.00
ATOM   53  N   PHE R 45    -30.805 -15.368   7.080  1.00  0.00
ATOM   54  CA  PHE R 45    -30.829 -15.256   8.526  1.00  0.00
ATOM   55  C   PHE R 45    -30.085 -13.996   8.932  1.00  0.00
ATOM   56  O   PHE R 45    -29.293 -13.430   8.175  1.00  0.00
ATOM   57  CB  PHE R 45    -30.243 -16.531   9.157  1.00  0.00
ATOM   58  CG  PHE R 45    -30.514 -16.587  10.647  1.00  0.00
ATOM   59  CD1 PHE R 45    -31.844 -16.581  11.126  1.00  0.00
ATOM   60  CD2 PHE R 45    -29.423 -16.628  11.539  1.00  0.00
ATOM   61  CE1 PHE R 45    -32.085 -16.592  12.512  1.00  0.00
ATOM   62  CE2 PHE R 45    -29.661 -16.637  12.927  1.00  0.00
ATOM   63  CZ  PHE R 45    -30.989 -16.611  13.400  1.00  0.00
ATOM   64  H   PHE R 45    -30.025 -15.788   6.623  1.00  0.00
ATOM   65  N   SER R 46    -30.382 -13.575  10.161  1.00  0.00
ATOM   66  CA  SER R 46    -29.961 -12.259  10.626  1.00  0.00
ATOM   67  C   SER R 46    -28.732 -12.274  11.517  1.00  0.00
```

```
ATOM   68 O   SER R 46   -28.497 -11.407  12.346 1.00 0.00
ATOM   69 CB  SER R 46   -31.156 -11.630  11.337 1.00 0.00
ATOM   70 OG  SER R 46   -31.890 -12.664  12.026 1.00 0.00
ATOM   71 H   SER R 46   -31.046 -14.080  10.714 1.00 0.00
ATOM   72 HG  SER R 46   -32.811 -12.512  11.820 1.00 0.00
ATOM   73 N   ASP R 47   -27.906 -13.314  11.317 1.00 0.00
ATOM   74 CA  ASP R 47   -26.772 -13.543  12.226 1.00 0.00
ATOM   75 C   ASP R 47   -25.567 -12.610  12.077 1.00 0.00
ATOM   76 O   ASP R 47   -24.410 -13.027  12.086 1.00 0.00
ATOM   77 CB  ASP R 47   -26.337 -15.025  12.168 1.00 0.00
ATOM   78 CG  ASP R 47   -25.807 -15.429  10.794 1.00 0.00
ATOM   79 OD1 ASP R 47   -26.456 -15.180   9.790 1.00 0.00
ATOM   80 OD2 ASP R 47   -24.712 -15.961  10.694 1.00 0.00
ATOM   81 H   ASP R 47   -28.048 -13.919  10.531 1.00 0.00
ATOM   82 N   VAL R 48   -25.857 -11.312  11.875 1.00 0.00
ATOM   83 CA  VAL R 48   -24.733 -10.395  11.691 1.00 0.00
ATOM   84 C   VAL R 48   -24.130  -9.906  13.003 1.00 0.00
ATOM   85 O   VAL R 48   -22.914  -9.763  13.131 1.00 0.00
ATOM   86 CB  VAL R 48   -25.108  -9.258  10.720 1.00 0.00
ATOM   87 CG1 VAL R 48   -26.299  -8.421  11.194 1.00 0.00
ATOM   88 CG2 VAL R 48   -23.886  -8.416  10.349 1.00 0.00
ATOM   89 H   VAL R 48   -26.767 -10.954  12.073 1.00 0.00
ATOM   90 N   VAL R 49   -25.034  -9.713  13.984 1.00 0.00
ATOM   91 CA  VAL R 49   -24.767  -9.685  15.431 1.00 0.00
ATOM   92 C   VAL R 49   -23.506  -9.045  16.022 1.00 0.00
ATOM   93 O   VAL R 49   -23.103  -9.361  17.142 1.00 0.00
ATOM   94 CB  VAL R 49   -25.003 -11.080  16.043 1.00 0.00
ATOM   95 CG1 VAL R 49   -26.440 -11.541  15.783 1.00 0.00
ATOM   96 CG2 VAL R 49   -23.973 -12.125  15.594 1.00 0.00
ATOM   97 H   VAL R 49   -25.987  -9.707  13.681 1.00 0.00
ATOM   98 N   SER R 50   -22.912  -8.118  15.261 1.00 0.00
ATOM   99 CA  SER R 50   -21.729  -7.376  15.719 1.00 0.00
ATOM  100 C   SER R 50   -21.546  -6.123  14.873 1.00 0.00
ATOM  101 O   SER R 50   -21.505  -4.977  15.336 1.00 0.00
ATOM  102 CB  SER R 50   -20.431  -8.205  15.623 1.00 0.00
ATOM  103 OG  SER R 50   -20.525  -9.489  16.273 1.00 0.00
```

```
ATOM  104  H  SER R  50    -23.312  -7.897  14.372  1.00  0.00
ATOM  105  HG SER R  50    -21.302  -9.403  16.827  1.00  0.00
ATOM  106  N  ALA R  51    -21.454  -6.446  13.572  1.00  0.00
ATOM  107  CA ALA R  51    -21.546  -5.403  12.562  1.00  0.00
ATOM  108  C  ALA R  51    -23.013  -5.196  12.263  1.00  0.00
ATOM  109  O  ALA R  51    -23.862  -5.866  12.848  1.00  0.00
ATOM  110  CB ALA R  51    -20.808  -5.825  11.288  1.00  0.00
ATOM  111  H  ALA R  51    -21.633  -7.392  13.330  1.00  0.00
ATOM  112  N  THR R  52    -23.266  -4.259  11.348  1.00  0.00
ATOM  113  CA THR R  52    -24.606  -3.698  11.228  1.00  0.00
ATOM  114  C  THR R  52    -25.679  -4.557  10.579  1.00  0.00
ATOM  115  O  THR R  52    -26.564  -5.091  11.239  1.00  0.00
ATOM  116  CB THR R  52    -24.481  -2.344  10.532  1.00  0.00
ATOM  117  OG1 THR R  52   -23.205  -1.766  10.845  1.00  0.00
ATOM  118  CG2 THR R  52   -25.624  -1.389  10.891  1.00  0.00
ATOM  119  H  THR R  52    -22.533  -3.835  10.820  1.00  0.00
ATOM  120  HG1 THR R  52   -23.136  -0.977  10.314  1.00  0.00
ATOM  121  N  GLU R  53    -25.602  -4.625   9.241  1.00  0.00
ATOM  122  CA GLU R  53    -26.765  -5.151   8.526  1.00  0.00
ATOM  123  C  GLU R  53    -26.656  -6.149   7.362  1.00  0.00
ATOM  124  O  GLU R  53    -27.702  -6.492   6.808  1.00  0.00
ATOM  125  CB GLU R  53    -27.678  -3.966   8.146  1.00  0.00
ATOM  126  CG GLU R  53    -27.452  -3.289   6.779  1.00  0.00
ATOM  127  CD GLU R  53    -25.983  -3.036   6.488  1.00  0.00
ATOM  128  OE1 GLU R  53   -25.530  -3.408   5.413  1.00  0.00
ATOM  129  OE2 GLU R  53   -25.284  -2.484   7.329  1.00  0.00
ATOM  130  H  GLU R  53    -24.901  -4.146   8.704  1.00  0.00
ATOM  131  N  PRO R  54    -25.448  -6.634   6.953  1.00  0.00
ATOM  132  CA PRO R  54    -25.503  -7.661   5.912  1.00  0.00
ATOM  133  C  PRO R  54    -26.227  -8.929   6.351  1.00  0.00
ATOM  134  O  PRO R  54    -26.254  -9.343   7.509  1.00  0.00
ATOM  135  CB PRO R  54    -24.032  -7.892   5.550  1.00  0.00
ATOM  136  CG PRO R  54    -23.286  -6.653   6.033  1.00  0.00
ATOM  137  CD PRO R  54    -24.070  -6.275   7.278  1.00  0.00
ATOM  138  N  CYS R  55    -26.841  -9.564   5.355  1.00  0.00
ATOM  139  CA CYS R  55    -27.561 -10.782   5.715  1.00  0.00
```

ATOM 140 C CYS R 55 -26.758 -12.020 5.403 1.00 0.00
ATOM 141 O CYS R 55 -25.722 -11.942 4.747 1.00 0.00
ATOM 142 CB CYS R 55 -28.884 -10.816 4.980 1.00 0.00
ATOM 143 SG CYS R 55 -29.966 -9.423 5.373 1.00 0.00
ATOM 144 H CYS R 55 -26.798 -9.206 4.422 1.00 0.00
ATOM 145 N LYS R 56 -27.264 -13.165 5.871 1.00 0.00
ATOM 146 CA LYS R 56 -26.589 -14.362 5.398 1.00 0.00
ATOM 147 C LYS R 56 -27.549 -15.386 4.837 1.00 0.00
ATOM 148 O LYS R 56 -28.519 -15.789 5.477 1.00 0.00
ATOM 149 CB LYS R 56 -25.714 -14.916 6.522 1.00 0.00
ATOM 150 CG LYS R 56 -24.805 -16.085 6.153 1.00 0.00
ATOM 151 CD LYS R 56 -23.591 -16.147 7.077 1.00 0.00
ATOM 152 CE LYS R 56 -23.022 -17.552 7.202 1.00 0.00
ATOM 153 NZ LYS R 56 -23.951 -18.331 8.015 1.00 0.00
ATOM 154 H LYS R 56 -28.051 -13.262 6.482 1.00 0.00
ATOM 155 1HZ LYS R 56 -23.881 -18.006 8.995 1.00 0.00
ATOM 156 2HZ LYS R 56 -23.728 -19.338 7.946 1.00 0.00
ATOM 157 3HZ LYS R 56 -24.928 -18.196 7.691 1.00 0.00
ATOM 158 N PRO R 57 -27.236 -15.830 3.598 1.00 0.00
ATOM 159 CA PRO R 57 -27.952 -16.989 3.057 1.00 0.00
ATOM 160 C PRO R 57 -27.718 -18.237 3.898 1.00 0.00
ATOM 161 O PRO R 57 -26.590 -18.524 4.312 1.00 0.00
ATOM 162 CB PRO R 57 -27.397 -17.079 1.631 1.00 0.00
ATOM 163 CG PRO R 57 -26.018 -16.418 1.682 1.00 0.00
ATOM 164 CD PRO R 57 -26.218 -15.301 2.698 1.00 0.00
ATOM 165 N CYS R 58 -28.842 -18.939 4.129 1.00 0.00
ATOM 166 CA CYS R 58 -28.833 -20.145 4.956 1.00 0.00
ATOM 167 C CYS R 58 -28.246 -21.406 4.309 1.00 0.00
ATOM 168 O CYS R 58 -27.067 -21.414 3.958 1.00 0.00
ATOM 169 CB CYS R 58 -30.219 -20.336 5.550 1.00 0.00
ATOM 170 SG CYS R 58 -31.446 -20.570 4.242 1.00 0.00
ATOM 171 H CYS R 58 -29.694 -18.544 3.776 1.00 0.00
ATOM 172 N THR R 59 -29.040 -22.485 4.171 1.00 0.00
ATOM 173 CA THR R 59 -28.405 -23.777 3.884 1.00 0.00
ATOM 174 C THR R 59 -29.331 -24.758 3.170 1.00 0.00
ATOM 175 O THR R 59 -30.560 -24.647 3.205 1.00 0.00

```
ATOM  176 CB  THR R 59   -27.872 -24.385   5.190 1.00 0.00
ATOM  177 OG1 THR R 59   -27.853 -23.393   6.235 1.00 0.00
ATOM  178 CG2 THR R 59   -26.489 -25.021   5.023 1.00 0.00
ATOM  179 H   THR R 59   -30.024 -22.480   4.346 1.00 0.00
ATOM  180 HG1 THR R 59   -27.610 -23.881   7.025 1.00 0.00
ATOM  181 N   GLU R 60   -28.701 -25.728   2.496 1.00 0.00
ATOM  182 CA  GLU R 60   -29.419 -26.674   1.647 1.00 0.00
ATOM  183 C   GLU R 60   -30.161 -27.753   2.390 1.00 0.00
ATOM  184 O   GLU R 60   -29.788 -28.927   2.459 1.00 0.00
ATOM  185 CB  GLU R 60   -28.473 -27.229   0.578 1.00 0.00
ATOM  186 CG  GLU R 60   -28.436 -26.362  -0.692 1.00 0.00
ATOM  187 CD  GLU R 60   -28.332 -24.886  -0.343 1.00 0.00
ATOM  188 OE1 GLU R 60   -29.269 -24.151  -0.619 1.00 0.00
ATOM  189 OE2 GLU R 60   -27.340 -24.471   0.243 1.00 0.00
ATOM  190 H   GLU R 60   -27.701 -25.728   2.526 1.00 0.00
ATOM  191 N   CYS R 61   -31.270 -27.273   2.945 1.00 0.00
ATOM  192 CA  CYS R 61   -32.170 -28.156   3.661 1.00 0.00
ATOM  193 C   CYS R 61   -33.085 -28.944   2.755 1.00 0.00
ATOM  194 O   CYS R 61   -34.299 -28.751   2.709 1.00 0.00
ATOM  195 CB  CYS R 61   -32.910 -27.347   4.714 1.00 0.00
ATOM  196 SG  CYS R 61   -31.740 -26.942   6.031 1.00 0.00
ATOM  197 H   CYS R 61   -31.509 -26.320   2.772 1.00 0.00
ATOM  198 N   VAL R 62   -32.425 -29.827   1.999 1.00 0.00
ATOM  199 CA  VAL R 62   -33.134 -30.711   1.091 1.00 0.00
ATOM  200 C   VAL R 62   -32.620 -32.122   1.268 1.00 0.00
ATOM  201 O   VAL R 62   -31.507 -32.351   1.744 1.00 0.00
ATOM  202 CB  VAL R 62   -32.966 -30.257  -0.371 1.00 0.00
ATOM  203 CG1 VAL R 62   -33.771 -28.988  -0.662 1.00 0.00
ATOM  204 CG2 VAL R 62   -31.491 -30.099  -0.762 1.00 0.00
ATOM  205 H   VAL R 62   -31.439 -29.935   2.116 1.00 0.00
ATOM  206 N   GLY R 63   -33.482 -33.057   0.831 1.00 0.00
ATOM  207 CA  GLY R 63   -33.115 -34.472   0.773 1.00 0.00
ATOM  208 C   GLY R 63   -32.332 -34.987   1.965 1.00 0.00
ATOM  209 O   GLY R 63   -32.817 -35.076   3.086 1.00 0.00
ATOM  210 H   GLY R 63   -34.346 -32.742   0.449 1.00 0.00
ATOM  211 N   LEU R 64   -31.064 -35.302   1.662 1.00 0.00
```

```
ATOM  212 CA  LEU R 64   -30.174 -35.897   2.660  1.00  0.00
ATOM  213 C   LEU R 64   -29.939 -35.063   3.905  1.00  0.00
ATOM  214 O   LEU R 64   -29.748 -35.602   4.993  1.00  0.00
ATOM  215 CB  LEU R 64   -28.818 -36.268   2.047  1.00  0.00
ATOM  216 CG  LEU R 64   -28.759 -37.594   1.273  1.00  0.00
ATOM  217 CD1 LEU R 64   -29.223 -38.770   2.135  1.00  0.00
ATOM  218 CD2 LEU R 64   -29.458 -37.548  -0.089  1.00  0.00
ATOM  219 H   LEU R 64   -30.789 -35.155   0.715  1.00  0.00
ATOM  220 N   GLN R 65   -29.920 -33.749   3.667  1.00  0.00
ATOM  221 CA  GLN R 65   -29.848 -32.806   4.767  1.00  0.00
ATOM  222 C   GLN R 65   -31.138 -32.025   4.898  1.00  0.00
ATOM  223 O   GLN R 65   -31.327 -30.896   4.444  1.00  0.00
ATOM  224 CB  GLN R 65   -28.607 -31.923   4.628  1.00  0.00
ATOM  225 CG  GLN R 65   -27.300 -32.698   4.852  1.00  0.00
ATOM  226 CD  GLN R 65   -27.227 -33.242   6.271  1.00  0.00
ATOM  227 OE1 GLN R 65   -28.016 -32.916   7.148  1.00  0.00
ATOM  228 NE2 GLN R 65   -26.211 -34.066   6.484  1.00  0.00
ATOM  229 H   GLN R 65   -30.093 -33.389   2.753  1.00  0.00
ATOM  230 1HE2 GLN R 65  -26.039 -34.449   7.390  1.00  0.00
ATOM  231 2HE2 GLN R 65  -25.596 -34.408   5.773  1.00  0.00
ATOM  232 N   SER R 66   -32.061 -32.731   5.554  1.00  0.00
ATOM  233 CA  SER R 66   -33.390 -32.190   5.816  1.00  0.00
ATOM  234 C   SER R 66   -33.405 -31.182   6.954  1.00  0.00
ATOM  235 O   SER R 66   -32.729 -31.340   7.966  1.00  0.00
ATOM  236 CB  SER R 66   -34.355 -33.332   6.140  1.00  0.00
ATOM  237 OG  SER R 66   -34.545 -34.205   5.013  1.00  0.00
ATOM  238 H   SER R 66   -31.773 -33.614   5.922  1.00  0.00
ATOM  239 HG  SER R 66   -33.695 -34.243   4.566  1.00  0.00
ATOM  240 N   MET R 67   -34.238 -30.147   6.731  1.00  0.00
ATOM  241 CA  MET R 67   -34.452 -29.049   7.683  1.00  0.00
ATOM  242 C   MET R 67   -34.580 -29.454   9.146  1.00  0.00
ATOM  243 O   MET R 67   -35.591 -30.030   9.547  1.00  0.00
ATOM  244 CB  MET R 67   -35.701 -28.290   7.216  1.00  0.00
ATOM  245 CG  MET R 67   -36.123 -27.081   8.053  1.00  0.00
ATOM  246 SD  MET R 67   -37.648 -26.329   7.454  1.00  0.00
ATOM  247 CE  MET R 67   -37.010 -25.683   5.898  1.00  0.00
```

```
ATOM  248  H   MET R  67    -34.671 -30.083   5.833  1.00  0.00
ATOM  249  N   SER R  68    -33.535 -29.137   9.905  1.00  0.00
ATOM  250  CA  SER R  68    -33.655 -29.183  11.360  1.00  0.00
ATOM  251  C   SER R  68    -34.023 -27.827  11.919  1.00  0.00
ATOM  252  O   SER R  68    -34.862 -27.691  12.800  1.00  0.00
ATOM  253  CB  SER R  68    -32.358 -29.637  12.009  1.00  0.00
ATOM  254  OG  SER R  68    -31.643 -30.509  11.115  1.00  0.00
ATOM  255  H   SER R  68    -32.761 -28.695   9.455  1.00  0.00
ATOM  256  HG  SER R  68    -31.558 -30.009  10.294  1.00  0.00
ATOM  257  N   ALA R  69    -33.375 -26.830  11.302  1.00  0.00
ATOM  258  CA  ALA R  69    -33.917 -25.487  11.420  1.00  0.00
ATOM  259  C   ALA R  69    -34.131 -24.964  10.022  1.00  0.00
ATOM  260  O   ALA R  69    -33.406 -25.351   9.101  1.00  0.00
ATOM  261  CB  ALA R  69    -32.949 -24.567  12.163  1.00  0.00
ATOM  262  H   ALA R  69    -32.643 -27.065  10.660  1.00  0.00
ATOM  263  N   PRO R  70    -35.166 -24.103   9.901  1.00  0.00
ATOM  264  CA  PRO R  70    -35.349 -23.341   8.665  1.00  0.00
ATOM  265  C   PRO R  70    -34.275 -22.271   8.587  1.00  0.00
ATOM  266  O   PRO R  70    -33.227 -22.350   9.229  1.00  0.00
ATOM  267  CB  PRO R  70    -36.770 -22.793   8.852  1.00  0.00
ATOM  268  CG  PRO R  70    -36.928 -22.604  10.359  1.00  0.00
ATOM  269  CD  PRO R  70    -36.166 -23.793  10.921  1.00  0.00
ATOM  270  N   CYS R  71    -34.550 -21.233   7.785  1.00  0.00
ATOM  271  CA  CYS R  71    -33.601 -20.119   7.809  1.00  0.00
ATOM  272  C   CYS R  71    -33.970 -19.007   8.772  1.00  0.00
ATOM  273  O   CYS R  71    -33.266 -18.019   8.957  1.00  0.00
ATOM  274  CB  CYS R  71    -33.418 -19.571   6.407  1.00  0.00
ATOM  275  SG  CYS R  71    -33.225 -20.894   5.186  1.00  0.00
ATOM  276  H   CYS R  71    -35.393 -21.195   7.252  1.00  0.00
ATOM  277  N   VAL R  72    -35.153 -19.212   9.378  1.00  0.00
ATOM  278  CA  VAL R  72    -35.518 -18.365  10.505  1.00  0.00
ATOM  279  C   VAL R  72    -35.220 -19.134  11.781  1.00  0.00
ATOM  280  O   VAL R  72    -34.442 -20.088  11.731  1.00  0.00
ATOM  281  CB  VAL R  72    -36.968 -17.871  10.369  1.00  0.00
ATOM  282  CG1 VAL R  72    -37.035 -16.768   9.311  1.00  0.00
ATOM  283  CG2 VAL R  72    -37.963 -18.992  10.064  1.00  0.00
```

ATOM 284 H VAL R 72 -35.684 -20.042 9.226 1.00 0.00
ATOM 285 N GLU R 73 -35.790 -18.668 12.904 1.00 0.00
ATOM 286 CA GLU R 73 -35.488 -19.248 14.217 1.00 0.00
ATOM 287 C GLU R 73 -34.000 -19.471 14.515 1.00 0.00
ATOM 288 O GLU R 73 -33.279 -18.511 14.794 1.00 0.00
ATOM 289 CB GLU R 73 -36.399 -20.461 14.483 1.00 0.00
ATOM 290 CG GLU R 73 -37.842 -20.111 14.899 1.00 0.00
ATOM 291 CD GLU R 73 -38.628 -19.399 13.805 1.00 0.00
ATOM 292 OE1 GLU R 73 -39.196 -20.066 12.948 1.00 0.00
ATOM 293 OE2 GLU R 73 -38.693 -18.173 13.816 1.00 0.00
ATOM 294 H GLU R 73 -36.613 -18.100 12.819 1.00 0.00
ATOM 295 N ALA R 74 -33.549 -20.733 14.428 1.00 0.00
ATOM 296 CA ALA R 74 -32.139 -20.969 14.723 1.00 0.00
ATOM 297 C ALA R 74 -31.209 -20.464 13.628 1.00 0.00
ATOM 298 O ALA R 74 -31.627 -19.858 12.643 1.00 0.00
ATOM 299 CB ALA R 74 -31.896 -22.456 14.994 1.00 0.00
ATOM 300 H ALA R 74 -34.142 -21.443 14.054 1.00 0.00
ATOM 301 N ASP R 75 -29.901 -20.717 13.841 1.00 0.00
ATOM 302 CA ASP R 75 -28.988 -20.165 12.838 1.00 0.00
ATOM 303 C ASP R 75 -28.978 -20.946 11.540 1.00 0.00
ATOM 304 O ASP R 75 -28.907 -22.175 11.568 1.00 0.00
ATOM 305 CB ASP R 75 -27.570 -19.881 13.412 1.00 0.00
ATOM 306 CG ASP R 75 -26.502 -20.949 13.148 1.00 0.00
ATOM 307 OD1 ASP R 75 -25.764 -20.841 12.170 1.00 0.00
ATOM 308 OD2 ASP R 75 -26.375 -21.893 13.918 1.00 0.00
ATOM 309 H ASP R 75 -29.610 -21.308 14.596 1.00 0.00
ATOM 310 N ASP R 76 -29.031 -20.167 10.438 1.00 0.00
ATOM 311 CA ASP R 76 -28.563 -20.650 9.133 1.00 0.00
ATOM 312 C ASP R 76 -28.887 -22.099 8.799 1.00 0.00
ATOM 313 O ASP R 76 -28.004 -22.960 8.851 1.00 0.00
ATOM 314 CB ASP R 76 -27.048 -20.433 9.048 1.00 0.00
ATOM 315 CG ASP R 76 -26.651 -19.628 7.832 1.00 0.00
ATOM 316 OD1 ASP R 76 -26.280 -20.197 6.821 1.00 0.00
ATOM 317 OD2 ASP R 76 -26.657 -18.412 7.895 1.00 0.00
ATOM 318 H ASP R 76 -29.310 -19.218 10.546 1.00 0.00
ATOM 319 N ALA R 77 -30.181 -22.342 8.504 1.00 0.00

```
ATOM  320 CA  ALA R 77   -30.727 -23.675  8.210 1.00 0.00
ATOM  321 C   ALA R 77   -29.903 -24.882  8.622 1.00 0.00
ATOM  322 O   ALA R 77   -28.947 -25.313  7.977 1.00 0.00
ATOM  323 CB  ALA R 77   -31.146 -23.786  6.745 1.00 0.00
ATOM  324 H   ALA R 77   -30.762 -21.532  8.486 1.00 0.00
ATOM  325 N   VAL R 78   -30.293 -25.370  9.804 1.00 0.00
ATOM  326 CA  VAL R 78   -29.473 -26.437 10.365 1.00 0.00
ATOM  327 C   VAL R 78   -29.674 -27.730  9.608 1.00 0.00
ATOM  328 O   VAL R 78   -30.689 -28.419  9.719 1.00 0.00
ATOM  329 CB  VAL R 78   -29.705 -26.621 11.875 1.00 0.00
ATOM  330 CG1 VAL R 78   -28.824 -27.731 12.461 1.00 0.00
ATOM  331 CG2 VAL R 78   -29.474 -25.311 12.630 1.00 0.00
ATOM  332 H   VAL R 78   -31.196 -25.121 10.147 1.00 0.00
ATOM  333 N   CYS R 79   -28.632 -28.038  8.838 1.00 0.00
ATOM  334 CA  CYS R 79   -28.713 -29.247  8.033 1.00 0.00
ATOM  335 C   CYS R 79   -27.339 -29.828  7.920 1.00 0.00
ATOM  336 O   CYS R 79   -26.525 -29.376  7.119 1.00 0.00
ATOM  337 CB  CYS R 79   -29.320 -28.928  6.669 1.00 0.00
ATOM  338 SG  CYS R 79   -31.114 -28.721  6.825 1.00 0.00
ATOM  339 H   CYS R 79   -27.953 -27.324  8.640 1.00 0.00
ATOM  340 N   ARG R 80   -27.136 -30.778  8.851 1.00 0.00
ATOM  341 CA  ARG R 80   -25.874 -31.473  9.118 1.00 0.00
ATOM  342 C   ARG R 80   -26.145 -32.410 10.286 1.00 0.00
ATOM  343 O   ARG R 80   -27.174 -32.258 10.947 1.00 0.00
ATOM  344 CB  ARG R 80   -24.794 -30.457  9.480 1.00 0.00
ATOM  345 CG  ARG R 80   -23.510 -30.612  8.671 1.00 0.00
ATOM  346 CD  ARG R 80   -23.609 -30.483  7.144 1.00 0.00
ATOM  347 NE  ARG R 80   -22.248 -30.464  6.602 1.00 0.00
ATOM  348 CZ  ARG R 80   -21.752 -29.350  6.025 1.00 0.00
ATOM  349 NH1 ARG R 80   -20.446 -29.201  5.899 1.00 0.00
ATOM  350 NH2 ARG R 80   -22.565 -28.390  5.605 1.00 0.00
ATOM  351 H   ARG R 80   -27.930 -31.029  9.408 1.00 0.00
ATOM  352 HE  ARG R 80   -21.632 -31.222  6.850 1.00 0.00
ATOM  353 1HH1 ARG R 80  -20.066 -28.349  5.510 1.00 0.00
ATOM  354 2HH1 ARG R 80  -19.803 -29.904  6.220 1.00 0.00
ATOM  355 1HH2 ARG R 80  -22.163 -27.510  5.312 1.00 0.00
```

```
ATOM  356 2HH2 ARG R  80    -23.555 -28.546   5.585  1.00  0.00
ATOM  357  N   CYS R  81    -25.254 -33.378  10.546  1.00  0.00
ATOM  358  CA  CYS R  81    -25.630 -34.302  11.618  1.00  0.00
ATOM  359  C   CYS R  81    -24.657 -34.425  12.779  1.00  0.00
ATOM  360  O   CYS R  81    -23.437 -34.482  12.654  1.00  0.00
ATOM  361  CB  CYS R  81    -25.971 -35.691  11.060  1.00  0.00
ATOM  362  SG  CYS R  81    -27.286 -35.685   9.805  1.00  0.00
ATOM  363  H   CYS R  81    -24.383 -33.437  10.057  1.00  0.00
ATOM  364  N   ALA R  82    -25.276 -34.521  13.965  1.00  0.00
ATOM  365  CA  ALA R  82    -24.515 -34.749  15.194  1.00  0.00
ATOM  366  C   ALA R  82    -25.304 -35.664  16.121  1.00  0.00
ATOM  367  O   ALA R  82    -26.298 -36.259  15.706  1.00  0.00
ATOM  368  CB  ALA R  82    -24.220 -33.410  15.880  1.00  0.00
ATOM  369  H   ALA R  82    -26.275 -34.483  13.959  1.00  0.00
ATOM  370  N   TYR R  83    -24.873 -35.700  17.401  1.00  0.00
ATOM  371  CA  TYR R  83    -25.613 -36.307  18.519  1.00  0.00
ATOM  372  C   TYR R  83    -25.565 -37.827  18.584  1.00  0.00
ATOM  373  O   TYR R  83    -24.974 -38.412  19.487  1.00  0.00
ATOM  374  CB  TYR R  83    -27.078 -35.829  18.634  1.00  0.00
ATOM  375  CG  TYR R  83    -27.226 -34.328  18.781  1.00  0.00
ATOM  376  CD1 TYR R  83    -26.962 -33.725  20.028  1.00  0.00
ATOM  377  CD2 TYR R  83    -27.670 -33.574  17.674  1.00  0.00
ATOM  378  CE1 TYR R  83    -27.210 -32.351  20.189  1.00  0.00
ATOM  379  CE2 TYR R  83    -27.914 -32.198  17.834  1.00  0.00
ATOM  380  CZ  TYR R  83    -27.710 -31.608  19.099  1.00  0.00
ATOM  381  OH  TYR R  83    -28.024 -30.273  19.294  1.00  0.00
ATOM  382  H   TYR R  83    -23.940 -35.374  17.555  1.00  0.00
ATOM  383  HH  TYR R  83    -28.217 -29.854  18.456  1.00  0.00
ATOM  384  N   GLY R  84    -26.236 -38.425  17.591  1.00  0.00
ATOM  385  CA  GLY R  84    -26.228 -39.880  17.476  1.00  0.00
ATOM  386  C   GLY R  84    -25.429 -40.269  16.256  1.00  0.00
ATOM  387  O   GLY R  84    -24.379 -40.900  16.321  1.00  0.00
ATOM  388  H   GLY R  84    -26.647 -37.841  16.890  1.00  0.00
ATOM  389  N   TYR R  85    -25.951 -39.784  15.120  1.00  0.00
ATOM  390  CA  TYR R  85    -25.110 -39.752  13.923  1.00  0.00
ATOM  391  C   TYR R  85    -24.142 -38.590  13.997  1.00  0.00
```

```
ATOM   392  O   TYR R  85    -24.434 -37.463  13.597  1.00  0.00
ATOM   393  CB  TYR R  85    -25.941 -39.668  12.637  1.00  0.00
ATOM   394  CG  TYR R  85    -26.885 -40.843  12.509  1.00  0.00
ATOM   395  CD1 TYR R  85    -26.367 -42.140  12.304  1.00  0.00
ATOM   396  CD2 TYR R  85    -28.271 -40.602  12.591  1.00  0.00
ATOM   397  CE1 TYR R  85    -27.258 -43.221  12.185  1.00  0.00
ATOM   398  CE2 TYR R  85    -29.161 -41.681  12.467  1.00  0.00
ATOM   399  CZ  TYR R  85    -28.645 -42.978  12.269  1.00  0.00
ATOM   400  OH  TYR R  85    -29.528 -44.039  12.161  1.00  0.00
ATOM   401  H   TYR R  85    -26.801 -39.267  15.189  1.00  0.00
ATOM   402  HH  TYR R  85    -30.392 -43.682  11.979  1.00  0.00
ATOM   403  N   TYR R  86    -23.001 -38.941  14.593  1.00  0.00
ATOM   404  CA  TYR R  86    -21.996 -37.958  14.983  1.00  0.00
ATOM   405  C   TYR R  86    -21.418 -37.177  13.824  1.00  0.00
ATOM   406  O   TYR R  86    -21.126 -35.992  13.937  1.00  0.00
ATOM   407  CB  TYR R  86    -20.809 -38.602  15.710  1.00  0.00
ATOM   408  CG  TYR R  86    -21.207 -39.697  16.673  1.00  0.00
ATOM   409  CD1 TYR R  86    -20.850 -41.023  16.352  1.00  0.00
ATOM   410  CD2 TYR R  86    -21.890 -39.374  17.863  1.00  0.00
ATOM   411  CE1 TYR R  86    -21.141 -42.050  17.264  1.00  0.00
ATOM   412  CE2 TYR R  86    -22.184 -40.403  18.774  1.00  0.00
ATOM   413  CZ  TYR R  86    -21.785 -41.722  18.473  1.00  0.00
ATOM   414  OH  TYR R  86    -22.023 -42.711  19.413  1.00  0.00
ATOM   415  H   TYR R  86    -22.958 -39.890  14.897  1.00  0.00
ATOM   416  HH  TYR R  86    -21.495 -43.480  19.212  1.00  0.00
ATOM   417  N   GLN R  87    -21.218 -37.946  12.732  1.00  0.00
ATOM   418  CA  GLN R  87    -20.570 -37.470  11.510  1.00  0.00
ATOM   419  C   GLN R  87    -19.097 -37.109  11.556  1.00  0.00
ATOM   420  O   GLN R  87    -18.514 -36.712  12.563  1.00  0.00
ATOM   421  CB  GLN R  87    -21.334 -36.316  10.855  1.00  0.00
ATOM   422  CG  GLN R  87    -22.628 -36.720  10.170  1.00  0.00
ATOM   423  CD  GLN R  87    -22.807 -35.859   8.937  1.00  0.00
ATOM   424  OE1 GLN R  87    -23.553 -34.880   8.908  1.00  0.00
ATOM   425  NE2 GLN R  87    -22.130 -36.305   7.879  1.00  0.00
ATOM   426  H   GLN R  87    -21.584 -38.879  12.734  1.00  0.00
ATOM   427 1HE2 GLN R  87    -22.399 -35.962   6.979  1.00  0.00
```

ATOM 428 2HE2 GLN R 87 -21.431 -37.016 7.960 1.00 0.00
ATOM 429 N ASP R 88 -18.536 -37.210 10.345 1.00 0.00
ATOM 430 CA ASP R 88 -17.727 -36.069 9.929 1.00 0.00
ATOM 431 C ASP R 88 -18.634 -35.318 8.978 1.00 0.00
ATOM 432 O ASP R 88 -19.200 -35.901 8.064 1.00 0.00
ATOM 433 CB ASP R 88 -16.408 -36.490 9.269 1.00 0.00
ATOM 434 CG ASP R 88 -15.384 -35.376 9.431 1.00 0.00
ATOM 435 OD1 ASP R 88 -14.915 -34.822 8.442 1.00 0.00
ATOM 436 OD2 ASP R 88 -15.051 -35.032 10.560 1.00 0.00
ATOM 437 H ASP R 88 -19.040 -37.751 9.666 1.00 0.00
ATOM 438 N GLU R 89 -18.883 -34.048 9.301 1.00 0.00
ATOM 439 CA GLU R 89 -20.163 -33.427 8.949 1.00 0.00
ATOM 440 C GLU R 89 -20.666 -33.353 7.500 1.00 0.00
ATOM 441 O GLU R 89 -21.862 -33.159 7.271 1.00 0.00
ATOM 442 CB GLU R 89 -20.252 -32.098 9.722 1.00 0.00
ATOM 443 CG GLU R 89 -19.934 -30.765 9.024 1.00 0.00
ATOM 444 CD GLU R 89 -18.588 -30.734 8.336 1.00 0.00
ATOM 445 OE1 GLU R 89 -18.494 -31.092 7.174 1.00 0.00
ATOM 446 OE2 GLU R 89 -17.616 -30.321 8.940 1.00 0.00
ATOM 447 H GLU R 89 -18.289 -33.640 9.988 1.00 0.00
ATOM 448 N THR R 90 -19.709 -33.499 6.555 1.00 0.00
ATOM 449 CA THR R 90 -19.933 -32.941 5.217 1.00 0.00
ATOM 450 C THR R 90 -21.285 -33.118 4.552 1.00 0.00
ATOM 451 O THR R 90 -21.938 -34.160 4.600 1.00 0.00
ATOM 452 CB THR R 90 -18.810 -33.347 4.255 1.00 0.00
ATOM 453 OG1 THR R 90 -17.674 -33.836 4.984 1.00 0.00
ATOM 454 CG2 THR R 90 -18.392 -32.204 3.324 1.00 0.00
ATOM 455 H THR R 90 -18.784 -33.648 6.889 1.00 0.00
ATOM 456 HG1 THR R 90 -17.327 -33.064 5.444 1.00 0.00
ATOM 457 N THR R 91 -21.647 -32.017 3.895 1.00 0.00
ATOM 458 CA THR R 91 -22.860 -31.897 3.097 1.00 0.00
ATOM 459 C THR R 91 -23.258 -33.149 2.323 1.00 0.00
ATOM 460 O THR R 91 -22.484 -33.676 1.526 1.00 0.00
ATOM 461 CB THR R 91 -22.647 -30.720 2.141 1.00 0.00
ATOM 462 OG1 THR R 91 -21.666 -29.793 2.666 1.00 0.00
ATOM 463 CG2 THR R 91 -23.964 -30.007 1.827 1.00 0.00

```
ATOM  464  H   THR R  91    -20.984 -31.271   3.860  1.00  0.00
ATOM  465  HG1 THR R  91    -20.894 -29.846   2.096  1.00  0.00
ATOM  466  N   GLY R  92    -24.499 -33.584   2.577  1.00  0.00
ATOM  467  CA  GLY R  92    -24.978 -34.710   1.781  1.00  0.00
ATOM  468  C   GLY R  92    -24.860 -36.093   2.409  1.00  0.00
ATOM  469  O   GLY R  92    -25.335 -37.085   1.850  1.00  0.00
ATOM  470  H   GLY R  92    -25.022 -33.210   3.337  1.00  0.00
ATOM  471  N   ARG R  93    -24.236 -36.138   3.595  1.00  0.00
ATOM  472  CA  ARG R  93    -24.173 -37.427   4.280  1.00  0.00
ATOM  473  C   ARG R  93    -24.418 -37.314   5.777  1.00  0.00
ATOM  474  O   ARG R  93    -24.453 -36.210   6.315  1.00  0.00
ATOM  475  CB  ARG R  93    -22.867 -38.152   3.925  1.00  0.00
ATOM  476  CG  ARG R  93    -21.604 -37.313   4.120  1.00  0.00
ATOM  477  CD  ARG R  93    -20.324 -38.083   3.779  1.00  0.00
ATOM  478  NE  ARG R  93    -19.135 -37.298   4.115  1.00  0.00
ATOM  479  CZ  ARG R  93    -18.683 -37.255   5.391  1.00  0.00
ATOM  480  NH1 ARG R  93    -17.741 -36.386   5.728  1.00  0.00
ATOM  481  NH2 ARG R  93    -19.200 -38.034   6.329  1.00  0.00
ATOM  482  H   ARG R  93    -23.801 -35.328   3.987  1.00  0.00
ATOM  483  HE  ARG R  93    -18.726 -36.705   3.421  1.00  0.00
ATOM  484 1HH1 ARG R  93    -17.400 -36.385   6.666  1.00  0.00
ATOM  485 2HH1 ARG R  93    -17.378 -35.697   5.095  1.00  0.00
ATOM  486 1HH2 ARG R  93    -18.999 -37.871   7.294  1.00  0.00
ATOM  487 2HH2 ARG R  93    -19.832 -38.785   6.135  1.00  0.00
ATOM  488  N   CYS R  94    -24.653 -38.506   6.371  1.00  0.00
ATOM  489  CA  CYS R  94    -24.768 -38.726   7.818  1.00  0.00
ATOM  490  C   CYS R  94    -24.488 -40.182   8.172  1.00  0.00
ATOM  491  O   CYS R  94    -25.041 -41.119   7.594  1.00  0.00
ATOM  492  CB  CYS R  94    -26.138 -38.358   8.397  1.00  0.00
ATOM  493  SG  CYS R  94    -26.692 -36.659   8.083  1.00  0.00
ATOM  494  H   CYS R  94    -24.611 -39.336   5.816  1.00  0.00
ATOM  495  N   GLU R  95    -23.572 -40.320   9.142  1.00  0.00
ATOM  496  CA  GLU R  95    -22.945 -41.588   9.514  1.00  0.00
ATOM  497  C   GLU R  95    -22.224 -41.383  10.836  1.00  0.00
ATOM  498  O   GLU R  95    -22.258 -40.278  11.382  1.00  0.00
ATOM  499  CB  GLU R  95    -21.981 -42.075   8.412  1.00  0.00
```

```
ATOM  500 CG  GLU R 95   -20.721 -41.229  8.154 1.00 0.00
ATOM  501 CD  GLU R 95   -21.085 -39.811  7.761 1.00 0.00
ATOM  502 OE1 GLU R 95   -21.467 -39.570  6.627 1.00 0.00
ATOM  503 OE2 GLU R 95   -20.997 -38.922  8.591 1.00 0.00
ATOM  504 H   GLU R 95   -23.203 -39.480  9.540 1.00 0.00
ATOM  505 N   ALA R 96   -21.599 -42.462 11.332 1.00 0.00
ATOM  506 CA  ALA R 96   -20.851 -42.305 12.578 1.00 0.00
ATOM  507 C   ALA R 96   -19.527 -41.574 12.413 1.00 0.00
ATOM  508 O   ALA R 96   -18.742 -41.952 11.544 1.00 0.00
ATOM  509 CB  ALA R 96   -20.605 -43.668 13.231 1.00 0.00
ATOM  510 OXT ALA R 96   -19.293 -40.619 13.151 1.00 0.00
ATOM  511 H   ALA R 96   -21.711 -43.344 10.871 1.00 0.00
END
```

REMARK 1 Second CRD of $p75^{NTR}$, bound to BDNF.

```
REMARK 2
ATOM    1 N   CYS R 39   -28.731 -23.425 17.186 1.00 0.00
ATOM    2 CA  CYS R 39   -29.491 -22.215 17.484 1.00 0.00
ATOM    3 C   CYS R 39   -30.988 -22.434 17.523 1.00 0.00
ATOM    4 O   CYS R 39   -31.773 -21.495 17.660 1.00 0.00
ATOM    5 CB  CYS R 39   -29.203 -21.102 16.474 1.00 0.00
ATOM    6 SG  CYS R 39   -27.698 -21.312 15.471 1.00 0.00
ATOM    7 1H  CYS R 39   -27.735 -23.264 17.148 1.00 0.00
ATOM    8 2H  CYS R 39   -28.868 -24.153 17.874 1.00 0.00
ATOM    9 3H  CYS R 39   -28.982 -23.835 16.298 1.00 0.00
ATOM   10 N   LEU R 40   -31.381 -23.704 17.336 1.00 0.00
ATOM   11 CA  LEU R 40   -32.802 -24.005 17.397 1.00 0.00
ATOM   12 C   LEU R 40   -33.098 -24.788 18.662 1.00 0.00
ATOM   13 O   LEU R 40   -32.371 -24.712 19.645 1.00 0.00
ATOM   14 CB  LEU R 40   -33.224 -24.736 16.114 1.00 0.00
ATOM   15 CG  LEU R 40   -33.141 -23.868 14.854 1.00 0.00
ATOM   16 CD1 LEU R 40   -33.498 -24.664 13.599 1.00 0.00
ATOM   17 CD2 LEU R 40   -33.987 -22.598 14.968 1.00 0.00
ATOM   18 H   LEU R 40   -30.734 -24.467 17.314 1.00 0.00
ATOM   19 N   ASP R 41   -34.194 -25.545 18.604 1.00 0.00
ATOM   20 CA  ASP R 41   -34.394 -26.559 19.630 1.00 0.00
```

```
ATOM   21  C   ASP R  41    -33.510 -27.762  19.326  1.00  0.00
ATOM   22  O   ASP R  41    -32.569 -27.678  18.542  1.00  0.00
ATOM   23  CB  ASP R  41    -35.888 -26.923  19.676  1.00  0.00
ATOM   24  CG  ASP R  41    -36.282 -27.631  18.391  1.00  0.00
ATOM   25  OD1 ASP R  41    -36.462 -28.842  18.426  1.00  0.00
ATOM   26  OD2 ASP R  41    -36.364 -26.975  17.359  1.00  0.00
ATOM   27  H   ASP R  41    -34.766 -25.640  17.790  1.00  0.00
ATOM   28  N   SER R  42    -33.860 -28.892  19.945  1.00  0.00
ATOM   29  CA  SER R  42    -33.192 -30.156  19.648  1.00  0.00
ATOM   30  C   SER R  42    -32.956 -30.499  18.173  1.00  0.00
ATOM   31  O   SER R  42    -31.967 -31.144  17.816  1.00  0.00
ATOM   32  CB  SER R  42    -33.975 -31.256  20.359  1.00  0.00
ATOM   33  OG  SER R  42    -34.507 -30.738  21.597  1.00  0.00
ATOM   34  H   SER R  42    -34.638 -28.916  20.568  1.00  0.00
ATOM   35  HG  SER R  42    -35.328 -31.194  21.757  1.00  0.00
ATOM   36  N   VAL R  43    -33.884 -30.042  17.310  1.00  0.00
ATOM   37  CA  VAL R  43    -33.712 -30.372  15.895  1.00  0.00
ATOM   38  C   VAL R  43    -32.454 -29.826  15.235  1.00  0.00
ATOM   39  O   VAL R  43    -31.932 -30.402  14.281  1.00  0.00
ATOM   40  CB  VAL R  43    -34.955 -30.058  15.044  1.00  0.00
ATOM   41  CG1 VAL R  43    -36.186 -30.773  15.604  1.00  0.00
ATOM   42  CG2 VAL R  43    -35.182 -28.560  14.824  1.00  0.00
ATOM   43  H   VAL R  43    -34.615 -29.433  17.633  1.00  0.00
ATOM   44  N   THR R  44    -31.938 -28.722  15.786  1.00  0.00
ATOM   45  CA  THR R  44    -30.651 -28.248  15.283  1.00  0.00
ATOM   46  C   THR R  44    -29.869 -27.538  16.372  1.00  0.00
ATOM   47  O   THR R  44    -30.165 -26.391  16.716  1.00  0.00
ATOM   48  CB  THR R  44    -30.833 -27.333  14.062  1.00  0.00
ATOM   49  OG1 THR R  44    -31.913 -27.770  13.215  1.00  0.00
ATOM   50  CG2 THR R  44    -29.538 -27.231  13.256  1.00  0.00
ATOM   51  H   THR R  44    -32.435 -28.226  16.507  1.00  0.00
ATOM   52  HG1 THR R  44    -31.927 -28.725  13.271  1.00  0.00
ATOM   53  N   PHE R  45    -28.911 -28.291  16.916  1.00  0.00
ATOM   54  CA  PHE R  45    -28.186 -27.770  18.069  1.00  0.00
ATOM   55  C   PHE R  45    -26.993 -26.926  17.656  1.00  0.00
ATOM   56  O   PHE R  45    -26.806 -26.646  16.478  1.00  0.00
```

```
ATOM   57  CB  PHE R 45     -27.822 -28.924  19.006  1.00  0.00
ATOM   58  CG  PHE R 45     -26.899 -29.937  18.362  1.00  0.00
ATOM   59  CD1 PHE R 45     -27.449 -31.094  17.770  1.00  0.00
ATOM   60  CD2 PHE R 45     -25.503 -29.718  18.376  1.00  0.00
ATOM   61  CE1 PHE R 45     -26.592 -32.040  17.179  1.00  0.00
ATOM   62  CE2 PHE R 45     -24.646 -30.663  17.785  1.00  0.00
ATOM   63  CZ  PHE R 45     -25.200 -31.813  17.186  1.00  0.00
ATOM   64  H   PHE R 45     -28.575 -29.099  16.440  1.00  0.00
ATOM   65  N   SER R 46     -26.169 -26.504  18.621  1.00  0.00
ATOM   66  CA  SER R 46     -25.321 -25.406  18.156  1.00  0.00
ATOM   67  C   SER R 46     -23.805 -25.596  18.062  1.00  0.00
ATOM   68  O   SER R 46     -23.139 -25.015  17.205  1.00  0.00
ATOM   69  CB  SER R 46     -25.722 -24.118  18.887  1.00  0.00
ATOM   70  OG  SER R 46     -27.050 -24.244  19.441  1.00  0.00
ATOM   71  H   SER R 46     -26.281 -26.700  19.596  1.00  0.00
ATOM   72  HG  SER R 46     -26.881 -24.590  20.319  1.00  0.00
ATOM   73  N   ASP R 47     -23.284 -26.424  18.982  1.00  0.00
ATOM   74  CA  ASP R 47     -21.847 -26.704  19.149  1.00  0.00
ATOM   75  C   ASP R 47     -20.914 -25.513  19.394  1.00  0.00
ATOM   76  O   ASP R 47     -19.707 -25.533  19.159  1.00  0.00
ATOM   77  CB  ASP R 47     -21.313 -27.830  18.204  1.00  0.00
ATOM   78  CG  ASP R 47     -20.687 -27.453  16.853  1.00  0.00
ATOM   79  OD1 ASP R 47     -20.787 -28.220  15.898  1.00  0.00
ATOM   80  OD2 ASP R 47     -20.046 -26.421  16.716  1.00  0.00
ATOM   81  H   ASP R 47     -23.930 -26.730  19.679  1.00  0.00
ATOM   82  N   VAL R 48     -21.525 -24.456  19.953  1.00  0.00
ATOM   83  CA  VAL R 48     -20.791 -23.190  20.089  1.00  0.00
ATOM   84  C   VAL R 48     -19.752 -23.030  21.212  1.00  0.00
ATOM   85  O   VAL R 48     -19.796 -22.163  22.083  1.00  0.00
ATOM   86  CB  VAL R 48     -21.762 -22.000  20.041  1.00  0.00
ATOM   87  CG1 VAL R 48     -22.331 -21.847  18.628  1.00  0.00
ATOM   88  CG2 VAL R 48     -22.865 -22.095  21.103  1.00  0.00
ATOM   89  H   VAL R 48     -22.434 -24.585  20.351  1.00  0.00
ATOM   90  N   VAL R 49     -18.722 -23.884  21.116  1.00  0.00
ATOM   91  CA  VAL R 49     -17.548 -23.718  21.974  1.00  0.00
ATOM   92  C   VAL R 49     -16.827 -22.386  21.754  1.00  0.00
```

```
ATOM   93 O   VAL R 49   -16.199 -21.808  22.647  1.00  0.00
ATOM   94 CB  VAL R 49   -16.621 -24.942  21.815  1.00  0.00
ATOM   95 CG1 VAL R 49   -16.113 -25.126  20.379  1.00  0.00
ATOM   96 CG2 VAL R 49   -15.490 -24.948  22.848  1.00  0.00
ATOM   97 H   VAL R 49   -18.738 -24.575  20.398  1.00  0.00
ATOM   98 N   SER R 50   -16.984 -21.895  20.512  1.00  0.00
ATOM   99 CA  SER R 50   -16.545 -20.542  20.170  1.00  0.00
ATOM  100 C   SER R 50   -17.478 -20.015  19.099  1.00  0.00
ATOM  101 O   SER R 50   -18.142 -20.822  18.450  1.00  0.00
ATOM  102 CB  SER R 50   -15.104 -20.582  19.665  1.00  0.00
ATOM  103 OG  SER R 50   -14.388 -21.603  20.381  1.00  0.00
ATOM  104 H   SER R 50   -17.472 -22.447  19.837  1.00  0.00
ATOM  105 HG  SER R 50   -14.702 -21.503  21.280  1.00  0.00
ATOM  106 N   ALA R 51   -17.535 -18.689  18.939  1.00  0.00
ATOM  107 CA  ALA R 51   -18.444 -18.111  17.945  1.00  0.00
ATOM  108 C   ALA R 51   -18.009 -18.327  16.502  1.00  0.00
ATOM  109 O   ALA R 51   -17.384 -17.480  15.860  1.00  0.00
ATOM  110 CB  ALA R 51   -18.633 -16.614  18.202  1.00  0.00
ATOM  111 H   ALA R 51   -16.914 -18.119  19.470  1.00  0.00
ATOM  112 N   THR R 52   -18.362 -19.542  16.034  1.00  0.00
ATOM  113 CA  THR R 52   -17.855 -20.040  14.756  1.00  0.00
ATOM  114 C   THR R 52   -18.740 -21.103  14.084  1.00  0.00
ATOM  115 O   THR R 52   -18.814 -22.264  14.488  1.00  0.00
ATOM  116 CB  THR R 52   -16.422 -20.581  14.935  1.00  0.00
ATOM  117 OG1 THR R 52   -15.633 -19.712  15.770  1.00  0.00
ATOM  118 CG2 THR R 52   -15.723 -20.802  13.589  1.00  0.00
ATOM  119 H   THR R 52   -18.809 -20.200  16.644  1.00  0.00
ATOM  120 HG1 THR R 52   -15.985 -18.832  15.634  1.00  0.00
ATOM  121 N   GLU R 53   -19.349 -20.674  12.968  1.00  0.00
ATOM  122 CA  GLU R 53   -20.398 -19.674  13.115  1.00  0.00
ATOM  123 C   GLU R 53   -21.732 -20.164  13.692  1.00  0.00
ATOM  124 O   GLU R 53   -22.195 -19.586  14.668  1.00  0.00
ATOM  125 CB  GLU R 53   -20.639 -18.835  11.840  1.00  0.00
ATOM  126 CG  GLU R 53   -19.550 -18.814  10.755  1.00  0.00
ATOM  127 CD  GLU R 53   -19.530 -20.110   9.955  1.00  0.00
ATOM  128 OE1 GLU R 53   -20.581 -20.583   9.522  1.00  0.00
```

```
ATOM  129 OE2 GLU R 53   -18.455 -20.666   9.758 1.00 0.00
ATOM  130 H   GLU R 53   -19.314 -21.243  12.150 1.00 0.00
ATOM  131 N   PRO R 54   -22.382 -21.186  13.062 1.00 0.00
ATOM  132 CA  PRO R 54   -23.801 -21.374  13.363 1.00 0.00
ATOM  133 C   PRO R 54   -24.087 -22.600  14.224 1.00 0.00
ATOM  134 O   PRO R 54   -23.206 -23.245  14.790 1.00 0.00
ATOM  135 CB  PRO R 54   -24.322 -21.543  11.933 1.00 0.00
ATOM  136 CG  PRO R 54   -23.279 -22.449  11.267 1.00 0.00
ATOM  137 CD  PRO R 54   -21.973 -22.056  11.958 1.00 0.00
ATOM  138 N   CYS R 55   -25.389 -22.945  14.169 1.00 0.00
ATOM  139 CA  CYS R 55   -25.953 -24.243  14.552 1.00 0.00
ATOM  140 C   CYS R 55   -25.269 -25.446  13.903 1.00 0.00
ATOM  141 O   CYS R 55   -24.242 -25.300  13.245 1.00 0.00
ATOM  142 CB  CYS R 55   -27.451 -24.242  14.222 1.00 0.00
ATOM  143 SG  CYS R 55   -28.150 -22.588  13.922 1.00 0.00
ATOM  144 H   CYS R 55   -26.029 -22.260  13.834 1.00 0.00
ATOM  145 N   LYS R 56   -25.873 -26.628  14.098 1.00 0.00
ATOM  146 CA  LYS R 56   -25.241 -27.917  13.821 1.00 0.00
ATOM  147 C   LYS R 56   -26.256 -29.045  13.957 1.00 0.00
ATOM  148 O   LYS R 56   -26.703 -29.417  15.037 1.00 0.00
ATOM  149 CB  LYS R 56   -24.073 -28.150  14.789 1.00 0.00
ATOM  150 CG  LYS R 56   -23.350 -29.501  14.702 1.00 0.00
ATOM  151 CD  LYS R 56   -22.658 -29.801  13.373 1.00 0.00
ATOM  152 CE  LYS R 56   -21.673 -30.966  13.503 1.00 0.00
ATOM  153 NZ  LYS R 56   -20.454 -30.524  14.191 1.00 0.00
ATOM  154 H   LYS R 56   -26.725 -26.673  14.623 1.00 0.00
ATOM  155 1HZ LYS R 56   -19.887 -31.370  14.402 1.00 0.00
ATOM  156 2HZ LYS R 56   -20.632 -30.000  15.073 1.00 0.00
ATOM  157 3HZ LYS R 56   -19.886 -29.946  13.544 1.00 0.00
ATOM  158 N   PRO R 57   -26.633 -29.599  12.787 1.00 0.00
ATOM  159 CA  PRO R 57   -27.416 -30.837  12.811 1.00 0.00
ATOM  160 C   PRO R 57   -26.644 -31.966  13.476 1.00 0.00
ATOM  161 O   PRO R 57   -25.420 -31.911  13.609 1.00 0.00
ATOM  162 CB  PRO R 57   -27.665 -31.109  11.323 1.00 0.00
ATOM  163 CG  PRO R 57   -27.447 -29.776  10.607 1.00 0.00
```

```
ATOM  164  CD  PRO R  57     -26.356 -29.119  11.441  1.00  0.00
ATOM  165  N   CYS R  58     -27.418 -32.994  13.860  1.00  0.00
ATOM  166  CA  CYS R  58     -26.761 -34.217  14.319  1.00  0.00
ATOM  167  C   CYS R  58     -26.309 -35.070  13.141  1.00  0.00
ATOM  168  O   CYS R  58     -26.576 -34.743  11.987  1.00  0.00
ATOM  169  CB  CYS R  58     -27.709 -34.963  15.259  1.00  0.00
ATOM  170  SG  CYS R  58     -27.015 -36.478  15.973  1.00  0.00
ATOM  171  H   CYS R  58     -28.408 -32.886  13.776  1.00  0.00
ATOM  172  N   THR R  59     -25.623 -36.173  13.459  1.00  0.00
ATOM  173  CA  THR R  59     -25.066 -37.074  12.445  1.00  0.00
ATOM  174  C   THR R  59     -26.048 -38.160  11.949  1.00  0.00
ATOM  175  O   THR R  59     -27.196 -38.234  12.397  1.00  0.00
ATOM  176  CB  THR R  59     -23.767 -37.636  13.055  1.00  0.00
ATOM  177  OG1 THR R  59     -23.270 -36.723  14.052  1.00  0.00
ATOM  178  CG2 THR R  59     -22.667 -37.924  12.029  1.00  0.00
ATOM  179  H   THR R  59     -25.398 -36.368  14.415  1.00  0.00
ATOM  180  HG1 THR R  59     -22.729 -37.252  14.644  1.00  0.00
ATOM  181  N   GLU R  60     -25.578 -38.985  10.999  1.00  0.00
ATOM  182  CA  GLU R  60     -26.467 -40.006  10.445  1.00  0.00
ATOM  183  C   GLU R  60     -26.899 -41.149  11.355  1.00  0.00
ATOM  184  O   GLU R  60     -26.152 -42.083  11.672  1.00  0.00
ATOM  185  CB  GLU R  60     -25.943 -40.541   9.111  1.00  0.00
ATOM  186  CG  GLU R  60     -27.011 -40.494   8.010  1.00  0.00
ATOM  187  CD  GLU R  60     -28.263 -41.228   8.450  1.00  0.00
ATOM  188  OE1 GLU R  60     -28.349 -42.428   8.253  1.00  0.00
ATOM  189  OE2 GLU R  60     -29.161 -40.605   9.003  1.00  0.00
ATOM  190  H   GLU R  60     -24.642 -38.859  10.693  1.00  0.00
ATOM  191  N   CYS R  61     -28.169 -41.001  11.750  1.00  0.00
ATOM  192  CA  CYS R  61     -28.775 -41.881  12.742  1.00  0.00
ATOM  193  C   CYS R  61     -29.712 -42.937  12.185  1.00  0.00
ATOM  194  O   CYS R  61     -30.148 -43.845  12.890  1.00  0.00
ATOM  195  CB  CYS R  61     -29.564 -41.086  13.782  1.00  0.00
ATOM  196  SG  CYS R  61     -28.791 -39.568  14.416  1.00  0.00
ATOM  197  H   CYS R  61     -28.690 -40.307  11.255  1.00  0.00
ATOM  198  N   VAL R  62     -30.069 -42.806  10.908  1.00  0.00
ATOM  199  CA  VAL R  62     -31.084 -43.768  10.496  1.00  0.00
```

```
ATOM  200  C  VAL R  62    -30.571 -44.884   9.598  1.00  0.00
ATOM  201  O  VAL R  62    -30.480 -46.055   9.964  1.00  0.00
ATOM  202  CB VAL R  62    -32.301 -43.050   9.878  1.00  0.00
ATOM  203  CG1 VAL R  62   -33.489 -44.005   9.713  1.00  0.00
ATOM  204  CG2 VAL R  62   -32.705 -41.812  10.685  1.00  0.00
ATOM  205  H  VAL R  62    -29.584 -42.202  10.268  1.00  0.00
ATOM  206  N  GLY R  63    -30.336 -44.466   8.349  1.00  0.00
ATOM  207  CA GLY R  63    -30.443 -45.442   7.270  1.00  0.00
ATOM  208  C  GLY R  63    -29.148 -45.809   6.584  1.00  0.00
ATOM  209  O  GLY R  63    -29.004 -46.882   6.009  1.00  0.00
ATOM  210  H  GLY R  63    -30.082 -43.508   8.197  1.00  0.00
ATOM  211  N  LEU R  64    -28.206 -44.867   6.628  1.00  0.00
ATOM  212  CA LEU R  64    -26.859 -45.283   6.260  1.00  0.00
ATOM  213  C  LEU R  64    -26.145 -45.795   7.489  1.00  0.00
ATOM  214  O  LEU R  64    -25.525 -46.855   7.545  1.00  0.00
ATOM  215  CB LEU R  64    -26.088 -44.113   5.644  1.00  0.00
ATOM  216  CG LEU R  64    -26.754 -43.525   4.397  1.00  0.00
ATOM  217  CD1 LEU R  64   -26.073 -42.229   3.958  1.00  0.00
ATOM  218  CD2 LEU R  64   -26.848 -44.540   3.255  1.00  0.00
ATOM  219  H  LEU R  64    -28.391 -43.992   7.076  1.00  0.00
ATOM  220  N  GLN R  65    -26.262 -44.951   8.515  1.00  0.00
ATOM  221  CA GLN R  65    -25.639 -45.245   9.796  1.00  0.00
ATOM  222  C  GLN R  65    -26.708 -45.080  10.851  1.00  0.00
ATOM  223  O  GLN R  65    -27.738 -44.460  10.612  1.00  0.00
ATOM  224  CB GLN R  65    -24.456 -44.300  10.006  1.00  0.00
ATOM  225  CG GLN R  65    -23.336 -44.444   8.965  1.00  0.00
ATOM  226  CD GLN R  65    -22.421 -45.624   9.253  1.00  0.00
ATOM  227  OE1 GLN R  65   -21.315 -45.443   9.762  1.00  0.00
ATOM  228  NE2 GLN R  65   -22.857 -46.816   8.833  1.00  0.00
ATOM  229  H  GLN R  65    -26.850 -44.141   8.449  1.00  0.00
ATOM  230 1HE2 GLN R  65   -22.292 -47.635   8.846  1.00  0.00
ATOM  231 2HE2 GLN R  65   -23.800 -46.898   8.500  1.00  0.00
ATOM  232  N  SER R  66    -26.473 -45.715  12.001  1.00  0.00
ATOM  233  CA SER R  66    -27.657 -45.886  12.838  1.00  0.00
ATOM  234  C  SER R  66    -27.604 -45.224  14.204  1.00  0.00
ATOM  235  O  SER R  66    -26.542 -44.815  14.682  1.00  0.00
```

```
ATOM  236 CB  SER R 66   -28.013 -47.373  12.884  1.00  0.00
ATOM  237 OG  SER R 66   -27.869 -47.927  11.565  1.00  0.00
ATOM  238 H   SER R 66   -25.586 -46.141  12.173  1.00  0.00
ATOM  239 HG  SER R 66   -28.474 -47.423  11.013  1.00  0.00
ATOM  240 N   MET R 67   -28.808 -45.110  14.779  1.00  0.00
ATOM  241 CA  MET R 67   -29.048 -44.257  15.939  1.00  0.00
ATOM  242 C   MET R 67   -28.294 -44.575  17.212  1.00  0.00
ATOM  243 O   MET R 67   -28.404 -45.649  17.800  1.00  0.00
ATOM  244 CB  MET R 67   -30.556 -44.203  16.197  1.00  0.00
ATOM  245 CG  MET R 67   -31.008 -42.933  16.916  1.00  0.00
ATOM  246 SD  MET R 67   -32.793 -42.833  17.123  1.00  0.00
ATOM  247 CE  MET R 67   -33.244 -42.903  15.380  1.00  0.00
ATOM  248 H   MET R 67   -29.573 -45.360  14.189  1.00  0.00
ATOM  249 N   SER R 68   -27.557 -43.553  17.633  1.00  0.00
ATOM  250 CA  SER R 68   -26.992 -43.620  18.977  1.00  0.00
ATOM  251 C   SER R 68   -27.868 -42.986  20.035  1.00  0.00
ATOM  252 O   SER R 68   -27.813 -43.326  21.215  1.00  0.00
ATOM  253 CB  SER R 68   -25.615 -42.989  18.978  1.00  0.00
ATOM  254 OG  SER R 68   -25.029 -43.228  17.693  1.00  0.00
ATOM  255 H   SER R 68   -27.423 -42.756  17.044  1.00  0.00
ATOM  256 HG  SER R 68   -24.083 -43.177  17.834  1.00  0.00
ATOM  257 N   ALA R 69   -28.706 -42.060  19.521  1.00  0.00
ATOM  258 CA  ALA R 69   -29.837 -41.437  20.214  1.00  0.00
ATOM  259 C   ALA R 69   -30.311 -40.307  19.312  1.00  0.00
ATOM  260 O   ALA R 69   -29.592 -39.924  18.387  1.00  0.00
ATOM  261 CB  ALA R 69   -29.406 -40.835  21.565  1.00  0.00
ATOM  262 H   ALA R 69   -28.493 -41.701  18.610  1.00  0.00
ATOM  263 N   PRO R 70   -31.506 -39.724  19.607  1.00  0.00
ATOM  264 CA  PRO R 70   -31.722 -38.322  19.207  1.00  0.00
ATOM  265 C   PRO R 70   -30.580 -37.436  19.699  1.00  0.00
ATOM  266 O   PRO R 70   -29.722 -37.895  20.456  1.00  0.00
ATOM  267 CB  PRO R 70   -33.063 -37.990  19.869  1.00  0.00
ATOM  268 CG  PRO R 70   -33.779 -39.331  20.022  1.00  0.00
ATOM  269 CD  PRO R 70   -32.637 -40.289  20.334  1.00  0.00
ATOM  270 N   CYS R 71   -30.549 -36.191  19.227  1.00  0.00
ATOM  271 CA  CYS R 71   -29.381 -35.417  19.642  1.00  0.00
```

```
ATOM  272  C  CYS R  71    -29.730 -34.124  20.337  1.00  0.00
ATOM  273  O  CYS R  71    -30.848 -33.618  20.262  1.00  0.00
ATOM  274  CB CYS R  71    -28.418 -35.200  18.474  1.00  0.00
ATOM  275  SG CYS R  71    -27.801 -36.785  17.835  1.00  0.00
ATOM  276  H  CYS R  71    -31.299 -35.781  18.711  1.00  0.00
ATOM  277  N  VAL R  72    -28.733 -33.641  21.079  1.00  0.00
ATOM  278  CA VAL R  72    -28.793 -32.337  21.739  1.00  0.00
ATOM  279  C  VAL R  72    -27.441 -31.695  21.515  1.00  0.00
ATOM  280  O  VAL R  72    -26.587 -32.323  20.897  1.00  0.00
ATOM  281  CB VAL R  72    -29.087 -32.477  23.244  1.00  0.00
ATOM  282  CG1 VAL R  72   -30.554 -32.827  23.502  1.00  0.00
ATOM  283  CG2 VAL R  72   -28.125 -33.455  23.932  1.00  0.00
ATOM  284  H  VAL R  72    -27.860 -34.132  21.089  1.00  0.00
ATOM  285  N  GLU R  73    -27.282 -30.465  22.038  1.00  0.00
ATOM  286  CA GLU R  73    -25.992 -29.787  21.908  1.00  0.00
ATOM  287  C  GLU R  73    -24.848 -30.522  22.569  1.00  0.00
ATOM  288  O  GLU R  73    -24.610 -30.447  23.773  1.00  0.00
ATOM  289  CB GLU R  73    -26.073 -28.328  22.365  1.00  0.00
ATOM  290  CG GLU R  73    -24.825 -27.556  21.923  1.00  0.00
ATOM  291  CD GLU R  73    -24.974 -26.067  22.159  1.00  0.00
ATOM  292  OE1 GLU R  73   -25.947 -25.478  21.698  1.00  0.00
ATOM  293  OE2 GLU R  73   -24.103 -25.484  22.793  1.00  0.00
ATOM  294  H  GLU R  73    -28.030 -30.065  22.564  1.00  0.00
ATOM  295  N  ALA R  74    -24.183 -31.276  21.690  1.00  0.00
ATOM  296  CA ALA R  74    -22.982 -32.030  22.006  1.00  0.00
ATOM  297  C  ALA R  74    -22.211 -32.099  20.717  1.00  0.00
ATOM  298  O  ALA R  74    -22.796 -32.213  19.640  1.00  0.00
ATOM  299  CB ALA R  74    -23.328 -33.451  22.455  1.00  0.00
ATOM  300  H  ALA R  74    -24.600 -31.329  20.777  1.00  0.00
ATOM  301  N  ASP R  75    -20.889 -31.945  20.853  1.00  0.00
ATOM  302  CA ASP R  75    -20.105 -31.837  19.633  1.00  0.00
ATOM  303  C  ASP R  75    -20.167 -33.101  18.799  1.00  0.00
ATOM  304  O  ASP R  75    -20.254 -34.213  19.326  1.00  0.00
ATOM  305  CB ASP R  75    -18.676 -31.418  19.976  1.00  0.00
ATOM  306  CG ASP R  75    -18.194 -30.327  19.038  1.00  0.00
ATOM  307  OD1 ASP R  75   -17.534 -29.398  19.470  1.00  0.00
```

ATOM 308 OD2 ASP R 75 -18.410 -30.388 17.841 1.00 0.00
ATOM 309 H ASP R 75 -20.452 -31.968 21.747 1.00 0.00
ATOM 310 N ASP R 76 -20.194 -32.858 17.466 1.00 0.00
ATOM 311 CA ASP R 76 -20.556 -33.842 16.433 1.00 0.00
ATOM 312 C ASP R 76 -21.294 -35.063 16.965 1.00 0.00
ATOM 313 O ASP R 76 -20.725 -36.140 17.153 1.00 0.00
ATOM 314 CB ASP R 76 -19.324 -34.222 15.591 1.00 0.00
ATOM 315 CG ASP R 76 -18.850 -33.033 14.765 1.00 0.00
ATOM 316 OD1 ASP R 76 -18.213 -32.134 15.285 1.00 0.00
ATOM 317 OD2 ASP R 76 -19.132 -32.953 13.580 1.00 0.00
ATOM 318 H ASP R 76 -19.875 -31.943 17.215 1.00 0.00
ATOM 319 N ALA R 77 -22.571 -34.806 17.303 1.00 0.00
ATOM 320 CA ALA R 77 -23.290 -35.694 18.218 1.00 0.00
ATOM 321 C ALA R 77 -23.531 -37.073 17.651 1.00 0.00
ATOM 322 O ALA R 77 -23.725 -37.259 16.456 1.00 0.00
ATOM 323 CB ALA R 77 -24.619 -35.075 18.644 1.00 0.00
ATOM 324 H ALA R 77 -23.001 -34.012 16.881 1.00 0.00
ATOM 325 N VAL R 78 -23.455 -38.052 18.556 1.00 0.00
ATOM 326 CA VAL R 78 -22.704 -39.281 18.232 1.00 0.00
ATOM 327 C VAL R 78 -23.295 -40.388 17.344 1.00 0.00
ATOM 328 O VAL R 78 -23.041 -41.583 17.543 1.00 0.00
ATOM 329 CB VAL R 78 -22.160 -39.877 19.542 1.00 0.00
ATOM 330 CG1 VAL R 78 -21.189 -38.911 20.224 1.00 0.00
ATOM 331 CG2 VAL R 78 -23.287 -40.288 20.497 1.00 0.00
ATOM 332 H VAL R 78 -23.598 -37.743 19.493 1.00 0.00
ATOM 333 N CYS R 79 -24.111 -40.011 16.349 1.00 0.00
ATOM 334 CA CYS R 79 -24.667 -41.058 15.490 1.00 0.00
ATOM 335 C CYS R 79 -23.639 -41.706 14.569 1.00 0.00
ATOM 336 O CYS R 79 -23.161 -41.097 13.611 1.00 0.00
ATOM 337 CB CYS R 79 -25.854 -40.535 14.695 1.00 0.00
ATOM 338 SG CYS R 79 -27.265 -40.010 15.706 1.00 0.00
ATOM 339 H CYS R 79 -24.146 -39.049 16.105 1.00 0.00
ATOM 340 N ARG R 80 -23.326 -42.955 14.966 1.00 0.00
ATOM 341 CA ARG R 80 -22.220 -43.688 14.354 1.00 0.00
ATOM 342 C ARG R 80 -22.617 -45.027 13.739 1.00 0.00
ATOM 343 O ARG R 80 -22.898 -45.120 12.547 1.00 0.00

```
ATOM   344  CB  ARG R  80     -21.047 -43.866  15.333  1.00  0.00
ATOM   345  CG  ARG R  80     -19.958 -42.787  15.285  1.00  0.00
ATOM   346  CD  ARG R  80     -19.283 -42.600  13.916  1.00  0.00
ATOM   347  NE  ARG R  80     -18.739 -43.844  13.361  1.00  0.00
ATOM   348  CZ  ARG R  80     -19.343 -44.423  12.298  1.00  0.00
ATOM   349  NH1 ARG R  80     -18.915 -45.588  11.814  1.00  0.00
ATOM   350  NH2 ARG R  80     -20.397 -43.844  11.740  1.00  0.00
ATOM   351  H   ARG R  80     -23.849 -43.366  15.715  1.00  0.00
ATOM   352  HE  ARG R  80     -17.952 -44.277  13.804  1.00  0.00
ATOM   353 1HH1 ARG R  80     -19.409 -46.064  11.082  1.00  0.00
ATOM   354 2HH1 ARG R  80     -18.080 -46.022  12.174  1.00  0.00
ATOM   355 1HH2 ARG R  80     -20.880 -44.269  10.976  1.00  0.00
ATOM   356 2HH2 ARG R  80     -20.749 -42.984  12.102  1.00  0.00
ATOM   357  N   CYS R  81     -22.630 -46.086  14.566  1.00  0.00
ATOM   358  CA  CYS R  81     -22.946 -47.400  14.002  1.00  0.00
ATOM   359  C   CYS R  81     -23.527 -48.331  15.049  1.00  0.00
ATOM   360  O   CYS R  81     -22.830 -49.080  15.728  1.00  0.00
ATOM   361  CB  CYS R  81     -21.732 -48.025  13.284  1.00  0.00
ATOM   362  SG  CYS R  81     -22.046 -48.494  11.547  1.00  0.00
ATOM   363  H   CYS R  81     -22.342 -45.997  15.517  1.00  0.00
ATOM   364  N   ALA R  82     -24.869 -48.212  15.160  1.00  0.00
ATOM   365  CA  ALA R  82     -25.712 -49.047  16.033  1.00  0.00
ATOM   366  C   ALA R  82     -25.041 -49.677  17.246  1.00  0.00
ATOM   367  O   ALA R  82     -24.801 -50.881  17.310  1.00  0.00
ATOM   368  CB  ALA R  82     -26.390 -50.148  15.212  1.00  0.00
ATOM   369  H   ALA R  82     -25.322 -47.577  14.537  1.00  0.00
ATOM   370  N   TYR R  83     -24.697 -48.786  18.189  1.00  0.00
ATOM   371  CA  TYR R  83     -23.809 -49.240  19.256  1.00  0.00
ATOM   372  C   TYR R  83     -24.319 -50.384  20.116  1.00  0.00
ATOM   373  O   TYR R  83     -25.492 -50.522  20.451  1.00  0.00
ATOM   374  CB  TYR R  83     -23.268 -48.059  20.087  1.00  0.00
ATOM   375  CG  TYR R  83     -24.247 -47.511  21.108  1.00  0.00
ATOM   376  CD1 TYR R  83     -25.207 -46.556  20.715  1.00  0.00
ATOM   377  CD2 TYR R  83     -24.147 -47.951  22.445  1.00  0.00
ATOM   378  CE1 TYR R  83     -26.058 -46.003  21.688  1.00  0.00
ATOM   379  CE2 TYR R  83     -25.001 -47.400  23.417  1.00  0.00
```

```
ATOM  380 CZ  TYR R 83   -25.937 -46.419  23.031  1.00  0.00
ATOM  381 OH  TYR R 83   -26.753 -45.849  23.995  1.00  0.00
ATOM  382 H   TYR R 83   -25.061 -47.858  18.145  1.00  0.00
ATOM  383 HH  TYR R 83   -27.139 -45.055  23.619  1.00  0.00
ATOM  384 N   GLY R 84   -23.359 -51.236  20.478  1.00  0.00
ATOM  385 CA  GLY R 84   -23.783 -52.411  21.232  1.00  0.00
ATOM  386 C   GLY R 84   -23.284 -53.694  20.609  1.00  0.00
ATOM  387 O   GLY R 84   -23.189 -54.732  21.259  1.00  0.00
ATOM  388 H   GLY R 84   -22.420 -51.099  20.167  1.00  0.00
ATOM  389 N   TYR R 85   -22.925 -53.551  19.317  1.00  0.00
ATOM  390 CA  TYR R 85   -21.764 -54.346  18.941  1.00  0.00
ATOM  391 C   TYR R 85   -20.520 -53.484  19.090  1.00  0.00
ATOM  392 O   TYR R 85   -20.632 -52.266  19.248  1.00  0.00
ATOM  393 CB  TYR R 85   -21.930 -54.959  17.539  1.00  0.00
ATOM  394 CG  TYR R 85   -21.890 -53.946  16.413  1.00  0.00
ATOM  395 CD1 TYR R 85   -23.084 -53.333  15.975  1.00  0.00
ATOM  396 CD2 TYR R 85   -20.649 -53.671  15.805  1.00  0.00
ATOM  397 CE1 TYR R 85   -23.042 -52.477  14.860  1.00  0.00
ATOM  398 CE2 TYR R 85   -20.609 -52.814  14.697  1.00  0.00
ATOM  399 CZ  TYR R 85   -21.808 -52.257  14.215  1.00  0.00
ATOM  400 OH  TYR R 85   -21.760 -51.493  13.062  1.00  0.00
ATOM  401 H   TYR R 85   -23.172 -52.734  18.790  1.00  0.00
ATOM  402 HH  TYR R 85   -20.964 -51.753  12.596  1.00  0.00
ATOM  403 N   TYR R 86   -19.354 -54.143  19.022  1.00  0.00
ATOM  404 CA  TYR R 86   -18.070 -53.498  19.330  1.00  0.00
ATOM  405 C   TYR R 86   -17.547 -52.466  18.319  1.00  0.00
ATOM  406 O   TYR R 86   -16.457 -52.635  17.784  1.00  0.00
ATOM  407 CB  TYR R 86   -17.072 -54.652  19.552  1.00  0.00
ATOM  408 CG  TYR R 86   -15.786 -54.368  20.316  1.00  0.00
ATOM  409 CD1 TYR R 86   -15.322 -53.061  20.597  1.00  0.00
ATOM  410 CD2 TYR R 86   -15.053 -55.502  20.719  1.00  0.00
ATOM  411 CE1 TYR R 86   -14.087 -52.896  21.255  1.00  0.00
ATOM  412 CE2 TYR R 86   -13.825 -55.340  21.380  1.00  0.00
ATOM  413 CZ  TYR R 86   -13.346 -54.040  21.627  1.00  0.00
ATOM  414 OH  TYR R 86   -12.110 -53.911  22.244  1.00  0.00
ATOM  415 H   TYR R 86   -19.425 -55.102  18.757  1.00  0.00
```

ATOM 416 HH TYR R 86 -11.829 -53.003 22.149 1.00 0.00
ATOM 417 N GLN R 87 -18.334 -51.399 18.081 1.00 0.00
ATOM 418 CA GLN R 87 -17.800 -50.310 17.258 1.00 0.00
ATOM 419 C GLN R 87 -17.117 -49.255 18.112 1.00 0.00
ATOM 420 O GLN R 87 -17.704 -48.681 19.022 1.00 0.00
ATOM 421 CB GLN R 87 -18.910 -49.706 16.371 1.00 0.00
ATOM 422 CG GLN R 87 -18.725 -48.273 15.812 1.00 0.00
ATOM 423 CD GLN R 87 -17.729 -48.089 14.663 1.00 0.00
ATOM 424 OE1 GLN R 87 -17.701 -47.027 14.040 1.00 0.00
ATOM 425 NE2 GLN R 87 -16.936 -49.120 14.374 1.00 0.00
ATOM 426 H GLN R 87 -19.143 -51.256 18.647 1.00 0.00
ATOM 427 1HE2 GLN R 87 -16.239 -49.104 13.659 1.00 0.00
ATOM 428 2HE2 GLN R 87 -16.869 -50.003 14.846 1.00 0.00
ATOM 429 N ASP R 88 -15.845 -49.028 17.759 1.00 0.00
ATOM 430 CA ASP R 88 -15.041 -48.001 18.429 1.00 0.00
ATOM 431 C ASP R 88 -14.442 -47.101 17.361 1.00 0.00
ATOM 432 O ASP R 88 -14.123 -47.592 16.276 1.00 0.00
ATOM 433 CB ASP R 88 -13.968 -48.725 19.273 1.00 0.00
ATOM 434 CG ASP R 88 -12.942 -47.819 19.953 1.00 0.00
ATOM 435 OD1 ASP R 88 -11.758 -48.104 19.876 1.00 0.00
ATOM 436 OD2 ASP R 88 -13.294 -46.831 20.580 1.00 0.00
ATOM 437 H ASP R 88 -15.429 -49.592 17.039 1.00 0.00
ATOM 438 N GLU R 89 -14.306 -45.805 17.710 1.00 0.00
ATOM 439 CA GLU R 89 -13.680 -44.795 16.839 1.00 0.00
ATOM 440 C GLU R 89 -14.515 -44.403 15.614 1.00 0.00
ATOM 441 O GLU R 89 -15.309 -43.460 15.616 1.00 0.00
ATOM 442 CB GLU R 89 -12.257 -45.283 16.493 1.00 0.00
ATOM 443 CG GLU R 89 -11.293 -44.524 15.571 1.00 0.00
ATOM 444 CD GLU R 89 -10.219 -45.518 15.145 1.00 0.00
ATOM 445 OE1 GLU R 89 -9.962 -45.681 13.957 1.00 0.00
ATOM 446 OE2 GLU R 89 -9.644 -46.177 15.998 1.00 0.00
ATOM 447 H GLU R 89 -14.511 -45.638 18.676 1.00 0.00
ATOM 448 N THR R 90 -14.293 -45.184 14.553 1.00 0.00
ATOM 449 CA THR R 90 -14.096 -44.591 13.232 1.00 0.00
ATOM 450 C THR R 90 -15.313 -44.151 12.444 1.00 0.00
ATOM 451 O THR R 90 -16.239 -44.933 12.212 1.00 0.00

```
ATOM  452 CB  THR R  90   -13.307 -45.598  12.397  1.00  0.00
ATOM  453 OG1 THR R  90   -12.719 -46.613  13.229  1.00  0.00
ATOM  454 CG2 THR R  90   -12.269 -44.936  11.490  1.00  0.00
ATOM  455 H   THR R  90   -14.031 -46.141  14.672  1.00  0.00
ATOM  456 HG1 THR R  90   -11.932 -46.206  13.613  1.00  0.00
ATOM  457 N   THR R  91   -15.264 -42.906  11.946  1.00  0.00
ATOM  458 CA  THR R  91   -16.086 -42.598  10.774  1.00  0.00
ATOM  459 C   THR R  91   -15.551 -43.214   9.474  1.00  0.00
ATOM  460 O   THR R  91   -15.041 -42.576   8.553  1.00  0.00
ATOM  461 CB  THR R  91   -16.263 -41.089  10.611  1.00  0.00
ATOM  462 OG1 THR R  91   -15.526 -40.320  11.595  1.00  0.00
ATOM  463 CG2 THR R  91   -17.753 -40.737  10.608  1.00  0.00
ATOM  464 H   THR R  91   -14.546 -42.271  12.218  1.00  0.00
ATOM  465 HG1 THR R  91   -16.170 -40.159  12.292  1.00  0.00
ATOM  466 N   GLY R  92   -15.638 -44.548   9.437  1.00  0.00
ATOM  467 CA  GLY R  92   -14.952 -45.240   8.341  1.00  0.00
ATOM  468 C   GLY R  92   -14.947 -46.747   8.485  1.00  0.00
ATOM  469 O   GLY R  92   -15.038 -47.506   7.517  1.00  0.00
ATOM  470 H   GLY R  92   -16.190 -45.008  10.134  1.00  0.00
ATOM  471 N   ARG R  93   -14.906 -47.132   9.766  1.00  0.00
ATOM  472 CA  ARG R  93   -15.165 -48.526  10.101  1.00  0.00
ATOM  473 C   ARG R  93   -16.597 -48.659  10.561  1.00  0.00
ATOM  474 O   ARG R  93   -17.179 -47.725  11.108  1.00  0.00
ATOM  475 CB  ARG R  93   -14.257 -49.027  11.231  1.00  0.00
ATOM  476 CG  ARG R  93   -12.866 -49.498  10.801  1.00  0.00
ATOM  477 CD  ARG R  93   -12.088 -50.205  11.924  1.00  0.00
ATOM  478 NE  ARG R  93   -11.530 -49.278  12.906  1.00  0.00
ATOM  479 CZ  ARG R  93   -11.885 -49.270  14.210  1.00  0.00
ATOM  480 NH1 ARG R  93   -11.321 -48.407  15.046  1.00  0.00
ATOM  481 NH2 ARG R  93   -12.806 -50.108  14.666  1.00  0.00
ATOM  482 H   ARG R  93   -14.866 -46.429  10.469  1.00  0.00
ATOM  483 HE  ARG R  93   -10.826 -48.644  12.583  1.00  0.00
ATOM  484 1HH1 ARG R  93   -11.678 -48.273  15.969  1.00  0.00
ATOM  485 2HH1 ARG R  93   -10.552 -47.825  14.774  1.00  0.00
ATOM  486 1HH2 ARG R  93   -13.112 -50.146  15.616  1.00  0.00
ATOM  487 2HH2 ARG R  93   -13.266 -50.761  14.058  1.00  0.00
```

```
ATOM   488  N   CYS R  94    -17.121 -49.864  10.349  1.00  0.00
ATOM   489  CA  CYS R  94    -18.327 -50.307  11.053  1.00  0.00
ATOM   490  C   CYS R  94    -18.187 -51.790  11.280  1.00  0.00
ATOM   491  O   CYS R  94    -18.340 -52.598  10.361  1.00  0.00
ATOM   492  CB  CYS R  94    -19.611 -50.063  10.264  1.00  0.00
ATOM   493  SG  CYS R  94    -20.314 -48.399  10.429  1.00  0.00
ATOM   494  H   CYS R  94    -16.640 -50.508   9.754  1.00  0.00
ATOM   495  N   GLU R  95    -17.798 -52.106  12.524  1.00  0.00
ATOM   496  CA  GLU R  95    -17.382 -53.477  12.826  1.00  0.00
ATOM   497  C   GLU R  95    -18.334 -54.564  12.388  1.00  0.00
ATOM   498  O   GLU R  95    -19.545 -54.380  12.270  1.00  0.00
ATOM   499  CB  GLU R  95    -17.063 -53.650  14.313  1.00  0.00
ATOM   500  CG  GLU R  95    -15.587 -53.436  14.658  1.00  0.00
ATOM   501  CD  GLU R  95    -15.185 -51.998  14.416  1.00  0.00
ATOM   502  OE1 GLU R  95    -14.757 -51.672  13.318  1.00  0.00
ATOM   503  OE2 GLU R  95    -15.280 -51.193  15.328  1.00  0.00
ATOM   504  H   GLU R  95    -17.570 -51.381  13.172  1.00  0.00
ATOM   505  N   ALA R  96    -17.715 -55.723  12.129  1.00  0.00
ATOM   506  CA  ALA R  96    -18.517 -56.877  11.727  1.00  0.00
ATOM   507  C   ALA R  96    -18.962 -57.733  12.900  1.00  0.00
ATOM   508  O   ALA R  96    -20.158 -57.994  13.010  1.00  0.00
ATOM   509  CB  ALA R  96    -17.748 -57.740  10.723  1.00  0.00
ATOM   510  OXT ALA R  96    -18.116 -58.127  13.704  1.00  0.00
ATOM   511  H   ALA R  96    -16.728 -55.754  12.290  1.00  0.00
END
```

---

*Principal residues are bolded.

Appendix 4. The Fortran-77 source code of the VBMC algorithm.*

```
      SUBROUTINE MONTE(XMIN,N,S0)
C*
C*    Variable Basis Monte Carlo simulated annealing:
C*    XMIN - initial configurational variables and
C*         final variables for subsequent local energy
C*         refinement.
C*    N - the number of configurational variables.
C*    S0 - initial energy.
C*    FUN - potential energy function.
C*
      IMPLICIT REAL*8(A-H,O-Z)
      DIMENSION XX(250),X(250),XMIN(1)
      DIMENSION Y(500,250),C(250,250),E(250),V(250,250)
      IYES=0
      ITEST=0
      READ(5,1)N1,N4,N5,NG1,ITE,IPR1,N33
      IF(N1.EQ.0)RETURN
      WRITE(6,3000)ITE,S0
      TT=ITE
 3000 FORMAT(/10X,'INITIAL TEMPERATURE',I7,
     1    ' INITIAL ENERGY ',F15.6/)
      PR1=IPR1
      PR2=PR1*2.D0
      WRITE(6,210)PR1,PR1
  210 FORMAT(' RANDOM TORSIONAL INCREMENT -'
     2    ,F5.2,' TO +',F5.2,' GRAD')
      WRITE(6,302)
  302 FORMAT(10X,'*VARIABLE BASIS MC SIMULATED ANNEALING*'/)
C*    Boltzmann factor.
      T=-1./(0.001987*TT)
C     *** TEMPERATURE T=ITE ***
    1 FORMAT(15I5)
      N1=N*N1
      N3=N
```

```
      K=N
C*    Cooling schedule.
      DT=(ITE-120)/(N5*N3)
      NG=NG1
      IF(NG.EQ.0)NG=1
C*    Initial set of random number generator.
      CALL SRAND(NG)
      WRITE(6,2)N1,N3,N4,N5,NG
    2 FORMAT(/5X,'MONTE-CARLO PARAMETERS:'/
     *5X,'BLIND CUT',I10/
     *5X,'BYPASS',I10/
     *5X,'FREQUENCY OF CONTROL OUTPUT',I10/
     *5X,'LENGTH OF ANNEALING REGION',I10/
     *5X,'INITIAL SET OF THE RANDOM GENERATOR ',I10/)
      IBEGIN=0
      MNCARL=0
      LQ=0
      I7=0
      L1=0
      EMIN=1.D37
      S3=0.
      S4=0.
C*    Initial set of basis of independent variables.
      DO 88 I=1,N
      DO 88 J=1,N
      V(I,J)=0.D0
      IF(I.EQ.J)V(I,J)=1.D0
   88 CONTINUE
      DO 2005 I=1,N
 2005 X(I)=XMIN(I)
  264 S1=0.
      S2=0.
      L=0
C*    Method Monte Carlo.
      IYES=0
      KG=0
```

```
      L2=0
      I=0
   26 I=I+1
C*      Random choice of a variable to move.
      H=RAND()
      IK=IDINT(H*N)+1
      RA=RAND()
      D=RA*PR2-PR1
C*      Variable Basis Markov chain: move along basis vectors.
      DO 513 II=1,N
  513 XX(II)=X(II)+V(II,IK)*D
      CALL FUN(N,XX,SS)
C*      SS - potential energy of the configuration XX.
      S=SS-S0
      BI=S*T
      IF(BI.GT.50.D0) GOTO 263
C*      CALCULATION OF TRANSITION PROBABILITY
      IF(BI.LT.-50.D0) GOTO 262
      B=DEXP(BI)
      W7=B/(B+1.D0)
C*      DOES TRANSITION TAKE PLACE ?
      Z=RAND()
      IF(W7-Z)262,263,263
C*      ** NO **
  262 CONTINUE
      GOTO 274
C*      ** YES ! **
  263 S0=SS
      IYES=IYES+1
      DO 1314 II=1,N
 1314 X(II)=XX(II)
C*      Blind cut off
  274 IF(IBEGIN.EQ.1) GOTO 266
      MNCARL=MNCARL+1
      IF(MNCARL-N1)26,1264,265
 1264 WRITE(6,1265)MNCARL,S0
```

```
 1265 FORMAT('Initial point has been cut off',I10,1PD17.9)
C*      Cut off upon criteria.
      GOTO 264
 265 S1=S1+S0
      S2=S2+S0*S0
      L=L+1
      IF(L.NE.20*N) GOTO 26
      L=0
      SR1=S1/I
      DISP1=S2/I-SR1**2
      IF(DABS(SR1-S0)-DSQRT(DISP1))270,270,271
 271 ITEST=0
      GOTO 272
 270  ITEST=ITEST+1
 272  YES=(1.D2*IYES)/I
      WRITE(6,268)I,S0,SR1,DISP1,ITEST,YES
 268  FORMAT('Cut off',I8,3D14.7,I3,2PF7.1)
      IF(I.GE.50000)GOTO 267
      IF(ITEST-3) 26,267,267
 267 IBEGIN=1
      WRITE(6,1265)MNCARL,S0
      WRITE(6,269)
 269  FORMAT(//45X,'Equilibrium has been reached '/)
      GOTO 264
C*      N3 - parameter of bypassing.
C*      DT - cooling schedule.
 266  L=L+1
      IF(TT.LE.120.D0)GOTO 3333
C*      Slow cooling.
      TT=TT-DT
C*      Boltzmann factor.
      T=-1.D0/(1.987D-3*TT)
      IF(L.LT.N3)GOTO 26
      L=0
      KG=KG+1
C*      Accumulating N33 sequential points of the Markov chain.
```

```
      DO 1992 J=1,N
1992 Y(KG,J)=X(J)
      L1=L1+1
      L2=L2+1
      IF(S0.GE.EMIN)GOTO 1957
      EMIN=S0
      DO 1961 IJ=1,N
1961  XMIN(IJ)=X(IJ)
      LQ=LQ+1
      WRITE(6,100)LQ,I,EMIN,TT,(XMIN(J),J=1,N)
100   FORMAT(/' LQ',2I7,D17.9,F7.1/(1X,10F12.3))
447   FORMAT(/' CR',2I7,D17.9,F7.1/(1X,10F12.3))
1957 IF(KG.LT.N33)GOTO 45
C*      Computing covariant matrix of the distribution of
C*      the N33 accumulated points in the configurational
C*      space.
      KG=0
      DO 71 II=1,K
      YYY=0.0
      DO 82 J=1,N33
   82 YYY=YYY+Y(J,II)
      YYY=YYY/N
      DO 54 J=1,N33
   54 Y(J,II)=Y(J,II)-YYY
   71 CONTINUE
      DO 710 II=1,K
      DO 710 J=1,K
      S=0.0
      DO 711 LL=1,N33
  711 S=S+Y(LL,II)*Y(LL,J)
  710 C(II,J)=S
C*      Covariant matrix is ready.
C*      Roration of basis V:
      CALL SDIAG2(250,K,C,E,V)
   45 IF(L2.LT.N4) GOTO 26
```

```
      L2=0
      YES=(1.D2*IYES)/I
      WRITE(6,72)I,L1,EMIN,S0,TT,YES
   72 FORMAT(' CO',2I10,2D15.6,F7.1,2PF7.1)
      IF(L1.LT.N5) GOTO 26
 3333 WRITE(6,1111)
 1111 FORMAT(//10X,'END OF MONTE CARLO STAGE')
      RETURN
      END
      SUBROUTINE SDIAG2(M,N,A,D,X)
C*
C*      Diagonalization of symmetric matrix A (NxN).
C*      Results: D - eigenvalues; X - eigenvectors.
C*
      IMPLICIT REAL*8(A-H,O-Z)
      DIMENSION A(M,M),D(M),X(M,M)
      DIMENSION E(250)
      EPS=1.0D-14
      TOL=1.0D-30
      IF(N.EQ.1)GOTO 400
      DO 10 I=1,N
      DO 10 J=1,I
   10 X(I,J)=A(I,J)
      DO 150 NI=2,N
      II=N+2-NI
      DO 150 I=II,II
      L=I-2
      H=.0D0
      G=X(I,I-1)
      IF(L)140,140,20
   20 DO 30 K=1,L
   30 H=H+X(I,K)**2
      S=H+G*G
      IF(S.GE.TOL)GOTO 50
      H=.0D0
      GOTO 140
```

```
 50 IF(H)140,140,60
 60 L=L+1
    F=G
    G=DSQRT(S)
    IF(F)75,75,70
 70 G=-G
 75 H=S-F*G
    X(I,I-1)=F-G
    F=.0D0
    DO 110 J=1,L
    X(J,I)=X(I,J)/H
    S=.0D0
    DO 80 K=1,J
 80 S=S+X(J,K)*X(I,K)
    J1=J+1
    IF(J1.GT.L)GOTO 100
    DO 90 K=J1,L
 90 S=S+X(K,J)*X(I,K)
100 E(J)=S/H
110 F=F+S*X(J,I)
    F=F/(H+H)
    DO 120 J=1,L
120 E(J)=E(J)-F*X(I,J)
    DO 130 J=1,L
    F=X(I,J)
    S=E(J)
    DO 130 K=1,J
130 X(J,K)=X(J,K)-F*E(K)-X(I,K)*S
140 D(I)=H
150 E(I-1)=G
160 D(1)=X(1,1)
    X(1,1)=1.D0
    DO 220 I=2,N
    L=I-1
    IF(D(I))200,200,170
170 DO 190 J=1,L
```

```
      S=.0D0
      DO 180 K=1,L
180 S=S+X(I,K)*X(K,J)
      DO 190 K=1,L
190 X(K,J)=X(K,J)-S*X(K,I)
200 D(I)=X(I,I)
      X(I,I)=1.D0
210 DO 220 J=1,L
      X(I,J)=.0D0
220 X(J,I)=.0D0
      B=.0D0
      F=.0D0
      E(N)=.0D0
      DO 340 L=1,N
      H=EPS*(DABS(D(L))+DABS(E(L)))
      IF(H.LE.B)GOTO 235
      B=H
235 DO 240 J=L,N
      IF(DABS(E(J)).LE.B)GOTO 250
240 CONTINUE
250 IF(J.EQ.L)GOTO 340
260 P=(D(L+1)-D(L))*.5D0/E(L)
      R=DSQRT(P*P+1.D0)
      IF(P)270,280,280
270 P=P-R
      GOTO 290
280 P=P+R
290 H=D(L)-E(L)/P
      DO 300 I=L,N
300 D(I)=D(I)-H
      F=F+H
      P=D(J)
      C=1.D0
      S=0.D0
      J1=J-1
      DO 330 NI=L,J1
```

```
      II=L+J1-NI
      DO 330 I=II,II
      G=C*E(I)
      H=C*P
      IF(DABS(P).LT.DABS(E(I)))GOTO 310
      C=E(I)/P
      R=DSQRT(C*C+1.D0)
      E(I+1)=S*P*R
      S=C/R
      C=1.D0/R
      GOTO 320
  310 C=P/E(I)
      R=DSQRT(C*C+1.D0)
      E(I+1)=S*E(I)*R
      S=1.D0/R
      C=C/R
  320 P=C*D(I)-S*G
      D(I+1)=H+S*(C*G+S*D(I))
      DO 330 K=1,N
      H=X(K,I+1)
      X(K,I+1)=X(K,I)*S+H*C
  330 X(K,I)=X(K,I)*C-H*S
      E(L)=S*P
      D(L)=C*P
      IF(DABS(E(L)).GT.B)GOTO 260
  340 D(L)=D(L)+F
      NI=N-1
  350 DO 380 I=1,NI
      K=I
      P=D(I)
      J1=I+1
      DO 360 J=J1,N
      IF(D(J).GE.P)GOTO 360
      K=J
      P=D(J)
  360 CONTINUE
```

```
      IF(K.EQ.I)GOTO 380
      D(K)=D(I)
      D(I)=P
      DO 370 J=1,N
      P=X(J,I)
      X(J,I)=X(J,K)
  370 X(J,K)=P
  380 CONTINUE
      RETURN
  400 D(1)=A(1,1)
      X(1,1)=1.D0
      RETURN
      END
```

---

*The essential places of the VBMC algorithm (different from conventional Monte Carlo technique) are bolded.

REFERENCES

All n, M.P., and D.J.Tild sley. 1987. Computer Simulation of Liquids. Claredon Press: Oxford.

Baldwin, A.N., and E.M. Shooter. 1994. *J.Biol.Chem.* 269:11456-11461.

Baldwin, A.N., and E.M. Shooter. 1995. *J.Biol.Chem.* 270:4594-4602.

Banner, D.W., A. D'Arcy, W. Janes, R. Gentz, H.-J. Schoenfeld, C. Broger, H. Loetscher, and W. Lesslauer. 1993. *Cell* 73:431-445.

Barbacid, M. 1993. *Oncogene* 8:2033-2042.

Barbacid, M. 1994. *J.Neurobiol.* 25:1386-1403.

Barde, Y.-A. 1989. *Neuron* 2:1525-1534.

Barker, P.A., and E.M.Shooter. 1994. *Neuron* 13:203-215.

Baumann, U.; Wu, S.; Flaherty, K.M.; McKay, D.B. 1993. *EMBO J.* 12: 3357-3364.

Ben Ari, Y.; Represa, A. 1990. *TINS* 13: 312-318.

Benedetti, M., A. Levi, and M.V. Chao. 1993. *Proc. Natl. Acad. Sci. U.S.A.* 90:7859-7863.

Berkemeier, L., J. Winslow, D. Kaplan, K. Nicolics, D. Goeddel, and A. Rosenthal. 1991. *Neuron* 7:857-866.

Bothwell, M.A. 1991. *Cell* 65:915-918.

Bothwell, M.A., Shooter, E.M. 1977. *J. Biol. Chem.* 23: 8532-8536.

Bradshaw, R.A., J. Murray-Rust, C.F. Ibáñez, N.Q. McDonald, R. Lapatto, and T.L. Blundell. 1994. *Protein Science* 3:1901-1913.

Brooks, B.R., R.E. Bruccoleri, B.D. Olason, D.J. States, S. Swaminathan, and M. Karplus. 1983. *J. Comput. Chem.* 4:187-217.

Brooks III, C.L., and D.A. Case, 1993. *Chem. Rev.* 93: 2487-2502.

Brünger, A.T. 1988. *J. Mol. Biol.* 203:803-816.

Burton, L.E., C.H. Schmelzer, E. Szönyi, C. Yedinak, and A. Gorrell. 1992. *J. Neurochem.* 59:1937-1945.

Burton, G., C. Schmelzer, M. Sadic, F. Hefti, and J. Treanor. 1995. *Soc. Neurosci. Abs.* 21:1061.

Carter, B.D., C. Kaltschmidt, B. Kaltschmidt, N. Offenhäuser, R. Böhm-Matthaei, P. A. Baeuerle, and Y.-A. Barde. 1996. *Science* 272:542-545.

Cassacia-Bonnefil, P., B.D. Carter, R.T. Dobrowsky, and M.V. Chao. 1996. *Nature* 383:716-719.

Chang, G., W.C. Guida, and W.C. Still. 1989. *J. Am. Chem. Soc.* 111:4379-4386.

Chao, M.V. 1992a. *Cell* 68:995-997.

Chao, M.V. 1992b. *Neuron* 9:583-593.

Chao, M. 1994. *J. Neurobiol.* 25:1373-1385.

Chao, M.V., and B.L. Hempst ad. 1995. *Trends Neurosci.* 18:321-326.

Clackson, T., and J.A. Wells. 1995. *Science* 267:383-386.

Clary, D.O., and L.F. Reichardt. 1994. *Proc. Natl. Acad. Sci. U.S.A.* 91:11133-11137.

Davies, A.M. 1994. *J. Neurobiol.* 25:1334-1348.

Dobrowsky, R., M.H. Werner, A.M. Castellino, M.V. Chao, and Y.A. Hannun. 1994. *Science* 265:1596-1599.

Drinkwater, C.C., P.A. Barker, U. Suter, and E.M. Shooter. 1993. *J. Biol. Chem.* 268:23202-23207.

Escandon, E., L.E. Burton, E. Szonyi, and K.J. Nikolics. 1993. *Neurosci. Res.* 34:601-613.

Frade, J.M., A. Rodrigues-Tébar, Y.-A. Barde. 1996. *Nature* 383:166-168.

Gibson, K.D., and H.A Scheraga. 1988. In *Structure and Expression: Vol. 1. From Proteins to Ribosomes*; Sarma, M.H., Sarma, R.H., Eds.; Adenine Press: Guilderland, NY, pp. 67-94.

Gidas, B. 1985. *J. Stat. Phys.* 39: 73-131.

Glass, D.; Nye, S.; Hantzopoulos, P.; Macchi, M.; Squinto, S.; Goldfarb, M.; Yancopoulos, G. 1991. *Cell* 66: 405-413.

Gotz, R.; Koster, R.; Winkler, C.; Raulf, F.; Lottspeich, F.; Schard, M.; Thoenen, H. 1994. *Nature* 372: 266-269.

Gregory, D.S., A.C.R. Martin, J.C. Cheetham, and A.R. Rees. 1993. *Protein Engineering* 6:29-35.

Gunningham, G.W.; Meijer, P.H.E. 1976. *J. Comp. Phys.* 20: 50-63.

Hallböök, F., C.F. Ibáñez, and H. Persson. 1991. *Neuron* 6:845-858.

Hefti, F.H. 1986. *J. Neurosci.* 6:2155-2162.

Hefti, F.H., and Weiner, W.J. 1986. *Annals of Neurology 20*:275-281.

Heldin, C.H., A. Ernlund, C. Rorsman, and L. Rönnstrand. 1989. *J. Biol. Chem.* 264:8905-8912.

Hempstead, B.L., D. Martin-Zanca, D.L. Kaplan, L.F. Parada, and M.V. Chao. 1991. *Nature* 350:678-683.

Herrmann, J.L., D.G. Menter, J. Hamada, D. Marchetti, M. Nakajima, and G.L. Nicolson. 1993. *Mol. Biol.* 4:1205-1216.

Hobza, P., H.L. Selzle, and E.W. Schlag. 1994. *J. Am. Chem. Soc.* 116:3500-3506.

Hodes, Z.I., G. Némethy, and H.A. Scheraga. 1979. *Biopolymers* 18:1565-1610.

Hohn, A.; Leibrock, J.; Bailey, K.; Barde, Y.-A. 1990. *Nature* 344: 339-341.

Hopfinger, A.J. 1973. Conformational Properties of Macromolecules. Academic Press, New York-London. pp. 70-85.

Hunter, C.A., and J.K.M. Sanders. 1990. *J. Am. Chem. Soc.* 112:5525-5534.

Hunter, C.A., J. Singh, and J.M. Thornton. 1991. *J. Mol. Biol.* 218:837-846.

Ibáñez, C.F., T. Ebendal, and H. Persson. 1991. *EMBO J.* 10:2105-2110.

Ibáñez, C.F., T. Ebendal, G. Barbany, J. Murray-Rust, T.L. Blundell, and H. Persson. 1992. *Cell* 69:329-341.

Ibáñez, C.F., L. Ilag, J. Murray-Rust, and H. Persson. 1993. *EMBO J.* 12:2281-2293.

Ibáñez, C.F. 1994. *J. Neurobiol.* 25:1349-1361.

Ibáñez, C.F. 1995. *Trends Biotech.* 13:217-227.

Ilag, L.L., P. Lönnerberg, H. Persson, and C.F. Ibáñez. 1994. *J. Biol. Chem.* 269:19941-19946.

IUPAC-IUB Commission on Biochemical Nomenclature. 1970. *Biochemistry* 9:3471-3479.

Jing, S.Q., P. Tapley, and M. Barbacid. 1992. *Neuron* 9:1067-1079.

Johnson, D., A. Lanahan, C.R. Buck, A. Sehgal, C. Morgan, E. Mercer, M. Bothwell, and M. Chao. 1986. *Cell* 47:545-554.

Judson, R.S.; Jaeger, E.P.; Treasurywala, A.M. 1994. *J. Mol. Struct. (Theochem)* 308: 191-206.

Kahle, P., L.E. Burton, C.H. Schmelzer, and C. Hertel. 1992. *J. Biol. Chem.* 267:22707-22710.

Kaplan, D.R.; Hempstead, B.L.; Martin-Zanca, D.; Chao, M.V.; Parada, L.F. 1991. *Science* 252: 554-558.

Kaplan, D.R., and R.M. Stephens. 1994. *J. Neurobiol.* 25:1404-1417.

Kincaid, R.H.; Scheraga, H.A. 1982. *J. Comput. Chem.* 3: 525-547.

Kirkpatrick, S., C.D. Gelatt, Jr., and M.P. Vecchi. 1983. *Science* 220:671-680.

Klein, R.; Jing, S.; Nanduri, V.; O'Rourke, E.; Barbacid, M. 1991. *Cell* 65: 189-197.

Klein, R.; Lamballe, F.; Bryant, S.; Barbacid, M. 1992. *Neuron* 8: 947-956.

Kobe, B., and J. Deisenhofer. 1993. *Nature* 366:751-756.

Kobe, B., and J. Deisenhofer. 1994. *Trends Biochem. Sci.* 19:415-421.

Kobe, B., and J. Deisenhofer. 1995. *Nature* 374:183-186.

Korsching, S. 1993. *J. Neurosci.* 13:2739-2748.

Krüttgen, A., J.V. Heymach, P. Kahle, and E.M. Shooter. 1996. *Soc. Neurosci. Abs.* 22:557.

Kullander, K., and T. Ebendal. 1994. *J. Neurosci. Res.* 39:195-210.

Kullander, K., and T. Ebendal. 1996. *Soc. Neurosci. Abs.* 22:557.

Kushner, H.J. 1987. *SIAM J. Appl. Math.* 47: 169-185.

Lai, K.-O., D.J. Glass, D. Geis, G.D. Yancopoulos, and N.Y. Ip. 1996. *J. Neurosci. Res.* 46:618-629.

Lamballe, F.; Klein, R.; Barbacid, M. 1991. *Cell* 66: 967-970.

Landreth, G.E., and E.M. Shooter. 1980. *Proc. Natl. Acad. Sci. U.S.A.* 77: 4751-4755.

Large, T.H., G. Weskamp, J.C. Helder, M.J. Radeke, T.P. Misko, E.M. Shooter, and L.F. Reichardt. 1989. *Neuron* 2:1123-1134.

Leibrock, J.; Lottspeich, A.H.; Hohn, A.; Hofer, M.; Hengerer, B.; Masiakowski, P.; Thoenen, H.; Barde, Y.-A. 1989. *Nature* 341: 149-152.

Lelj, F.; Grimaldi, P.; Cristianziano, P.L. 1991. *Biopolymers* 31: 663-670.

Leven, G.R.; Mendel, L.M. 1993. *TINS* 16: 353-359.

Levi-Montalcini, R. 1987. *EMBO J. 6*:1145-1154.

Li, Z.; Scheraga, H.A. 1988. *J. Mol. Struct. (Theochem)* 179: 333-352.

Livnah, O., E.A. Stura, D.L. Johnson, S.A. Middleton, L. S. Mulcahy, N.C. Wrighton, W.J. Dower, L.K. Jolliffe, and I.A. Wilson. 1996. *Science* 273:464-471.

Loeb, D.M.; Maragos, J.; Martin-Zanca, D.; Chao, M.V.; Parada, L.F.; Greene, L.A. 1991. *Cell* 66: 961-966.

Luo, Y., and K.E. Neet. 1992. *J. Biol. Chem.* 267:12275-12283.

MacDonald, J.I.S., and S.O. Meakin. 1996. *Mol. Cell. Neurosci.* 7:371-390.

Mahadeo, D., L. Kaplan, M.V. Chao, and B.L. Hempstead. 1994. *J. Biol. Chem.* 269:6884-6891.

Maisopierre, P.C.; Belluscio, L.S.S.; Squinto, S.; Ip, N.Y.; Furth, M.E.; Lindsay, R.M.; Yancopoulos, G.D. 1990. *Science* 247: 1446-1451.

Maness, L.M., A.J. Kastin, J.T. Weber, W.A. Banks, B.S. Beckman, and J.E. Zadina. 1994. *Neurosci. Biobehav. Rev.* 18:143-159.

Marchetti, D., McQuillan, D.J., W.C. Spohn, D.D. Carson, and G.L. Nicolson. 1996. *Cancer Res.* 56:2856-2863.

Matsumoto, K., R.K. Wada, J.M. Yamashiro, D.R. Kaplan, and C.J. Thiele. 1995. *Cancer Res.* 55:1798-1806.

McDonald, N.Q., R. Lapatto, J. Murray-Rust, J. Gunning, A. Wlodawer, and T.L. Blundell. 1991. *Nature* 354:411-414.

McKee, A.C.; Kosik, K.S.; Kowal, N.W. 1991. *Ann. Neurol.* 30: 156.

McMahon, S.B.; Bennett, D.L.H.; Priestley, J.V.; Shelton, D.L. 1995. *Nature Med.* 1: 774-780.

Meakin, S.O., and E.M. Shooter. 1992. *Trends Neurosci.* 15:323-331.

Merrell, R., M.W. Pulliam, L. Randono, L.F. Boyd, R.A. Bradshaw, and L. Glaser. 1975. *Proc. Natl. Acad. Sci. U.S.A.* 72:4270-4274.

Metropolis, N.; Rosenbluth, A.W.; Rosenbluth, M.N.; Teller, A.H.; Teller, E. 1953. *J. Chem. Phys.* 21: 1087-1092.

Moore, J.B., and E.M. Shooter. 1975. *Neurobiology* 5:369-381.

Morgan *et al.* 1989. In Annual Reports in Medicinal Chemistry. Ed.: Vinick, F.J. Academic Press, San Diego, CA, pp. 243-252.

Nayeem, A.; Vila, J.; Scheraga, H.A. 1991. *J. Comput. Chem.* 12: 594-605.

Nilges, M., G.M. Clore, and A.M. Gronenborn. 1988. *FEBS Lett.* 229:317-324.

Paine, G.H.; Scheraga, H.A. 1985. *Biopolymers* 24: 1391-1436.

Pérez, P., P.M. Coll, B.L. Hempstead, D. Martin-Zanca, and M.V. Chao. 1995. *Mol. Cell. Neurosci.* 6:97-105.

Persson, H., and C.F. Ibáñez. 1993. *Curr. Opin. Neurol. Neurosurg.* 6:11-18.

Piela, L.; Kostrowicki, J.; Scheraga, H.A. 1989. *J. Phys. Chem.* 93: 3339-3346.

Piela, L.; Olszewski, K.A.; Pillardy, J. 1994. *J. Mol. Struct. (Theochem)* 308: 229-239.

Ponnuswamy, P.K., and P. Manavalan. 1976. *J. Theor. Biol.* 60:481-486.

Purves, D. 1988. Body and Brain. A Trophic Theory of Neural Connectors. Cambridge, MA: Harvard University Press, pp. 1-1231.

Radeke, M.J., T.P. Misko, C. Hsu, L.A. Herzenberg, and E.M. Shooter. 1987. *Nature* 325:593-597.

Radziejewski, C., and R.C. Robinson. 1993. Biochemistry 32:13350-13356.

Radziejewski, C.; Robinson, R. C.; DiStefano, P.S.; Taylor, J.W. 1992. *Biochemistry* 31: 4431-4436.

Raj, N.; Morley, S.D.; Jackson, D.E. 1994. *J. Mol. Struct. (Theochem)* 308: 175-190.

Rao, M.; Pangali, C.; Berne, B.J. 1979. *Mol. Phys.* 37: 1773-1798.

Rashid, K.; van der Zee, C.E.E.M.; Ross, G.M.; Chapman, C.A.; Stanisz, J.; Riopelle, R.J.; Racine, R.J.; Fahnestock, M. 1995. *Proc. Natl. Acad. Sci. U.S.A.* 92: 9495-9499.

Ripoll, D.R.; Scheraga, H.A. 1988. *Biopolymers* 27: 283-1303.

Robinson, R.C., C. Radziejewski, D.I. Stuart, and E.Y. Jones. 1995. *Biochemistry* 34:4139-4146.

Rodrigues-Tébar, A., G. Dechant, and Y.-A. Barde. 1990. *Neuron* 4:487-492.

Rodrigues-Tébar, A., G. Dechant, R. Gotz, and Y.-A. Barde. 1992. *EMBO J.* 11:917-922.

Rosenthal, A.; Goeddel, D.V.; Nguyen, T.; Lewis, M.; Shih, A.; Laramee, G.R.; Nikolics, K.; Winslow, J.W. 1990. *Neuron* 4: 767-773.

Ross, A.H., M.-C. Daou, C. A. McKinnon, P.J. Condon, M.B. Lachyankar, R.M. Stephens, D.R. Kaplan, and D.E. Wolf. 1996. *J. Cell Biol.* 132:945-953.

Ross, G.M., I.L. Shamovsky, G. Lawrance, M. Solc, S.M. Dostaler, S.L. Jimmo, D.F. Weaver, and R.J. Riopelle. 1997. *Nature Med.* 3:872-878.

Rossky, P. J. ; Doll, J. D. ; Friedman, H. L. 1978. *J. Ch m. Phys.* 69: 4628-4633.

Rovelli, G.; Heller, R.A.; Canossa, M.; Shooter, E.M. 1993. *Proc. Natl. Acad. Sci. USA* 90: 8717-8721.

Ryckaert, J.-P., Ciccotti, G.; Berendsen, H.J.C. 1977. *J. Comput. Phys.* 23:327-341.

Rydén, M., J. Murray-Rust, D. Glass, L.L. Ilag, M. Trupp, G.D. Yancopoulos, N.Q. McDonald, and C.F. Ibáñez. 1995. *EMBO J.* 14:1979-1990.

Rydén, M., and C.F. Ibáñez, C.F. 1996. *J. Biol. Chem.* 271:5623-5627.

Schauer, M., and E.R. Bernstein. 1985. *J. Chem. Phys.* 82:3722-3727.

Schechter, A.L., and M.A. Bothwell. 1981. *Cell* 24:867-874.

Scheraga, H.A. 1989. *Prog. Clin. Biol. Res.* 289: 3-18.

Scheraga, H.A. 1994. *Pol. J. Chem.* 68: 889-891.

Schmelzer, C.H., L.E. Burton, W.-P. Chan, E. Martin, C. Gorman, E. Canova-Davis, V.T. Ling, M.B. Sliwkowski, G. McCray, J.A. Briggs, T.H. Nguyen, and G. Polastri. 1992. *J. Neurochem.* 59:1675-1683.

Schneider, R., E. Schneider-Scherzer, M. Thumher, B. Auer, and M. Schweiger. 1988. *EMBO J.* 7:4151-4156.

Schneider, R., and M. Schweiger. 1991. *Oncogene* 6:1807-1811.

Shamovsky, I.L.; Yarovskaya, I.Yu.; Khrapova, N.G.; Burlakova, E.B. 1992. *J. Mol. Struct. (Theochem)* 253: 149-159.

Shamovsky, I.L., G.M. Ross, R.J. Riopelle, and D.F. Weaver. 1996. *J. Am. Chem. Soc.* 118:9743-9749.

Shih, A., G.R. Laramee, C.H. Schmelzer, L.E. Burton, and J.W. Winslow. 1994. *J. Biol. Chem.* 269:27679-27686.

Simon, I.; Nemethy, G.; Scheraga, H.A. 1978. *Macromolecules* 11: 797-804.

Snider, W.D., and E.M. Johnson. 1989. *Ann. Neurol.* 26:489-506.

Snow, M.E. 1992. *J. Comput. Chem.* 13: 579-584.

Soppet, D.; Escandon, E.; Maragos, J.; Middlemas, D.S.; Reid, S.W.; Blair, J.; Burton, L.E.; Stanton, B.; Kaplan, D.R.; Hunter, T.; Nikolics, K.; Parada, L.F. 1991. *Cell* 65: 895-903.

Squinto, S.P.; Stitt, T.N.; Aldrich, T.H.; Davis, S.; Bianco, S.M.; Radziejewski, C.; Glass, D.J.; Masiakowski, P.; Furth, M.E.; Valenzuela, D.M.; DiStefano, P.S.; Yancopoulos, G.D. 1991. *Cell* 65: 885-893.

Suter, U., C. Angst, C.-L. Tien, C.C. Drinkwater, R.M. Lindsay, and E.M. Shooter. 1992. *J. Neurosci.* 12:306-318.

Sutter, A., R.J. Riopelle, R.M. Harris-Warrick, and E.M. Shooter. 1979. *J. Biol. Chem.* 254:5972-5982.

Szentpsly, L.V.; Shamovsky, I.L.; Nefedova, V.V.; Zubkus, V.E. 1994. *J. Mol. Struct.*

(Theochem) 308: 125-140.

Taylor, R.A.V., J.F. Kerrigan, F.M. Longo, M. deBoisblanc, and W.C. Mobley. 1991. *Soc. Neurosci. Abs.* 17: 712.

Thoenen, H. 1991. *Trends Neurosci.* 14: 165-170.

Treanor, J.J.S., C. Schmelzer, B. Knusel, J.W. Winslow, D.L. Shelton, F. Hefti, K. Nikolics, and L.E. Burton. 1995. *J. Biol. Chem.* 270: 23104-23110.

Ullrich, A., and J. Schlessinger. 1990. *Cell* 61: 203-212.

Urfer, R., P. Tsoulfas, D. Soppet, E. Escandón, L.F. Parada, and L.G. Presta. 1994. *EMBO J.* 13:5896-5909.

Urfer, R., P. Tsoulfas, L. O'Connell, D.L. Shelton, L.F. Parada, and L.G. Presta. 1995. *EMBO J.* 14:2795-2805.

Vale, R.D.; Shooter, E.M. 1985. *Methods Enzymol.* 109: 21-39.

Vanderbilt, D., and S.G. Louie. 1984. *J. Comput. Phys.* 56:259-271.

Van der Zee, C.E.E., G.M. Ross, R.J. Riopelle, and T. Hagg. 1996. *Science* 274: 1729-1732.

Villani, V.; Tamburro, A.M. 1994. *J. Mol. Struct. (Theochem)* 308: 141-157.

Warme, P.K., and R.S. Morgan. 1978. *J. Mol. Biol.* 118: 289-304.

Washiyama, K., Y. Muragaki, L.B. Rorke, V.M.-Y.Lee, S.C. Feinstein, M.J. Radeke, D. Blumberg, D.R. Kaplan, and J.Q. Trojanowski. 1996. *Amer. J. Path.* 148:929-940.

Weiner, S.J., P.A. Kollman, D.A. Case, U.C. Singh, C. Ghio, G. Alagona, S. Profeta Jr., and P.Weiner. 1984. *J.Am.Chem.Soc.* 106:765-784.

Weskamp, G.; Reichardt, L.F. 1991. *Neuron* 6: 649-663.

Wilson, C., and S. Doniach. 1989. *Proteins* 6:193-209.

Wilson, S.R., W. Cui, J.W. Moscowitz, and K.E. Schmidt. 1988. *Tetrahedron Lett.* 29:4373-4376.

Windisch, J.M., B. Auer, R. Marksteiner, M.E. Lang, and R. Schneider. 1995a. *FEBS Lett.* 374:125-129.

Windisch, J.M., R. Marksteiner, and R. Schneider. 1995b. *J. Biol. Chem.* 270: 28133-28138.

Windisch, J.M., R. Marksteiner, M.E. Lang, B. Auer, and R. Schneider. 1995c. *Biochemistry* 34:11256-11263.

Wolf, D.E., C.A. McKinnon, M.-C. Daou, R.M. Stephens, D.R. Kaplan, and A.H. Ross. 1995. *J. Biol. Chem.* 270:2133-2138.

Woo, S.B., D.E. Timm, and K.E. Neet. 1995. *J. Biol. Chem.* 270:6278-6285.

Woo, S.B., and K.E. Neet. 1996. *J. Biol. Chem.* 271:24433-24441.

Woolf, C.J.; Doubell, T.A. 1994. *Current Opinions in Neurobiol.* 4: 525-534.

Yan, H., and M.V. Chao. 1991. *J. Biol. Chem.* 266:12099-12104.

Yoder, M.D.; Keen, N.T.; Jumak, F. 1993. *Science* 260: 1503-1507.

WHAT IS CLAIMED IS:

1. A variable basis Monte-Carlo (VBMC) simulated annealing method for identifying an optimal structure in a molecular system, comprising:

(a) providing a Markov chain with an initial basis set of N configurational variables which define a structure for said molecular system;

(b) translating the N configurational variables simultaneously along a basis vector to produce a new structure for the molecular system, wherein magnitude of translation is randomly chosen within a preselected range;

(c) calculating potential energy of the new structure of the molecular system;

(d) deciding whether to accept or reject the new structure using an effective temperature dependent transition function, and if the new structure is accepted, replacing the current structure with the accepted structure;

(e) repeating steps (b) to (d), each repetition having a new basis vector, for a preselected first number of repetitions at a preselected upper temperature; then

(f) decreasing temperature according to a preselected cooling schedule;

(g) repeating steps (b) to (d) and (f), each repetition having a new basis vector, for a preselected second number of repetitions; then

(h) storing current structure of the molecular system;

(i) repeating steps (g) and (h) until a preselected number of stored structures have been accumulated; then

(j) rotating the basis set of configurational variables according to an effective distribution of the accumulated structures so that basis vectors are directed along low-energy valleys of a potential energy hypersurface thereby accelerating conformational motions and structural transitions of the molecular system, and erasing accumulated structures from steps (h) and (i);

(k) repeating steps (i) and (j) until, after an effective third number of repetitions, a preselected lower temperature limit is reached, thereby producing an unrefined global minimum structure; and

(l) refining the global energy minimum structure so that at least one local minimum on the potential energy hypersurface is identified.

2. The method of claim 1, wherein the basis vector is chosen randomly within said preselected range.

3. The method of claim 1, wherein the basis vector is chosen deterministically within said

preselected range.

4. The method of claim 1 wherein the preselected second number of repetitions is N or a multiple thereof.

5. The method of claim 1 wherein the preselected second number of repetitions is at least about 2N.

6. The method of claim 1 wherein the refining step is non-linear minimization.

7. The method of claim 6, wherein the refining step is gradient descent minimization.

8. The method of claim 6, wherein the refining step is conjugate gradient minimization.

9. The method of claim 6, wherein the refining step is a quasi-Newton minimization method.

10. The method of claim 9, wherein the quasi-Newton method is Newton -Raphson method.

11. The method of claim 6, wherein the refining step is Marquardt method.

12. The method of claim 6, wherein the refining step is a variable metric method.

13. The method of claim 6, wherein the refining step is Powell method.

14. The method of claim 1 wherein said molecular system is at least one peptide domain comprising amino acid residues, each amino acid residue comprising a main chain having α-carbon atoms, carbonyl carbon atoms and nitrogen atoms, said basis set of configurational variables comprising torsional angles (ψ_i) between said α-carbon atoms and neighbouring carbonyl carbon atoms, and torsional angles (ϕ_i) between said α-carbon atoms and neighbouring nitrogen atoms.

15. The method of claim 14 wherein torsional angles describing planar portions of said peptide domains are held constant.

16. The method of claim 14 wherein said effective temperature dependent transition function for screening a new stat x_{i+1} derived from a previous state x_i is given by:

$$W(x_i \Rightarrow x_{i+1}) = 1/[1 + \exp(\Delta E_i / kT)]$$

where ΔE_i is the difference between conformational energies of the states x_{i+1} and x_i, k is the Boltzmann constant and T is absolute temperature.

17. The method of claim 14 wherein said effective temperature dependent transition function for screening a new state x_{i+1} derived from a previous state x_i is given by:

$$W(x_i \Rightarrow x_{i+1}) = 1, \quad \text{if } E(x_{i+1}) \leq E(W(x_i))$$

$$= \exp(-\Delta E_i / kT), \quad \text{if } E(x_{i+1}) \geq E(W(x_i))$$

where ΔE_i is the difference between conformational energies of the states x_{i+1} and x_i, k is the Boltzmann constant and T is absolute temperature.

18. The method of claims 14, 15, 16 or 17 wherein said preselected upper temperature is about 1000^0K.

19. The method of claim 18 wherein said preselected lower temperature is about 120^0K.

20. A method of identifying structures of a peptide domain of a neurotrophin to bind with a binding site of a receptor, comprising;

a) providing a plurality of neurotrophin analogues wherein at least one neurotrophin analogue binds said receptor;

b) identifying an optimal or near-optimal structure for respective peptide domains of the neurotrophin analogues that bind said receptor by applying a preselected number of the variable basis Monte-Carlo (VBMC) annealing simulations according to claim 1 to each of the respective peptide domains to identify minimum or near-minimum energy structures for said peptide domains; and

c) comparing said minimum or near-minimum energy structures to identify common structural features shared by neurotrophin analogues exhibiting receptor mediated activity.

21. The method according to claim 20 wherein said common structural features are absent from neurotrophin analogues that do not exhibit receptor-mediated activity.

22. A method of identifying structures of a domain of a ligand to bind with a binding site of

a receptor, comprising;

a) providing a plurality of ligand analogues wherein at l ast one ligand analogue binds said receptor;

b) id ntifying an optimal or near-optimal structure for respective domains of the ligand analogues that bind said receptor by applying a preselected number of the variable basis Monte-Carlo (VBMC) annealing simulations according to claim 1 to each of the respective domains to identify minimum or near-minimum energy structures for said domains; and

c) comparing said minimum or near-minimum energy structures to identify common structural features shared by ligands exhibiting receptor mediated activity.

23. The method according to claim 22 wherein said common structural features are absent from ligand analogues that do not exhibit receptor-mediated activity.

24. The method according to claim 20 wherein said neurotrophin is NGF, and said receptor is TrkA.

25. The method according to claim 20 wherein said neurotrophin is brain-derived neurotrophic factor (BDNF), neurotrophin-3 (NT-3), or neurotrophin-4 (NT-4), and said receptor is TrkB.

26. The method according to claim 20 wherein said neurotrophin is neurotrophin-3 (NT-3) and said receptor is TrkC.

27. The method according to claim 20 wherein said receptor is the common neurotrophin receptor $p75^{NTR}$.

28. A ligand for binding with TrkA, wherein TrkA comprises a leucine rich motif (LRM) comprising amino acid residues 93 to 117, wherein coordinates of the residues of said LRM are given in Appendix 1, said LRM having five binding areas, area A comprising amino acid residue Phe^{105tA} capable of hydrophobic interaction, area B comprising amino acid residues Phe^{111tA}, Phe^{113tA}, and Thr^{114tA} capable of hydrophobic interaction, area C comprising amino acid residues Asp^{109tA} and His^{112tA} capable of ionic interaction, area D comprising amino acid residue Lys^{100tA} capable of ionic interaction, and area E comprising Asn^{95tA} to Ile^{98tA} capable of multiple parallel β-strand type hydrogen bonding, the ligand comprising;

at least three moieties each comprising effective atomic elements having spatial

occupancy, relative atomic position, bond type and charge to define a three dimensional conformation of said ligand so that a first moiety can bind with a first binding area, a second moiety can bind with a second binding area, and a third moiety can bind with a third binding area.

29. The ligand according to claim 28 wherein the first moiety can hydrophobically bond with binding area A, the second moiety can ionically bind with binding area C, and the third moiety can ionically bind with binding area D.

30. The ligand according to claim 29 comprising a fourth moiety effectively spaced with respect to the other moieties so it can hydrophobically bond with binding area B.

31. The ligand according to claim 29 comprising a fourth moiety effectively spaced with respect to the other moieties so it can hydrogen bond with binding area E.

32. The ligand according to claim 29 wherein the first moiety is capable of hydrophobic bonding to Phe^{105tA} in binding area A, the second moiety is positively charged and present in an effective position in said ligand to ionically interact with Asp^{109tA} and His^{112tA} in binding area C, and the third moiety is negatively charged and present in an effective position in said ligand to ionically interact with Lys^{100tA} in binding area D.

33. The ligand according to claim 32 wherein the moiety hydrophobically bonded to Phe^{105tA} in binding area A is Trp, wherein the positively charged moiety which ionically interacts with Asp^{109tA} and His^{112tA} in binding area C is Arg and Lys, and wherein the negatively charged moiety which ionically interacts with Lys^{100tA} in binding area D is Asp.

34. The ligand according to claim 32 wherein said first, second and third moieties are amino acids or isosteres thereof.

35. The ligand according to claim 30 wherein said fourth moiety is an amino acid or isostere thereof.

36. The ligand according to claim 31 wherein said fourth moiety is an amino acid or isostere thereof.

37. A method of designing a ligand to bind with a LRM of TrkA, comprising:

providing a template of said LRM of TrkA, said LRM comprising amino acid residue sequence 93 to 117 inclusiv , said amino acid residues having spatial Cartesian coordinates given in Appendix 1 wherein said binding area A comprises Phe^{105tA} capable of hydrophobic bonding, binding area B comprises Phe^{111tA}, Phe^{113tA}, Thr^{114tA} capable of hydrophobic bonding, binding area C comprises Asp^{109tA} and His^{112tA} capable of ionic interaction, binding area D comprises Lys^{100tA} capable of ionic interaction, and binding area E comprises Asn^{95tA} to Ile^{98tA} capable of hydrogen bonding; and

computationally evolving a ligand using an effective algorithm so that said evolved ligand comprises at least three effective moieties located relative to each other in the ligand so that a first moiety can bind with a first of said five binding areas, a second moiety can bind with a second of said five binding areas, and a third moiety can bind with a third of said binding areas.

38. The method according to claim 37 including the step of generating said ligand under a constraint that the evolved ligand comprises said first effective moiety spatially located to hydrophobically bind with binding area A, said second moiety spatially located to ionically interact with binding area C, and said third moiety spatially located to ionically interact with binding area D.

39. The method according to claim 37 including the step of generating said ligand under a constraint that the evolved ligand comprises an effective moiety spatially located to hydrophobically interact with binding area B.

40. The method according to claim 37 including the step of generating said ligand under a constraint that the evolved ligand comprises an effective moiety spatially located to hydrogen bond with binding area E.

41. A ligand for binding with TrkB, wherein TrkB comprises a leucine-rich motif (LRM) comprising amino acid residues 93 to 117, the coordinates of the residues of said LRM given in Appendix 2, said LRM having five binding areas, binding area F comprising amino acid residue Asp^{100tB} capable of ionic interaction, binding area G comprising amino acid residue Lys^{109tB} capable of ionic interaction, binding area H comprising amino acid residue Lys^{113tB} capable of ionic interaction, binding area I comprising amino acid residue Arg^{94tB} capable of ionic interaction, and binding area K comprising amino acid residue Lys^{104tB} capable of hydrogen bonding or ionic interaction, the ligand comprising:

at least three moieties each comprising effective atomic elements having spatial

occupancy, relative atomic position, bond typ and charge to define a three dimensional conformation of said ligand so that a first moiety can bind with a first binding area, a second moiety can bind with a second binding area, and a third moiety can bind with a third binding area.

42. The ligand according to claim 41 wherein one of said at least three moieties can ionically bind with binding area F, another of said at least three moieties can ionically bind with binding area G, and another of said at least three moieties can form a hydrogen bond or ionically bind with binding area K.

43. The ligand according to claim 42 wherein said ligand includes a fourth moiety effectively spaced relative to said at least three moieties so that it can ionically bind with binding area H.

44. The ligand according to claim 42 wherein said ligand includes a fourth moiety effectively spaced relative to said at least three moieties so that it can ionically bind with binding area I.

45. The ligand according to claim 41 wherein the first moiety is positively charged and present in an effective position in said ligand to ionically bind to Asp^{100tB} in binding area F, the second moiety is negatively charged and present in an effective position in said ligand to ionically interact with Lys^{109tB} in binding area G, and the third moiety is neutral or negatively charged and capable of hydrogen bonding or ionically bonding to Lys^{104tB} in binding area K.

46. The ligand according to claim 45 wherein a fourth moiety is negatively charged and present in an effective position in said ligand to ionically bind to Lys^{113tB} in binding area H, and wherein a fifth moiety is negatively charged and present in an effective position in said ligand to ionically bind to Arg^{94tB} in binding area I.

47. The ligand according to claim 46 wherein the positively charged moiety ionically bonded to Asp^{100tB} in binding area F is Arg, wherein the charged moiety which ionically interacts with Lys^{109tB} in binding area G is Glu and Lys, and wherein the negatively charged moiety ionically bonded with Lys^{113tB} in binding area H is Asp.

48. The ligand according to claim 47 wherein the negatively charged amino acid residue ionically bonded to Arg^{94tB} in binding area I is Glu.

49. The ligand according to claim 45 wherein the neutral or negatively charged moiety capable of hydrogen bonding or ionically bonding to Lys^{104B} in binding area K is Thr.

50. The ligand according to claim 45 wherein said first, second and third moieties are amino acids or isosteres thereof.

51. The ligand according to claim 46 wherein said fourth and fifth moieties are amino acids or isosteres thereof.

52. A method of designing a ligand to bind with TrkB, wherein TrkB comprises a leucine-rich motif (LRM) comprising amino acid residues 93 to 117, the coordinates of the residues of said LRM given in Appendix 2, said LRM having five binding areas, binding area F comprising amino acid residue Asp^{100B} capable of ionic interaction, binding area G comprising amino acid residue Lys^{109B} capable of ionic interaction, binding area H comprising amino acid residue Lys^{113B} capable of ionic interaction, binding area I comprising amino acid residue Arg^{94B} capable of ionic interaction, and binding area K comprising amino acid residue Lys^{104B} capable of hydrogen bonding or ionic interaction, the method comprising:

computationally evolving a ligand using an effective algorithm so that said evolved ligand comprises at least three effective moieties located relative to each other in the ligand so that a first moiety can bind with a first of said five binding areas, a second moiety can bind with a second of said five binding areas, and a third moiety can bind with a third of said binding areas.

53. A ligand for binding with the common neurotrophin receptor $p75^{NTR}$, wherein $p75^{NTR}$ comprises a binding site including amino acid residues Cys^{39p} to Cys^{94p} inclusive, said residues of said binding site having spatial coordinates given in Appendix 3, said binding site having three binding areas including binding loop 2A comprising region Cys^{39p} to Cys^{58p} capable of attractive electrostatic interaction, binding loop 2B comprising region Cys^{58p} to Cys^{79p} capable of attractive electrostatic interaction, and binding loop 3A comprising region Cys^{79p} to Cys^{94p} capable of attractive electrostatic interaction, the ligand comprising;

at least two moieties each comprising effective atomic elements having spatial occupancy, relative atomic position, bond type and charge to define a three dimensional conformation of said ligand so that a first moiety can bind with a first binding area, and a second moiety can bind with a second binding area.

54. The ligand according to claim 53 wherein said ligand is an agonist, and wherein one

of said at least two moieties binds to loop 2B.

55. The ligand according to claim 53 further comprising a third moiety wh rein said first moiety can bind to loop 2A, said second moiety can bind to loop 2B and said third moiety can bind to loop 3A.

56. The ligand according to claim 53 wherein said first moiety binds to any two of Asp^{47p}, Lys^{56p} and Glu^{53p}.

57. The ligand according to claim 53 wherein said binding loop 2A includes amino acid residues Asp^{47p} and Lys^{56p} and said first moiety ionically binds to said residues Asp^{47p} and Lys^{56p}.

58. The ligand according to claim 53 wherein said binding loop 2B includes amino acid residues Asp^{75p} and Asp^{76p} and said second moiety ionically binds to said residues Asp^{75p} and Asp^{76p}.

59. The ligand according to claim 55 wherein said binding loop 3A includes amino acid residues Asp^{88p} and Glu^{89p} and said third moiety ionically binds to said residues Asp^{88p} and Glu^{89p}.

60. The ligand according to claim 55 wherein said third moiety binds to any two of Asp^{88p}, Glu^{89p} and Arg^{80p}.

61. A method of designing a ligand for binding with the common neurotrophin receptor $p75^{NTR}$, wherein $p75^{NTR}$ comprises a binding site including amino acid residues Cys^{39p} to Cys^{94p} inclusive, said residues of said binding site having spatial coordinates given in Appendix 3, said binding site having three binding areas including binding loop 2A comprising region Cys^{39p} to Cys^{58p} capable of attractive electrostatic interaction, binding loop 2B comprising region Cys^{58p} to Cys^{79p} capable of attractive electrostatic interaction, and binding loop 3A comprising region Cys^{79p} to Cys^{94p} capable of attractive electrostatic interaction, the method comprising;

computationally evolving a ligand using an effective algorithm so that said evolved ligand comprises at least two effective moieties located relative to each other in the ligand so that a first moiety can bind to a first of said three loops and a second moiety can bind to a second loop of said three loops.

62. A method of identifying a ligand to bind with a leucin rich motif (LRM) of TrkA, comprising:

providing a three dimensional conformation for said LRM, said LRM comprising amino acid residue sequence 93 to 117 inclusive, said amino acid residues having spatial Cart sian coordinates given in Appendix 1, said LRM having five binding areas, area A comprising amino acid residue Phe^{105tA} capable of hydrophobic interaction, area B comprising amino acid residues Phe^{111tA}, Phe^{113tA}, and Thr^{114tA} capable of hydrophobic interaction, area C comprising amino acid residues Asp^{109tA} and His^{112tA} capable of ionic interaction, area D comprising amino acid residue Lys^{100tA} capable of ionic interaction, and area E comprising Asn^{95tA} to Ile^{98tA} capable of multiple parallel β-strand type hydrogen bonding;

providing a data base containing molecules coded for spatial occupancy, relative atomic position, bond type and/or charge; and

screening said data base to select those molecules comprising moieties having a three dimensional conformation and effective charge that can bind with at least three of said five binding areas.

63. A method of identifying a ligand to bind with a leucine rich motif (LRM) of TrkB, comprising:

providing a three dimensional conformation for said LRM, said LRM comprising amino acid residues 93 to 117, the coordinates of the residues of said LRM given in Appendix 2, said LRM having five binding areas, binding area F comprising amino acid residue Asp^{100tB} capable of ionic interaction, binding area G comprising amino acid residue Lys^{109tB} capable of ionic interaction, binding area H comprising amino acid residue Lys^{113tB} capable of ionic interaction, binding area I comprising amino acid residue Arg^{94tB} capable of ionic interaction, and binding area K comprising amino acid residue Lys^{104tB} capable of hydrogen bonding or ionic interaction;

providing a data base containing molecules coded for spatial occupancy, relative atomic position, bond type and/or charge; and

screening said data base to select those molecules comprising moieties having a three dimensional conformation and effective charge that can bind with at least three of said five binding areas.

64. A method of identifying a ligand to bind with common neurotrophin receptor $p75^{NTR}$, comprising:

providing a three dimensional conformation for the common neurotrophin receptor $p75^{NTR}$, wherein $p75^{NTR}$ comprises a binding site including amino acid residues Cys^{39p} to

Cys^{94p} inclusive, said residues of said binding site having spatial coordinates given in Appendix 3, said binding site having three binding areas including binding loop 2A comprising region Cys^{39p} to Cys^{58p} capable of attractiv lectrostatic int raction, binding loop 2B comprising region Cys^{58p} to Cys^{79p} capable of attractive electrostatic interaction, and binding loop 3A comprising region Cys^{79p} to Cys^{94p} capable of attractive electrostatic interaction;

providing a data base containing molecules coded for spatial occupancy, relative atomic position, bond type and/or charge; and

screening said data base to select those molecules comprising moieties that can bind with at least two of said three binding loops.

First monomer: amino terminus

	1				5					10					15
hNGF	S	S	S	H	P	I	F	H	R	G	E	F	S	V	C ...
mNGF	S	S	T	H	P	V	F	H	M	G	E	F	S	V	C ...
mNGFΔ3-9	-	-	-	-	-	-	-	S	S	G	E	F	S	V	C ...
hNGF-H4D	S	S	S	D	P	I	F	H	R	G	E	F	S	V	C ...
mNGFΔ1-8	-	-	-	-	-	-	-	-	M	G	E	F	S	V	C ...
BDNF	-	-	H	S	D	P	A	R	R	G	E	L	S	V	C ...

Second monomer: carboxyl terminus

	112'									118'
hNGF	... C	V	C	V	L	S	R	K	A	V R
mNGF	... C	V	C	V	L	S	R	K	A	T R
mNGFΔ3-9	... C	V	C	V	L	S	R	K	A	T R
hNGF-H4D	... C	V	C	V	L	S	R	K	A	V R
mNGFΔ1-8	... C	V	C	V	L	S	R	K	A	T R
BDNF	... C	V	C	T	L	T	I	K	R	G R

Figure 1

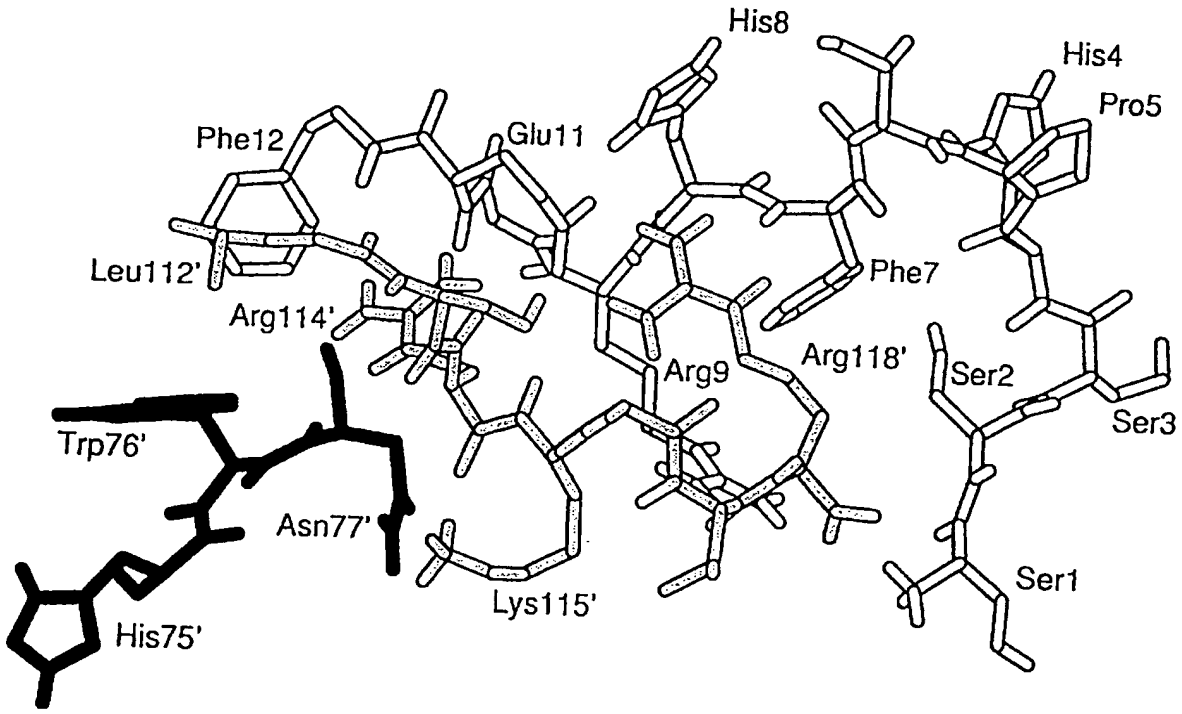
His8
His4
Pro5
Phe12
Glu11
Leu112'
Phe7
Arg114'
Arg118'
Ser2
Arg9
Ser3
Trp76'
Asn77'
Ser1
Lys115'
His75'

Figure 2

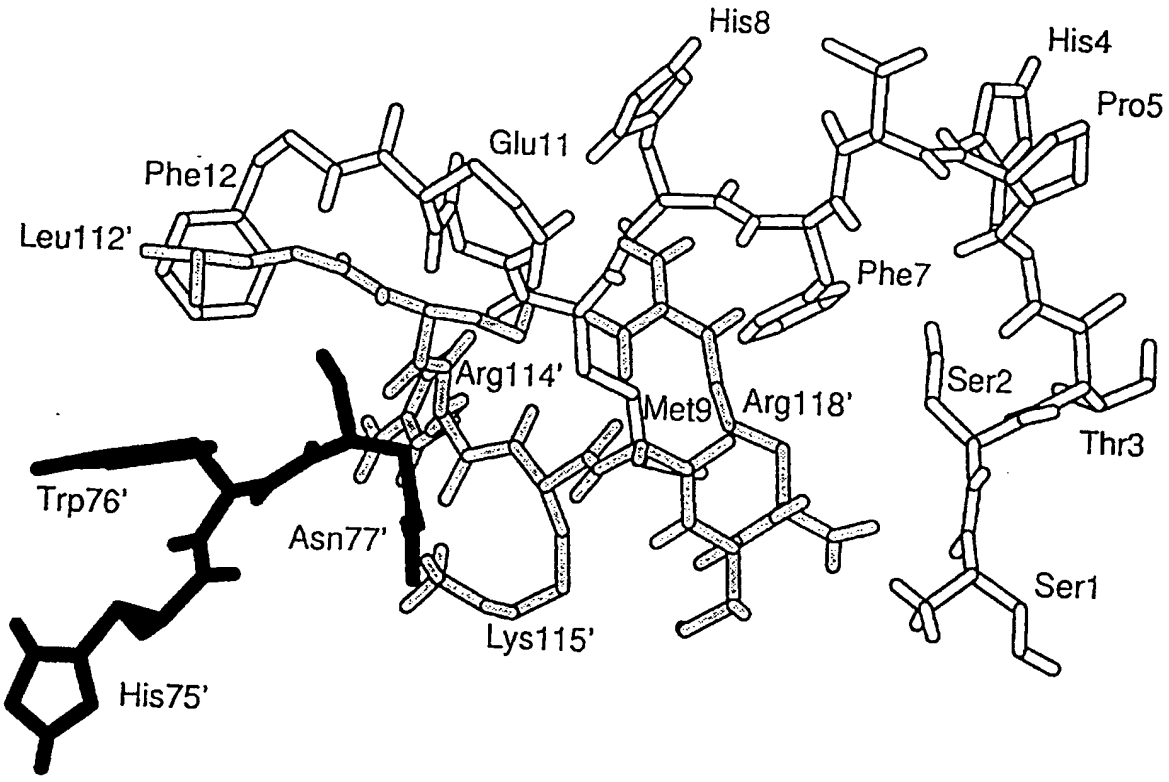
His8
His4
Pro5
Glu11
Phe12
Leu112'
Phe7
Arg114'
Met9
Arg118'
Ser2
Thr3
Trp76'
Asn77'
Ser1
Lys115'
His75'

Figure 3

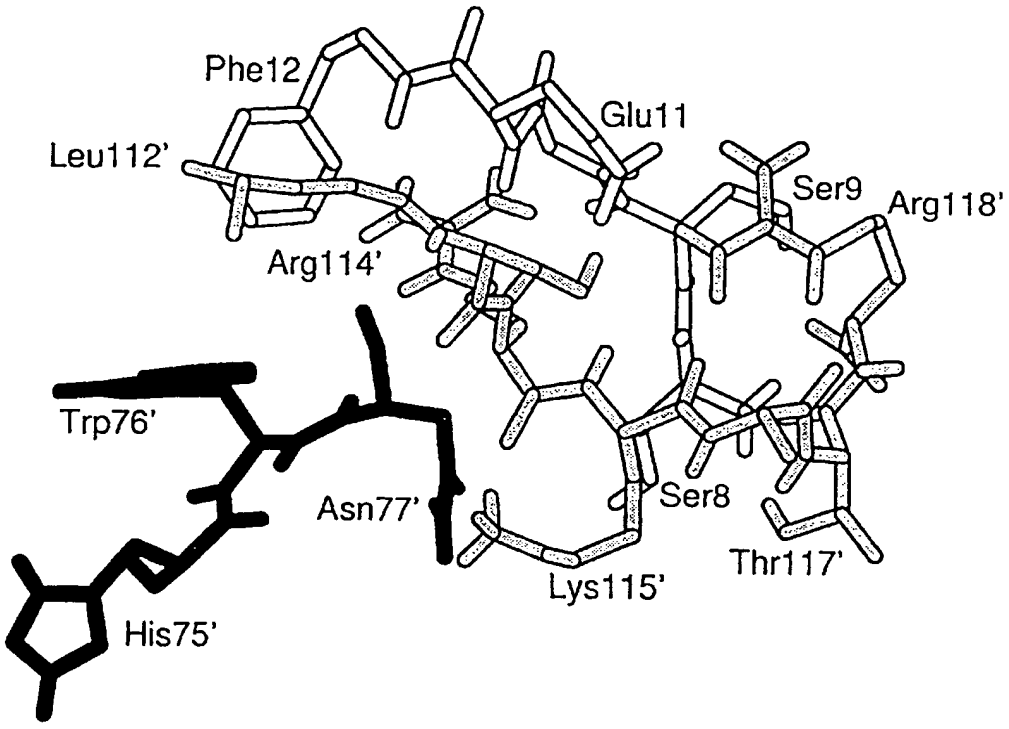
Phe12
Glu11
Leu112'
Ser9
Arg118'
Arg114'
Trp76'
Asn77'
Ser8
Thr117'
Lys115'
His75'

Figure 4

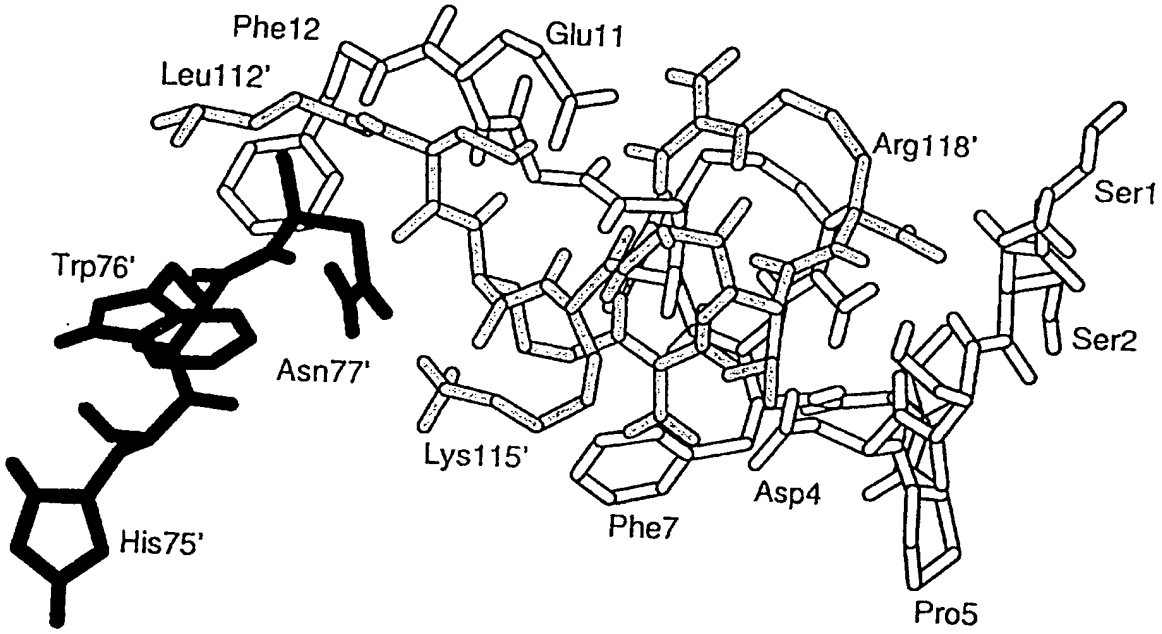
Phe12
Glu11
Leu112'
Arg118'
Ser1
Trp76'
Ser2
Asn77'
Lys115'
Asp4
Phe7
His75'
Pro5

Figure 5

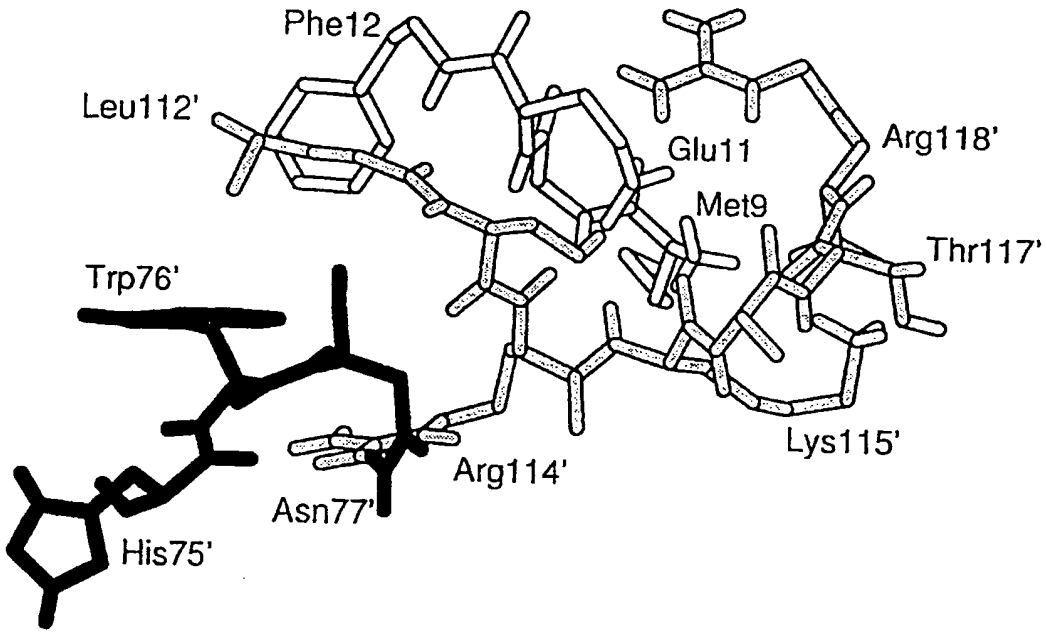
Phe12
Leu112'
Glu11
Arg118'
Met9
Thr117'
Trp76'
Lys115'
Arg114'
Asn77'
His75'

Figure 6

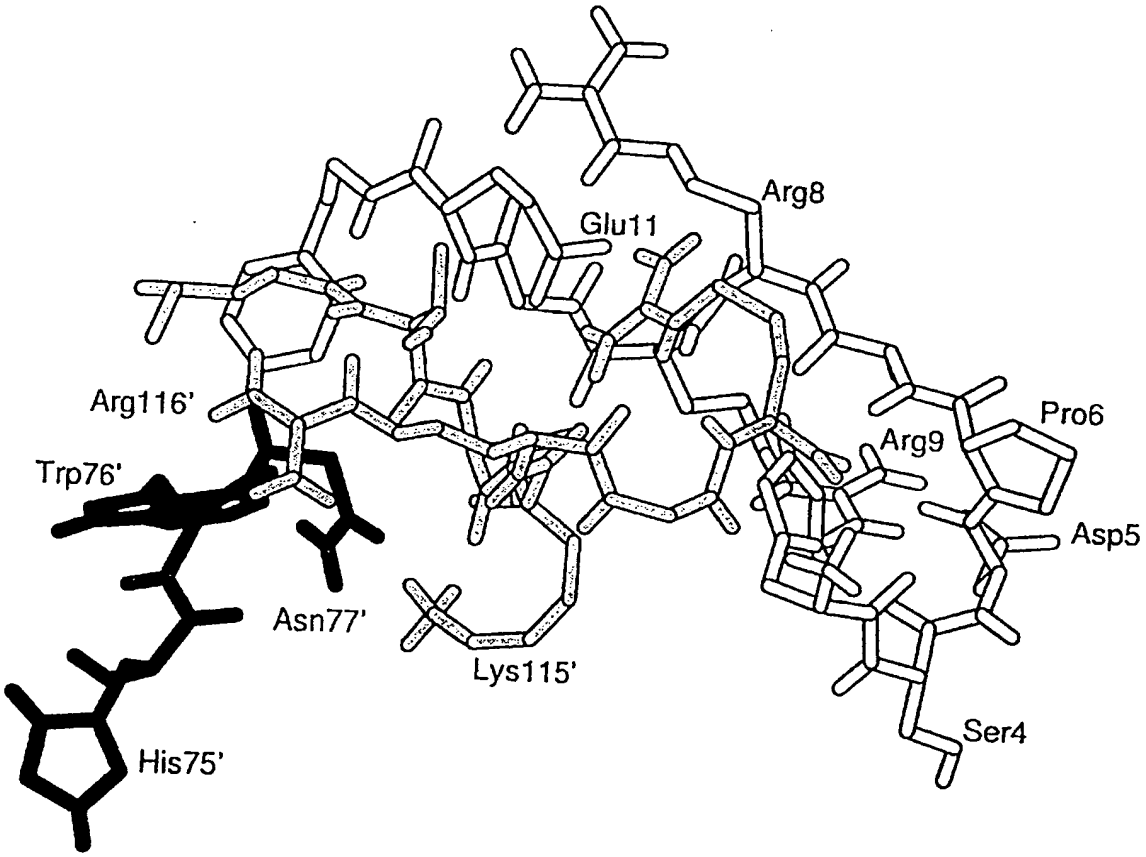
Arg8
Glu11
Arg116'
Trp76'
Pro6
Arg9
Asp5
Asn77'
Lys115'
Ser4
His75'

Figure 7

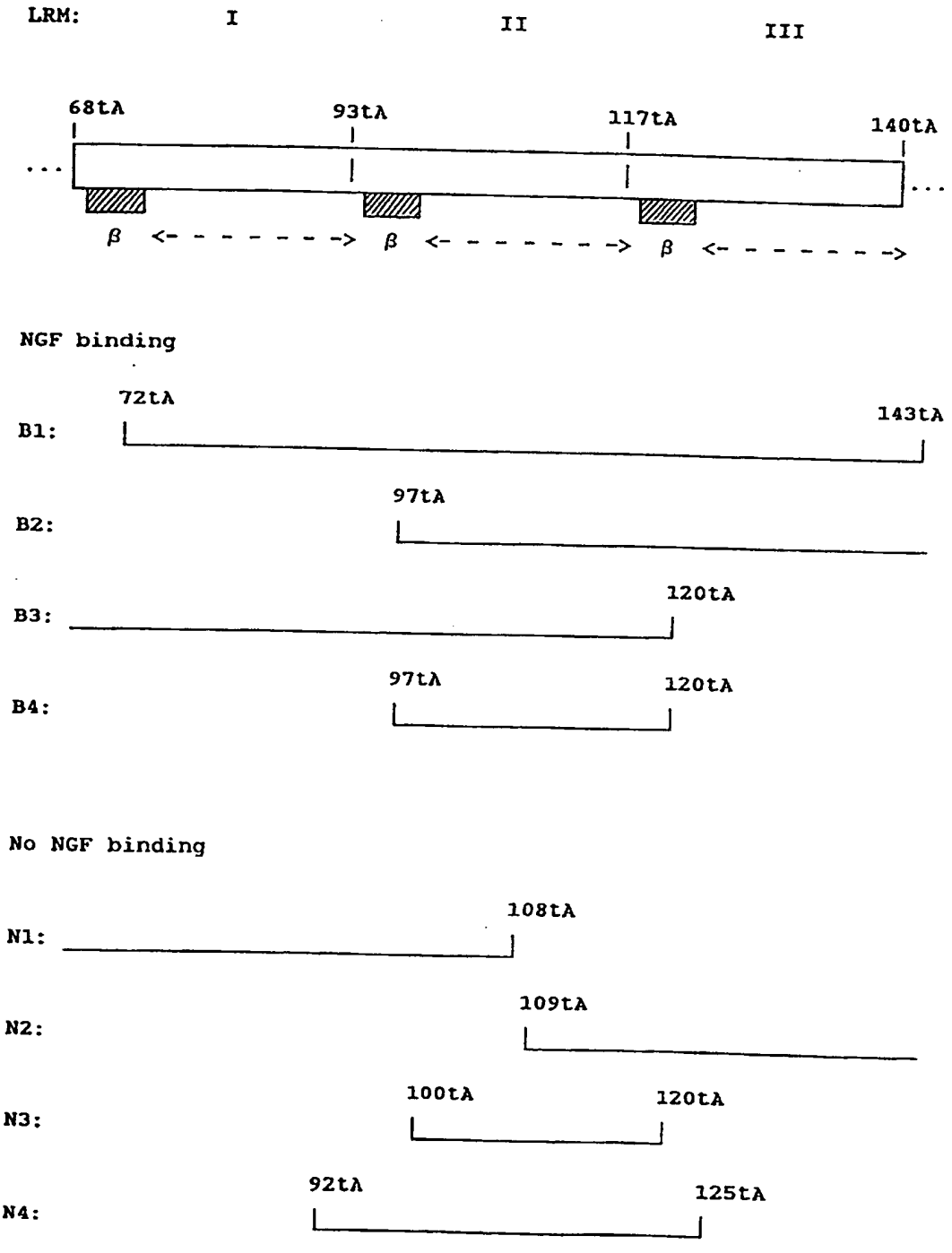
LRM:
I
II
III
68tA
93tA
117tA
140tA
β <- - - - - - -> β <- - - - - - -> β <- - - - - - ->
NGF binding
B1:
72tA
143tA
B2:
97tA
B3:
120tA
B4:
97tA
120tA
No NGF binding
N1:
108tA
N2:
109tA
N3:
100tA
120tA
N4:
92tA
125tA

Figur 8

Figure 9

First monomer: amino terminus

	1				5					10					15
hNGF	S	S	S	H	P	I	F	H	R	G	E	F	S	V	C	D ...
mNGF	S	S	T	H	P	V	F	H	M	G	E	F	S	V	C	D ...
mNGFΔ3-9	-	-	-	-	-	-	-	S	S	G	E	F	S	V	C	D ...
hNGF:NT-4/5	S	S	S	H	P	I	F	H	R	G	E	F	S	V	C	D ...

Second monomer: carboxyl terminus

	75'						110'					115'					118'
hNGF	... K	H	W	N	...	C	V	C	V	L	S	R	K	A	V	R
mNGF	... K	H	W	N	...	C	V	C	V	L	S	R	K	A	T	R
mNGFΔ3-9	... K	H	W	N	...	C	V	C	V	L	S	R	K	A	T	R
hNGF:NT-4/5	... R	H	W	V	...	C	V	C	T	L	L	S	R	T	G	R

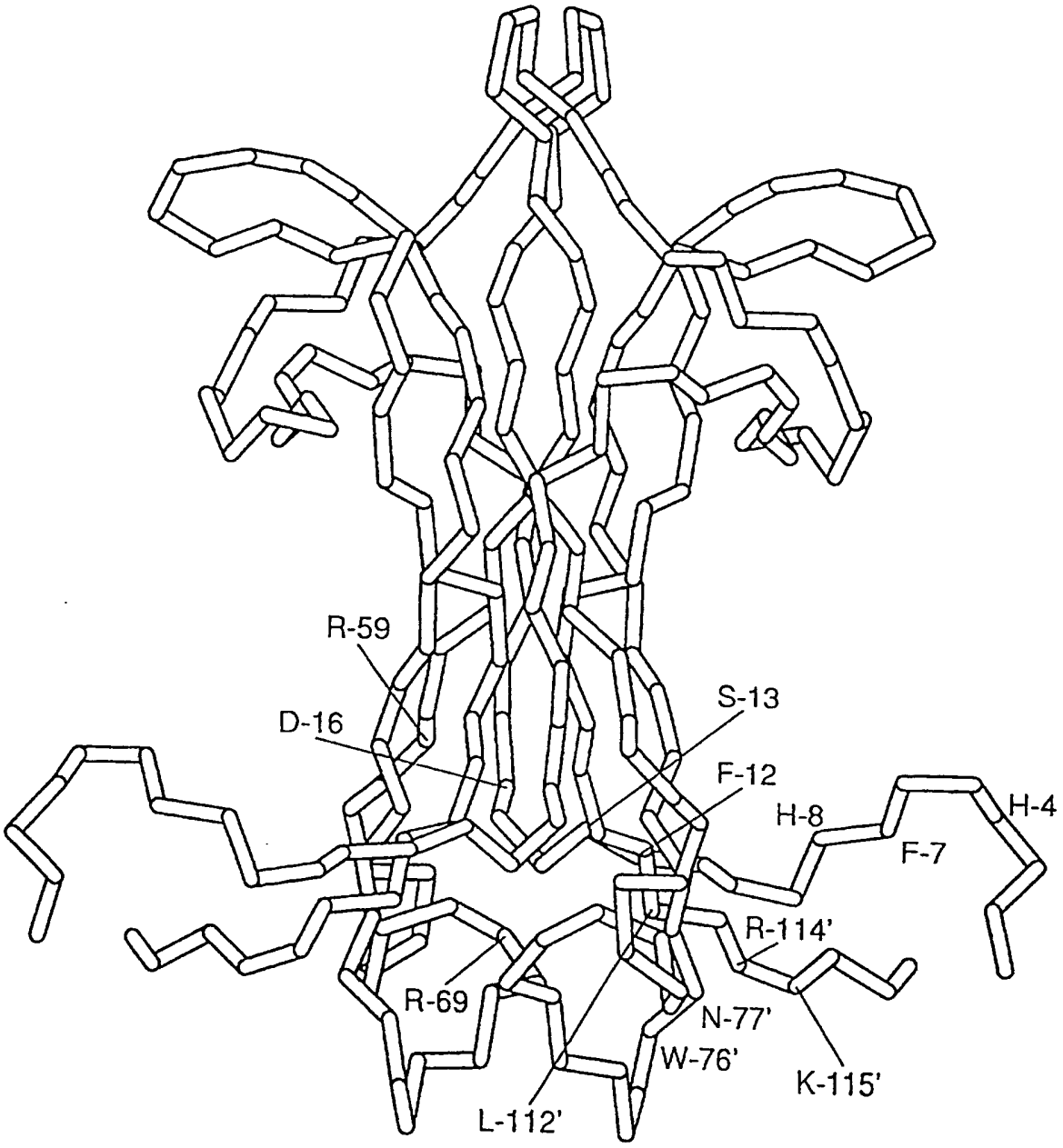

Figure 10a

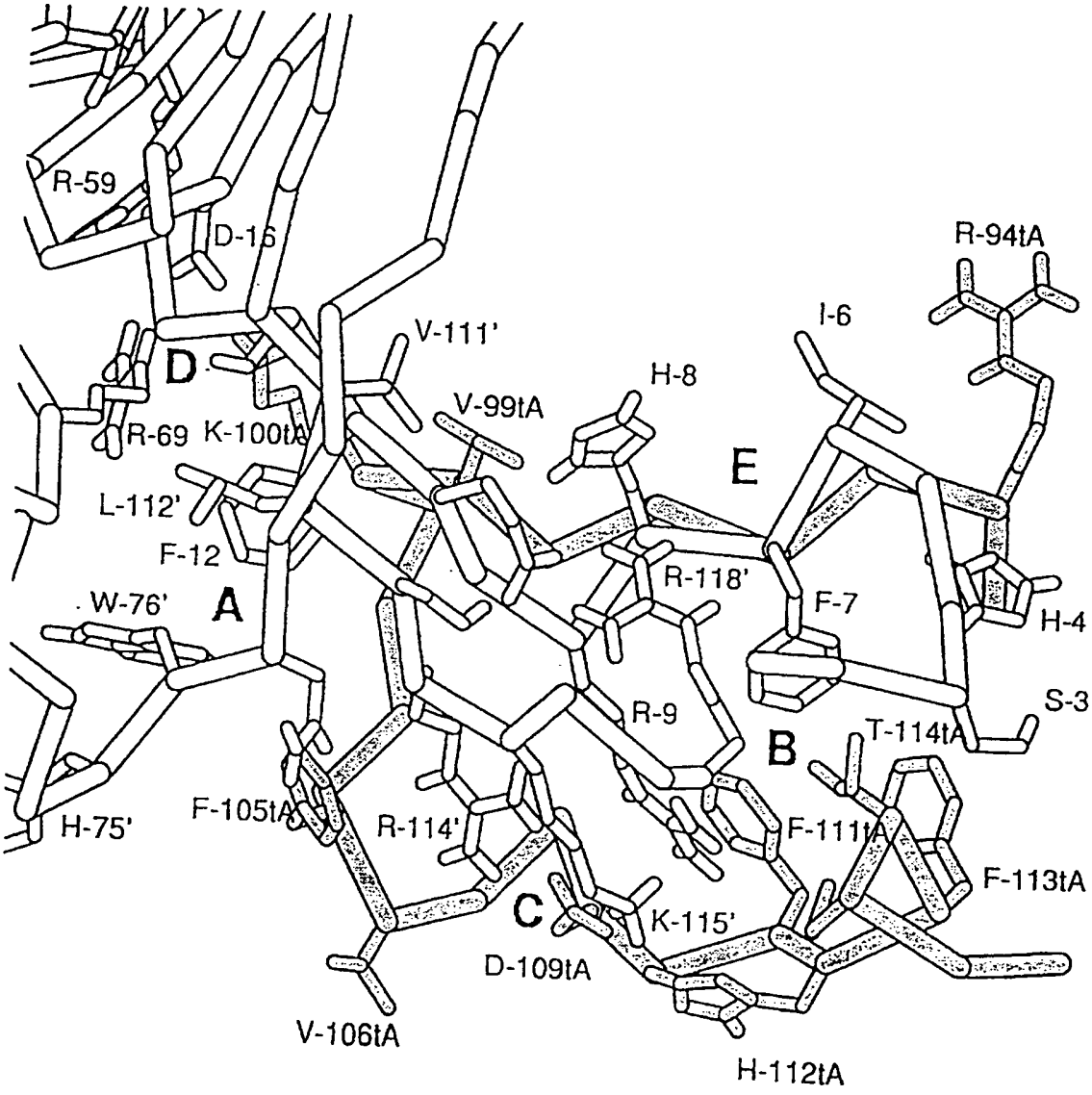
R-59
D-16
R-94tA
I-6
V-111'
D
H-8
V-99tA
R-69
K-100tA
E
L-112'
F-12
R-118'
W-76'
A
F-7
H-4
S-3
R-9
T-114tA
B
H-75'
F-105tA
R-114'
F-111tA
F-113tA
C
K-115'
D-109tA
V-106tA
H-112tA

Figure 10b

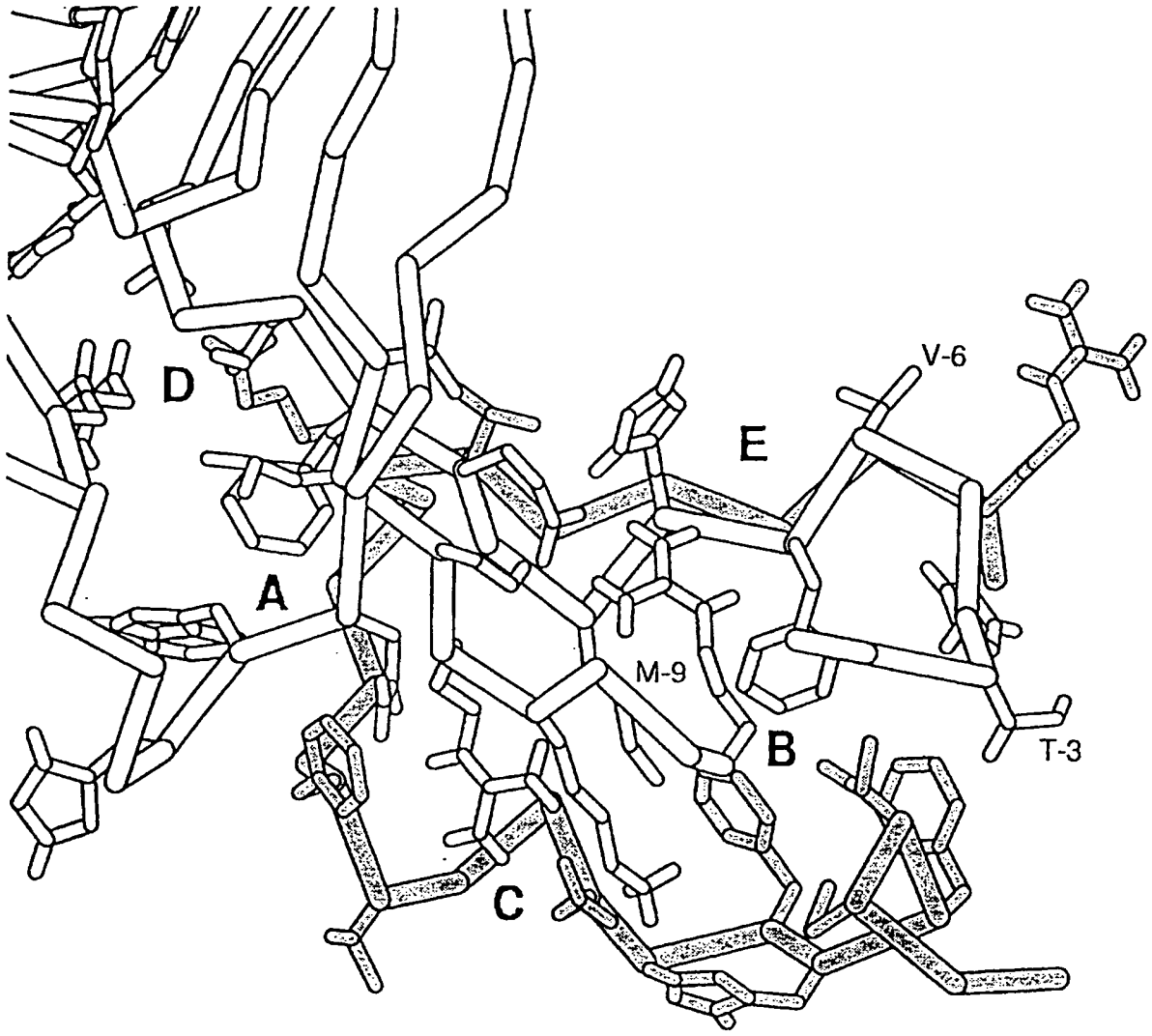

Figure 10c

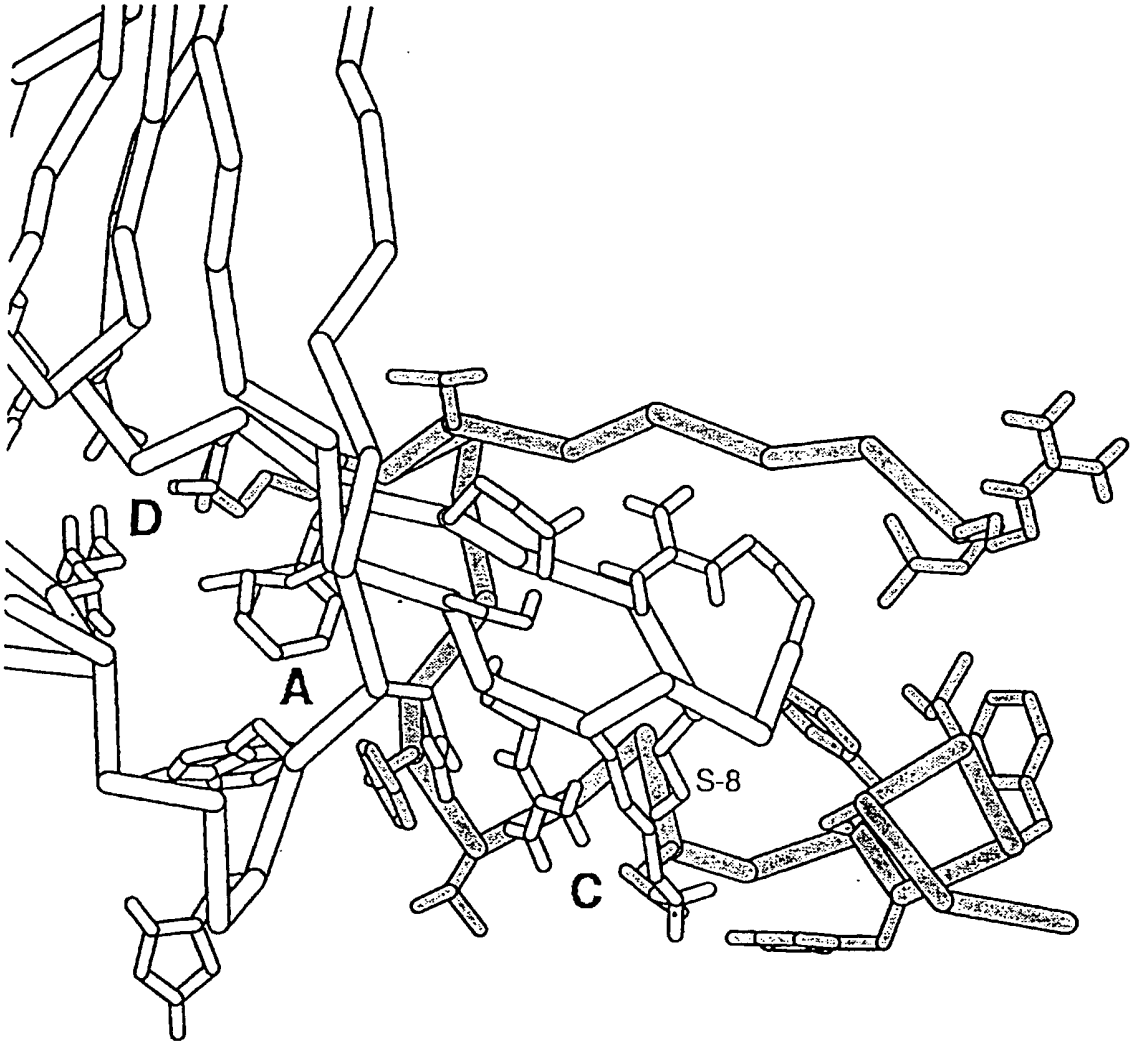

Figure 10d

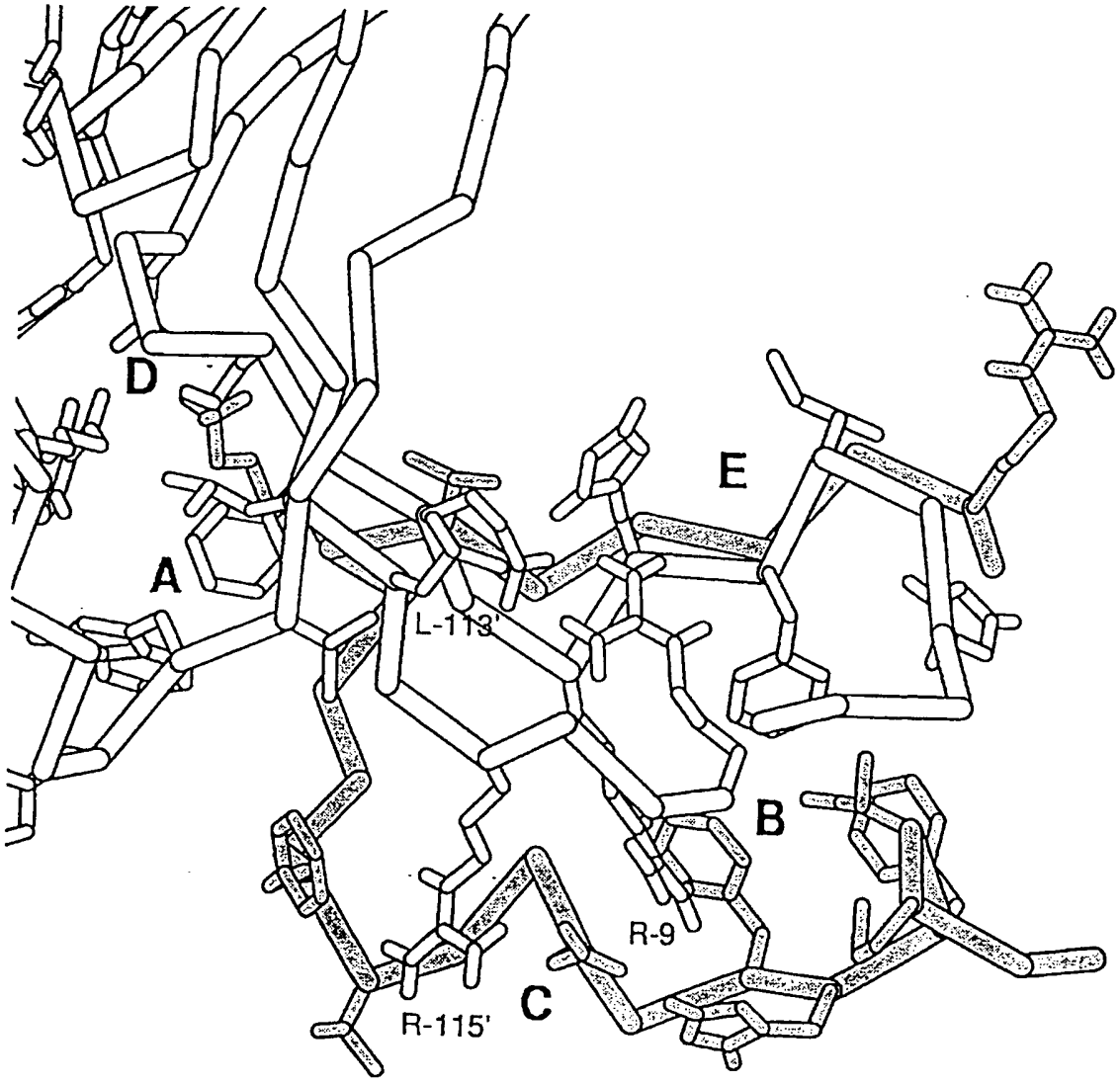

Figure 10e

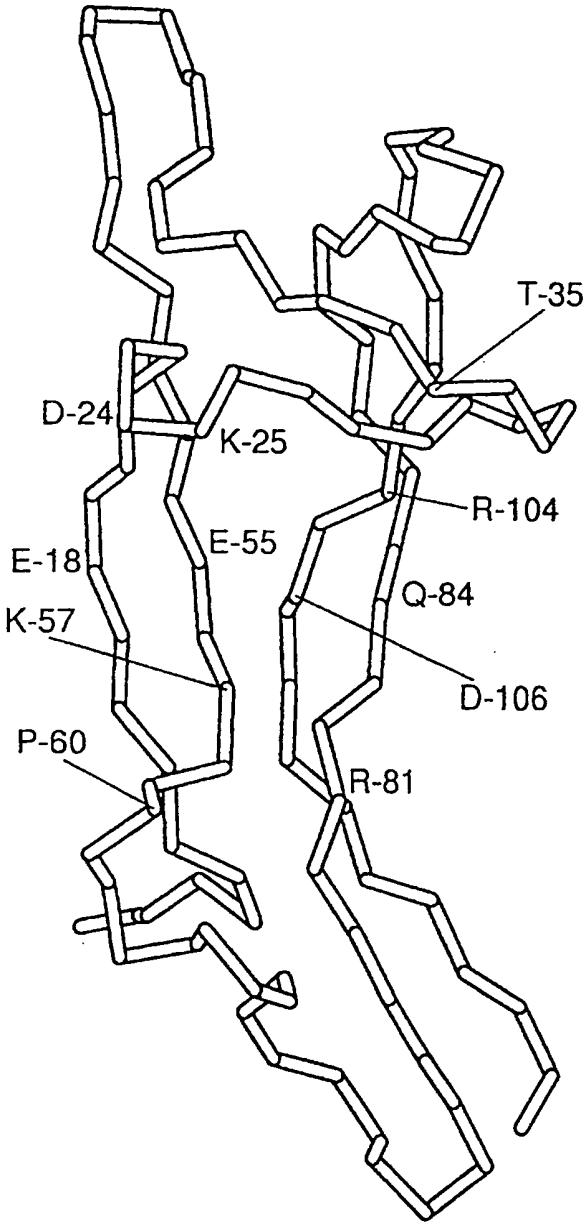

Figure 11a

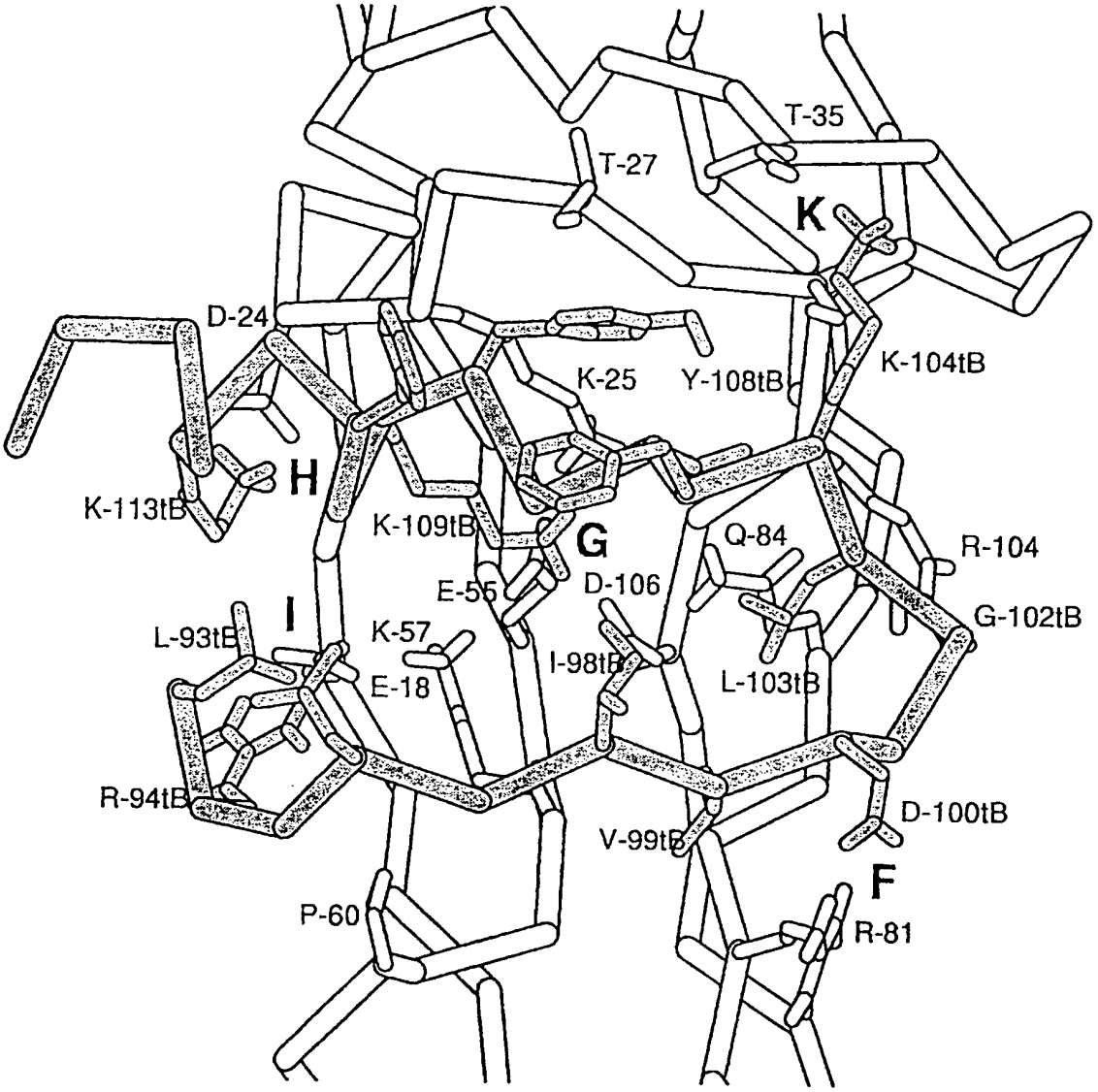
T-35
T-27
K
D-24
K-25
Y-108tB
K-104tB
H
K-113tB
K-109tB
G
Q-84
R-104
E-55
D-106
I
L-93tB
K-57
G-102tB
I-98tB
E-18
L-103tB
R-94tB
D-100tB
V-99tB
F
P-60
R-81

Figure 11b

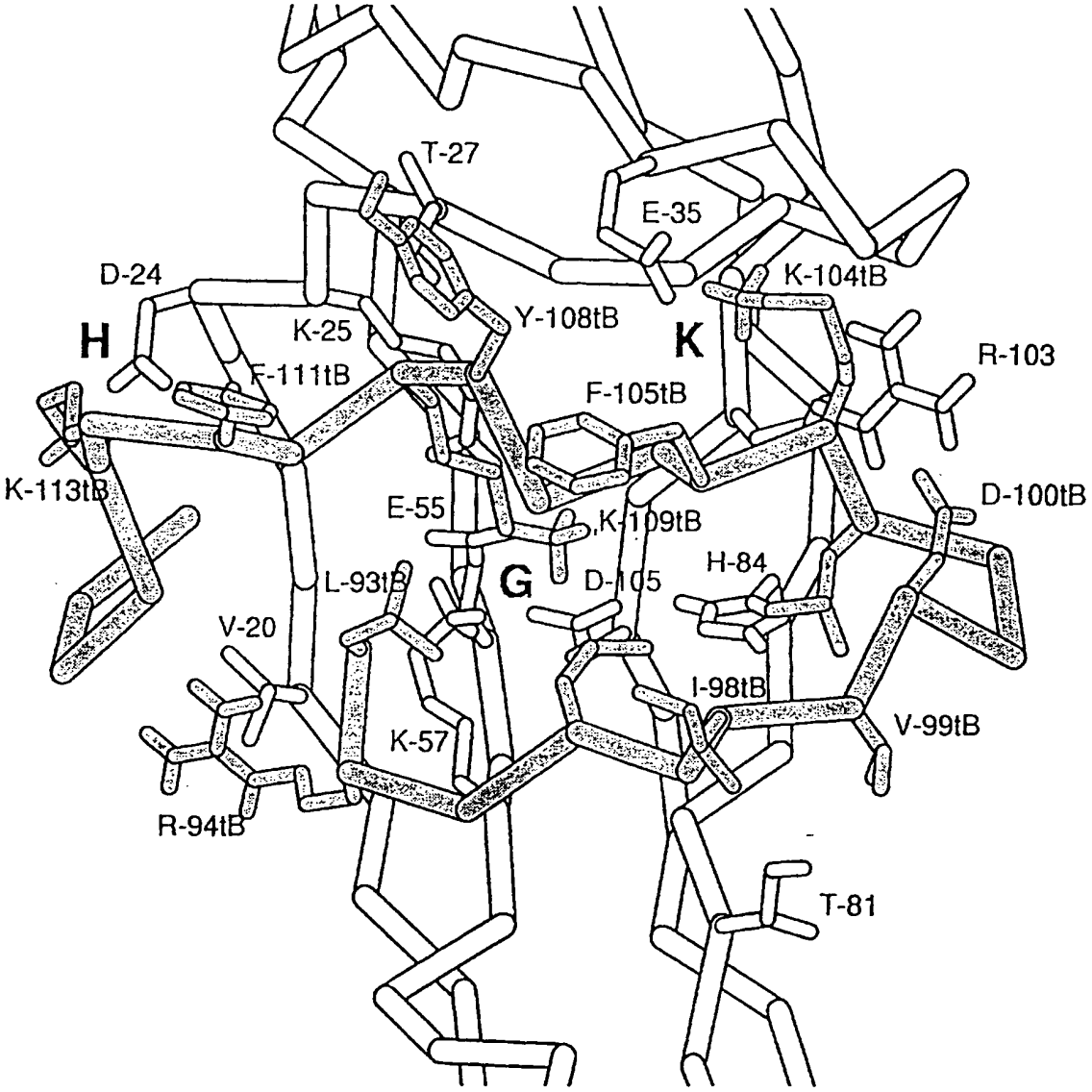
T-27
E-35
D-24
K-104tB
H
K-25
Y-108tB
K
R-103
F-111tB
F-105tB
K-113tB
D-100tB
E-55
K-109tB
H-84
L-93tB
G
D-105
V-20
I-98tB
V-99tB
K-57
R-94tB
T-81

Figure 11c

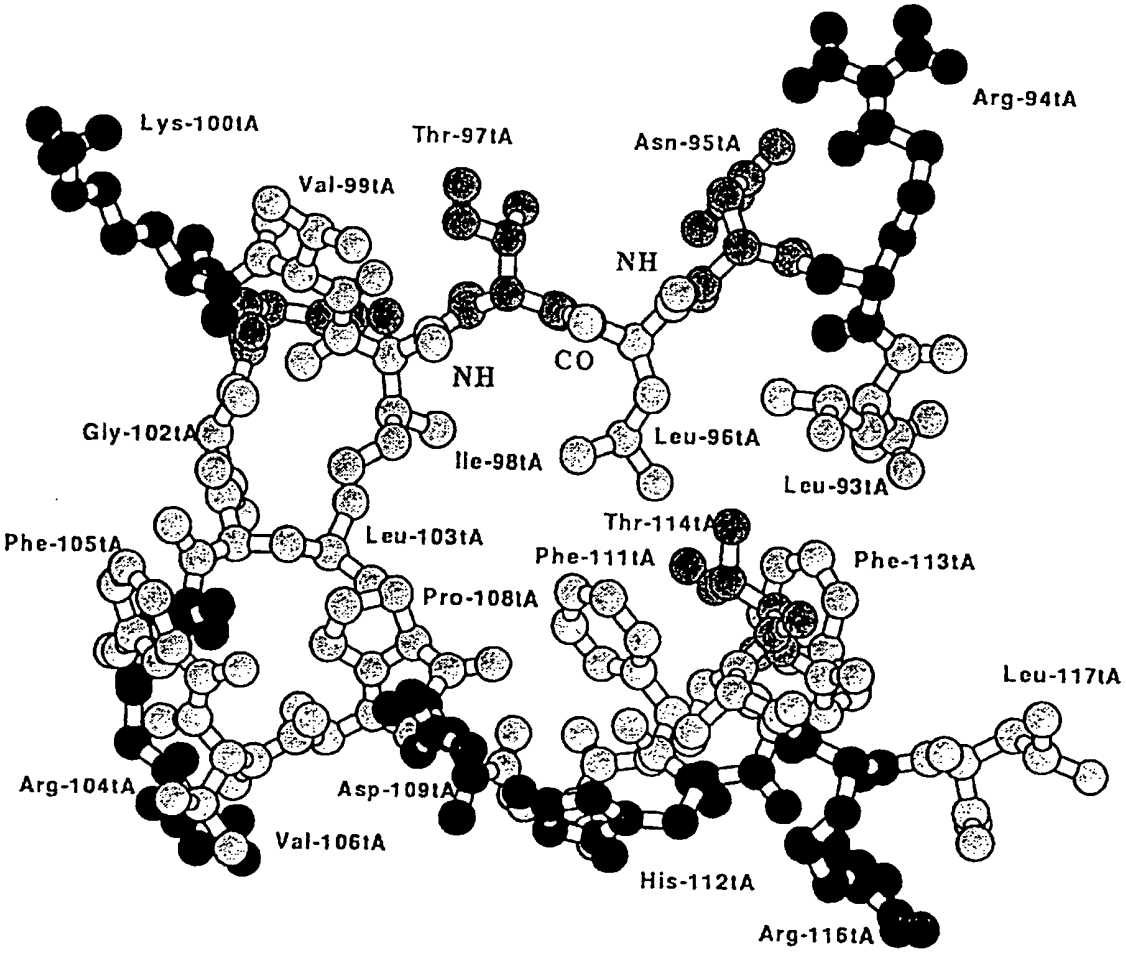
Lys-100tA
Thr-97tA
Asn-95tA
Arg-94tA
Val-99tA
NH
CO
NH
Gly-102tA
Ile-98tA
Leu-96tA
Leu-93tA
Thr-114tA
Phe-105tA
Leu-103tA
Phe-111tA
Phe-113tA
Pro-108tA
Leu-117tA
Arg-104tA
Asp-109tA
Val-106tA
His-112tA
Arg-116tA

Figure 12

Amino terminus

	1				5					10					15		
hNGF sequence	S	S	S	H	P	I	F	H	R	G	E	F	S	V	C	D	...
Conserved in NGF	-	-	-	X	X	X	-	X	X	X	X	-	X	X	X	X	
Determine structure	-	-	-	X	X	X	-	X	X	X	X	X	-	X	X	-	
Interact with LRM	-	-	-	-	-	X	X	X	-	-	X	-	X	-	-	X	
LRM binding sites						E	B	E			E		D			D	

Figure 13

Carboxyl terminus

	...	K	75' H	W	N	...	C	V	C	110' V	L	S	R	115' K	A	V	R
hNGF sequence																	
Conserved in NGF		-	X	X	X		X	X	X	X	X	X	X	X	-	-	X
Determine structure		-	X	X	X		X	X	X	X	X	X	-	-	-	-	X
Interact with LRM		-	-	X	-		-	-	-	-	-	-	X	X	-	-	-
LRM binding sites				A									C	C			

	93tA	95tA		100tA			105tA			110tA			115tA		
LRM sequence	L	R	N	L	T	I	V	K	S	G	L	R	F	V	A
Specific for trkA	-	-	-	-	-	-	-	X	-	-	-	X	X	-	-
Consensus	X	-	-	X	-	X	-	-	-	X	-	-	X	-	-
Interact with NGF	-	-	-	X	-	-	X	X	-	-	-	-	X	-	-
Form binding site			<--E-->		D					A		C			

LRM sequence	P	D	A	F	H	F	T	P	R	L					
Specific for trkA	X	X	-	-	X	X	X	X	-						
Consensus	-	-	-	X	-	-	-	-	-	X					
Interact with NGF	X	X	-	X	X	X	X	X	-	-					
Form binding site		C		B	C	B	B	C							

Figure 14

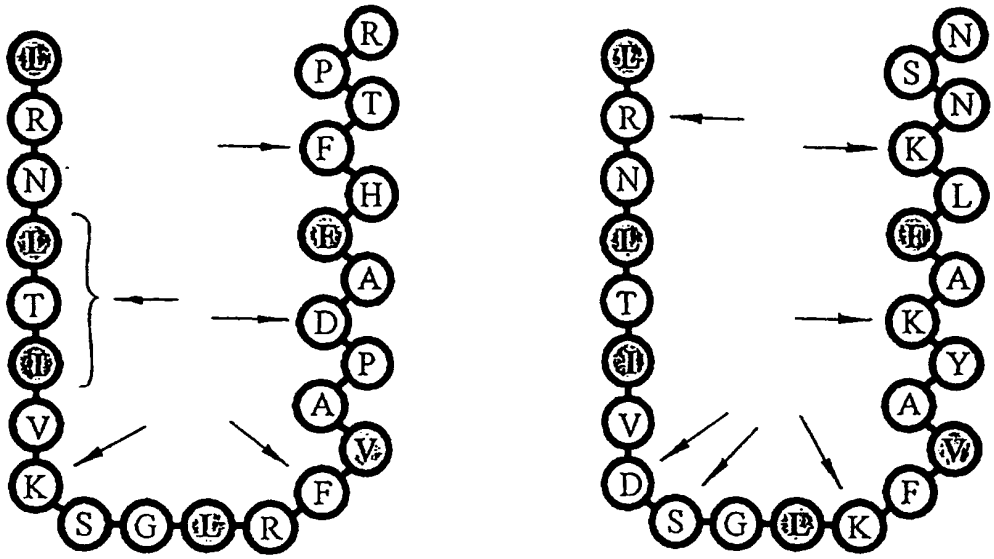

a *b*

Figure 15

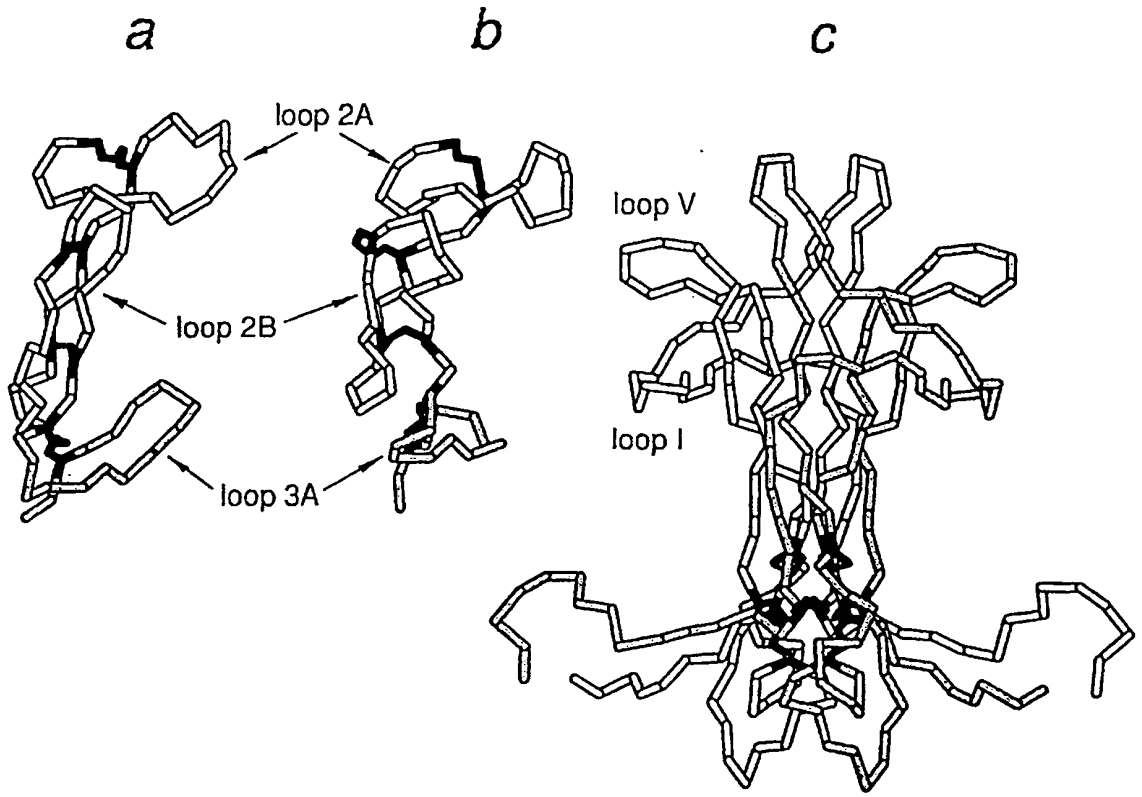

Figure 16

Second Cysteine-Rich Domain

$p75^{NTR}$(h)	39	C L D S V T F S D V V S A T E P C K P C T
$p75^{NTR}$(r)	39	C L D N V T F S D V V S A T E P C K P C T
$p75^{NTR}$(c)	40	C L D S V T Y S D T V S A T E P C K P C T
$p55^{TNFR}$	41	C - E S G S F T A S E N H L R H C L S C S
$p75^{NTR}$(h)	60	E C V G L Q S M S A - - P C V E A D D A V C
$p75^{NTR}$(r)	60	E C L G L Q S M S A - - P C V E A D D A V C
$p75^{NTR}$(c)	61	Q C V G L H S M S A - - P C V E S D D A V C
$p55^{TNFR}$	61	K C R K E M G Q V E I S S C T V D R D T V C

Third Cysteine-Rich Domain

$p75^{NTR}$(h)	80	R C A Y G Y Y Q D E - - - T T G R C E A
$p75^{NTR}$(r)	80	R C A Y G Y Y Q D E - - - E T G H C E A
$p75^{NTR}$(c)	81	R C A Y G Y F Q D E - - - L S G S C K E
$p55^{TNFR}$	83	G C R K N Q Y R H Y W S E N L F Q C F N

Figure 17

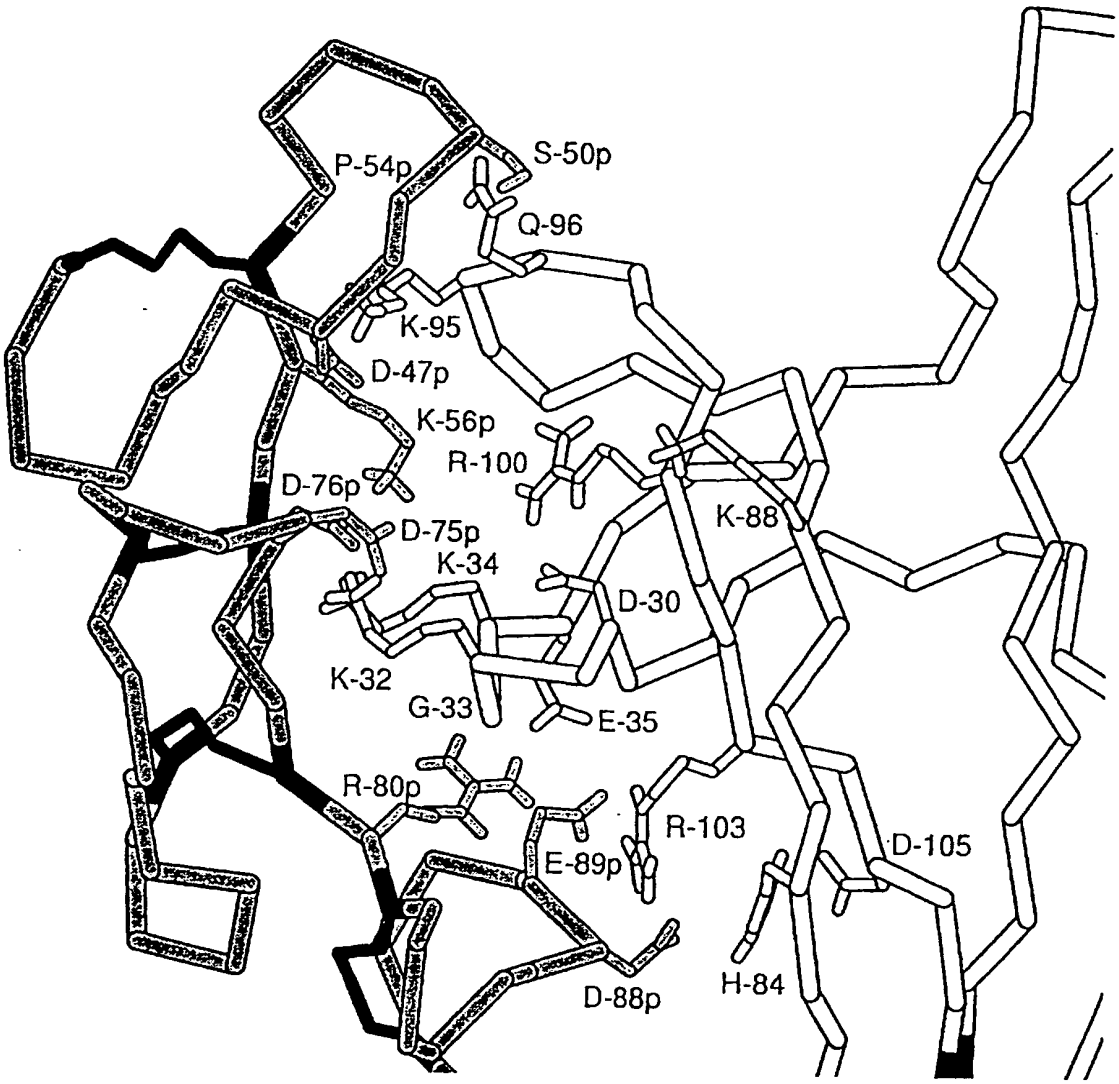
P-54p
S-50p
Q-96
K-95
D-47p
K-56p
R-100
D-76p
D-75p
K-34
K-88
D-30
K-32
G-33
E-35
R-80p
R-103
D-105
E-89p
H-84
D-88p

Figure 18a

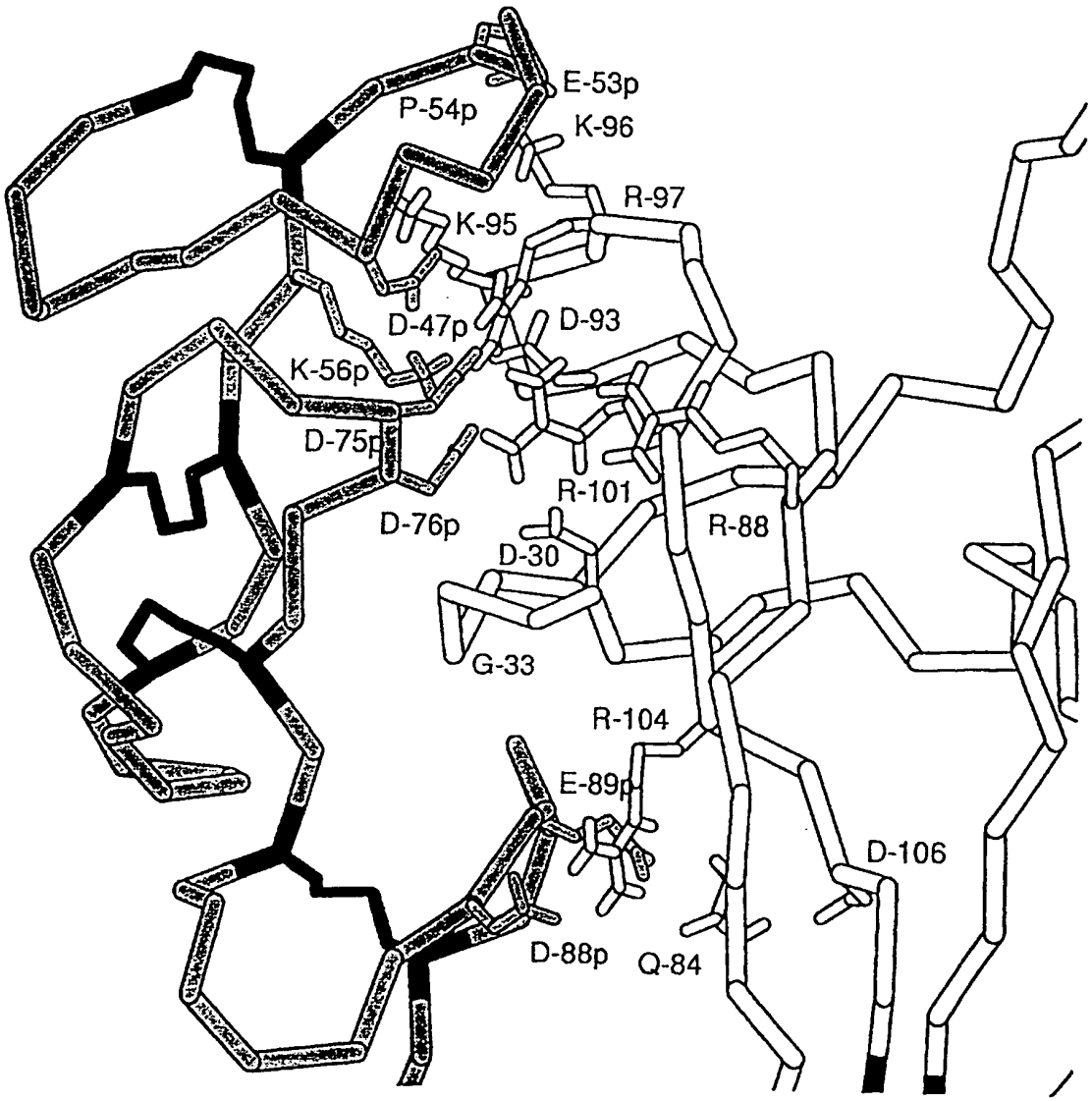
E-53p
P-54p
K-96
R-97
K-95
D-47p
D-93
K-56p
D-75p
R-101
D-76p
R-88
D-30
G-33
R-104
E-89p
D-106
D-88p
Q-84

Figure 18b

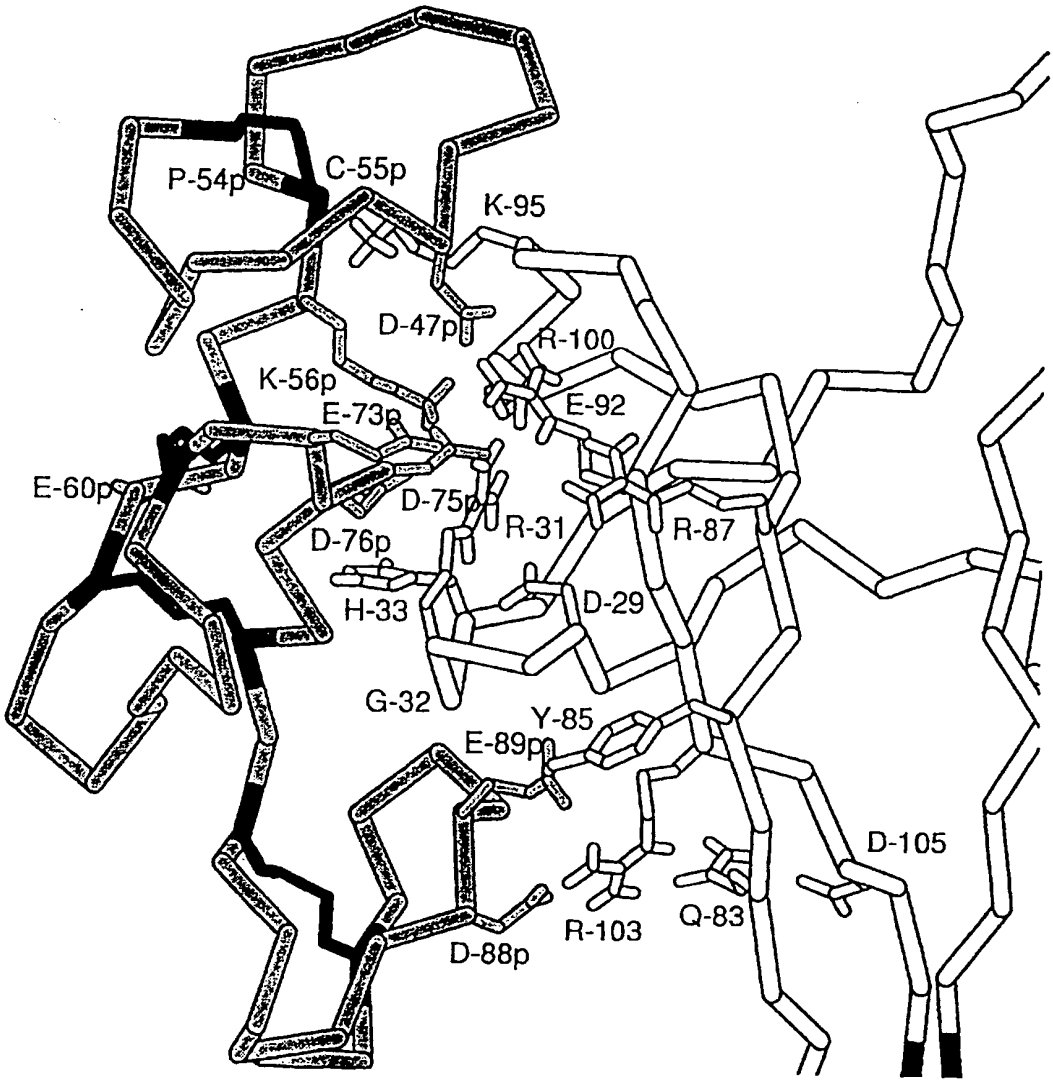
P-54p
C-55p
K-95
D-47p
R-100
K-56p
E-92
E-73p
E-60p
D-75p
R-31
R-87
D-76p
H-33
D-29
G-32
Y-85
E-89p
D-105
R-103
Q-83
D-88p

Figure 18c

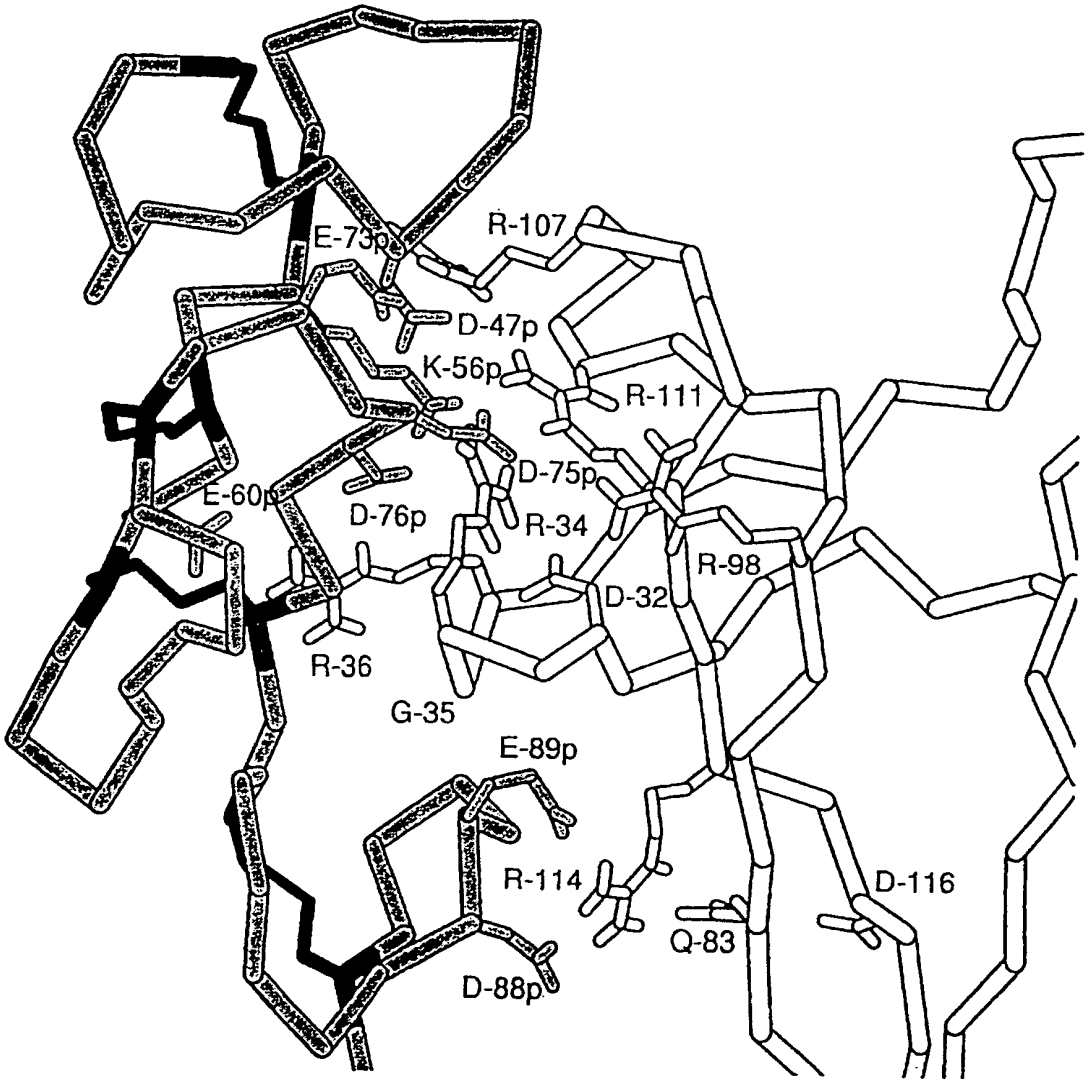
E-73p
R-107
D-47p
K-56p
R-111
D-75p
E-60p
D-76p
R-34
R-98
D-32
R-36
G-35
E-89p
R-114
D-116
Q-83
D-88p

Figure 18d

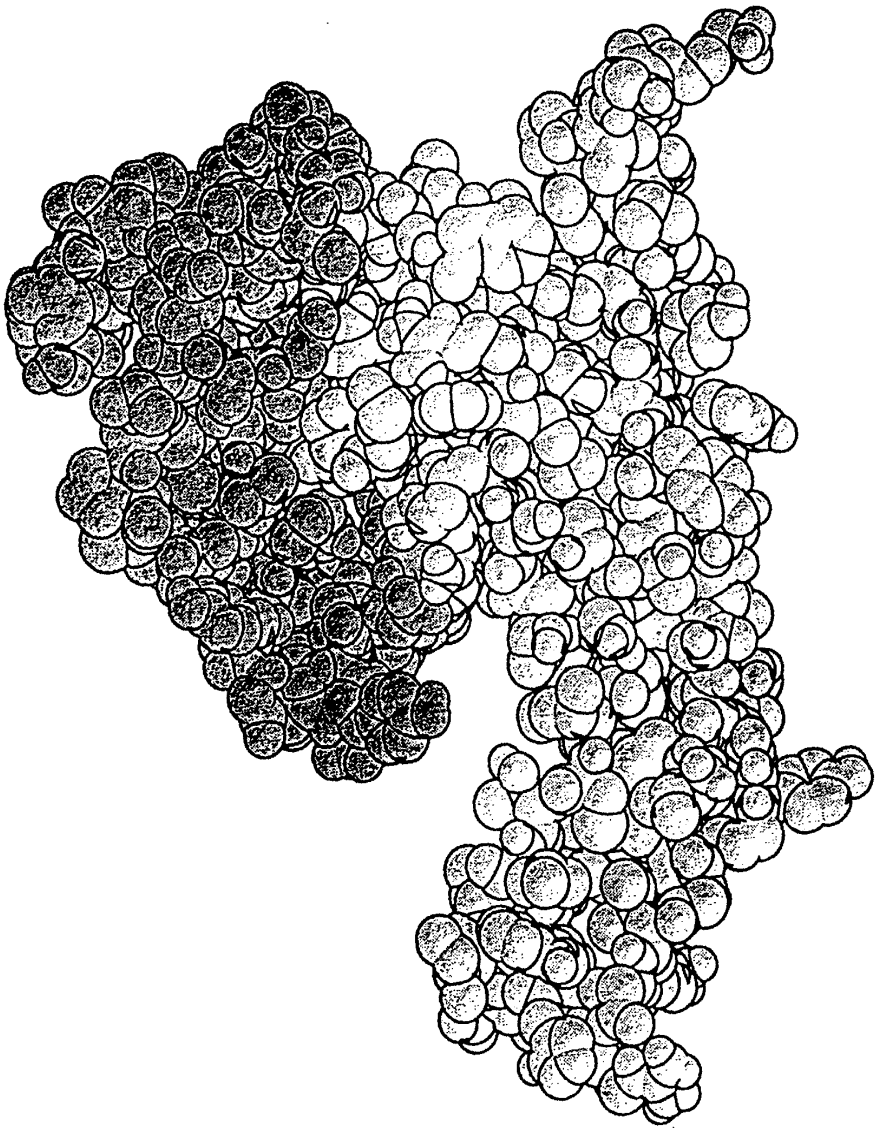

Figure 19

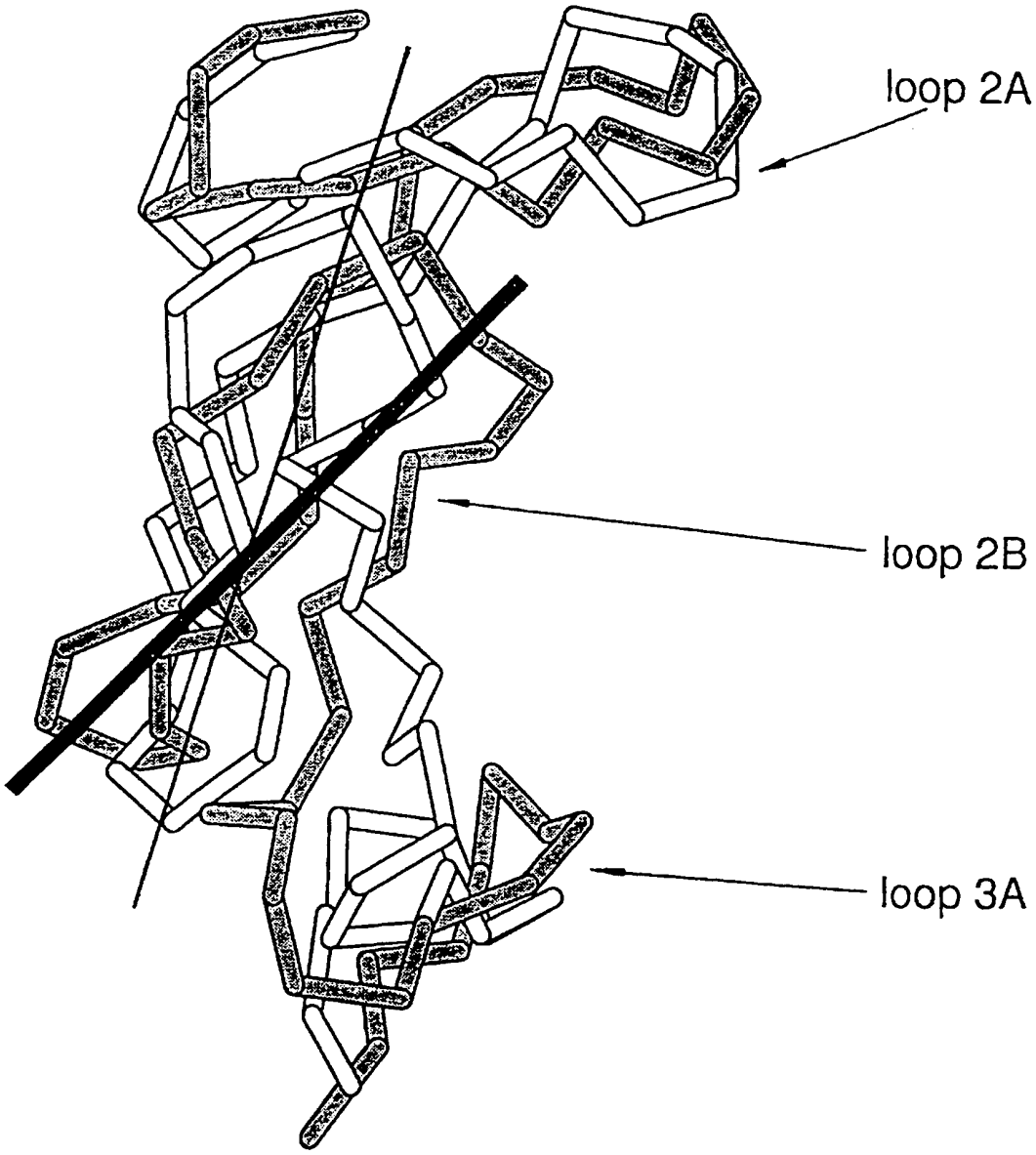

Figure 20